NCHRP Web Document 40 (Project 20-50[8/13]): Contractor's Final Report

LTPP Data Analysis: Factors Affecting Pavement Smoothness

Prepared for:

National Cooperative Highway Research Program
Transportation Research Board
National Research Council

Submitted by:

R. W. Perera
S. D. Kohn
Soil and Materials Engineers, Inc.
Plymouth, Michigan

August 2001

ACKNOWLEDGMENT

This work was sponsored by the American Association of State Highway and Transportation Officials (AASHTO), in cooperation with the Federal Highway Administration, and was conducted in the National Cooperative Highway Research Program (NCHRP), which is administered by the Transportation Research Board (TRB) of the National Research Council.

CONTENTS

ACKNOWLEDGMENTS

The research reported herein was performed under NCHRP Project 20-50(08/13) by Soil and Materials Engineers (SME). Dr. Starr D. Kohn, Manager of Pavement Services, and Dr. Rohan W. Perera, Project Engineer, served as co-principal investigators for this project. The analysis work for this project was performed by Dr. Rohan Perera. Ken Dani of SME created the analysis database, while Christopher Byrum of SME worked on development of models for GPS-1 sections and cumulative traffic analysis. Dr. Julian Faraway of University of Michigan provided input on the statistical analysis, and introduced the team to longitudinal data analysis.

SUMMARY

It is believed that the general public perceives a good road as one that provides a smooth ride. Studies at the road test sponsored by the American Association of State Highway Officials showed that the subjective evaluation of the pavement based on mean panel ratings was primarily influenced by roughness. Therefore, the development of roughness on pavements is a major issue for highway agencies.

Although pavement smoothness has been recognized as one of the important measures of pavement performance, the contribution of factors such as pavement structure, rehabilitation techniques, climatic conditions, traffic levels, layer materials and properties, and pavement distress to changes in pavement smoothness are not well documented. Without this information, the selection of appropriate pavement design structure, design features, and rehabilitation strategies that will ensure long-term smoothness is a difficult task. The data collected for the Long Term Pavement Performance (LTPP) study provides an opportunity to investigate the effect of these factors on the development of roughness.

In this research project, data available in the LTPP Information Management System (IMS) was used to determine the effect of factors such as design and rehabilitation parameters, climatic conditions, traffic levels, material properties, and extent and severity of distress that cause changes in pavement smoothness. For the purposes of this research, the International Roughness Index (IRI) was used as the measure of pavement smoothness. The IRI is a smoothness index that is widely used in the United States, and can be calculated for any profile that is measured by an inertial profiler. The LTPP program consists of two complementary programs, the General Pavement Studies(GPS) and Specific Pavement Studies (SPS).

The General Pavement Studies (GPS), is a study of the performance of in-service pavement test sections that were in either their original design phase or in their first overlay phase. The pavement types in the GPS experiment that were studied in this research project were: asphalt concrete (AC) on granular base, AC on stabilized base, jointed plain concrete, jointed reinforced concrete, continuously reinforced concrete, AC overlays of AC pavements,

and AC overlays on concrete pavements. Roughness trends over time for each of these pavement types were studied. Subgrade, climatic and pavement material properties that influence the roughness progression on each of these pavement types were identified.

The SPS projects that were analyzed in this project were the SPS-1, SPS-2, SPS-5 and SPS-6 experiments. The SPS projects are located throughout the United States. Each SPS project consists of several test sections, with the number of test sections being different for each SPS project. In the SPS-1 experiment, the structural factors affecting the performance of flexible pavements is studied. New flexible pavements were built for this study. The SPS-2 experiment is a study of structural factors affecting rigid pavement performance. New PCC pavements were built for this study. The SPS-5 experiment studies different treatment factors that can be used to rehabilitate AC pavements. All of these treatment factors involve overlays, with the factors being studied being overlay thickness, millimg, and type of AC used (virgin and recycled). The SPS-6 experiment studies different rehabilitation treatments that can be applied to rigid pavements. The treatments studied in this experiment include repairs to existing PCC, diamond grinding, AC overlays (with and without intensive restoration of existing surface prior to overlay), and crack/break seat with different AC thicknesses. The roughness characteristics of the different test sections in each of these projects were studied. Differences in performance between different rehabilitation strategies that were used for rehabilitation of flexible and rigid pavements were analyzed.

CHAPTER 1
INTRODUCTION AND PROJECT OBJECTIVES

INTRODUCTION

It is believed that the general public perceives a good road as one that provides a smooth ride. Studies at the road test sponsored by the American Association of State Highway Officials showed that the subjective evaluation of the pavement based on mean panel ratings was primarily influenced by roughness (1). Therefore, the development of roughness on pavements is a major issue for highway agencies.

Although pavement smoothness has been recognized as one of the important measures of pavement performance, the contribution of factors such as pavement structure, rehabilitation techniques, climatic conditions, traffic levels, layer materials and properties, and pavement distress to changes in pavement smoothness are not well documented. Without this information, the selection of appropriate pavement design structure, design features, and rehabilitation strategies that will ensure long-term smoothness is a difficult task. The data collected for the Long Term Pavement Performance (LTPP) study provides an opportunity to investigate the effect of these factors on the development of roughness.

PROJECT OBJECTIVES AND SCOPE

The objectives of this research project are to use the Level E data available in the LTPP Information Management System (IMS) to determine the effect of factors such as design and rehabilitation parameters, climatic conditions, traffic levels, material properties, and extent and severity of distress that cause changes in pavement smoothness, and to quantify the contribution of these factors to pavement smoothness. For the purposes of this research, the International Roughness Index (IRI) was used as the measure of pavement smoothness. The IRI is a smoothness index that is widely used in the United States, and can be calculated for any profile that is measured by an inertial profiler (2). The IRI values that are available in the IMS have

been computed from profile measurements that have been obtained at test sections. The research was limited to using Level E data that is available in the IMS. The data at Level E have passed a series of quality control checks. The findings of this research will provide guidance for considering long-term smoothness in the design of new and rehabilitated pavements.

The LTPP program consists of two complementary programs, the General Pavement Studies and Specific Pavement Studies. The General Pavement Studies (GPS), is a study of the performance of in-service pavement test sections that were in either their original design phase or in their first overlay phase. Table 1 shows the GPS experiments that were studied in this research project.

Table 1. GPS experiments.

GPS Experiment Number	Description
GPS-1	AC on Granular Base
GPS-2	AC on Stabilized Base
GPS-3	Jointed Plain Concrete
GPS-4	Jointed Reinforced Concrete
GPS-5	Continuously Reinforced Concrete
GPS-6	AC Overlay of AC Pavements
GPS-7	AC Overlay of PCC Pavement

The Specific Pavement Studies (SPS), investigated the effect of specific design features on pavement performance. The SPS experiments that were studied in this research project are shown in table 2.

Table 2. SPS experiments.

SPS Experiment	Description
SPS-1	Strategic Study of Structural Factors for Flexible Pavements
SPS-2	Strategic Study of Structural Factors for Rigid Pavements
SPS-5	Rehabilitation of Asphalt Concrete Pavements
SPS-6	Rehabilitation of Jointed Concrete Pavements

The work performed for the research project was divided into five tasks. The following is a brief description of the work performed for each task.

Task 1: Perform a literature review of LTPP reports that deal with pavement smoothness to obtain information needed to accomplish project objectives. From the data elements available in the LTPP database, identify elements needed to conduct the research and determine the extent of availability of each.

Task 2: Based on the information obtained in Task 1, develop a data analysis plan to address the changes in smoothness encountered at the GPS and SPS experiments that were studied in this research project.

Task 3: Submit for NCHRP review and approval a progress report that documents the research performed under Tasks 1 and 2, and giving details of the data analysis plan.

Task 4: Revise the data analysis plan in accordance with the review comments, and execute the approved data analysis plan.

Task 5: Submit a final report that documents the entire research effort.

ORGANIZATION OF REPORT

Chapter 2 presents the review of literature related to factors affecting pavement smoothness and roughness development in pavements. Chapter 3 presents the data elements that were selected for analysis and data synthesis methods that were used with the data obtained from the IMS. Chapter 4 presents the data analysis methods that were utilized during the study. Chapter 5 describes roughness characteristics of new pavements, and describes the results obtained from the SPS-1 and SPS-2 experiments. Chapter 6 describes roughness characteristics of rehabilitated pavements, and describes results obtained from SPS –5 and SPS-6 experiments.

Chapter 7 presents the results obtained for GPS experiments in the first design phase, which are GPS experiments 1 through 5. Chapter 8 presents the results obtained for GPS experiments 6 and 7, which are overlaid pavements. Chapter 9 presents the conclusions and recommendations for future research.

CHAPTER 2
LITERATURE REVIEW

LONG TERM PAVEMENT PERFORMANCE PROGRAM

The LTPP program is a 20-year study that was started in 1987. The objectives of the LTPP program are to: (1) evaluate existing design methods; (2) develop improved design methods and strategies for the rehabilitation of existing pavements; (3) develop improved design equations for new and reconstructed pavements; (4) determine the effects of loading, environment, material properties and variability, construction quality, and maintenance levels on pavement distress and performance; (5) determine the effects of specific design features on pavement performance; and (6) establish a national long-term pavement database (3). The Strategic Highway Research Program (SHRP) administrated the first five years of the program, and thereafter, the administration of the program was transferred to Federal Highway Administration (FHWA).

The GPS experiments that were analyzed in this study were the GPS experiments 1 through 7. GPS experiments 1 through 5 study the performance of different types of pavements in the first design phase, while experiments 6 and 7 study the performance of AC overlays on AC and PCC pavements, respectively. Table 1 (in Chapter 1) gives the pavement type in each GPS experiment. Each GPS section is 152 m long. The GPS sections generally represent pavements that incorporate materials and structural designs used in standard engineering practice in the United States. The GPS test sections had been in service for some time when they were accepted into the LTPP program. Roughness data collection at these test sections have been performed at regular intervals after the test sections were accepted into the LTPP program. However, the initial IRI of these test sections are not known.

The SPS experiments were designed to study the effect of specific design features on pavement performance. Each SPS experimental test site consists of multiple test sections, each of which is 152 m in length. The SPS experiments that were studied in this research project were experiments 1, 2, 5 and 6. New pavements were constructed for SPS-1 and SPS-2 experiments,

and profile data were collected on these pavements after construction. Thereafter, these test sections have been profiled at regular intervals. For these sections, the roughness of the pavement when it was opened to traffic, as well as roughness data collected at approximately annual intervals are available. The SPS-5 and SPS-6 experiments study the effect of different rehabilitation treatments on asphalt concrete and jointed concrete pavements, respectively. For these two experiments, profile data were collected at the test sections prior to and after rehabilitation, and thereafter at approximately annual intervals.

ROUGHNESS STUDIES

Several research projects that used LTPP data to study roughness progression have been performed during the past several years. The first ever comprehensive analysis of roughness progression at LTPP sections was performed by Perera et al. (4). This research project investigated the time-sequence roughness data at GPS test sections to study trends in development of roughness, and developed models to predict roughness. An evaluation of roughness data collected for the SPS-1, -2, -5 and –6 experiments were also performed in this study. Khazanovich et al. (5) used LTPP data to investigate common characteristics of good and poorly performing PCC pavements. They grouped jointed plain concrete (JPC), jointed reinforced concrete (JRC) and continuously reinforced concrete (CRC) pavements into three groups (poor, normal and good) based on time vs IRI relationships, and examined factors contributing to differences in pavement performance. Owusu-Antwi et al. (6) and Titus-Glover et al. (7,8) used LTPP data to analyze the performance of PCC pavements. They determined design features and construction practices that enhance pavement performance, and developed models to predict roughness. Simpson et al. (9) performed a sensitivity analysis of IRI data at the GPS sections. Very few time-sequence IRI values were available when this study was performed. Byrum (10) analyzed profile data collected at GPS-3 and 4 sections and developed a curvature index to quantify slab shape from profile elevation data, and showed that slab curvature was related to PCC pavement performance. An analysis of pavement performance trends for test sections in SPS-5 and SPS-6 projects was performed by Daleiden et al. (11). In this study, a comparison of performance trends of different test sections were made to evaluate the effect of

different rehabilitation treatments. The parameters studied in this research were pavement distress (e.g., fatigue cracking, longitudinal cracking, transverse cracking), roughness, rutting, and deflection data.

In the NCHRP project 10-47 (12), variations in roughness statistics due to distress, lateral wander of traveled path, and temperature differential in PCC slabs were studied. This study utilized roughness data collected from test sections that were established on in-service roads specifically for this study, as well as data collected at LTPP sites. Paterson (13) utilized data from a study that was conducted in Brazil to develop models to predict roughness. Von Qunitus et al. (14) used LTPP data to study the relationship between changes in pavement surfaces distress of flexible pavements to incremental changes in IRI.

ROUGHNESS DEVELOPMENT OF AC PAVEMENTS

In investigating roughness characteristics of GPS sections, Perera et al. (4) found a strong relationship between pavement performance and environmental factors. When they performed this study, each GPS sections had been profiled an average of four times. When roughness progression for test sections in each GPS experiment was plotted for each of the four environmental zones (i.e., wet-freeze, wet no-freeze, dry-freeze, and dry no-freeze), there were distinct trends in roughness progression between the regions. The observed roughness development trends in GPS-1 sections seem to indicate that pavement roughness remains relatively constant over the initial life of the pavement, and then after a certain point show a rapid increase. The IRI plots show several sections that were over 15 years old, but had low IRI values. An analysis of these sections indicated they have carried a relatively low cumulative traffic volume when compared to the theoretical cumulative traffic volume the section was capable of carrying. A preliminary analysis of the sections that were showing a high increase in roughness over the monitored period indicated that these sections were close to or have exceeded their design life based on equivalent axle loads.

ROUGHNESS DEVELOPMENT OF PCC PAVEMENTS

A comprehensive analysis of IRI trends of GPS-3, GPS-4 and GPS-5 pavements was performed by Perera et al. (4). At the time this study was performed, these sections had an average of four time-sequence IRI values. This analysis indicated distinct IRI trends for each of these experiments.

Perera et al. (4) found that for JPC pavements (i.e., GPS-3), there were distinct differences in IRI progression between doweled and non-doweled pavements. Generally, the non-doweled pavements showed higher rates of increase in roughness when compared to doweled pavements. For both doweled and non-dowelled pavements, higher IRI values were generally indicated for pavements located in areas that received higher precipitation, had higher freezing indices, and had a higher content of fines in the subgrade. In the non-freeze regions, pavements located in areas that had a higher number of days above 32°C had lower IRI values for both doweled and non-doweled pavements. Pavements that had higher modulus values for PCC had higher IRI values. These observations indicate that mix design factors and the type of aggregate used may influence the performance of the pavements from a roughness point of view.

Khazanovich et al. (5) analyzed roughness trends in JPC (i.e., GPS-3) sections by dividing the sections into three groups based on IRI vs. time performance. The three groups were classified as poor, normal and good. The performance of a pavement section was classified to be good if the IRI satisfied the following condition: IRI < 0.631 + 0.0631 * Age, where IRI is in m/km, and age is the pavement age in years. The performance of a pavement section was classified to be poor if the IRI satisfied the following condition: IRI > 1.263 + 0.0947 * Age, where IRI is in m/km, and age is the pavement age in years. Pavement sections falling between the good and poor cut-off limits were considered to be performing normally. Of the poor performing sections, approximately 71 percent were located in wet-freeze region, 24 percent in dry-freeze region, and 6 percent in wet no-freeze region. None of the poorly performing sections were located in dry no-freeze regions. Higher IRI values were related to high freeze index values, higher freeze thaw cycles, and higher annual days below 0 °C. They also found that the presence of increased moisture over an extended period of time, characterized by the average

number of wet days per year, caused higher roughness. Pavements in warmer climates generally had lower IRI values. They also found a strong relationship between pavement performance and subgrade type. Approximately 67 percent of sections constructed on fine-grained subgrade had a poor IRI performance, while only 33 percent of sections on coarse-grained soils had a poor IRI performance. No trend between traffic and IRI was found. Sections with stabilized bases had lower IRI compared to sections with granular bases. In the poor performance group, 82 percent of the sections had granular bases while 18 percent of the sections had stabilized bases. Sections with asphalt stabilized bases had significantly lower IRI than all other bases. They used linear regression to backcast an estimate of the initial as-constructed roughness and to obtain a rate of increase of roughness. They found that poor performing sections had the highest average rate of increase of roughness, while good performing sections had the lowest rate. They also found that poor performing sections had higher backcasted initial roughness when compared to normal and good sections.

Perera et al. (4) found that for JRCP (i.e., GPS-4) pavements, higher IRI values were associated with higher precipitation, higher moisture content in subgrade, thicker slabs, longer joint spacing, lower water cement ratios, and higher modulus values for PCC. Khazanovich et al. (5) performed an analysis of JRCP sections using an approach similar to that used in the analysis of GPS-3 sections. They determined JRCP constructed on coarse-grained soil performs better than JRCP constructed on fine grained subgrade. All JRCP rated as poor were constructed on fine grained subgrade, while no JRCP rated as poor was constructed on coarse grained soil. They indicated where poor subgrade soil exists, the specification of a thick granular layer will be beneficial. They did not find any specific trends between IRI and traffic, but observed JRCP in good IRI performance category carried much higher ESALs than those in the poor or normal group. Higher IRI values were associated with thicker slabs, which indicated thicker slabs were constructed rougher than thinner slabs. Pavements in areas having a greater annual precipitation or a higher number of wet days had a higher IRI. There were no significant differences in IRI between granular and stabilized bases. They used a linear regression on the time-sequence IRI data to backcast the initial roughness value and obtain a rate of increase of IRI. This analysis indicated that both the initial IRI and rate of increase of IRI over time were greater for the JRCP rated as poor when compared to the normal and good performing category. They found that the

mean backcasted initial IRI of JRCP rated as poor was 2.38 m/km, while the sections that were rated as good had a mean backcasted initial IRI of 1.10 m/km. The sections that were rated as poor had an IRI increase per year that was twice as high for JRCP rated as good. They also found that on average, sections with higher k-values had lower IRI values.

Perera et al. (4) analyzed roughness trends of CRCP pavements and observed that CRCP pavements appear to maintain a relatively constant IRI over the monitored period. The IRI behavior pattern was observed to be similar for new as well as old pavements. They report that there were many sections that are over 15 years old, but are still very smooth (IRI < 1.5 m/km). Lower IRI values were associated with higher percentage of longitudinal steel and higher water cement ratios for PCC mix, while higher IRI values were associated with higher values of PCC modulus. In non-freezing areas, higher IRI values were noted for pavements in areas that had higher number of days above 32°C. Khazanovich et al. (5) analyzed roughness trends in CRCP pavements by dividing the LTPP sections into three groups based on time vs IRI performance. The three groups were classified as poor, normal and good. They found higher percentage of steel reinforcement resulted in smoother pavements. They indicate in general, pavements constructed over coarse grained subgrade performed better than those constructed over fine grained subgrade. Of all poorly performing sections, 63 percent were located on fine grained subgrade while 37 percent was located on coarse grained subgrade. They did not find any trends between IRI and traffic, but found that sections that were in the good category had higher traffic volumes.

EFFECT OF SLAB CURVATURE ON ROUGHNESS

Analysis of LTPP data by Byrum (10) as well as data analyzed for the NCHRP Project 10-47 (12) have shown that jointed PCC pavements can take a shape where the slab is curled upwards or downwards. Figure 1 shows an example of a PCC slab that is curled downwards, where the joints are at a lower elevation with respect to the center of the slab. This PCC pavement has a joint spacing of 9 m, which can be seen in this figure. Figure 2 shows an example of a PCC slab that is curled upward with respect to the center of the slab, which has a

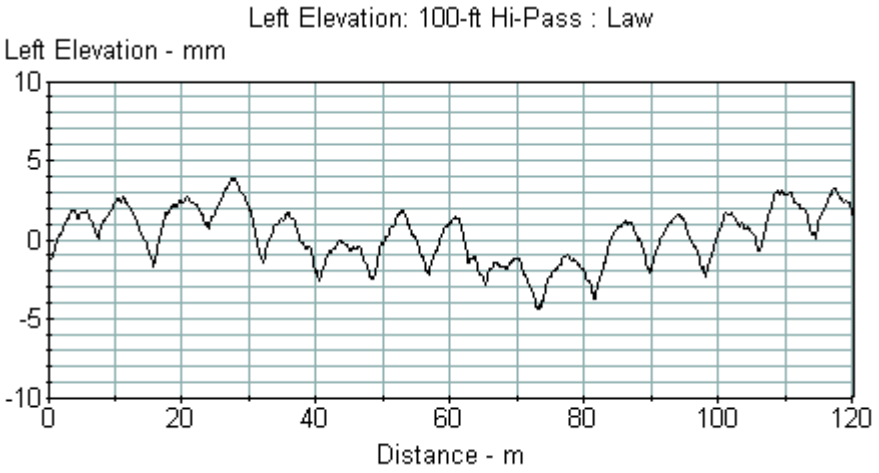

Figure 1. Slab with joints curled down.

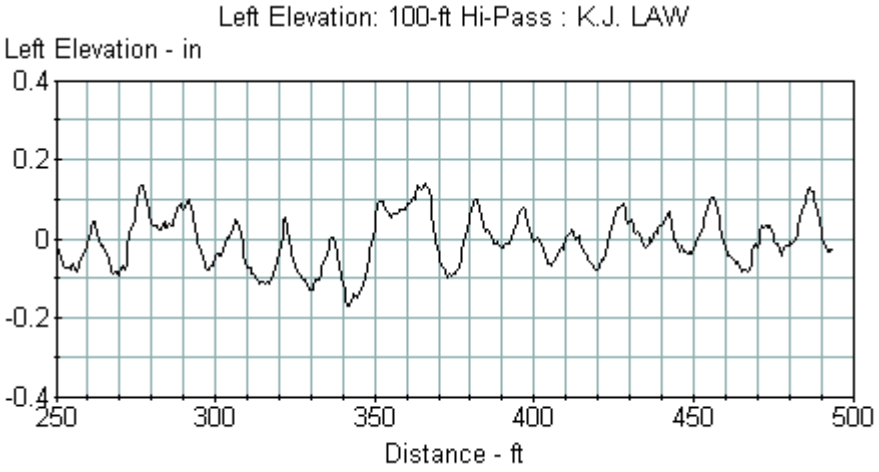

Figure 2. Slab with joints curled up.

joint spacing of 15 feet. These shapes were observed during a period when the temperature differential between the top and bottom of the slab was low, and therefore the shapes were not a result of the temperature gradient. These curvatures are a result of the locked-in curvature in the slab that occurs because of construction conditions or are related to moisture variations in the slab. Pavements that are severely curved downwards as shown in figure 1 can suffer from excessive mid panel deflections and premature cracking that begin at the bottom of the slab. Pavements that are severely curved upward as shown in figure 2 suffer excessive joint

deflections, resulting in premature faulting and spalling, and may experience mid-panel transverse cracking that starts from the top of the slab.

Byrum (10) used LTPP profile data to develop a curvature index for JPC slabs. This index presents a measure of the curvature that is present in PCC pavements. A complex interaction of temperature, moisture, and material creep that occurs early in the pavement life can apparently result in the development of large locked-in slab curvature. Byrum showed that the curvature index of PCC slabs was related to performance of PCC pavements. He showed that JPC pavements without dowels have more curvature than PCC pavements without dowels. The distribution of the curvatures that were observed for doweled and non-doweled pavements is shown in figure 3.

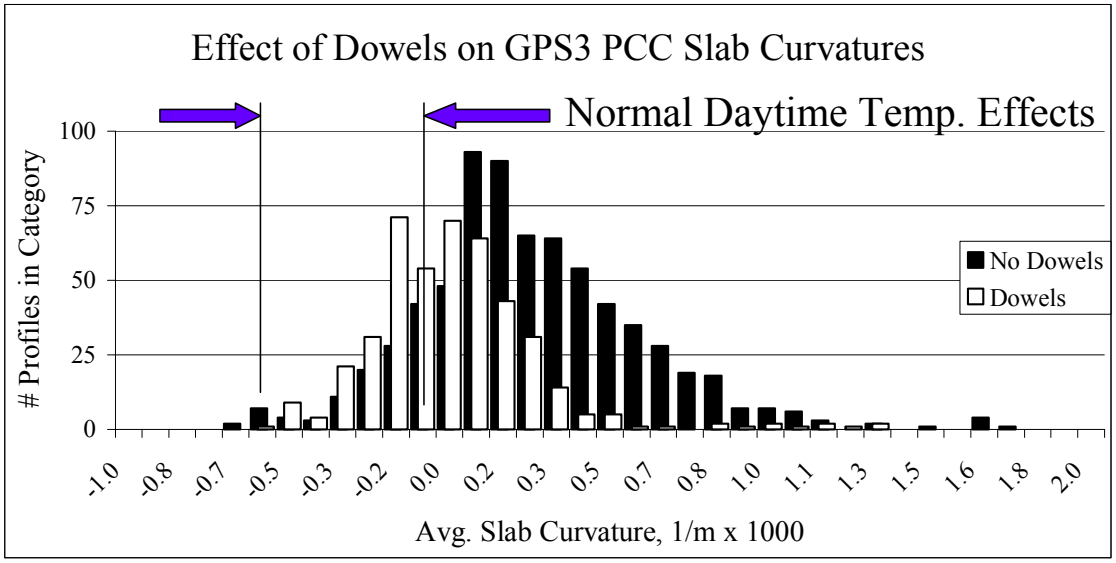

No Dowels	LCI	RCI
Minimum	-0.68	-0.68
Maximum	1.62	1.70
Average	0.21	0.22
Std Dev	0.34	0.35
Count	351	351

Dowels	LCI	RCI
Minimum	-0.54	-0.61
Maximum	1.30	1.28
Average	-0.03	-0.02
Std Dev	0.27	0.26
Count	218	218

Figure 3 Average slab curvatures for GPS-3 pavements along the wheel paths (10).

ROUGHNESS CHARACTERISTICS OF OVERLAID PAVEMENTS

Perera et al. (4) investigated roughness characteristics of SPS-5 projects that deal with the performance of selected asphalt concrete rehabilitation treatment factors. The study found that irrespective of the roughness before overlay of a section, the roughness after overlay of the sections for a specific project would fall within a relatively narrow band. They also analyzed IRI data from the GPS-6B and GPS-7B pavements for which IRI before and after the overlay was available. The analysis indicated that a relatively thin overlay could reduce the IRI of a pavement dramatically. For example, a 100 mm thick AC overlay reduced the IRI of a flexible pavement from 3.15 to 0.63 m/km. Similarly, a 84 mm thick AC overlay reduced the IRI of a PCC pavement from 2.68 to 0.87 m/km. Sufficient time-sequence IRI data were not available for the GPS-6B and GPS-7B experiments to see the how the rate of IRI development is affected by the IRI before the overlay.

SPS EXPERIMENTS

An initial evaluation of the SPS-1, SPS-2, SPS-5 and SPS-6 projects has been performed under the FHWA data analysis contract (14, 15, 16, 17). These studies looked at available data for the projects, summarized construction deviations and construction problems in each project, and performed an initial evaluation of the data trends. Daleiden et al. (11) performed an analysis of performance trends at SPS –5, -6 and –7 sites. They presented time-sequence plots for cracking, rutting, deflection and roughness data. However, no clear conclusions on pavement performance could be obtained from this study, as limited monitoring data were available at the time this study was conducted.

TRANSVERSE VARIATIONS, SEASONAL VARIATIONS AND DAILY VARIATIONS OF IRI

Several experiments were conducted using an inertial profiler for NCHRP project 10-47 (12) to investigate the effect of lateral variations of the profiled path on IRI. A shift in the wheel

path of 0.3 m typically caused variations of IRI ranging from 5 to 10 percent. In this project, IRI values from LTPP seasonal sites were analyzed to study variations in IRI due to seasonal effects. (12). Also, data from PCC seasonal sites were used to study daily variations in IRI. The report prepared for the project (12) describes the seasonal variations in roughness that was observed at the LTPP seasonal monitoring sites. When daily variations in IRI at the seasonal monitoring sites were analyzed, it was noted for slabs that were curled downwards, the roughness of the pavement increased in the afternoon when compared to the morning. The roughness of slabs that are curled upwards decreased in roughness from morning to afternoon. The magnitude of this change in roughness observed during the day due to temperature effects was generally less than 0.1 m/km for most sections.

MODELS TO PREDICT ROUGHNESS DEVELOPMENT

Perera et al. (4) developed models to predict the development of roughness for GPS experiments 1 through 4 using an optimization technique. These models predict the initial IRI of the pavement with the use of subgrade properties and structural properties of the pavement, and then predict a growth rate as a function of time, traffic, subgrade properties, and pavement structure. Models to predict roughness that were developed using LTPP data for PCC pavements are presented by Titus-Golver (7,8). Paterson (13) used data from Brazil to develop models to predict roughness based on traffic, structural parameters of pavement and distress data. The incremental change in roughness was modeled through three groups of components, dealing with structural, surface distress, and environmental-age-condition factors. Von Quintus et al. (18) studied relationships between changes in pavement surface distress in flexible pavements to incremental changes in IRI using LTPP data. Models to predict IRI based on pavement distress was developed in this study.

CHAPTER 3

SELECTION OF DATA ELEMENTS AND DATA SYNTHESIS

IMS DATABASE

The data collected for the LTPP program are stored in the LTPP Information Management System (IMS) database. This data can be divided into the following categories: inventory, maintenance, climatic, monitoring, traffic, materials testing, and rehabilitation. A brief description of the data elements contained in each category follows.

Inventory Data: Inventory tables contain information related to the location of the section, historical information about the section, and material characteristics of the pavement obtained from State transportation agency archives.

Maintenance Data: Data tables in this category record maintenance activities that have been performed on the test sections.

Climatic Data: The climatic data at the GPS sections are derived from weather data collected by the National Oceanic and Atmospheric Administration and the Canadian Climatic Center (for Canadian test sections). Data collected from five weather stations that are close to each GPS section are used in deriving the climatic data. Weather stations have been installed at SPS sites and site specific weather data are collected.

Monitoring Data: Data tables in this category contain data that are obtained by monitoring activities that are performed at the test sections. These include profile data, deflection data, friction data, surface distress data, and transverse profile data.

Traffic Data: Traffic data tables contain historical traffic estimates provided by State highway agencies as well as monitored traffic data collected by weigh in motion equipment.

Materials Testing: Laboratory test data for pavement and subgrade materials are contained in these tables. Samples were obtained from pavement layers and subgrade at each tests section from just outside the section limits. Extensive laboratory tests were performed on these samples to characterize pavement layer and subgrade properties.

Rehabilitation Data: Major improvements that are made at test sections are documented in the data tables that are in this category.

The data for the test sections are uploaded into the IMS database after undergoing quality control checks. The data that have satisfied the quality control checks are referred to as "Level E" data

IDENTIFICATION OF DATA ELEMENTS

The objectives of this research was to determine the effect of factors such as design and rehabilitation parameters, climatic conditions, traffic levels, material properties, and extent and severity of distress that cause changes in pavement smoothness. The first step in the study was to identify variables that are available in the LTPP database that could be related to the development of roughness.

The information obtained from the literature review was used to identify data elements that have been identified in past research projects as having an effect on roughness development. The data tables in IMS that contain the data elements were then identified. All data tables in the IMS were reviewed, and data elements that could have an impact on roughness development that were not identified previously were selected based on engineering judgment. Table 3 presents the data elements that were identified to be included in the analysis database that was built for this research study.

Table 3. Identified data elements.

Description	Data Element	Applicable Experiment	
		GPS	SPS
Section Data			
LTPP experiment number	EXPERIMENT_SECTION	1-7	1,2,5,6
Construction date	INV_AGE	1-7	1,2,5,6
Drainage type	INV_GENERAL	1-7	5, 6
Drainage location	INV_GENERAL	1-7	5, 6
Roughness			
IRI Value	MON_PROFILE_MASTER	1-7	1,2,5,6
Profile Data	MON_PROFILE_DATA		Selected Sections
Pavement Layer Data			
AC Thickness	TST_L05B	1,2,6,7	1,5,6
PCC thickness	TST_L05B	3,4,5,7	2,6
Base thickness	TST_L05B	1-7	1,2,5,6
Subbase thickness	TST_L05B	1-7	1,2,5,6
Material code for base/subbase	TST_L05B	1-7	1,2,5,6
Base gradation	TST_SS01_UG01_UG02	1-7	1,2,5,6
Base moisture content	TST_SS01_UG01_UG02	1-7	1,2,5,6
Base/subbase liquid limit	TST_UG04_SS03	1-7	1,2,5,6
Base/subbase plastic limit	TST_UG04_SS03	1-7	1,2,5,6
Base/subbase plasticity index	TST_UG04_SS03	1-7	1,2,5,6
Traffic Data			
Historical ESALs	TRF_EST_ANL_TOT_GPS_LN	1-7	1,2,5,6
Monitored ESALs	TRAFFIC_MONITOR_BASIC_INFO	1-7	1,2,5,6
Subgrade Data			
Subgrade plastic limit	TST_UG04_SS03	1-7	1,2,5,6
Subgrade liquid limit	TST_UG04_SS03	1-7	1,2,5,6
Subgrade plasticity index	TST_UG04_SS03	1-7	1,2,5,6
Subgrade gradation properties	TST_SS01_UG01_UG02	1-7	1,2,5,6
Subgrade moisture content	TST_SS01_UG01_UG02	1-7	1,2,5,6
Subgrade material code	TST_L05B	1-7	1,2,5,6
Subgrade resilient modulus	TST_SS07	1-7	1,2,5,6
% Greater than 2mm	TST_SS02_UG03	1-7	1,2,5,6
% Coarse sand	TST_SS02_UG03	1-7	1,2,5,6
% Fine sand	TST_SS02_UG03	1-7	1,2,5,6
% Silt	TST_SS02_UG03	1-7	1,2,5,6
% Clay	TST_SS02_UG03	1-7	1,2,5,6

Table 3. Identified data elements (Continued).

Description	Data Element	Applicable Experiment	
		GPS	SPS
Shoulder Information			
Shoulder surface type	INV_SHOULDER	1-7	5, 6
Shoulder width	INV_SHOULDER	1-7	5, 6
Shoulder paved width	INV_SHOULDER	1-7	5, 6
Shoulder base type	INV_SHOULDER	1-7	5, 6
Shoulder surface thickness	INV_SHOULDER	1-7	5, 6
Shoulder base thickness	INV_SHOULDER	1-7	5, 6
Rehabilitation Data			
Overlay thickness	RHB_IMP, INV_MAJOR_IMP	6,7	5, 6
Overlay date	RHB_IMP	6,7	5, 6
Climatic Data			
Annual precipitation	CLM_VWS_PRECIP_ANNUAL	1-7	1,2,5,6
Intense precipitation days	CLM_VWS_PRECIP_ANNUAL	1-7	1,2,5,6
Number of wet days/yr	CLM_VWS_PRECIP_ANNUAL	1-7	1,2,5,6
Average maximum temperature	CLM_VWS_TEMP_ANNUAL	1-7	1,2,5,6
Average minimum temperature	CLM_VWS_TEMP_ANNUAL	1-7	1,2,5,6
Number of days below 0° C/yr	CLM_VWS_TEMP_ANNUAL	1-7	1,2,5,6
Number of days above 32 °C/yr	CLM_VWS_TEMP_ANNUAL	1-7	1,2,5,6
Number of freeze thaw cycles/yr	CLM_VWS_TEMP_ANNUAL	1-7	1,2,5,6
Annual Freeze index	CLM_VWS_TEMP_ANNUAL	1-7	1,2,5,6
PCC Test Data			
PCC compressive strength	TST_PC01	3, 4, 5, 7	2, 6,
PCC Poisson's ratio	TST_PC04	3, 4, 5, 7	2, 6,
PCC unit weight	TST_PC05	3, 4, 5, 7	2, 6,
PCC elastic modulus	TST_PC04	3, 4, 5, 7	2, 6,
PCC split tensile strength	TST_PC02	3, 4, 5, 7	2, 6,
PCC density	TST_PC05	N/A	2, 6,
PCC percent voids	TST_PC05	N/A	2, 6,
PCC air content (hardened PCC)	TST_PC08	N/A	2
PCC flexural strength	TST_PC09	N/A	2
PCC Steel Information			
Reinforcing type	INV_PCC_STEEL	4,5	6
Transverse bar diameter	INV_PCC_STEEL	4,5	6
Transverse bar spacing	INV_PCC_STEEL	4,5	6
Longitudinal bar diameter	INV_PCC_STEEL	4,5	6
Longitudinal bar spacing	INV_PCC_STEEL	4,5	6
Longitudinal steel percentage	INV_PCC_STEEL	4,5	6

Table 3. Identified data elements (Continued).

Description	Data Element	Applicable Experiment	
		GPS	SPS
PCC Mix Data			
Entrained air	INV_PCC_MIXTURE	3,4,5,7	6
Coarse aggregate in mix - weight	INV_PCC_MIXTURE	3,4,5,7	2, 6
Fine aggregate in mix - weight	INV_PCC_MIXTURE	3,4,5,7	2, 6
Cement in mix - weight	INV_PCC_MIXTURE	3,4,5,7	2, 6
Water in mix - weight	INV_PCC_MIXTURE	3,4,5,7	2, 6
Curing method	INV_PCC_MIXTURE	3,4,5,7	6
Paver type	INV_PCC_MIXTURE	3,4,5,7	6
Cement type	INV_PCC_MIXTURE	3,4,5,7	2, 6
Slump	INV_PCC_MIXTURE	3,4,5,7	6
PCC mix temperature	TST_FRESH_PCC	N/A	2
Slump	TST_FRESH_PCC	N/A	2
Air content	TST_FRESH_PCC	N/A	2
PCC Joint Information			
Joint spacing	INV_PCC_JOINT	3, 4	6, 7
Load transfer	INV_PCC_JOINT	3	6, 7
Joint skewness	INV_PCC_JOINT	3	6, 7
Dowel diameter	INV_PCC_JOINT	3, 4	6, 7
Dowel coating	INV_PCC_JOINT	3, 4	6, 7
AC Properties			
Extraction results	TST_AC_04	1,2,6,7	1,5,6,8
Resilient modulus	TST_AC07	1,2,6,7	1,5,6,8
Bulk specific gravity	TST_AC02	1,2,6,7	1,5,6,8
Maximum specific gravity	TST_AC03	1,2,6,7	1,5,6,8
Distress Data			
AC manual distress data	MON_DIS_AC_REV	1,2,6	1,5,8
AC automated distress data	MON_DIS_PADIAS_AC	1,2,6	1,5,8
Jointed PCC manual distress data	MON_DIS_JPCC_REV	3,4	2
Jointed PCC automated distress	MON_DIS_PADIAS_JPCC	3,4	2
CRCP manual distress	MON_DIS_CRCP_REV	5	N/A
CRCP automated distress	MON_DIS_PADIAS_CRCP	5	N/A
Faulting data	MON_DIS_JPCC_FAULT_SECT	3,4	2
Rutting data	MON_RUT_DEPTH_POINT	1,2,6,7	1,5,6

Note: N/A – Not Available

BUILDING THE ANALYSIS DATABASE

The analysis database used for this project was built using Access 97. The data tables containing the data elements that were identified were obtained from the IMS. The data obtained corresponded to IMS Release 10.2. Computer programs were written using visual basic programming language to extract the identified data elements from IMS data tables, and to build the analysis database. Several values were available for a test section for some data elements. For example, for a specific section, thickness values were available from several coring locations. A similar situation existed for materials test data, where results were available for multiple samples obtained at different locations for a test section. For cases where multiple data values were available for a data element, the values were averaged to obtain a unique value for the section.

For this research project, the mean IRI of the test section, which is the average IRI of the left and right wheel paths, was used to characterize the roughness. For a specific test date at a test section, the LTPP database generally has five IRI values that have been obtained from five profile runs. The mean IRI values of these multiple profile runs were averaged to obtain the roughness for that specific test date.

TRAFFIC DATA

The IMS database has historical as well as monitored traffic data. Monitored traffic data is available only after the section was accepted into the LTPP program. Weigh-in-Motion (WIM) scales and Automatic Vehicle Classification systems have been installed at some LTPP test sections. At some test sections, portable equipment is used to collect WIM and classification data. As both historical and monitored traffic data are available at a site, a procedure was developed to obtain the cumulative traffic that has been applied at the site. This procedure consisted of developing a traffic growth curve for the site using both the historical and monitored traffic data. A best fit exponential curve of the following form was fitted to the time sequence historical and monitored traffic data at each site.

$$KESAL(t) = (KESAL_0)\, e^{rt}$$

where,

$KESAL(t)$	=	Kilo Equivalent Axle Loads (KESAL) at time t years
$KESAL_0$	=	Kilo Equivalent Single Axles (KESAL) per year at traffic open date
r	=	Average annual traffic growth rate, percent
t	=	Time, years

In some cases there was good agreement in the trend between the historical and monitored traffic data, while in other cases there were significant differences between the two trends. Figure 4 shows two cases, where for one case the trend between the historical and monitored traffic is poor, while for the other case the two trends show good agreement. Figure 4 shows the individual trends for the historical and monitored data as well as the combined trend for the data that was obtained by fitting an exponential curve to the data.

Once the initial KESAL and the traffic growth rate for a site is known, the cumulative traffic at any point in time can be determined. It should be noted that acceptable curve fits could not be made at several sites because of large variability in the traffic data between the years. For such sites, an appropriate growth curve was assigned based on the traffic data trend at that site.

DATA AVAILABILITY

Backcalculated moduli are not currently available in the IMS. However, a data analysis contractor had performed backcalculation using the deflection data collected at GPS sections. This data had not passed Level E quality checks. This data was obtained through the NCHRP. A review of the data indicated backcalculated moduli were not available for a significant number of sections, and also there appeared to be many outliers in the data. Because of these limitations, backcalculated moduli were not used in the analysis. Resilient moduli values for base and subgrade were also not available for most GPS sections, and therefore were not used in the analysis. Table 4 presents the availability of some key data elements for GPS sections.

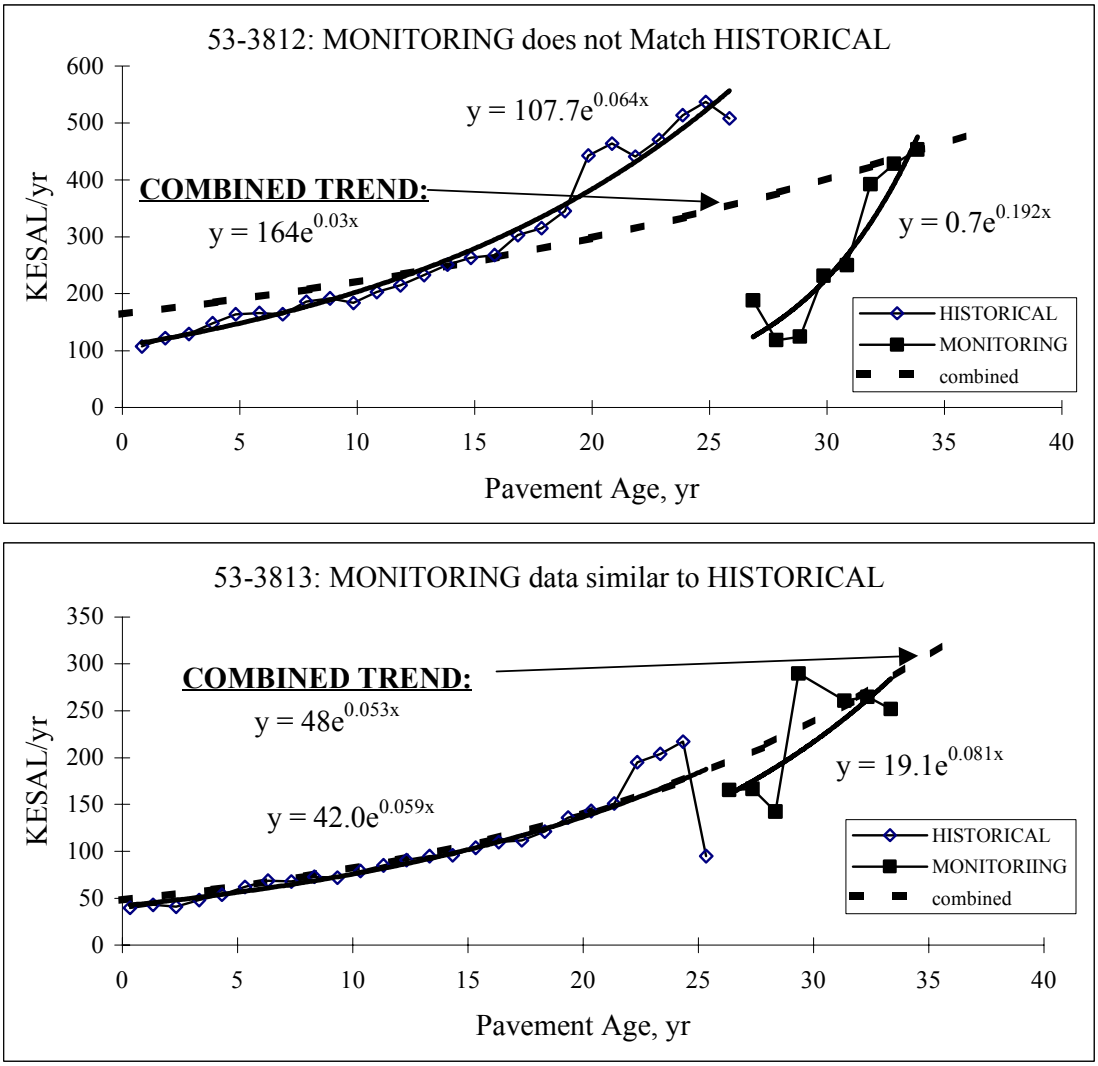

Figure 4. Comparison of historical, monitoring and combined traffic trends.

Generally, sufficient data were available for GPS sections to investigate the effect of design, climatic and materials test parameters on roughness development. Materials test data as well as traffic data were not available for most SPS sections. Therefore, the effect of materials properties and traffic effects on roughness development could not be studied for SPS sections.

Table 4. Data availability at GPS sections

Parameter	Percentage Sections Where Data is Available									
	GPS Experiment									
	GPS 1	GPS 2	GPS 3	GPS 4	GPS 5	GPS 6A	GPS 6B	GPS 7A	GPS 7B	GPS 9
Traffic	98	98	100	100	100	98	100	100	100	88
Construction Date	100	100	100	100	100	100	100	100	100	100
Climatic Data	99	99	100	100	100	100	100	100	100	100
Drainage Information	100	99	100	100	100	100	100	100	100	100
Shoulder Information	100	99	100	100	100	100	100	100	100	96
Surface Thickness	91	98	98	100	99	98	100	100	100	69
Overlay Thickness						75	80	94	81	69
Base Thickness	83	97	92	89	98	74	95	79	90	54
Base Gradation	83		79	94	100	100	98	100	88	100
Base Moisture Content	80		79	91	93	97	98	100	82	100
Base- Plasticity Index	81		81	97	100	100	98	100	88	100
Subgrade Gradation	92	95	91	97	98	100	96	97	100	92
Subgrade Plasticity Index	93	95	91	98	98	100	96	97	100	92
Subgrade Moisture Content	90	95	89	97	98	100	96	97	100	92
Subgrade Hydrometer Analysis	86	90	86	95	93	98	93	94	100	88
Extracted AC Content	89	96				95	97	35	20	
AC - Max. Specific Gravity	89	96				95	97	35	20	
AC - Bulk Specific Gravity	90	96				95	97	35	20	
PCC - Tensile Strength			92	86	95			91	94	88
PCC - Elastic Modulus			92	92	99			100	97	96
PCC - Compressive Strength			85	92	96			97	90	96
PCC - Unit Weight			92	92	99			100	97	96
PCC - Poissons Ratio			91	92	99			100	97	96
PCC - Air Content			84	66	87			44	65	77
PCC - Mix Design			89	80	89			56	65	73
PCC - Curing Method			84	85	90			44	77	69
PCC - Slump			73	51	77			26	42	65
PCC - Steel				58	98			32	45	42
PCC - Joint Spacing			100	100				82	61	85
PCC - Load Transfer			97	97				65	58	73

This page left intentionally blank.

CHAPTER 4

DATA ANALYSIS METHODS

RELATIONSHIP BETWEEN IRI AND DATA ELEMENTS

Once the databases containing the data elements selected for analysis were assembled, statistical procedures such as univariate analysis and bivarate analysis were performed on the data. The univariate analysis consisted of an investigation of the distribution of each data element. The analysis was carried out separately for each GPS and SPS experiment. Data distributions were analyzed using histograms and box-plots. A box-plot is a simple graphical representation showing the center and the spread of the distribution, along with outliers. Figure 5 presents an example of a box plot that shows the distribution of the first IRI value that was obtained at SPS-2 sections that have a lean concrete base. The horizontal line at the interior of the box is located at the median of the data. The height of the box is equal to the interquartile distance (IQD), which is the difference between the third quartile of the data and the first quartile. The whiskers (the lines extending from the top and the bottom of the box) extend to the extreme values of the data or a distance of 1.5 X IQD from the center, whichever is less. For data having a normal distribution, approximately 99.3% of the data falls inside the whiskers. Data points that fall outside the whiskers may be outliers, and are indicated by horizontal lines. For the box-plot shown in figure 5, the median IRI value is 1.34 m/km. The first and the third quartile values that are indicated by the lower and the upper limits of the box are 1.19 m/km and 1.50 m/km, respectively. The horizontal lines above the top whisker show the outliers in the data set.

The bivariate analysis consisted of computing the Pearson's correlation coefficient between the data elements selected for analysis and the median IRI value over the monitored period at a section, and/or the change in IRI value over the monitored period at a section. This analysis was carried out for GPS sections as these sections had sufficient data to carry out this analysis. The correlation coefficient has a value between 1 and -1, with values approaching 1 indicating a strong positive correlation, values near zero indicating no correlation, and values approaching -1 indicating an inverse relationship between parameters. As it is possible to have a strong correlation

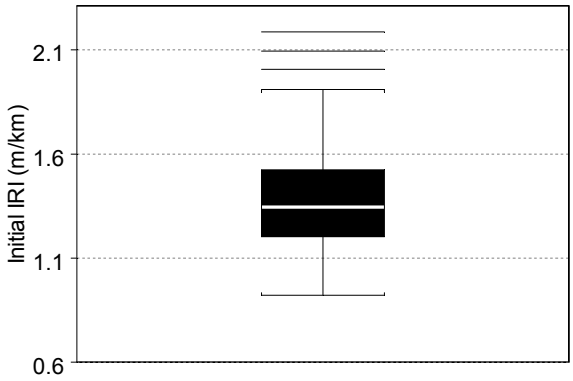

Figure 5. Example of a box-plot.

between two variables simply because of biases in the data distribution and influential observations, scatter plots were used to obtain an insight into the relationship between the two parameters to identify the true trends in the data. Two way scatter plots between each data element and median IRI of the section over the monitored period, and the rate of change of IRI over the monitored period were examined to identify data trends. The scatter plot between the data element and the median IRI provides an insight into the relationship between the data element and the level of IRI, while the scatter plot between the rate of change of IRI and the data elements provides an insight into the effect of the data element on the change in roughness. Scatter plots between the different data elements were also examined to investigate correlations between data elements. This study provided information on which data elements to use in model building, as using data elements that are correlated with each other in model building will not yield accurate models. For each GPS experiment, scatter plots were used initially to examine trends for the whole data set. Thereafter, for each GPS experiment, data trends were examined separately for the different environmental zones. The data elements that were used in the analysis of the GPS sections are shown in table 5.

Four environmental zones were considered in this analysis, and they correspond to the four environmental zones that are used in the LTPP program, which are wet-freeze, wet no-freeze, dry-freeze and dry no-freeze. The boundary between wet and dry regions was taken as 508 mm of annual precipitation, and the boundary between the freezing and non-freezing zones

Table 5. Data elements analyzed.

Parameter	Applicable GPS Experiment
Pavement Age	1-7
Surface Thickness	1-7
Base Thickness	1-7
Total Pavement Thickness	1-7
Structural Number	1,2,6
Overburden Pressure	1-7
AC Bulk Specific Gravity	1,2,6
AC Air Voids	1,2,6
Asphalt Content	1,2,6
Annual Precipitation	1-7
Intense Precipitation Days per year	1-7
Annual Wet Days	1-7
Mean Temperature	1-7
Days with Temperature > 32 °C, per year	1-7
Days with Temperature < 0 °C, per year	1-7
Annual Freezing Index	1-7
Freeze Thaw Cycles per Year	1-7
Plasticity Index Subgrade	1-7
Plastic Limit Subgrade	1-7
Moisture Content Subgrade	1-7
Silt Content in Subgrade	1-7
Clay Content in Subgrade	1-7
Percent Passing No. 200 Sieve, Subgrade	1-7
Moisture Content Base	1-7
Percent Passing No. 200 Sieve, Base	1-7
Joint Spacing PCC	3,4
PCC Elastic Modulus	3,4,5
PCC Compressive Strength	3,4,5
PCC Tensile Strength	3,4,5
PCC Poisson's Ratio	3,4,5
PCC Unit Weight	3,4,5
PCC - Coarse Aggregate, Weight	3,4,5
PCC – Fine Aggregate, Weight	3,4,5
PCC - Cement, Weight	3,4,5
PCC – Water Cement Ratio	3,4,5
PCC – Air	3,4,5
PCC – Slump	3,4,5
Traffic	1-7

was taken as an annual freezing index of 89 °C days. Figure 6 shows the general distribution of the four environmental zones in the United States.

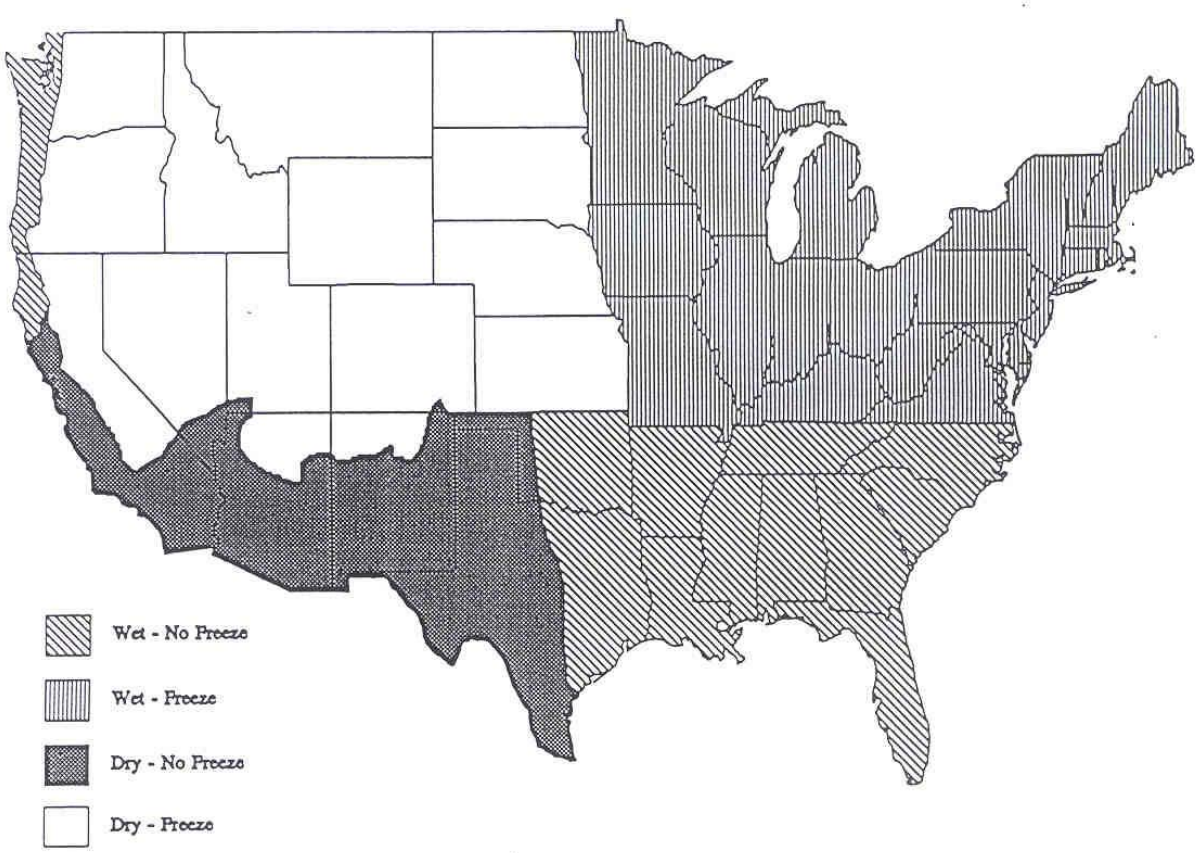

Figure 6. Environmental zones.

MODELING APPROACH

One popular approach that might be considered for modeling roughness development is regression analysis, where each roughness observation is considered to be an independent observation. The IRI or some function of IRI could be taken as the response and the time of measurement and other variables could be used as predictors. However, this approach would not be appropriate for this time-sequence IRI data for two main reasons. First, one of the

fundamental assumptions of regression analysis is that the observations are independent. This assumption is clearly violated in this data since observations are grouped by pavement section. The time-sequence IRI values that are obtained for a specific pavement section would be dependent on the past roughness at the section. If this dependence is ignored and regression analysis is used, the typical drawback is that the significance of predictors is overstated. The other main drawback to regression analysis is that it fails to take advantage of the information provided by following a given section over time.

Consider the relationship between IRI and pavement age that is shown in figure 7. If each observation was considered to be an independent variable, the data points will be treated as shown in figure 7(a). Longitudinal data analysis methods take into account the time sequence nature of the IRI values at a section to predict future IRI. Figure 7(b) illustrates the approach that is used in longitudinal data analysis, where the time sequence aspect of IRI values is considered in the analysis. The results that are obtained by such an analysis will be different from an analysis that considers each point as an independent observations as shown in figure 7(a). Longitudinal data analysis is performed by using a mixed effects model analysis.

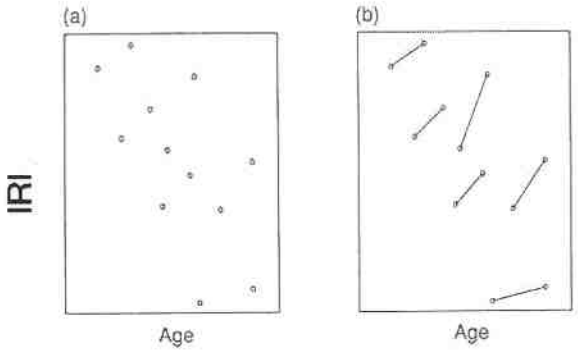

Figure 7. Modeling of time-sequence data.

Mixed effects models are commonly used in the biomedical and social sciences where one might be interested in the progress of a patient or subject over time as a function of treatment and/or environmental factors. This modeling approach is well established and has been found effective in these applications. The data under consideration here are similar to those found in epidemiological applications where subjects are measured at varying time points, where there are

a large number of potential predictors and a complex pattern of missing observations. A mixed effects model analysis is similar to a regression analysis in that many of the steps are familiar. Diagnostic plots need to be checked, variables selected and possibly transformed. However, one well-known feature of a regression model that is not found in a mixed model is the R^2. In a regression model, there is only one kind of random variation - the R^2 tells us the relative size of this residual random variation compared to the variation explained by the model. In a mixed model, there are multiple sources of residual variation. At a minimum, there will be the variation in individual IRI measurements and the variation in whole pavement sections. There is no simple equivalent to R^2. Nevertheless, the random effect standard errors do tell how well the model can predict future observations. These models may indicate that a great deal of variation is not explained by the available predictors. This does not mean that the models do not fit well. On the contrary, the mixed effects model does a good job of describing the inherent variation in the data.

The general form of the model that is used in a mixed model analysis is:

$$y_i(t_{ij}) = \beta_0 + \beta_t t_{ij} + \sum_{k=1}^{p} \beta_k \chi_{ik} + \gamma_i + \varepsilon_{ij}$$

$y_i(tij)$ = Response of pavement section i at time t_{ij}

β_t = Coefficient that controls the growth of roughness over time

$\sum_{k=1}^{p} \beta_k \chi_{ik}$ = The term which indicates how the predictors affect roughness. There are p predictors where x_{ik} denotes the value of predictor k for section i, while coefficients $\beta_1, \ldots \beta_p$ controls the size of these effects

γ_i = Random effects term drawn from a normal distribution with mean zero and variance to be estimated. This term represents variations among pavement sections not explained by predictors

ε_{ij} = Error term. In the simplest form of the model, these errors are independent and normally distributed with a variance to be estimated.

The statistical software package S-Plus (19) contains a procedure for performing mixed model analysis. The mixed model analysis was carried out to build models to predict development of roughness for GPS sections. Selection of data elements to use as predictor variables were made based on the observations from the two-way scatter plots. Models to predict development of roughness for SPS projects could not be carried out as sufficient traffic and materials test data were not available for these projects. However, the mixed model method was used in the analysis of SPS projects to test the significance of available data elements to development of roughness.

This page left intentionally blank.

CHAPTER 5

ROUGHNESS CHARACTERISTICS OF SPS-1 AND SPS-2 PROJECTS

SPS-1 EXPERIMENT: STRATEGIC STUDY OF STRUCTURAL FACTORS FOR FLEXIBLE PAVEMENTS

Introduction

The SPS-1 experiment was developed to investigate the effect of selected structural factors on the long-term performance of flexible pavements that were constructed on different subgrade types and in different environmental regions. New pavements were constructed for the SPS-1 experiment. In the SPS-1 experiment, twelve test sections were constructed at a project location. The twelve test sections in a project were either section numbers 1 through 12, or section numbers 13 through 24. The pavement structure of the test sections in the SPS-1 experiment is shown in table 6. The subgrade types considered in this experiment are classified as fine grained and coarse grained, and the environmental regions considered are the four LTPP environmental regions: wet freeze, wet-no freeze, dry freeze and dry-no freeze. The structural factors considered in this experiment are asphalt thickness, base type, base thickness and drainability (presence or lack of it as provided by an open graded permeable asphalt treated layer and edge drains). Five different base types are used in this experiment: dense graded aggregate base (DGAB), asphalt treated base (ATB), asphalt treated base (ATB) over dense graded aggregate base (DGAB), permeable asphalt treated base (PATB) over dense graded aggregate base (DGAB), and asphalt treated base (ATB) over permeable asphalt treated base (PATB). The test sections are profiled immediately after construction, and thereafter at approximately annual intervals.

Analyzed Projects

A review of the LTPP database indicated profile data were available for sixteen SPS-1 projects. Table 7 presents the SPS-1 projects for which IRI data were available. Table 7 also

Table 6. Structural properties of SPS-1 sections.

Test Section Number	AC Thickness (mm)	Layer 2		Layer 3	
		Material	Thickness (mm)	Material	Thickness (mm)
1	175	DGAB	200	-	-
2	100	DGAB	300	-	-
3	100	ATB	200	-	-
4	175	ATB	300	-	-
5	100	ATB	100	DGAB	100
6	175	ATB	200	DGAB	100
7	100	PATB	100	DGAB	100
8	175	PATB	100	DGAB	200
9	175	PATB	100	DGAB	300
10	175	ATB	100	PATB	100
11	100	ATB	200	PATB	100
12	100	ATB	300	PATB	100
13	100	DGAB	200	-	-
14	175	DGAB	300	-	-
15	175	ATB	200	-	-
16	100	ATB	300	-	-
17	175	ATB	100	DGAB	100
18	100	ATB	200	DGAB	100
19	175	PATB	100	DGAB	100
20	100	PATB	100	DGAB	200
21	100	PATB	100	DGAB	300
22	100	ATB	100	PATB	100
23	175	ATB	200	PATB	100
24	175	ATB	300	PATB	100
Note: DGAB - Dense Graded Aggregate Base, ATB - Asphalt Treated Base, PATB – Permeable Asphalt Treated Base					

presents the following information for each project: test section numbers in project, climatic zone, subgrade type, construction date, last profile date in the database, age of project at first profile date, age of project at last available profile date, time difference between first and last profile dates, the number of times the project has been profiled, and the estimated annual ESALs at the site.

Ten projects have been profiled within one year of construction, four projects between one and two years after construction, and one project (in Florida) two years or after construction, and one project (in Alabama) three years after construction. Four SPS-1 projects have been profiled only once. The others were profiled two to seven times.

Table 7. SPS-1 projects.

Location	State Code	Section Numbers in Project	Climatic Zone (Note 1)	Subgrade Type	Construction Date	Last Available Profile Date	Age of Project at First Profile Date (Years)	Age of Project at Last Profile Date (Years)	Time Difference Between First And Last Profile Dates (Years)	Number of Times Profiled	Estimated Traffic (KESAL/Yr)
Alabama	AL	1-12	WNF	Fine	1/1/93	1/27/98	3.0	5.1	2.1	3	237
Arizona	AZ	13-24	DNF	Coarse	8/1/93	12/4/98	0.5	5.3	4.8	5	223
Arkansas	AR	13-24	WNF	Coarse	9/1/94	7/1/97	0.8	2.8	2.0	2	210
Delaware	DE	1-12	WF	Coarse	5/1/96	11/5/98	0.6	2.5	1.9	7	203
Florida	FL	1-12	WNF	Coarse	2/1/95	1/27/97	2.0	2.0	0.0	1	1463
Iowa	IA	1-12	WF	Fine	11/19/92	7/19/99	0.9	6.7	5.8	6	N/A
Kansas	KS	1-12	DF	Fine	11/1/93	3/21/99	0.5	5.4	4.9	5	130
Louisiana	LA	13-24	WNF	Fine	7/1/97	11/17/97	0.4	0.4	0.0	1	524
Michigan	MI	13-24	WF	Fine	11/1/95	6/25/97	1.2	1.6	0.4	3	72
Nebraska	NE	13-24	DF	Fine	8/1/95	5/16/98	0.3	2.8	2.5	4	145
Nevada	NV	1-12	DF	Coarse	9/1/95	8/28/98	1.6	3.0	1.4	3	799
New Mexico	NM	1-12	DNF	Fine	11/1/95	3/11/97	1.4	1.4	0.0	1	393
Ohio	OH	1-12	WF	Fine	1/1/95	11/12/98	1.6	3.9	2.3	4	N/A
Oklahoma	OK	13-24	WNF	Fine	6/1/97	11/19/97	0.5	0.5	0.0	1	393
Texas	TX	13-24	WNF	Fine	4/1/97	4/2/98	0.4	1.0	0.6	2	N/A
Virginia	VA	13-24	WF	Fine	11/28/95	10/29/98	0.4	2.9	2.5	7	N/A
Note 1: DF - Dry Freeze, DNF - Dry No-Freeze, WF - Wet Freeze, WNF - Wet No-Freeze											

Analysis of Early Age IRI

An analysis was performed to study the early-age IRI characteristics of SPS-1 projects. The initial IRI values for the SPS-1 projects were obtained at varying times after construction. Therefore, the initial IRI may not necessarily correspond to the IRI that is obtained immediately after construction. Therefore, the term early-age IRI is used in this analysis to differentiate from the initial IRI of the pavement, which is the IRI immediately after construction. All SPS-1 projects on which the IRI was obtained less than two years after construction were used in this analysis. This excluded two projects, Florida and Alabama from the analysis.

Figure 8 shows the average early-age IRI of the test sections within each project, differentiated according to the asphalt concrete thickness. The value shown for a project in figure 8 is the average IRI of six test sections that have an AC thickness of 100 mm or 175 mm. The average IRI values for the 100 mm AC and 175 mm AC sections were close to each other for each project, but for most projects the average IRI of 175 mm thick AC sections was lower than the average IRI of 100 mm sections. The maximum difference between the two thicknesses occurred for the project in Ohio, where the average IRI for the 175 mm thick AC was 0.2 m/km lower than the average IRI for the 100 mm thick AC. The projects in Nebraska and Ohio had the highest early-age IRI values, while the projects in Louisiana, Nevada and New Mexico had the lowest early-age IRI values. The standard deviation of early-age IRI for the SPS-1 projects is shown in figure 9. The project in Ohio had the highest standard deviation in IRI between the test sections.

The frequency distribution of early-age IRI values of the test sections in the SPS-1 projects separated according to the two AC thicknesses is shown in figure 10, while the cumulative frequency distribution is shown in figure 11. The cumulative frequency distribution curve shows that 175 mm AC surfaces have lower IRI values than 100 mm AC surfaces. The curve shows that an IRI value of less than 0.8 m/km was achieved on 40 percent of sections that received a 100 mm AC surface and 55 percent of the sections that received a 175 mm AC

surface. An IRI value of less than 1.0 m/km was obtained by 75 percent of the sections that received a 100 mm AC surface and 85 percent of the sections that received a 175 mm AC surface

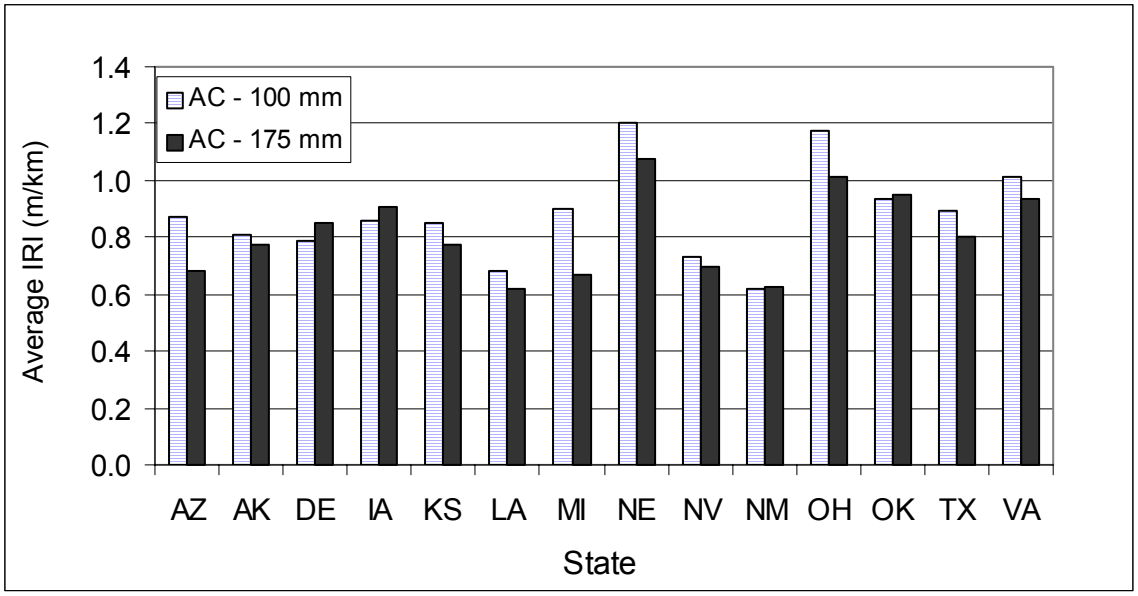

Figure 8. Average early-age IRI of SPS-1 projects.

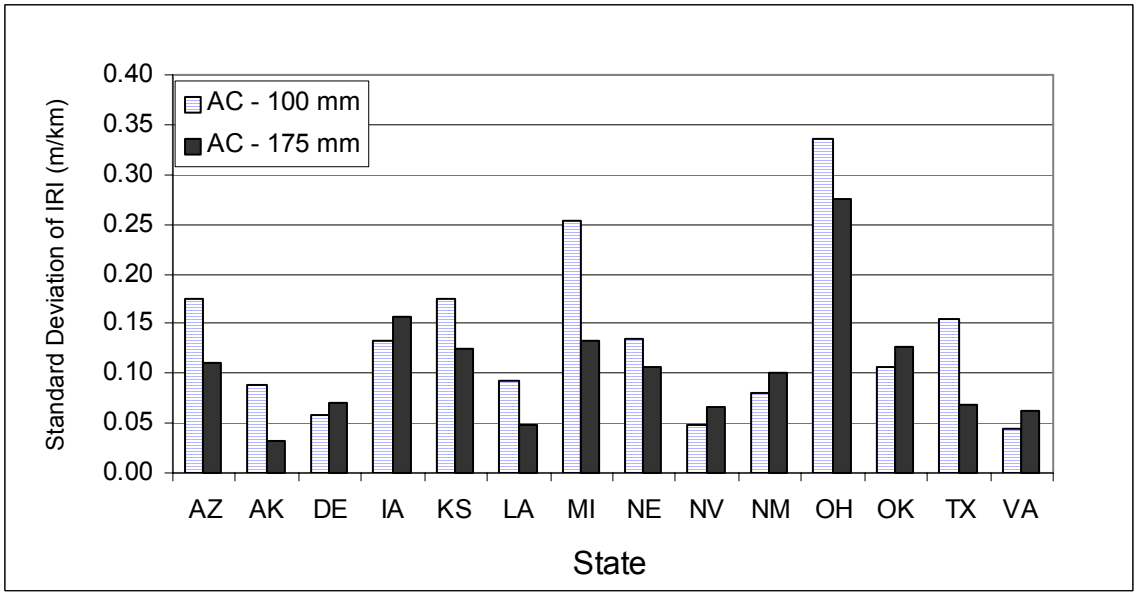

Figure 9. Standard deviation of early-age IRI for SPS-1 projects.

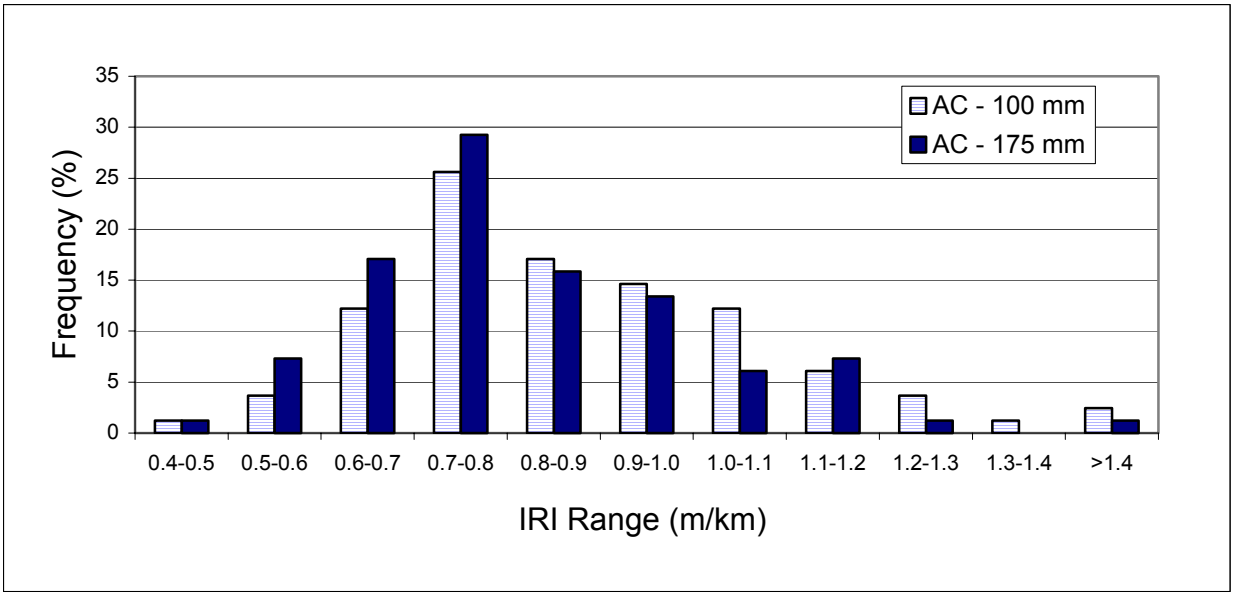

Figure 10. Frequency distribution of early-age IRI.

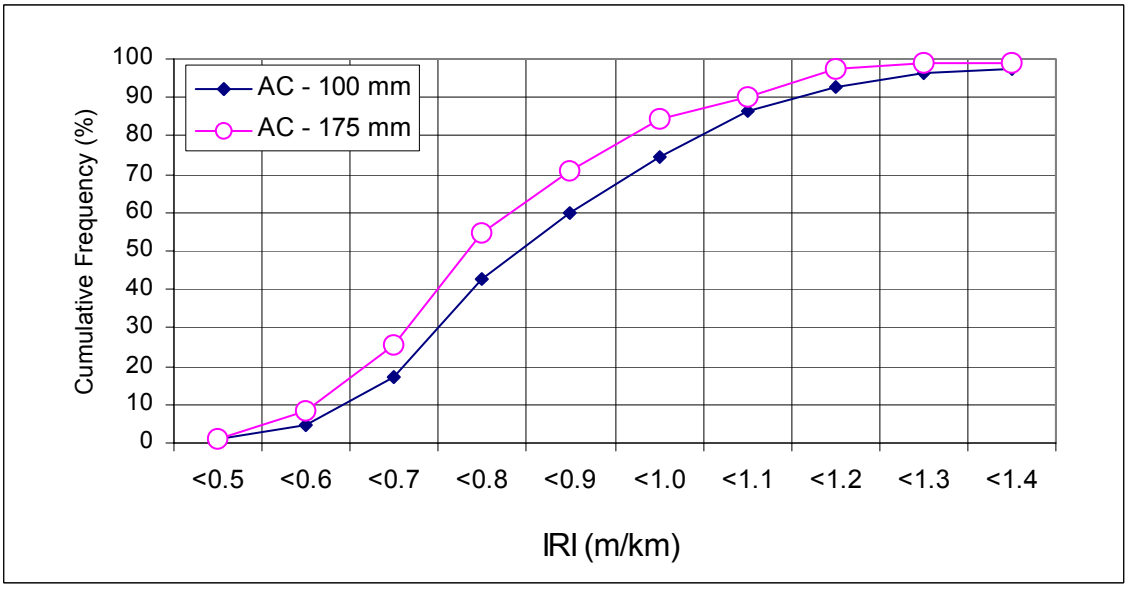

Figure 11. Cumulative frequency distribution of early-age IRI.

The average and the standard deviation of early-age IRI values that were obtained for the 100 mm and 175 mm AC surfaces are shown in table 8. A two-way ANOVA on early-age IRI that was conducted by treating AC Thickness (two levels) and three base types (three levels – DGAB, ATB, PATB) indicated that AC thickness was significant (p-value 0.03).

Table 8. Average and standard deviation of early-age IRI: SPS-1.

AC Thickness (mm)	IRI (m/km)	
	Average	Std. Dev
100	0.88	0.21
175	0.82	0.18

An analysis was performed to study if there was an influence of base type on which the AC surface is placed on the early-age IRI. The AC surfaces in SPS-1 projects were placed on three different base types: dense graded aggregate base (DGAB), asphalt treated base (ATB) and permeable asphalt treated base (PATB). For each project, the AC surface was placed on DGAB for two sections, on ATB for seven sections, and on PATB for three sections. Figure 12 shows a box-plot of the range of early-age IRI values that were obtained for each base type.

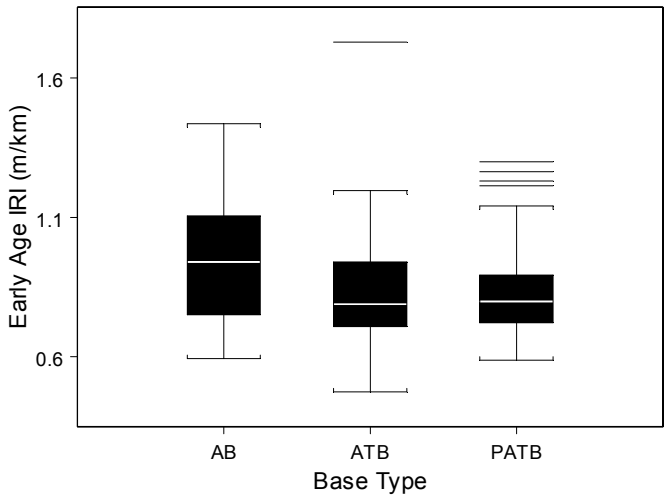

Figure 12. Distribution of early-age IRI for each base type.

The average early-age IRI values for the three base types are: DGAB – 0.94 m/km, ATB – 0.82 m/km, and PATB – 0.84 m/km. A two-way ANOVA on early-age IRI was conducted by treating AC Thickness (two levels) and base types (three levels – DGAB, ATB, PATB). The analysis indicated that base type was significant (p-value 0.02). A multiple comparison of the IRI values indicated that the IRI values obtained on DGAB and ATB were significantly different.

The analysis indicated there were no differences between IRI values obtained on AC surfaces placed on PATB when compared to ATB or DGAB. The box-plot of IRI values showed that there were several PATB sections that had high IRI values, but these are indicated to be outliers when compared to the other PATB sections.

Changes in IRI for SPS-1 Projects

Plots showing the change in IRI over time at individual SPS-1 projects are included in Appendix A. Table 9 presents the changes in IRI for the test sections in each SPS-1 project. The change in IRI was computed by subtracting the IRI at the first profile date from the IRI at the last available profile date. Table 9 also shows the age of project at last profile date, age of the project when it was first profiled, and the time difference corresponding to the change in IRI. In table 9, cases that show an IRI increase of 0.1 m/km or greater are shown in bold. Table 10 presents the percent change in IRI at the test sections, with respect to the IRI at the first profile date. Cases where the percent increase is greater or equal to 10 percent are shown in bold. The average IRI at the first profile date for all SPS-1 test sections was 0.85 m/km. Ten percent of this value is 0.09 m/km, which is a small increase in IRI if the magnitude of the change is considered. A study of transverse profile variations at a new AC pavement by Karamihas et al. (12) indicated IRI variations of 5 percent could occur due to lateral wander of 0.3 m from the wheel path. Therefore, for sections that show a percent change of less than 5 percent, the change in roughness may have been caused by variations in the profiled path.

All sections in the Delaware SPS-1 show a negative percent change in IRI, except for one section that shows no change in IRI. This project has been profiled seven times since construction, with the first profile date being 12/5/96. The IRI of all sections for the first profile date is higher than the subsequent six IRI values that were obtained. This indicates that either there was an error in the profiling equipment at the first profile date or the higher IRI was caused by variations in the pavement profile due to environmental causes (e.g., shrink or swell of subgrade). The difference in IRI between the last profile date and second profile date indicated the change in IRI for the test sections to be between –0.03 and 0.02 m/km, except for one section

Table 9. Changes in IRI for SPS-1 sections.

State	Age of Project at First Profile Date (Yrs)	Age of Project at Last Profile Date (Yrs)	Time Difference for IRI Change (Years)	Change in IRI (IRI at Last Profile Date - IRI at First Profile Date) (m/km)											
				Section Number											
				1	2	3	4	5	6	7	8	9	10	11	12
Alabama	3.0	5.1	2.1	0.02	0.08	0.01	0.05	0.02	0.07	0.01	-0.01	-0.05	0.07	0.01	0.05
Delaware	0.6	2.5	1.9	-0.10	0.00	-0.09	-0.13	-0.10	-0.08	-0.12	-0.11	-0.13	-0.15	-0.13	-0.15
Iowa	0.9	6.7	5.8	**0.46**	**1.27**	**0.37**	**0.30**	**0.34**	**0.30**	**1.13**	**0.71**	0.07	**0.54**	**0.34**	**0.31**
Kansas	0.5	5.4	4.9	**0.41**	**0.41**	**0.75**	**0.18**	**1.56**	**0.39**	**0.15**	**0.60**	**0.37**	**0.19**	**0.13**	0.00
Nevada	1.6	3.0	1.4	0.02	0.04	0.01	0.00	-0.01	0.01	0.01	-0.01	0.01	0.01	0.01	0.01
Ohio	1.6	3.9	2.3	**2.68**	**0.31**	**2.71**	**0.47**	**0.99**	**0.61**	**0.16**	**0.99**	**0.74**	**0.40**	**0.49**	**0.49**

State	Age of Project at First Profile Date (Yrs)	Age of Project at Last Profile Date (Yrs)	Time Difference for IRI Change (Years)	Change in IRI (IRI at Last Profile Date - IRI at First Profile Date) (m/km)											
				Section Number											
				13	14	15	16	17	18	19	20	21	22	23	24
Arizona	0.5	5.3	4.8	0.03	0.07	-0.02	0.03	0.00	-0.01	0.09	0.02	0.01	0.05	0.02	0.02
Arkansas	0.8	2.8	2.0	0.02	0.08	0.04	-0.05	0.00	0.00	0.04	0.03	0.00	0.02	-0.01	0.01
Michigan	1.2	1.6	0.4	N/A	N/A	0.02	0.03	0.04	-0.04	N/A	**1.36**	**0.14**	N/A	0.04	0.02
Nebraska	0.3	2.8	2.5	**0.51**	**0.25**	-0.02	**0.17**	-0.03	**0.19**	0.08	**0.12**	**0.14**	**0.31**	**0.18**	0.04
Texas	0.4	1.0	0.6	0.03	**0.15**	**0.12**	-0.02	0.01	-0.06	**0.10**	**0.13**	0.06	0.05	0.05	**0.19**
Virginia	0.4	2.9	2.5	**0.67**	0.05	0.03	0.01	0.01	0.03	0.08	**0.11**	0.09	0.06	0.07	0.07

Note: N/A - Sections not accepted into the LTPP program because of deviations from construction guidelines.

Table 10. Percent change in IRI for SPS-1 sections.

State	Age of Project at First Profile Date (Yrs)	Age of Project at Last Profile Date (Yrs)	Time Difference for IRI Change (Years)	Percent Change in IRI (Note 1) (m/km)											
				Section Number											
				1	2	3	4	5	6	7	8	9	10	11	12
Alabama	3.0	5.1	2.1	2	8	1	8	4	**11**	2	-1	-7	9	1	7
Delaware	0.6	2.5	1.9	-12	0	-11	-16	-14	-11	-20	-15	-18	-24	-19	-26
Iowa	0.9	6.7	5.8	**28**	**59**	**34**	**27**	**25**	**25**	**100**	**47**	**8**	**36**	**30**	**30**
Kansas	0.5	5.4	4.9	**29**	**26**	**49**	**19**	**64**	**34**	**19**	**44**	**34**	**22**	**15**	0
Nevada	1.6	3.0	1.4	2	6	1	0	-1	1	1	-1	2	2	2	2
Ohio	1.6	3.9	2.3	**66**	**20**	**100**	**39**	**48**	**35**	**11**	**53**	**51**	**25**	**39**	**35**

State	Age of Project at First Profile Date (Yrs)	Age of Project at Last Profile Date (Yrs)	Time Difference for IRI Change (Years)	Percent Change in IRI (Note 1) (m/km)											
				Section Number											
				13	14	15	16	17	18	19	20	21	22	23	24
Arizona	0.5	5.3	4.8	3	**10**	-3	4	1	-1	9	2	1	5	2	3
Arkansas	0.8	2.8	2.0	2	**10**	5	-6	0	0	5	4	0	3	-2	1
Michigan	1.2	1.6	0.4	N/A	N/A	3	5	5	-4	N/A	**60**	**10**	N/A	8	3
Nebraska	0.3	2.8	2.5	**26**	**18**	-2	**14**	-3	**14**	6	9	**10**	**22**	**16**	3
Texas	0.4	1	0.6	3	**17**	**12**	-2	1	-7	**12**	**15**	7	6	5	**18**
Virginia	0.4	2.9	2.5	**41**	5	3	1	1	2	**7**	9	8	5	7	8

Note 1: Percent Change in IRI = 100 X (IRI Last Profile Date - IRI First Profile Date)/(IRI at First Profile Date)

N/A: Sections not accepted to the LTPP program because of deviations from construction guidelines..

that had a change in IRI of 0.09 m/km. Thus, all sections in this project have more or less maintained their roughness values from the second to the last profile date. Therefore, it appears there was an error in the profiling equipment when this project was profiled the first time.

Most of the SPS-1 projects are still young, and many projects are not showing changes in roughness. Material test data and monitored traffic data for most of the SPS-1 projects are not yet available in the IMS. Therefore, a comprehensive statistical analysis to identify parameters that relate to development of pavement roughness cannot be performed yet.

The projects located in Alabama, Arizona, Iowa and Kansas are between five and seven years old. All sections in the Alabama and Arizona projects have not shown much change in IRI, in fact the highest percentage change in IRI for a test section in the Arizona project is 10 percent and in the Alabama project is 11 percent. The test sections in the Iowa and Kansas projects show an increase in IRI with only one section in each project showing a percent change in IRI that is less than 10 percent. The other sections in these two projects are showing an increase in IRI that range from 15 to 100 percent. The only other project where the majority of the sections show an increase in roughness is the project in Ohio, which is 3.9 years old and the test sections show an increase in IRI ranging from 11 to 100 percent.

An evaluation of the pavement distress at the SPS-1 projects was performed to see if the distresses that contribute to increase in roughness could be identified. The distress survey date that was closest to the last profile date was selected in the database, and the distresses for this date were summarized. Distresses that were evaluated were fatigue cracking, block cracking, longitudinal cracking in the wheel path, number of transverse cracks, and the length of transverse cracking. The summarized distresses are shown in table 11. The number of sections in each project that exhibit fatigue cracking, longitudinal cracking in the wheel path and transverse cracking are shown in table 11. Block cracking was not noted in any SPS-1 project. Table 11 also presents the average distress, which was computed by summing each type of distress for all sections and dividing this value by the number of sections in the project that exhibited that distress. For each distress type all severity levels were combined when computing the average values.

Table 11. Pavement distress at SPS-1 projects.

State	Last Profile Date	Distress Survey Date	Distress Survey Method	Sections Exhibiting Distress			Average Distress (see Note 1)			
				Fatigue Cracking	Longitudinal Cracking in Wheel Path	Transverse Cracking	Fatigue Cracking (m^2)	Longitudinal Cracking Wheel Path (m)	Transverse Cracks (No)	Transverse Cracking (m)
Alabama	1/98	2/00	Pasco	0	1	4	-	1	1	2
Arizona	12/98	2/99	Manual	6	10	1	8	33	1	1
Arkansas	7/97	6/97	Manual	5	4	3	11	4	3	3
Delaware	11/98	6/99	Pasco	1	0	2	2	-	1	1
Florida	1/97	12/96	Manual	0	0	0	-	-	-	-
Iowa	7/99	8/99	Pasco	4	10	12	10	36	11	20
Kansas	3/99	12/99	Manual	12	4	9	158	34	6	17
Louisiana	11/97	5/98	Manual	0	0	0	-	-	-	-
Michigan	6/97	10/98	Manual	2	2	3	14	31	1	2
Nebraska	5/98	10/98	Manual	0	2	2	-	8	2	3
Nevada	8/98	12/98	Manual	3	2	0	4	13	-	-
New Mexico	3/97	5/97	Manual	0	0	0	-	-	-	-
Ohio	11/98	8/99	Pasco	0	0	0	-	-	-	-
Oklahoma	11/97	12/97	Manual	0	0	0	-	-	-	-
Texas	4/98	3/98	Manual	1	1	0	3	61	-	-
Virginia	10/98	10/99	Manual	2	1	1	72	15	1	1

Note 1: Average Distress = Sum of Distresses / Number of Sections With Distress
- Distress type not present.

All sections in the Iowa SPS-1 project exhibited transverse cracking, with ten of these sections also exhibiting longitudinal cracking in the wheel path. The increase in roughness for the sections in this project is attributed to these two distresses. All sections in the Kansas project exhibited fatigue cracking, with nine of these sections also exhibiting transverse cracking, and the increase in roughness for this project is attributed to these two distresses. The project in Ohio also showed a large increase in roughness, but as shown in table 11 none of the sections in this project had any distresses at the last distress survey date. However, this section has non-wheel path longitudinal cracking and rutting. The increase in roughness for this project is attributed to rutting. Table 11 shows that ten sections in the Arizona SPS-1 project have longitudinal cracking in the wheel path that are either low or medium severity, but the sections in the projects have shown no increase in roughness. It is likely that the dry no-freeze environment and the coarse subgrade at this project is helping to prevent differential movement between the two sides of the crack, and therefore not causing an increase in roughness. Some sections in the project in Texas, which is one year old, are showing an increase in roughness. At the time of last profile date, the rutting in the left wheel path of the sections ranged from 0 to 18 mm with an average of 9.8 mm and the rutting in the right wheel path ranged from 0 to 8 mm, with an average of 4 mm. The increase in roughness of this project is attributed to rutting of the sections.

The three projects that showed the largest increase in roughness were located in Iowa, Kansas and Ohio, and all these three projects had test section numbers 1 through 12. All three projects are located on a fine grained subgrade. An ANOVA was conducted using the data from these three projects to see if differences in performance between test sections could be identified. The two-way ANOVA was conducted with state and section number being considered as independent variables, and the percent increase in roughness as the dependant variable. The ANOVA indicated there was no significant difference in IRI between the test sections. That is the statistical analysis did not indicate that stronger pavement sections behaved differently from some of the weaker test sections, or if the provision of drainage caused a difference in IRI of the test sections. Sufficient materials test data are not available in the LTPP database to investigate the cause for the increase in roughness at the projects in Iowa, Kansas, and Ohio, or for the cause

of the good performance for the projects in Arizona and Alabama (both of which are older than 5 years).

Summary of Findings

The data from the SPS-1 projects indicated the sections with a 100 mm thick AC surface had an average early-age IRI of 0.88 m/km, and a standard deviation of IRI of 0.21 m/km. The sections with a 175 mm thick AC surface had an average IRI of 0.82 m/km, and a standard deviation of IRI of 0.18 m/km. IRI values less than 0.8 m/km was achieved on 40 percent of the sections that received a 100 mm AC surface and 55 percent of the sections that received a 175 mm AC surface. An IRI of less than 1.0 m/km was obtained by 75 percent of the sections that received a 100 mm AC surface and 85 percent of the sections that received a 175 mm AC surface.

The AC surfaces in SPS-1 projects have been placed on three different types of bases: DGAB, ATB, and PATB. The average IRI of sections placed on base types of DGAB, ATB and PATB were 0.94 m/km, 0.82 m/km, and 0.84 m/km. The statistical analysis indicated that there was a significant difference in early age IRI of pavements placed on DGAB and ATB. The analysis also indicated there was no significant difference between early age IRI obtained on pavements placed on PATB when compared to the other two base types.

The SPS-1 projects that showed the highest increase in IRI were located in Kansas, Iowa and Ohio. In both the Iowa and Kansas projects, all sections except for one are showing a percent increase in IRI between 15 to 100 percent. This increase in IRI occurred in approximately 6 years for the Iowa project, and approximately 5 years for the Kansas project. The increase in IRI at the project in Iowa is attributed to transverse cracking and longitudinal cracking in the wheel path, while the increase in IRI for the project in Kansas is attributed to fatigue cracking and transverse cracking. The percent increase in IRI at the test sections in the Ohio project ranged from 11 to 100 percent, with this increase occurring approximately in 4 years. The increase in IRI at the sections in the Ohio project is attributed to rutting. Some of the test sections in the

Texas project are showing an increase in IRI of over 10 percent within an approximately 6-month period. This increase in IRI is attributed to rutting. A statistical analysis was conducted using the percent increase in roughness of the test sections in Kansas, Iowa and Ohio to see if differences in test sections could be identified. The analysis indicated that there were no significant differences between the test sections.

The average project IRI, which is the average of the IRI of all sections in the project for the projects in Iowa, Kansas and Ohio were 0.88 m/km, 0.81 m/km and 1.10 m/km, respectively. Although the pavements in these projects achieved a smooth pavement initially, many sections, including very thick sections had high increases in roughness during the initial life of the pavement. This demonstrates that achieving a smooth pavement initially does not guarantee that it will remain smooth even during the initial life. Factors such as mix design problems in the AC, inadequate preparation of the subgrade prior to placing the pavement, or other construction problems can cause a pavement that is built smooth initially to increase its roughness within a short time period.

SPS-2 EXPERIMENT: STRATEGIC STUDY OF STRUCTURAL FACTORS FOR RIGID PAVEMENTS

Introduction

The SPS-2 experiment was designed to investigate the effect of selected structural factors on the long-term performance of rigid pavements constructed on different subgrades and in different environmental regions. New pavements were constructed for the SPS-2 experiment. In the SPS-2 experiment, twelve test sections were constructed at a project location. All test sections were doweled jointed PCC with a joint spacing of 4.6 m. The twelve test sections constructed for a project were either section numbers 1 through 12, or section numbers 13 through 24. The pavement structure of the test sections is shown in table 12. The structural factors considered in this experiment are: thickness of PCC layer (200 and 275 mm), flexural strength of the PCC at 14 days (3.8 and 6.2 MPa), base type (lean concrete base, dense graded

Table 12. Structural properties of SPS-2 sections.

Test Section Number	PCC Thickness (mm)	Flexural Strength (MPa)	Lane Width (m)	Layer 2		Layer 3	
				Material	Thickness (mm)	Material	Thickness (mm)
1	200	3.8	3.66	DGAB	150	-	-
2	200	6.2	4.27	DGAB	150	-	-
3	275	3.8	4.27	DGAB	150	-	-
4	275	6.2	3.66	DGAB	150	-	-
5	200	3.8	3.66	LCB	150	-	-
6	200	6.2	4.27	LCB	150	-	-
7	275	3.8	4.27	LCB	150	-	-
8	275	6.2	3.66	LCB	150	-	-
9	200	3.8	3.66	PATB	100	DGAB	100
10	200	6.2	4.27	PATB	100	DGAB	100
11	275	3.8	4.27	PATB	100	DGAB	100
12	275	6.2	3.66	PATB	100	DGAB	100
13	200	3.8	4.27	DGAB	150	-	-
14	200	6.2	3.66	DGAB	150	-	-
15	275	3.8	3.66	DGAB	150	-	-
16	275	6.2	4.27	DGAB	150	-	-
17	200	3.8	4.27	LCB	150	-	-
18	200	6.2	3.66	LCB	150	-	-
19	275	3.8	3.66	LCB	150	-	-
20	275	6.2	4.27	LCB	150	-	-
21	200	3.8	4.27	PATB	100	DGAB	100
22	200	6.2	3.66	PATB	100	DGAB	100
23	275	3.8	3.66	PATB	100	DGAB	100
24	275	6.2	4.27	PATB	100	DGAB	100

Note: DGAB – Dense Graded Aggregate Base, LCB - Lean Concrete Base, PATB - Permeable Asphalt Treated Base

aggregate base and permeable asphalt treated base over dense graded aggregate base), lane width (3.65 and 4.27 m), and drainability (presence or lack of it as provided by an open graded permeable asphalt treated layer and edge drains). The subgrade types considered in this experiment are classified as fine grained and coarse grained, while the environmental regions considered are the four LTPP regions: wet-freeze, wet no-freeze, dry-freeze and dry-no freeze. The test sections in a SPS-2 project were profiled immediately after construction, and thereafter at approximately annual intervals.

Analyzed Projects

A review of the IMS database indicated that profile data were available for twelve SPS-2 projects. Table 13 presents the following information for each SPS-2 project: section numbers in project, climatic zone, subgrade type, construction date, last available profile date, age of project at first profile date, age of project at last profile date, time difference between first and last profile dates, the number of times the project was profiled, and the traffic volume. Ten of the twelve SPS-2 projects have been profiled within one year after construction, with the other two projects being profiled when their age was between one and two years. The SPS-2 project in Arkansas was profiled only once after construction, while the others were profiled 2 to 9 times.

Analysis of Early Age IRI

The SPS-2 projects were first profiled at varying times after construction. Therefore, the IRI obtained during the first profile date may not necessarily correspond to the IRI that is obtained immediately after construction. Therefore, the term early-age IRI is used in this analysis to differentiate from the initial IRI of the pavement, which corresponds to the IRI immediately after construction. The early-age IRI values of all SPS-2 projects were used in this analysis.

Figure 13 shows the average early-age IRI of the test sections in each project, differentiated according to the PCC thickness. The IRI shown for a project in figure 13 is the average IRI of the six test sections that have a PCC thickness of 200 mm or 275 mm. The average IRI for the 200 mm PCC and 275 mm PCC sections were close to each other for most projects, but for a majority of the projects the average IRI of the 275 mm thick PCC pavements were higher than the average IRI of the 200 mm thick PCC pavement. The maximum difference in the average IRI between the two thicknesses occurred for the project in Delaware, where the average IRI of the 275 mm thick PCC sections were 0.3 m/km greater than the average IRI of the

Table 13. SPS-2 projects.

Location	State Code	Section Numbers in Project	Climatic Zone (Note 1)	Subgrade Type	Construction Date	Last Available Profile Date	Age of Project at First Profile Date (Years)	Age of Project At Last Profile Date (Years)	Time Difference Between First And Last Profile Date (Years)	Number of Times Profiled	Traffic (KESAL/yr)
Arizona	AZ	13-24	DNF	Coarse	10/1/93	12/8/98	0.3	5.2	4.9	5	1094
Arkansas	AR	13-24	WNF	Fine	11/1/95	2/6/97	1.3	1.3	0.0	1	N/A
Colorado	CO	13-24	DF	Coarse	11/1/93	8/14/98	0.4	4.8	4.3	3	487
Delaware	DE	13-24	WF	Coarse	5/1/96	7/28/98	0.6	2.2	1.6	6	N/A
Iowa	IA	13-24	WF	Fine	12/1/94	7/17/99	0.2	4.6	4.4	5	56
Kansas	KS	1-12	DF	Fine	8/1/92	3/15/99	0.0	6.6	6.6	8	639
Michigan	MI	13-24	WF	Fine	11/1/93	4/12/99	0.8	5.4	4.6	9	1600
Nevada	NV	1-12	DF	Coarse	9/1/95	8/28/98	0.8	3.0	2.2	4	N/A
North Carolina	NC	1-12	WNF	Fine	1/1/94	11/4/98	0.2	4.8	4.6	8	728
North Dakota	ND	13-24	DF	Fine	11/1/94	5/14/99	1.8	4.5	2.7	2	N/A
Ohio	OH	1-12	WF	Fine	6/1/96	11/12/98	0.2	2.4	2.2	4	N/A
Washington	WA	1-12	DF	Coarse	11/1/95	5/7/99	0.0	3.5	3.5	4	N/A
Note 1: DF: Dry Freeze, DNF - Dry No-Freeze, WF - Wet Freeze, WNF - Wet No-Freeze											

200 mm sections. The standard deviations of early-age IRI for the SPS-2 projects are shown in figure 14. The 275 mm PCC sections in Iowa and Nevada had the highest standard deviation in IRI.

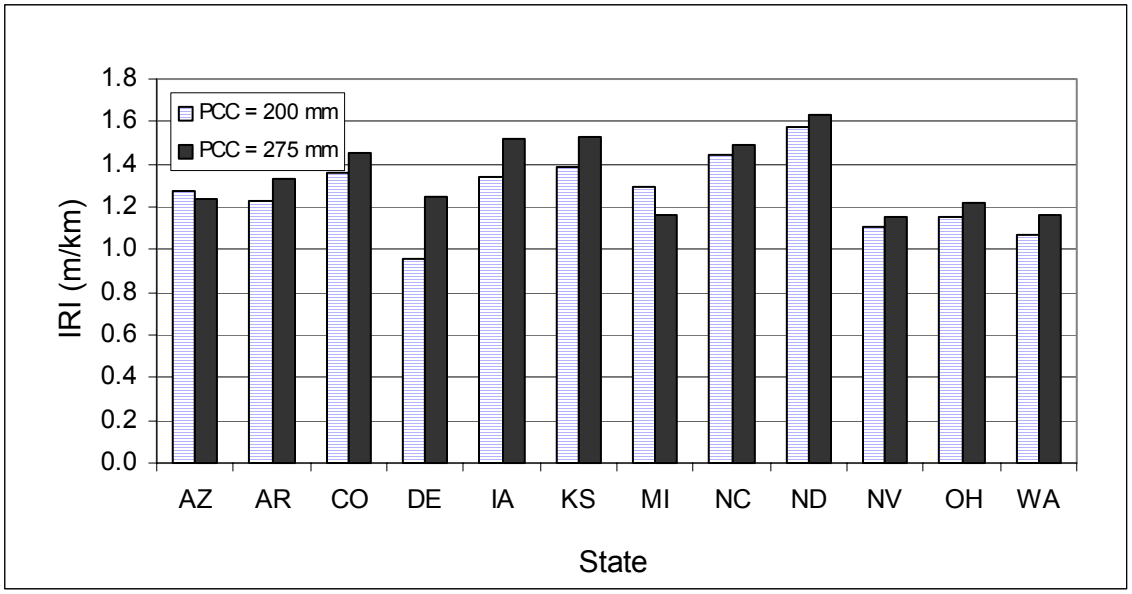

Figure 13. Average early-age IRI of SPS-2 projects.

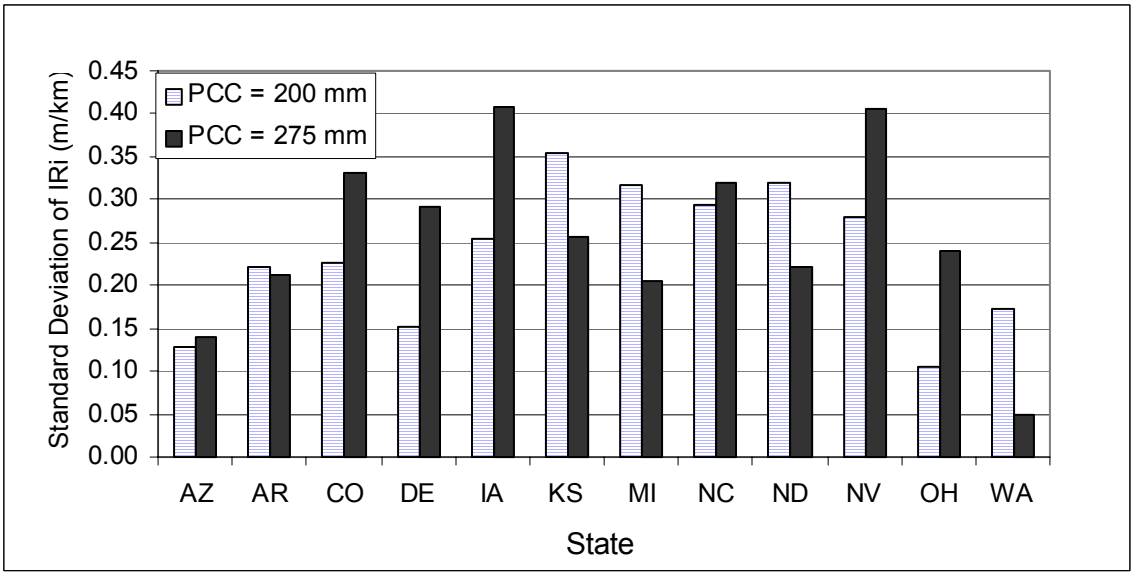

Figure 14. Standard deviation of early-age IRI for SPS-2 projects.

The frequency distribution of the early-age IRI values of the test sections in the SPS-2 projects separated according to the two PCC thicknesses is shown in figure 15, while the cumulative frequency distribution is shown in figure 16.

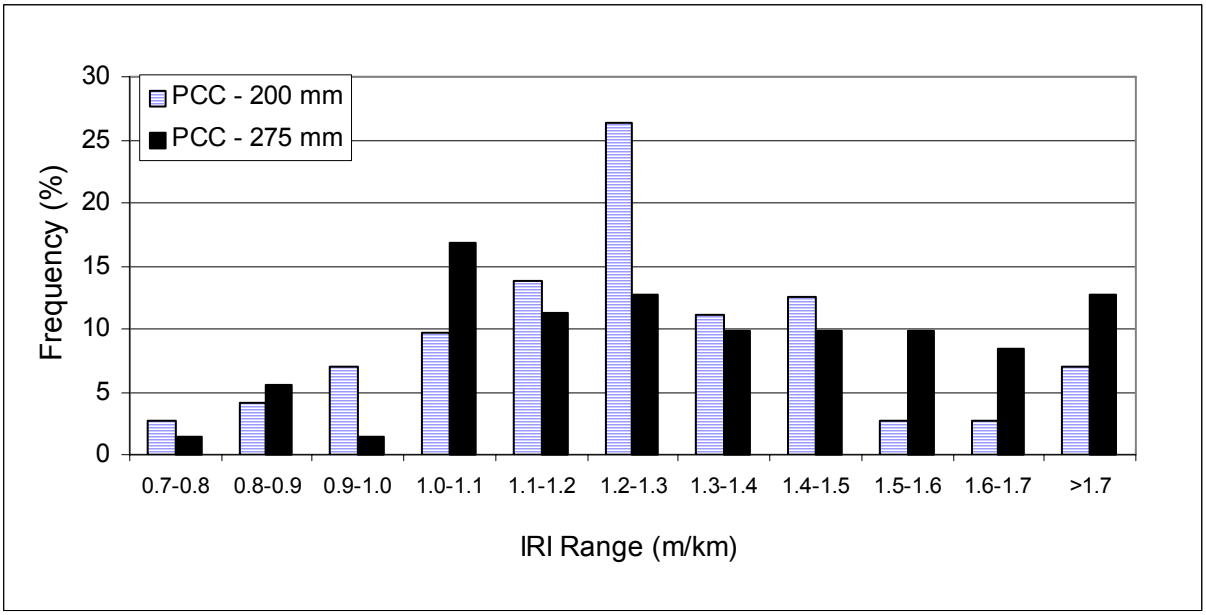

Figure 15. Frequency distribution of early-age IRI.

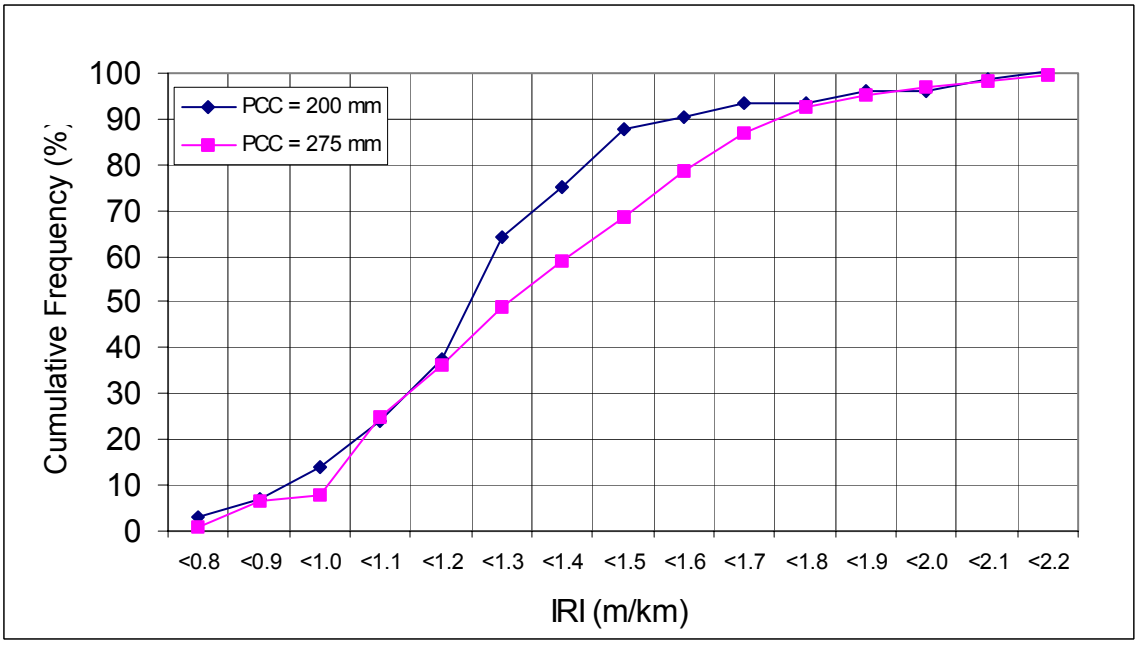

Figure 16. Cumulative frequency distribution of early-age IRI.

About 40 percent of the sections had an IRI of less than 1.2 m/km for both 200 mm and 275 mm thick PCC pavements. About 90 percent of 200 mm PCC sections and 70 percent of the 275 mm PCC sections had an IRI of less than 1.5 m/km.

The average and the standard deviation of early-age IRI values for the two different PCC thicknesses are shown in table 14.

Table 14. Average and standard deviation of early-age IRI: SPS-2 .

PCC Thickness (mm)	IRI (m/km)	
	Average	Std. Dev
200	1.27	0.28
275	1.30	0.30

An analysis was performed to study if the early-age IRI depended on the base type, PCC thickness, and flexural strength of PCC. The PCC surface in SPS-2 projects was placed on three different base types: dense graded aggregate base (DGAB), lean concrete base (LCB), and permeable asphalt treated base (PATB). In a SPS-2 project, four sections were placed on each of the three base types. The two flexural strengths used in the SPS-2 projects were 3.8 and 6.2 Mpa, while the two PCC thicknesses are 200 mm and 275 mm.

A three way ANOVA was conducted using the early-age IRI as the dependant variable, and PCC thickness, base type, and flexural strength as independent variables. The ANOVA indicated PCC thickness and flexural strength were not significant while the base type was significant (p-value = 0.02). A multiple comparison indicated IRI values of PCC pavements on LCB was significantly different than PATB. Figure 17 shows a box-plot of the distribution of the early-age IRI values categorized according to the base type. As shown in the box-plot, the pavements placed on LCB had the highest median IRI value. Three sections placed on LCB had IRI values greater than 2.0 m/km, and are considered to be outliers. Two sections placed on PATB also had early-age IRI values that were greater than 2.0 m/km, and are also considered to be outliers. Table 15 presents the average, standard deviation, and 15^{th} and 85^{th} percentile early-IRI values classified according to base type. As shown in table 15, the highest early-age IRI values were obtained on PCC pavements that were placed on LCB bases.

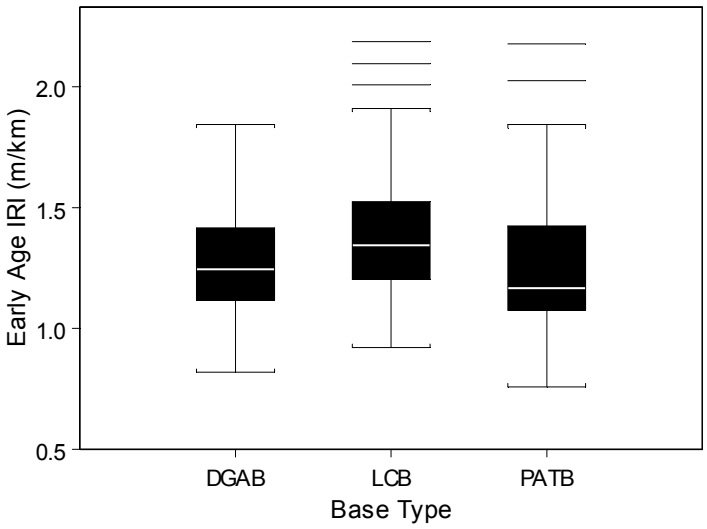

Figure 17. Box-plot of early-age IRI.

Table 15. Average and standard deviation of early-age IRI classified according to base type.

Base Type	Early Age IRI (m/km)			
	Average	Standard Dev	15th Percentile	85th Percentile
Aggregate Base	1.27	0.24	1.02	1.49
Lean Concrete Base	1.40	0.29	1.10	1.60
Permeable Asphalt Treated Base	1.25	0.32	0.98	1.55

Changes in IRI for SPS-2 Projects

Plots showing the changes in IRI of the test sections in individual SPS-2 projects are included in Appendix B. The SPS-2 projects are still young, with 27 percent of the projects being between 5 and 7 years old, and 63 percent of the projects being less than five years old. Table 16 presents the changes in IRI for the test sections in each SPS-2 project relative to the IRI at the first profile date. Table 16 also shows the age of the project when it was first profiled, age of project at last profile date, and the time difference corresponding to the change in IRI. In table

Table 16. Change in IRI at SPS-2 sections.

State	Age of Project at First Profile Date (Yrs)	Age of Project at Last Profile Date (Yrs)	Time Difference for IRI Change (Years)	Change in IRI (IRI at Last Profile Date - IRI at First Profile Date) (m/km)											
				Section Number											
				1	2	3	4	5	6	7	8	9	10	11	12
Delaware	0.6	2.2	1.6	**0.17**	0.07	-0.03	-0.01	0.05	-0.29	0.04	0.05	0.01	**0.13**	0.04	0.03
Kansas	0.0	6.6	6.6	**0.30**	-0.23	0.06	**0.11**	0.04	-0.48	0.03	**0.12**	-0.06	**0.12**	-0.05	-0.07
N. Carolina	0.2	4.8	4.6	**0.31**	**0.39**	**0.21**	**0.13**	0.06	**0.19**	0.09	**0.23**	**0.18**	0.02	**0.10**	**0.12**
Nevada	0.8	3.0	2.2	**0.51**	**0.61**	**0.24**	**0.54**	**0.19**	**0.10**	**0.44**	**0.12**	**0.39**	**0.37**	**0.50**	N/A
Ohio	0.2	2.1	1.9	**0.21**	**0.20**	0.01	0.09	**0.10**	0.09	-0.14	-0.21	**0.13**	-0.06	-0.04	-0.10
Washington	0.1	3.5	3.5	**0.14**	0.03	0.02	0.03	0.01	**0.54**	**0.11**	**0.13**	**0.10**	**0.23**	0.00	**0.10**

State	Age of Project at First Profile Date (Yrs)	Age of Project at Last Profile Date (Yrs)	Time Difference for IRI Change (Years)	Change in IRI (IRI at Last Profile Date - IRI at First Profile Date) (m/km)											
				Section Number											
				13	14	15	16	17	18	19	20	21	22	23	24
Arizona	0.3	5.2	4.9	**0.31**	-0.23	**0.28**	-0.05	-0.09	-0.35	**0.12**	-0.12	**0.11**	-0.10	**0.21**	0.04
Colorado	0.5	4.8	4.4	-0.04	-0.08	0.00	-0.06	0.05	-0.06	0.07	0.08	-0.08	0.00	-0.17	-0.06
Iowa	0.2	4.6	4.4	0.01	0.06	0.06	**0.10**	**0.26**	**0.11**	-0.10	0.02	**0.12**	0.06	-0.15	-0.11
Michigan	0.9	5.5	4.7	**1.15**	**0.22**	**0.73**	-0.12	**2.15**	**0.36**	**0.18**	0.02	0.07	-0.07	-0.02	-0.08
North Dakota	1.8	4.5	2.7	-0.24	-0.11	-0.04	0.06	-0.10	N/A	-0.01	0.03	-0.11	-0.15	-0.05	-0.13

Note: N/A - IRI at first profile date incorrect, therefore change not computed.

16, cases that show an IRI increase of 0.10 m/km or greater are shown in bold. Table 17 shows the percent change in IRI at the test sections, with respect to the IRI at the first profile date. Cases where the percent increase is greater than or equal to 10 percent are shown in bold.

In the Nevada project, all sections except for two sections showed 21 to 64 percent increase in IRI, which occurred during 2.2 years. Several sections in the Michigan project show a high increases in roughness. Section 17 in the Michigan project that shows an IRI increase of 214 percent failed because of pumping occurring in the LCB layer. In the North Carolina project, 66 percent of the sections show an increase in IRI of greater than 10 percent within a 4.6 year period. All projects that have section 1 show an increase in IRI that is greater than 10 percent, with the age of the sections ranging from 2.1 to 6.6 years. There are five projects that have section 13 that has similar characteristics as section 1 except that the lane width is 4.27 m. Two of these projects are showing an increase in IRI that is greater than 10 percent. No other trends can be seen for individual projects, or for similar sections across the projects. There are sections that are showing a decrease in roughness from the initial IRI, and some projects have sections that are showing large increases in roughness when compared to other sections in that project.

It is not possible to do a comprehensive analysis on the performance of the SPS-2 projects because of the lack of materials testing data. However, some of the specific observations that were described previously can be investigated to determine if the cause of the change in IRI can be identified from the profile data.

Investigation of Specific Cases

Based on the findings from the analysis of changes in IRI at SPS-2 sections, the following cases were identified for analysis.

1. Investigate the cause for the high increase in roughness at some sections.
2. Investigate the cause of the high reduction in roughness at some sections.
3. Investigate the cause of the increase in roughness in the North Carolina project.

Table 17. Percent change in IRI at SPS-2 sections.

State	Age of Project at First Profile Date (Yrs)	Age of Project at Last Profile Date (Yrs)	Time Difference for IRI Change (Years)	Percent Change in IRI (Note 1)											
				Section Number											
				1	2	3	4	5	6	7	8	9	10	11	12
Delaware	0.6	2.2	1.6	**16**	8	-3	0	5	-28	4	3	1	**14**	4	2
Kansas	0.0	6.6	6.6	**24**	-19	4	8	3	-23	2	6	-5	9	-4	-4
N. Carolina	0.2	4.8	4.6	**23**	**29**	**12**	**11**	3	**13**	5	**13**	**15**	2	8	11
Nevada	0.8	3.0	2.2	**56**	**41**	**29**	**35**	**21**	7	**45**	7	**48**	**33**	**64**	N/A
Ohio	0.2	2.1	1.9	**17**	**17**	1	**10**	8	7	-10	-14	**13**	-5	-3	-9
Washington	0.1	3.5	3.5	**11**	3	2	2	1	**52**	9	**11**	8	**29**	0	**9**

State	Age of Project at First Profile Date (Yrs)	Age of Project at Last Profile Date (Yrs)	Time Difference for IRI Change (Years)	Percent Change in IRI (Note 1)											
				13	14	15	16	17	18	19	20	21	22	23	24
Arizona	0.3	5.2	4.9	**21**	-18	**20**	-4	-7	-26	**10**	-10	**10**	-9	**18**	4
Colorado	0.5	4.8	4.4	-4	-7	0	-6	3	-4	5	5	-5	0	-10	-3
Iowa	0.2	4.6	4.4	1	5	3	8	**20**	9	-6	2	9	3	-7	-8
Michigan	0.9	5.5	4.7	**95**	**12**	**83**	-8	**214**	**24**	**15**	2	7	-6	-2	-7
North Dakota	1.2	3.2	2.0	-16	-9	-2	3	-7	N/A	-1	2	-8	-9	-4	-6

Note 1: Percent Change in IRI = 100 X (IRI Last Profile Date - IRI First Profile Date)/(IRI at First Profile Date)

Note: N/A - IRI at first profile date incorrect, therefore change not computed.

4. Investigate the cause for the increase in roughness in the Nevada project.
5. Investigate the cause of high variability in roughness over the years at some sections.

These investigations were carried out by analyzing profile data of the selected sites. The profile data in the IMS database has been filtered with a 100 m cut-off filter. It is difficult to see specific features that affect roughness by viewing these profiles. A closer look at the features that affect roughness was performed by using different filters on the profile data. Band-pass filters that look at specific wavelengths were extensively used in this analysis. All plots in this section that are indicated to have been band-pass filtered have been filtered using with a band pass filter that will keep only the wavelengths between 1.6 and 8 m. Power spectral density (PSD) plots were also extensively used in this analysis. The application of PSD plots for pavement profiles is described by Sayers and Karamihas (20). The PSD plots were used to analyze the distribution of the wavelengths that are contained in a profile. In the PSD plots, the x-axis shows the wavenumber, which is the inverse of wavelength.

Investigate Cause for High Increase in Roughness at Some Sections

Some sections in some SPS-2 projects have shown a high increases in roughness when compared to other sections in that project. Three of the test sections (section 13 in Arizona, section 13 in Michigan, and section 6 in Washington) were selected for detailed investigation.

Arizona – Section 13

Section 13 in Arizona has shown an increase in IRI of 21 percent from the first measured IRI within a period of 4.9 years. This section has a 200 mm PCC slab that rests on a DGAB base, and has a slab width of 4.27 m. This section is showing the highest increase in IRI of all test sections in the Arizona SPS-2 project. The profile date, profile time and the IRI values for this section are shown in table 18. The mean IRI at this section decreased from 1.44 m/km at the first profile date (1994) to 1.20 m/km at the second profile date (1995), and increased to 1.75 m/km at the last profile date (1998).

Table 18. IRI values – section 13 – Arizona.

Profile Date	Profile Time	IRI (m/km)
1/25/94	6:10 AM	1.44
3/5/95	11:21 AM	1.20
12/4/97	11:06 AM	1.71
12/8/98	10:28 AM	1.75

The band-pass filtered profile plots of the right wheel path for the first, second and last profile dates are shown in figure 18. As seen from this plot, the curvature of the slabs is less pronounced at second profile date (date = 1995, IRI = 1.20 m/km) when compared to the first profile date (date = 1994, IRI = 1.44 m/km), but the curvature increases significantly at the last profile dates (date = 1998, IRI = 1.75 m/km).

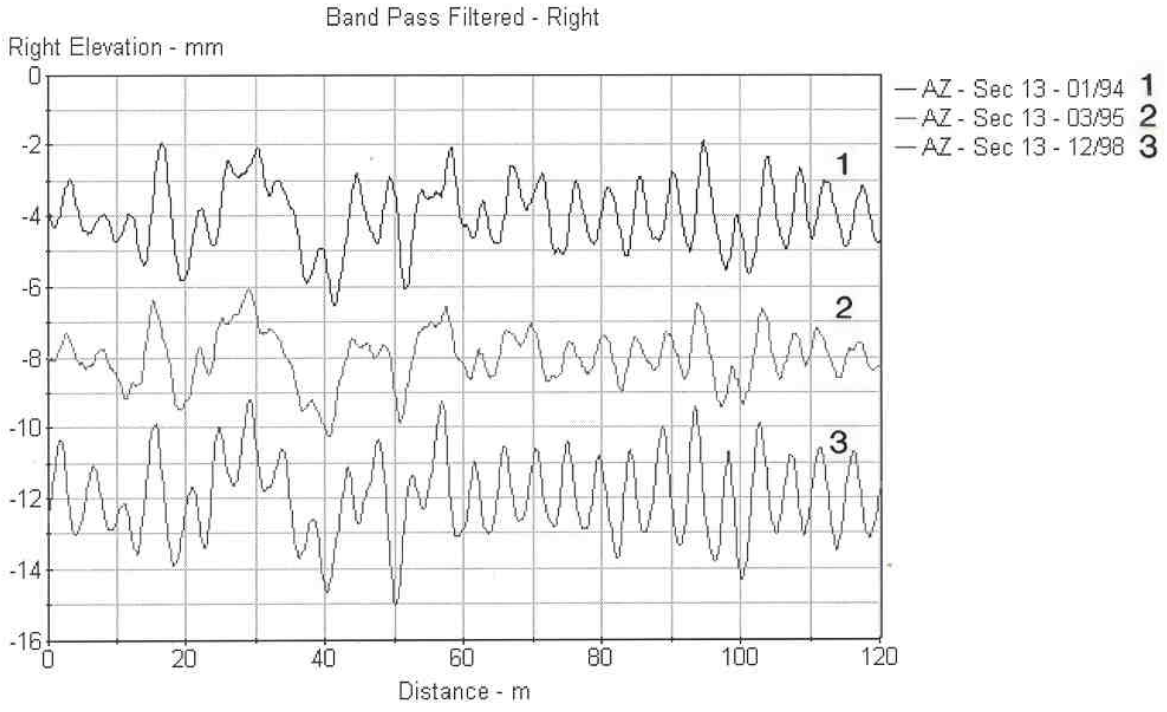

Figure 18. Band pass filtered profile plots – section 13 – Arizona.

The slabs at this section are curved upwards, where the edges of the slab are at a higher elevation when compared to the center of the slab. The distance between two-peaks in the plot corresponds to 4.6 m, which is the joint spacing of the PCC slabs. Generally, for slabs showing

this type of curvature, the curling of the joints is maximum in the early morning when the temperature differential between the top and the bottom of the slab is maximum. The cause for the higher IRI at the first profile date when compared to the second profile date is attributed to this, as this site was first profiled in the early morning. The curvature of the slab at the last profile date when the site was profiled in the mid morning is more pronounced than the curvature at the first profile date when the slab was profiled early in the morning. From these observations it appears that the curled-up shape of the slab is increasing over time, with moisture variations in the slab having a possible effect on slab curling.

The PSD plots for the second profile date (IRI = 1.20 m/km) and last profile date (IRI = 1.75 m/km) are shown in figure 19. A comparison of these two figures show a pronounced peak at a wavenumber of 0.21 cycles/m for the last profiling date of 12/98 when compared to the second profiling date of 03/95. The wavenumber of 0.21 corresponds to a wavelength of 4.6 m, which is the slab length. Therefore, these plots clearly show that the slab curvature is affecting the wavelength distribution in the profile.

Michigan – Section 13

Section 13 in the Michigan SPS-2 project has shown an increase in IRI of 95 percent from its initial IRI. This section has a 200 mm PCC slab that rests on a DGAB base, and has a slab width of 4.27 m. The profile dates, profile times, and IRI values for this section are shown in table 19. The mean IRI at this section has ranged between 1.10 m/km and 1.38 m/km for the first six profile dates from 9/94 to 4/97. From 4/97 to 4/99, the IRI has increased from 1.10 m/km to 2.36 m/km.

The band-pass filtered profile plots of the right wheel path for 1994 (IRI = 1.21 m/km) and 1998 (1.72 m/km) are shown in figure 20. The slabs at this section are curved upwards. The curvature of the slabs in 1998 is much more pronounced than the curvatures in 1994. The site was profiled around noon in 1994 and in the afternoon in 1998, so the profile shapes seen are not influenced by early morning curling behavior. The increase in roughness at this site is attributed to the increase in upward curvature of the slabs.

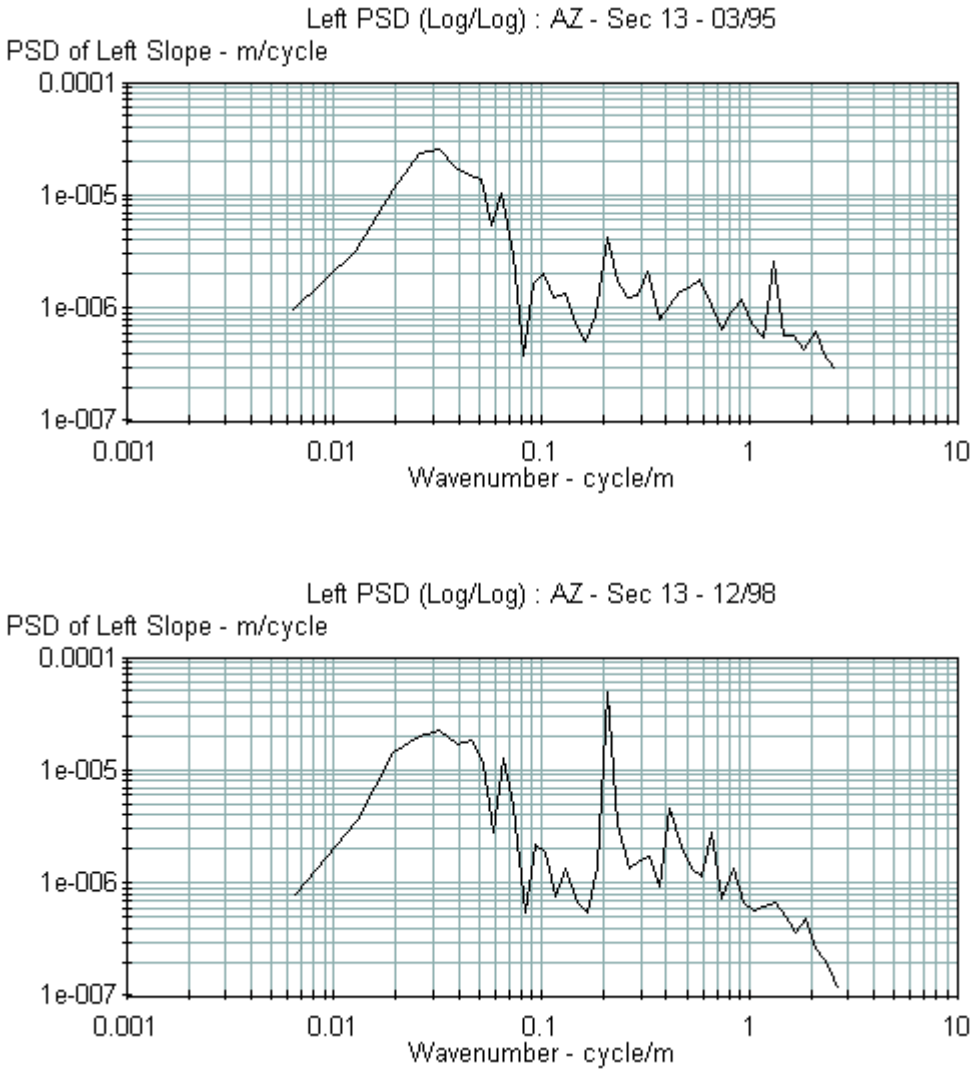

Figure 19. PSD plots – left wheel path profiles – section 13 – Arizona.

Washington – Section 6

Section 6 in the Washington SPS-2 project showed the highest increase in IRI for that project. The profile dates, profile times and IRI for this section are shown in table 20. The IRI of this section increased from 1.04 m/km in 1995 to 1.58 m/km in 1999, an increase of 52 percent that occurred in about three and a half years.

Table 19. IRI values – Section 13 – Michigan.

Profile Date	Profile Time	IRI (m/km)
9/6/94	11:30 AM	1.21
8/11/95	9:35 AM	1.11
1/8/96	4:34 PM	1.23
4/9/96	10:11 AM	1.38
12/29/96	10:28 AM	1.23
4/15/97	1:05 PM	1.10
7/1/97	9:23 AM	1.47
11/5/98	4:35 PM	1.72
4/12/99	12:15 PM	2.36

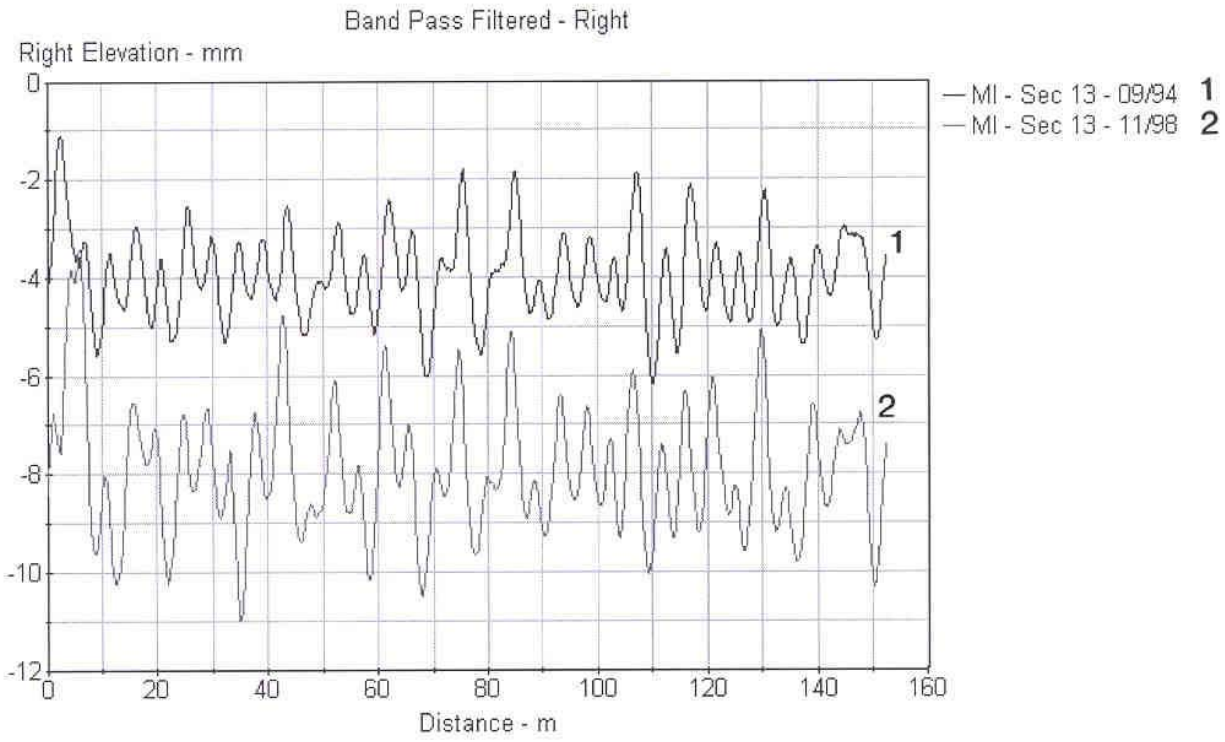

Figure 20. Band pass filtered profile plots – section 13 – Michigan.

Table 20. IRI values – Section 6 – Washington.

Profile Date	Profile Time	IRI (m/km)
11/18/95	1:18 PM	1.04
10/6/97	4:48 PM	1.28
5/15/98	2:27 PM	1.44
5/7/99	1:02 PM	1.58

The 100-m filtered right wheel path profile plots for this section for the four profiling dates are shown in figure 21. As seen from this figure, the slabs take a pattern where the middle of the slab is at a higher elevation compared to the joints. This pattern is clearly seen at the beginning of the section where the humps occur at 4.6 m intervals.

The band-pass filtered right wheel path profiles for this section are shown in figure 22. This figure shows the downward curvature has increased from the first profile date (1995) to the last profile date (1999). The increase in the downward curvature of this site over time contributed to the increase in roughness at this site. The increase in the downward curvature for this section may have been due to changes in moisture conditions within the slab.

Investigate the Cause of High Decrease in Roughness

Test sections in some SPS-2 projects have shown a high decrease in roughness when compared to other test sections in that project. Three test sections that showed a high decrease in roughness, section 18 in Arizona, section 6 in Delaware, and section 6 in Kansas were selected to investigate if the cause of the reduction in roughness could be identified.

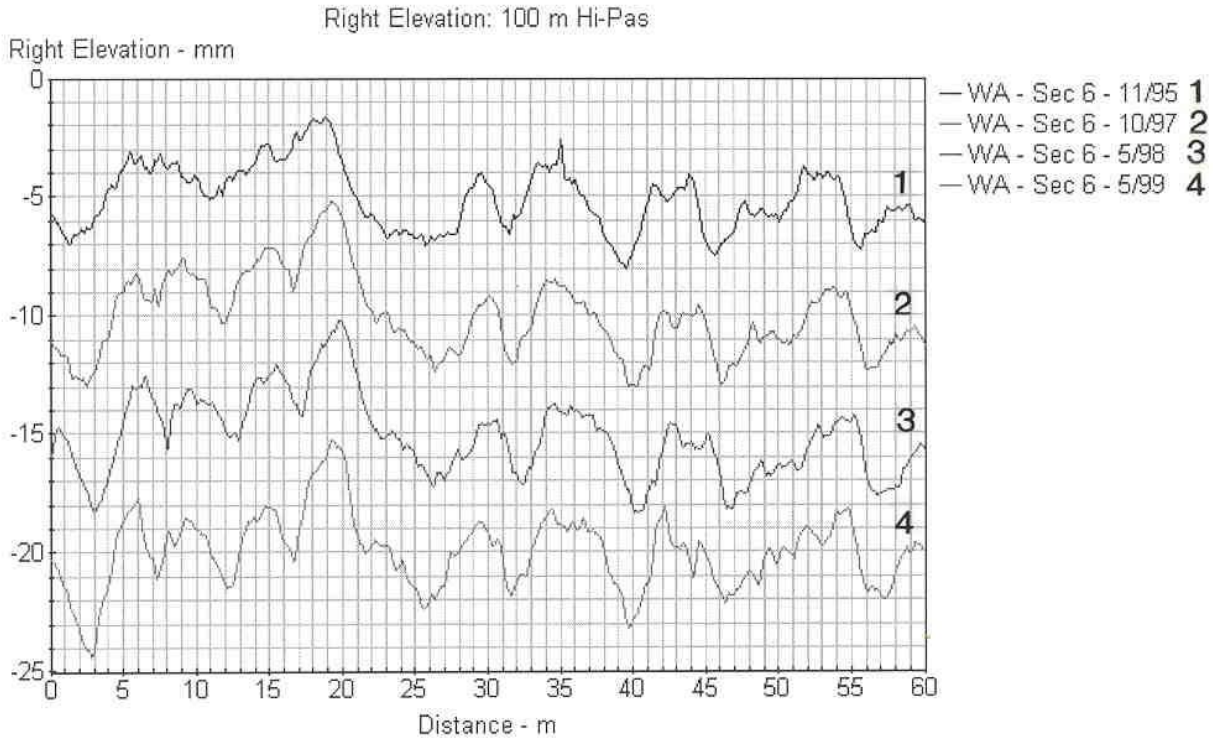

Figure 21. High pass filtered (100 m) right wheel path profile – section 6 – Washington.

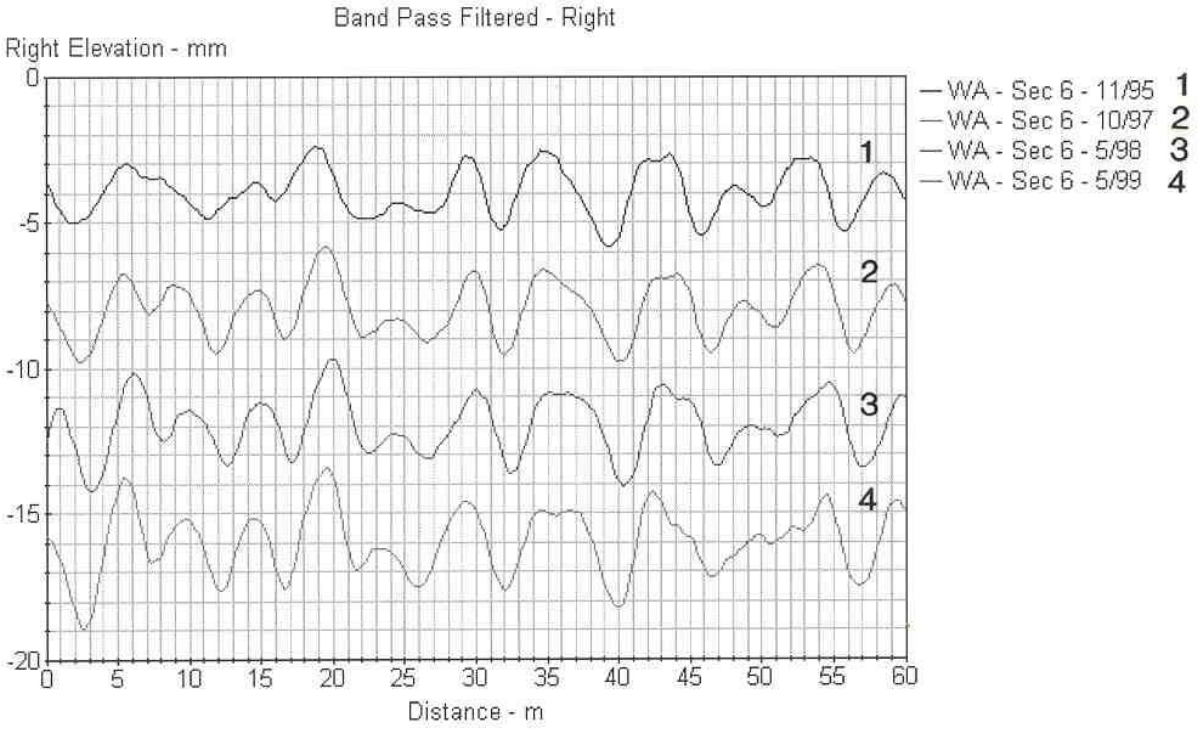

Figure 22. Band pass filtered profile plots – section 6 – Washington.

Arizona – Section 18

Section 18 in the Arizona SPS-2 project has shown a decrease in IRI of 26 percent when compared to the IRI at first profile date. This section has a 200 mm PCC slab with a LCB base, and has a slab width of 3.66 m. The profile dates, profile times and IRI for this section are shown in table 21. The IRI of this section at the first profile date was 1.36 m/km, and thereafter for the other three profile dates the IRI ranged between 0.95 to 1.01 m/km.

Table 21. IRI values – section 18 – Arizona.

Profile Date	Profile Time	IRI (m/km)
1/25/94	6:10 AM	1.36
3/5/95	11:21 AM	0.95
1/27/97	11:22 AM	0.98
12/4/97	11:06 AM	1.01
12/8/98	10:28 AM	1.01

The band-pass filtered left wheel path profile for test dates in 1994, 1995 and 1998 are shown in figure 23. The slabs at this section are curled upwards. The plot for the first profile date shows a high curvature, when compared to the profile plots for the other two profile dates. The site was profiled very early in the morning on the first profile date, and for other dates it was profiled between approximately 10:30 A.M. and 11:30 AM. The cause for the higher curvature for the first profile date is attributed to curling of the slab due to the temperature differential between the top and the bottom of the slab, that is maximum during the early morning. This effect can be clearly seen in a PSD plot by the high peak that occurs at a wavenumebr of 0.23 cycles per meter, which corresponds to a wavelength of 4.6 m. The decrease in roughness noted at the site was therefore caused by the higher initial IRI that was caused by curling due to temperature effects.

Figure 24 shows a bar graph of the IRI values of the test sections in the Arizona SPS-2 project. This figure shows the difference in IRI values between the first profile date when the site was profiled very early in the morning and the second profiling date when the site was profiled

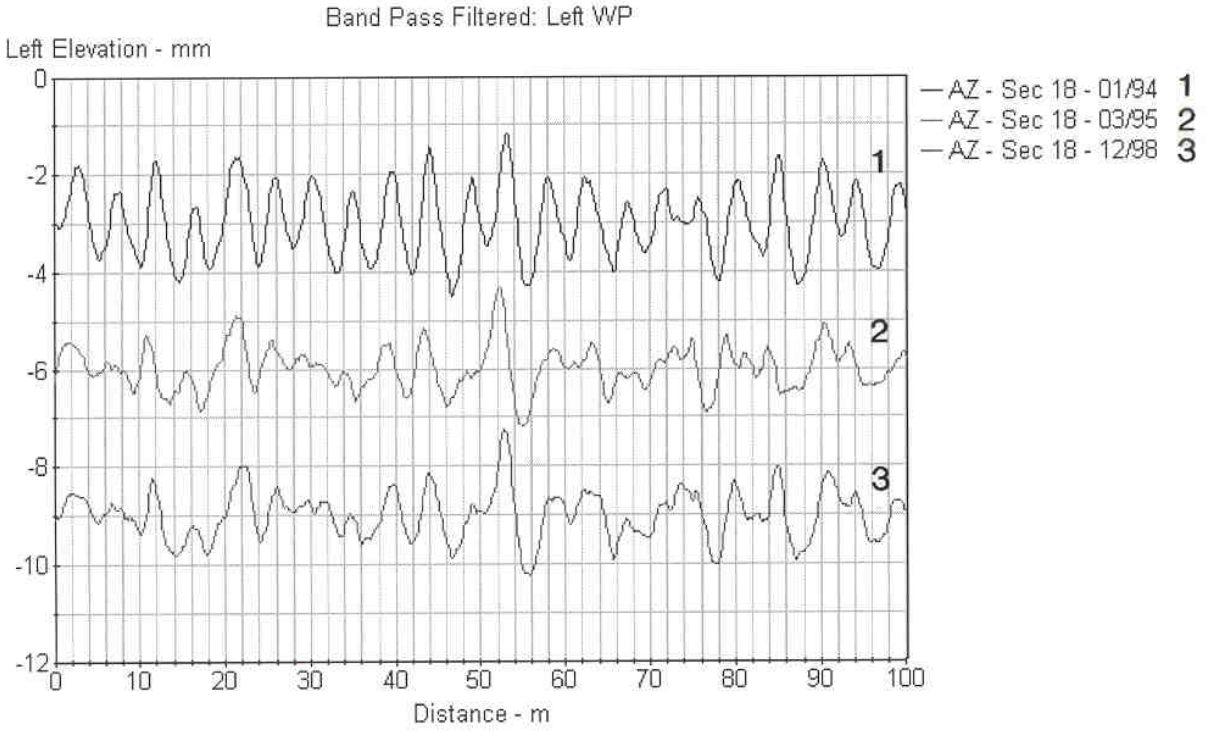

Figure 23. Band pass filtered profile plots – section 18 – Arizona.

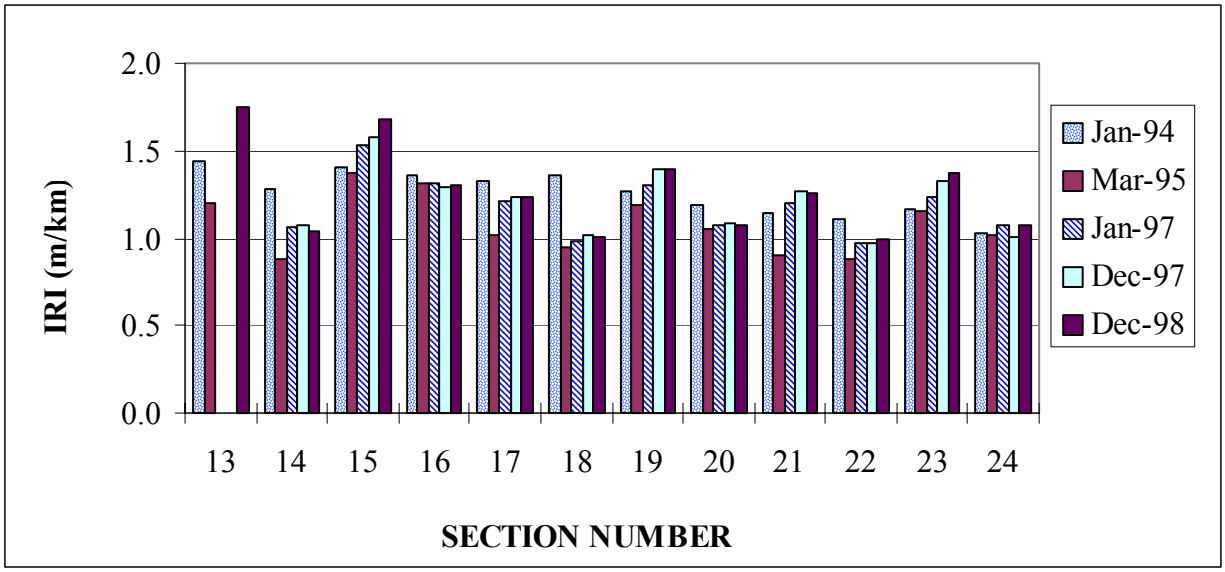

Figure 24. IRI values at SPS-2 project in Arizona.

approximately at 11:20 AM varied from section to section. This difference was minimal for sections that had 275 mm thick PCC slabs (sections 15, 16, 19, 20 23, 24), when compared to the other sections that had 200 mm thick PCC slabs.

Delaware – Section 6

Test section 6 in the Delaware SPS-2 project had a decrease in IRI of 28 percent when compared to the IRI at the first profile date. This section has a 200 mm PCC slab, which is on a DGAB base, and has a slab width of 4.27 m. The only other section in this project to show a decrease in IRI was section 3, which showed a decrease in IRI of 3 percent. The profile dates, profile times and IRI for this section are shown in table 22. The IRI of section 6 decreased from 1.04 m/km at the first profile date (1996) to 0.75 m/km at the last profile date (1998).

Table 22. IRI values – Section 6 – Delaware.

Profile Date	Profile Time	IRI (m/km)
12/6/96	10:53 AM	1.04
6/10/97	10:30 AM	0.74
9/29/97	10:57 AM	0.86
2/25/98	8:26 AM	0.90
5/13/98	1:33 PM	0.71
7/28/98	10:24 AM	0.75

The band-pass filtered left wheel path profile plots for three profile dates, first (12/96, IRI = 1.04 m/km), third (9/97, IRI = 0.86 m/km), and last (7/98, IRI = 0.75 m/km) are shown in figure 25. The profile plot shows the decrease in the curvature effect over the years, which contributed to the decrease in IRI over the years. As all three profiles were taken around 10:30 in the morning, the changes in curvatures should not be related to early morning curling effects.

Kansas - Section 6

Test section 6 in the Kansas SPS-2 project showed a decrease in IRI of 23 percent, when compared to the IRI obtained at the first profile date. This section has a 200 mm PCC slab, which is on a DGAB base, and has a slab width of 4.27 m. The profile dates, profile times and IRI for

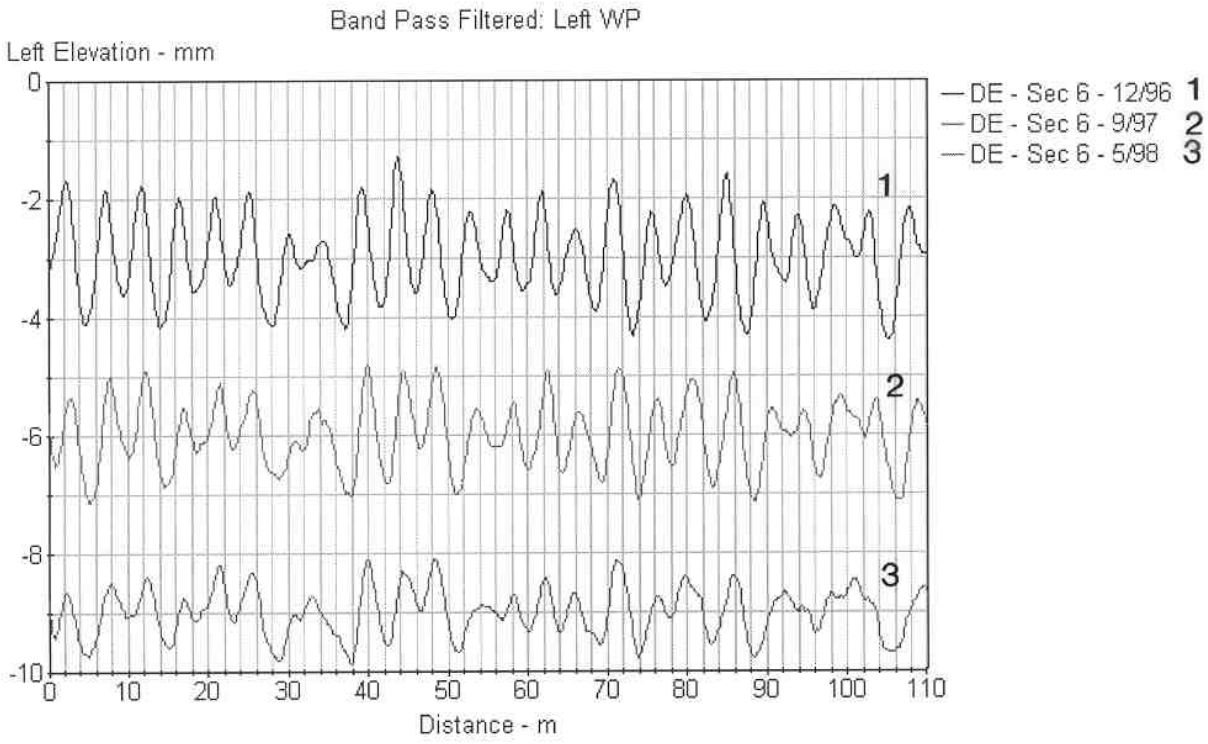

Figure 25. Band pass filtered profile plots – section 6 – Delaware.

this section are shown in table 23. The IRI of this section decreased from 2.09 m/km at the first profile date (1992) to 1.62 m/km at the last profile date (1999). The band pass filtered left wheel path profiles for the first (date = 1992, IRI = 2.09 m/km) and last profile dates (date = 1999, IRI = 1.62 m/km), as well as the profile for 1995 (IRI = 1.39 m/km) are shown in figure 26. The highest curvature in the profile plots is seen for the first profile date (1992) that had the highest IRI, while the least curvature is seen for 1995 when the IRI was the lowest. The effect of curvature is clearly seen in the last part of the profile. The variation in the IRI at this section can be attributed to curvature variations of the slabs. The highest IRI at the section occurred at the first profile date, when the section was profiled past noon. Therefore, the high IRI for this date cannot be attributed to early morning slab curling effects. The profiles in 1995 and 1999 were obtained relatively early in the morning, but yet the IRI at these two dates were less than the IRI obtained at the first profile date. The variation of slab curling observed at the site may be related to moisture variations in the PCC slab.

Table 23. IRI values – Section 6 – Kansas.

Profile Date	Profile Time	IRI (m/km)
8/14/92	1:52 PM	2.09
3/10/93	11:26 AM	1.51
5/15/94	11:00 AM	1.38
2/18/95	9:12 AM	1.39
4/20/96	1:31 PM	1.41
3/3/97	11:40 AM	1.70
5/15/98	10:26 AM	1.57
3/15/99	8:34 AM	1.62

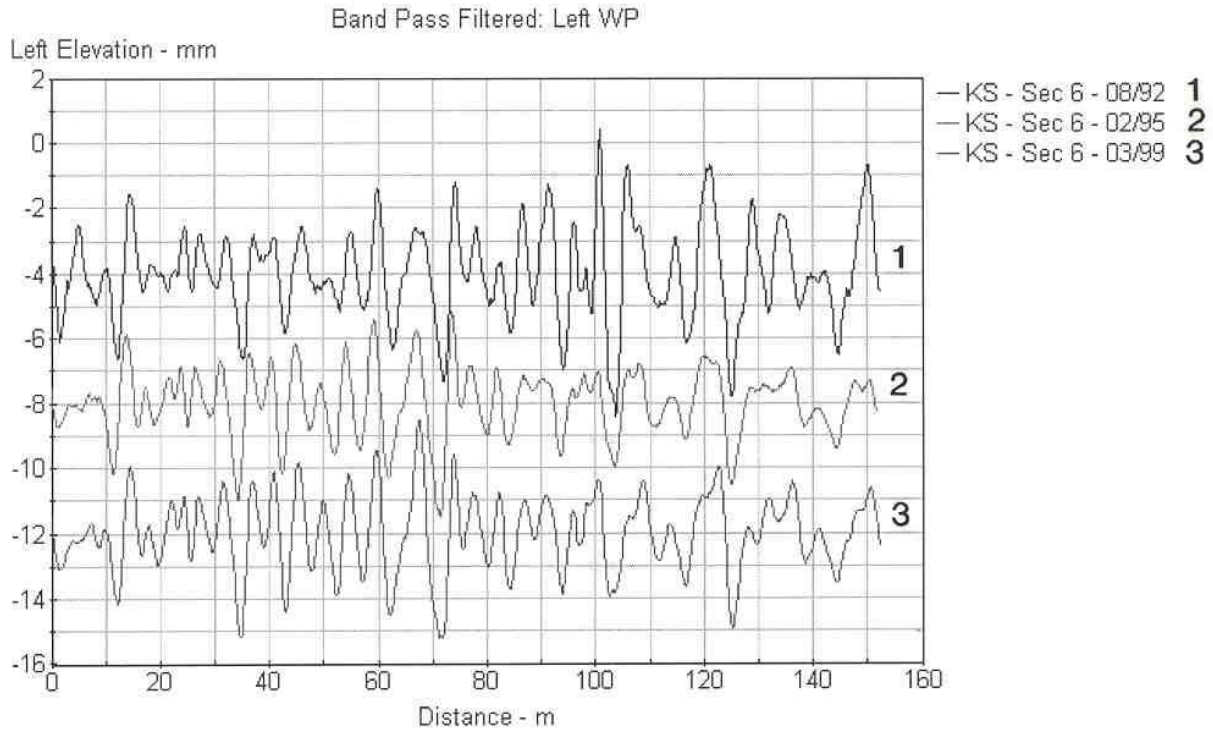

Figure 26. Band pass filtered profile plots – section 6 – Kansas.

Investigate Cause of Increase in Roughness at Test Sections in the North Carolina Project

All sections in the North Carolina project show an increase in IRI when compared to the IRI at the first profile date, with seven test sections showing an increase in IRI of over 10 percent. Section 2 in the project showed the highest percentage increase in IRI of 29 percent. This section has a 200 mm PCC slab, has a 150 mm thick DGAB base, and a slab width of 4.27 m. The profile dates, profile times, and IRI values for this test section is shown in table 24. The IRI of this section from the first profile date (3/94) to the seventh profile date (7/98) ranged from 1.37 m/km to 1.44 m/km. However, at the last (eighth) profile date, the IRI suddenly increased to 1.77 m/km.

Table 24. IRI values – section 2- North Carolina.

Profile Date	Profile Time	IRI (m/km)
3/30/94	10:28 AM	1.37
1/6/96	5:46 AM	1.42
2/28/96	10:43 AM	1.44
10/7/97	1:12 PM	1.41
2/18/98	1:57 PM	1.41
5/19/98	10:36 AM	1.38
7/24/98	11:31 AM	1.42
11/4/98	8:45 AM	1.77

The band pass filtered right wheel path profile plots for 10/97 (IRI = 1.41 m/km), 7/98 (IRI = 1.42 m/km), and last profile date of 11/98 (IRI = 1.77 m/km) are shown in figure 27. The slabs in this section are curled upwards. The plot shows that the slab curvature for the profile date of 11/98 is more than that of the other two dates. The increase in roughness at this test section at the last profile date was due to the increase in slab curvature. The IRI at the last profile date was obtained at 8:45 A.M. in the morning, and the increase in IRI that occurred for that date are attributed to early morning curling effects in the slab.

The PSD plots for profile dates of 10/97 (IRI = 1.41 m/km) and 11/98 (IRI = 1.77 m/km) are shown in figure 28. Note the difference in the plots at a wavenumber of 0.2, where there is a pronounced peak in the profile plot for the profile date of 11/98. The wave number of 0.2

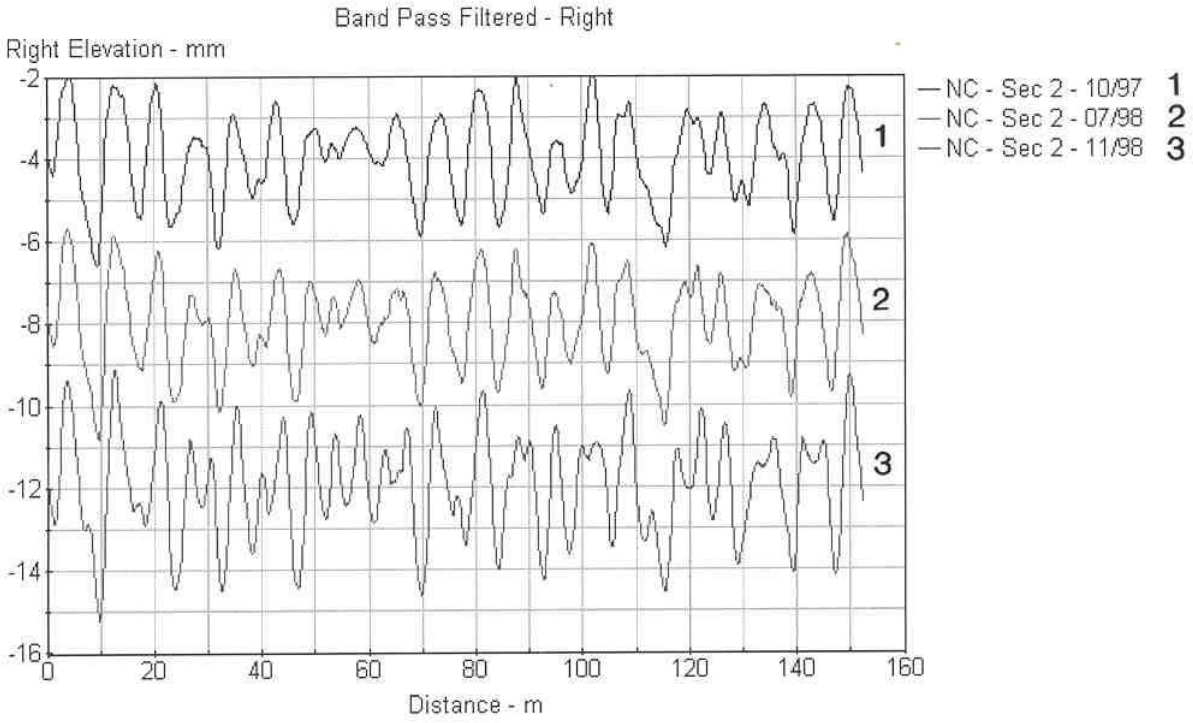

Figure 27. Band pass filtered profile plots – section 2 – North Carolina.

corresponds to a wavelength of 4.6 m, which is the slab length. The curling of the slabs, that are 4.6 m in length, caused a contribution to the IRI and made the IRI to increase at the last profile date.

The IRI values of all test sections in the North Carolina project for the different profiling dates are shown in figure 29. All sections in this project, except for section 10 show a sudden increase in IRI at the last profile dates. This is caused by early morning curling of the slabs. For this project, the effect of curling is seen for both slab thicknesses of 200 and 275 mm.

Investigate Cause for Increase in Roughness at the Nevada Project

All sections in the Nevada project show an increase in IRI when compared to the first profile date, with 5 sections showing an increase in IRI of over 40 percent. This increase in IRI occurred within a 2.2 year period. Section 7 in the Nevada project, which showed an increase in

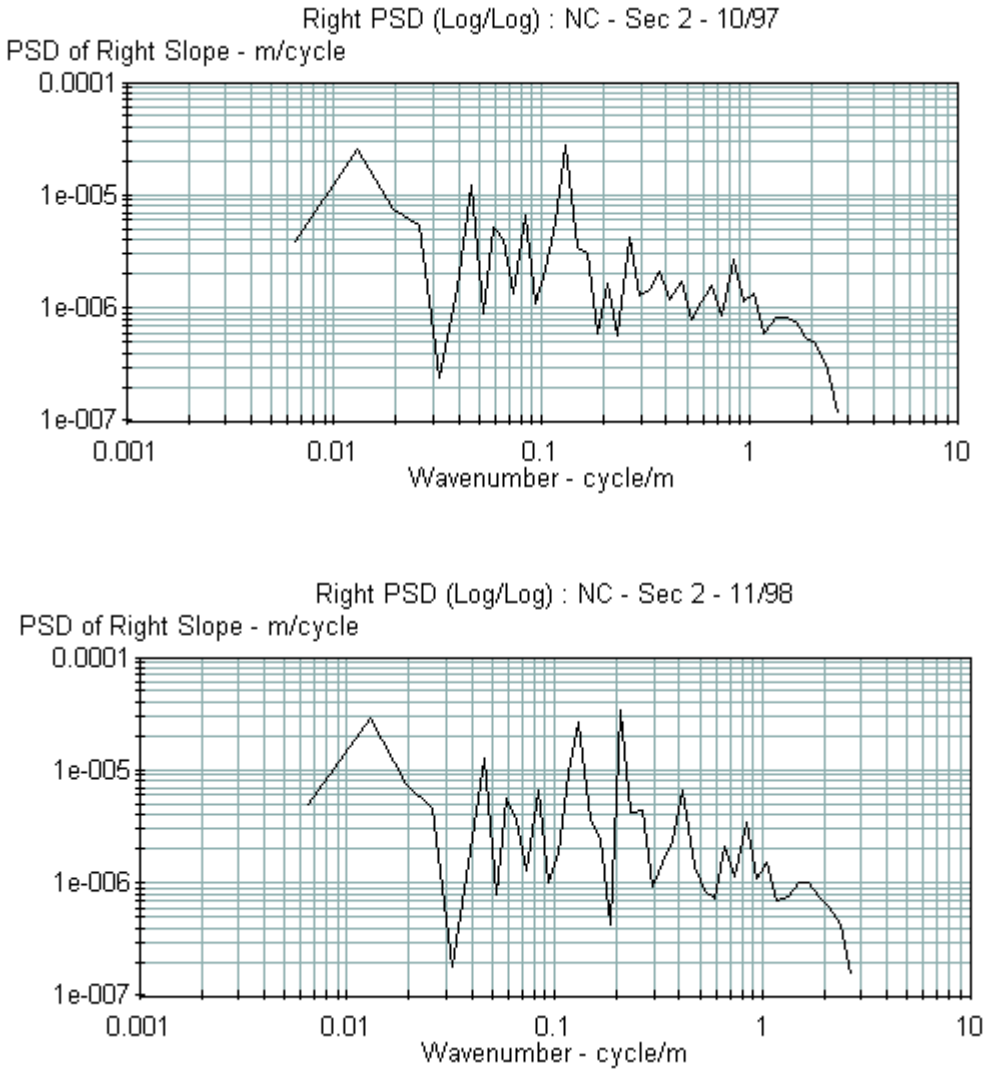

Figure 28. PSD plots – left wheel path profiles – section 2 – North Carolina.

IRI of 45 percent, was analyzed. This section has a 275 PCC slab, with a 150 mm LCB base, and a slab width of 4.27 m. The profile date, profile time and IRI values of test section 7 in the Nevada SPS-2 project are shown in table 25.

The IRI of this section at the first profile date was 1.0 m/km, but within 1.5 years it increased to 1.43 m/km at the third profile date, and remained close to this value at the last profile date. The band pass filtered right wheel path profile plots for the four profile dates are shown in figure 30. The slabs in this section are curled upwards. The profile plots show that the

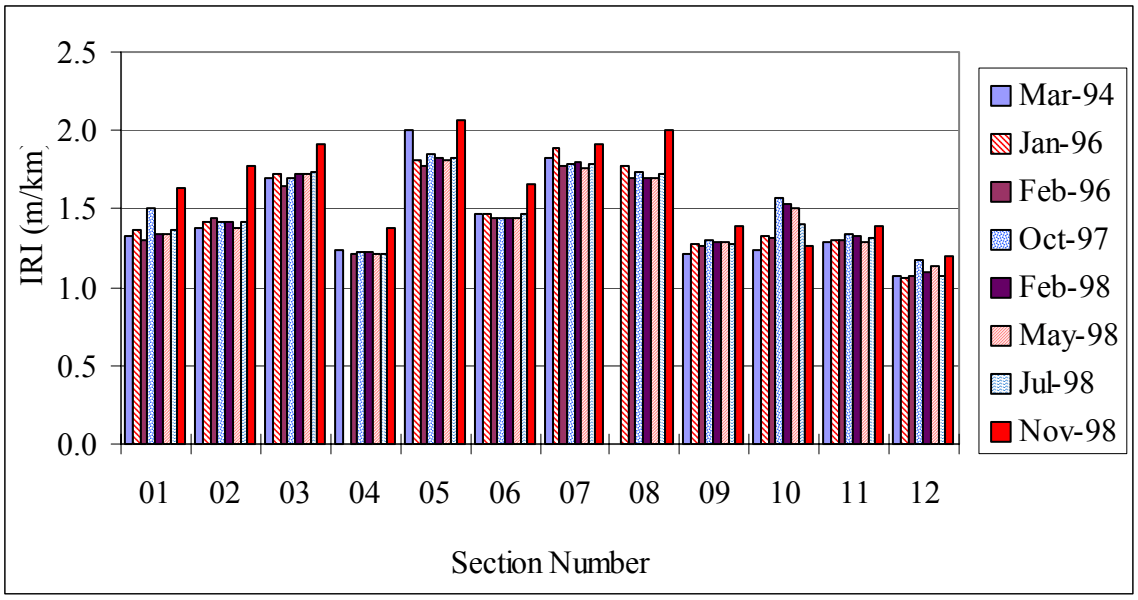

Figure 29. IRI values for North Carolina SPS-2 project.

Table 25. IRI values – Section 7- Nevada.

Profile Date	Profile Time	IRI (m/km)
6/28/96	1:01 PM	1.00
4/22/97	9:51 AM	1.12
11/18/97	2:47 PM	1.43
8/28/98	10:14 AM	1.44

slab curvature for the third and fourth profile dates are much more pronounced than the curvatures for the first and second profile dates. The increase in roughness at this section is attributed to the increase in curvature of the slabs. The other sections in this project that are showing a large increase in IRI also show a similar increase in slab curvature.

The construction report for this project indicated that construction difficulties were encountered during the construction of this project as the contractor had difficulties in working with the PCC mixes which were different than the mixes used in Nevada (15). Extensive transverse cracking had occurred throughout this project at a very early age.

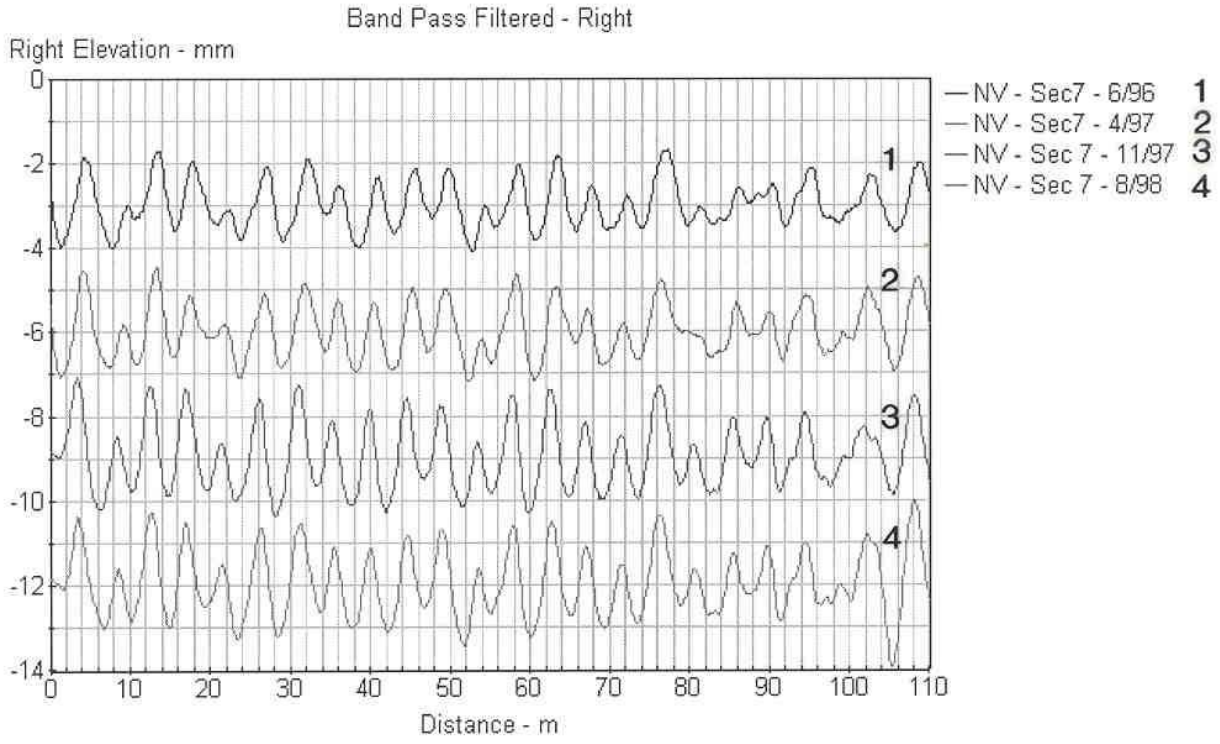

Figure 30. Band pass filtered profile plots – section 7 – Nevada.

Investigate Cause of High Variability in Roughness Over the Years

Section 14 in the Michigan SPS-2 project has shown highly variable IRI values over the years. This section has 200 mm PCC slab that is on a DGAB base, and has a 3.66 m slab width. The profile date, profile time and IRI values of this section are shown in table 26.

The IRI of this section at the first profile date in 1994 was 1.84 m/km, while the IRI at the last profile date in 1999 was 2.06 m/km. But between these years, the IRI of this section has ranged from a low of 1.22 m/km to a high of 2.71 m/km. Figure 31 shows the right wheel path band pass filtered profiles for 1994 (IRI = 1.84 m/km), 1997 (1.62 m/km), and 1998 (2.71 m/km). The variations in curvature for these three test dates are clearly seen in the plot, with increasing curvature corresponding to increasing roughness. The lowest IRI for this section

Table 26. IRI values – section 14 – Michigan.

Profile Date	Profile Time	IRI (m/km)
9/6/94	11:30 AM	1.84
8/11/95	9:35 AM	1.22
1/8/96	4:34 PM	2.17
4/9/96	10:11 AM	2.10
12/29/96	10:28 AM	2.03
4/15/97	1:05 PM	1.60
7/1/97	9:23 AM	1.62
11/5/98	4:35 PM	2.71
4/12/99	12:15 PM	2.06

occurred in 1995, with that profile being obtained at 9:35 AM. The IRI values shown in table 26 show that the IRI is not being influenced by early morning temperature effects. The curling effects seen at this section may be related to moisture variations within the PCC slab.

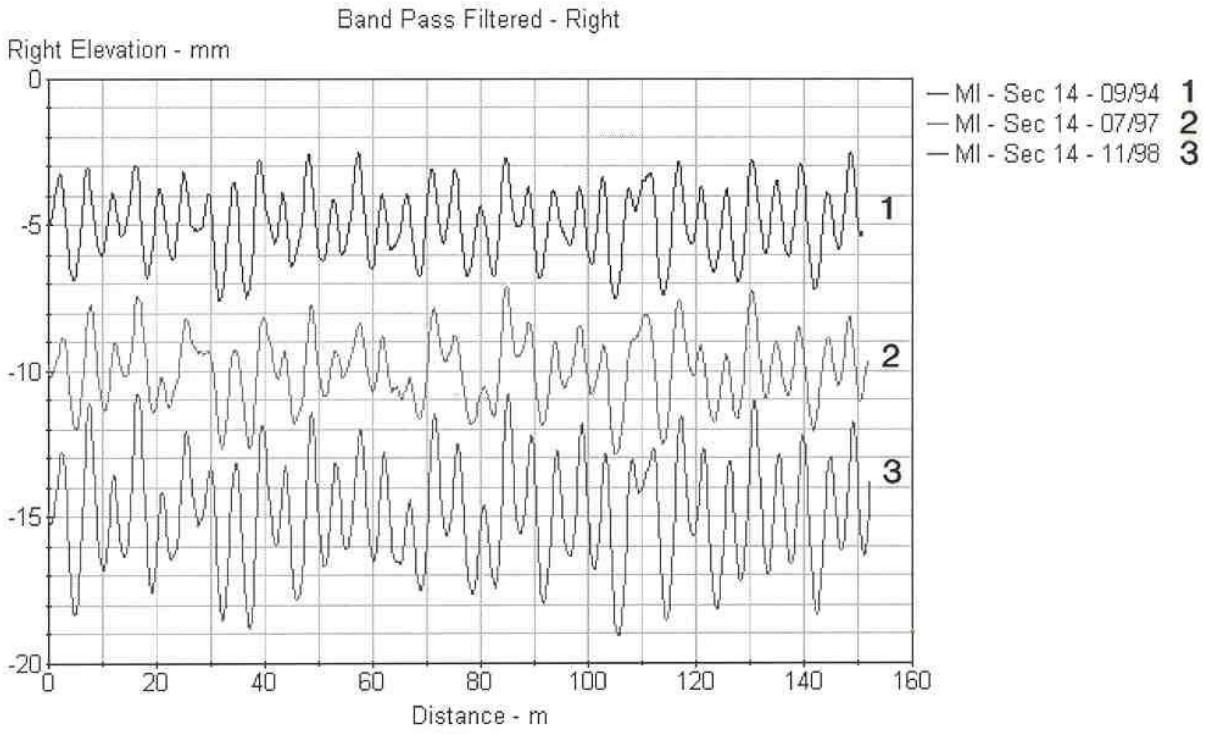

Figure 31. Band pass filtered profile plots – section 14 – Michigan.

Relationship Between Changes in IRI and Distress

Byrum (21) has shown that distresses in PCC slabs such as faulting is related to slab curvature. The sections that show high curvature or high variations in curvature are expected to show pavement distress early in the life. The distress data in the LTPP database was reviewed to see if the sections showing a high increase in IRI or a high reduction in IRI had higher distress when compared to the other sections. However, a clear relationship between IRI changes and pavement distress was not found. The only exception was the project in Nevada, where transverse cracking was noted at most sections in the Nevada project.

Summary of Findings

The data from the SPS-2 projects indicated the average early-age IRI of the 200 mm thick PCC pavements to be 1.27 m/km, with the standard deviation of IRI being 0.28 m/km. For the 275 mm thick PCC pavements, the average IRI was 1.30 m/km, with the standard deviation of IRI being 0.30 m/km. A statistical test on the early-age IRI considering the two PCC thicknesses of 200 mm and 275 mm indicated that PCC thickness was not significant. The PCC surface in the SPS-2 projects have been placed on three different base types: DGAB, LCB and PATB. The average early-age IRI values for PCC pavements placed on DGAB, LCB, and PATB were 1.27 m/km, 1.40 m/km, and 1.25 m/km, respectively. The highest early-age IRI was obtained for PCC surfaces placed on LCB.

An evaluation of the changes in roughness that had occurred over the monitored period at the SPS-2 sections indicated several distinct patterns: (1) some sections in some of the projects showed high increases in roughness, (2) some sections in some projects showed a reduction in roughness, (3) most of the sections in the Nevada project showed very high increases in roughness, (4) most of the sections in the North Carolina project showed an increase in roughness in excess of 10 percent, (5) Some sections in some projects showed very high variability in roughness between the years. An investigation was carried out using the profile

data to determine if the cause for the changes in roughness that have occurred for the cases described previously could be found. In all of the investigated cases, it was found that the changes in roughness that had occurred could be related to changes in curvature of the PCC slabs.

Some of the sections that have shown a high increase in roughness are: (1) section 13 in the Arizona project that showed an increase in IRI of 21 percent over a 5 year period, (2) section 13 in the Michigan project that showed an increase in IRI of 95 percent over a 4.5 year period, and section 6 in Washington that showed an increase in roughness of 52 percent over a 3.5 year period. The cause for the increase in roughness of the sections in the Arizona and Michigan projects was the increase in upward slab curvature over time. For the section in the Washington project, the increase in roughness was caused by the increase in downward slab curvature over time. These changes were not due to temperature variations, and may have been caused by changes in moisture conditions within the PCC slab over time.

Some of the sections that have shown a decrease in roughness are: (1) section 18 in Arizona that showed a decrease in IRI of 26 percent, (2) Section 6 in Delaware that showed a decrease in IRI of 26 percent, (3) Section 6 in Kansas that showed a decrease in IRI of 23 percent. The cause for the decrease in IRI for the project in Arizona was because the section was first profiled early in the morning, when temperature related curling was present in the slab. For the sections in Delaware and Kansas, the reduction in roughness was not due to a temperature effect, but caused by a decrease in slab curvature over time, which may have been caused by variations in the moisture conditions in the PCC slab over time.

Most of the sections in the project in North Carolina showed a sudden increase in roughness at the last profile date, with some sections showing an increase as much as 25 percent. The cause for this increase in roughness was because the section was last profiled early in the morning when slab curling due to temperature was present, and this resulted in an increase in roughness. Most of the sections in the Nevada project showed very high increases in roughness with 5 sections showing an increase in IRI of over 40 percent that occurred with a 2 year period. The cause for the increase in roughness of these sections was the increase in slab curvature that

occurred over time. A few of the SPS-2 sections showed large variations in roughness over the monitored period. Section 14 in Michigan had an IRI of 1.84 m/km the first time it was profiled, and an IRI of 2.06 m/km after five years. In between these two dates, the section had been profiled seven times, with the IRI ranging between 1.22 m/km and 2.71 m/km during this period. The variations in IRI at this section were caused by changes in slab curvature, which was not caused by temperature affects.

In the Nevada project, large changes in IRI occurred at both 200 mm and 275 mm thick PCC slabs. However, in other project large changes in roughness generally occurred on sections that had 200 mm thick PCC slabs. Test section 1 in all projects showed an increase in IRI of over 10 percent. Test section 1 has a 200 mm thick PCC slab that had a 14-day flexural strength target of 3.8 Mpa, and rests on a DGAB base. Section 1 in all projects showed an increase in curvature over the years, and the cause for the increase in IRI is attributed to the increase in curvature. It appears that this particular pavement section is more susceptible to changes in curvature than the rest of the pavement sections in the SPS-2 experiment.

CHAPTER 6

ROUGHNESS CHARACTERISTICS OF SPS-5 AND SPS-6 PROJECTS

SPS-5 EXPERIMENT: REHABILITATION OF ASPHALT CONCRETE PAVEMENTS

Introduction

The specific pavement studies SPS-5 experiment was developed to investigate the performance of selected AC rehabilitation treatment factors. The rehabilitation treatment factors include overlay mix type (recycled and virgin), overlay thickness (50 mm and 125 mm), and surface preparation of the existing AC surface prior to overlay (minimal and intensive preparation). Nine test sections are included in each SPS-5 project, with eight sections being experimental sections and one section being the control section. The overlay thickness, type of AC used for the overlay (virgin or recycled) and the type of surface preparations that is carried out on the test sections prior to placing the AC overlay are shown in table 27.

Table 27. Treatments applied to SPS-5 test sections.

Section Number	Surface Preparation	Type of AC	Overlay Thickness (mm)
1	Routine Maintenance	-	0
2	Minimum surface preparation	Recycled	50
3	Minimum surface preparation	Recycled	125
4	Minimum surface preparation	Virgin	125
5	Minimum surface preparation	Virgin	50
6	Intensive surface preparation	Virgin	50
7	Intensive surface preparation	Virgin	125
8	Intensive surface preparation	Recycled	125
9	Intensive surface preparation	Recycled	50

Table 28 presents a description of the types of surface preparation activities that were carried out at the sections prior to placing the AC overlay. Section 1 is designated as a control section, which receives only limited routine-type maintenance. Repair activities on the control

Table 28. Surface preparation activities for SPS-5 test sections.

Test Section Details	Surface Preparation								
Treatment Options		Minimal				Intense			
Section Number	1	2	3	4	5	6	7	8	9
Overlay Thickness (mm)	0	50	125	125	50	50	125	125	50
Overlay Material	-	R	R	V	V	V	V	R	R
Patching	X	X	X	X	X	P	P	P	P
Crack Sealing	X	-	-	-	-	P	P	P	P
Leveling	-	A	A	A	A	-	-	-	-
Milling	-	F	F	F	F	X	X	X	X
Seal Coat	B	-	-	-	-	-	-	-	-

R - Recycled Hot Mixed Asphalt Concrete
V - Virgin Hot Mixed Asphalt Concrete
X - Perform
A - If ruts are > 12 mm
B - Not permitted in first year of study
P - Perform after milling as required
F - Milling permitted only to remove open graded friction courses

section are limited to those maintenance activities needed to keep the section in a safe and functional condition. Repair activities on this section were carried out according to the guidelines of the State highway agency. The minimal level of surface preparation applies to test sections 2 through 5, and consists primarily of patching of severely distressed areas and potholes and placement of a leveling course in ruts that are greater than 12 mm. The intensive level of preparation applies to test sections 6 through 9, and includes milling of the existing AC surface, patching of distressed areas, and crack sealing after milling. Milling of the surface is the primary difference between the minimal and intensive preparation levels in this experiment. Milling was performed in the intensive surface preparation sections to a depth of 38 to 50 mm, and the depth of material removed by milling was replaced with an equal thickness of AC overlay material. This material is a virgin mix on test sections 6 and 7 and a recycled mix on test sections 8 and 9. The depth of replacement material is not counted as a part of the overlay thickness specified in the experiment. The recycled AC that is used consisted of 30 percent recycled asphalt mix.

Analyzed Projects

A review of the IMS database indicated that profile data were available for seventeen SPS-5 projects. Table 29 presents the following information for each SPS-5 project: state located, climatic zone, subgrade type, if pre-rehabilitation IRI and distress data are available for the project, rehabilitation date, age of project at first profile date, age of project at last available profile date, number of times the project has been profiled after rehabilitation, pre-rehabilitation IRI of the project, and the annual ESALs at the site. The pre-rehabilitation IRI of the project was computed by averaging the pre-rehabilitation IRI of all test sections in the SPS-5 project.

Figure 32 shows the pre-rehabilitation IRI of the SPS-5 projects. The pre-rehabilitation IRI was computed by averaging the pre-rehabilitation IRI of all test sections in a SPS-5 project. Out of the fifteen projects for which pre-rehabilitation IRI values were available, 53 percent of the projects had an IRI over 1.5 m/km, while 47 percent of the projects had an IRI of less than 1.5 m/km. Considering that an IRI value of 1.5 m/km corresponds to a present serviceability rating of 3.4 (22), 47 percent of the projects were in a fairly good condition from a roughness point of view when rehabilitation was performed. In fact the projects in Alabama, Florida, Georgia and Maine had project IRI values between 1.0 and 1.2 m/km, which are very low IRI values.

Figure 33 presents the pre-rehabilitation standard deviation of IRI of the test sections that are contained in each SPS-5 project. There were large differences in the variability of IRI values between the test sections for the different projects. The standard deviation of IRI between the projects ranged from a low of 0.11 m/km (Georgia) to a high of 0.56 m/km (Colorado).

Table 30 presents the average distress per section at the SPS-5 projects prior to rehabilitation for the following distress types: fatigue cracking, block cracking, longitudinal cracking, transverse cracking and patching. The average distress per section for a specific distress type in a project was computed by averaging the distresses present in all test sections. For each distress type, all severity levels were combined in computing the average. Table 30 also

Table 29. SPS-5 projects.

State	State Code	Climatic Zone (Note 1)	Subgrade Type	Availability of Pre-Rehabilitation Data		Rehab. Date	Age of Project After Rehabilitation at First Profile Date (yr)	Age of Project at Last Profile Date (yr)	Number of Times Profiled After Rehabilitation	Pre-Rehab. Project IRI (m/km)	Traffic KESAL (per year)
				IRI	Distress						
Alabama	AL	WNF	Coarse	Yes	Yes	12/19/91	0.3	4.3	3	1.2	N/A
Alberta	AB	DF	Coarse	Yes	Yes	10/3/90	0.0	8.6	9	1.9	N/A
Arizona	AZ	DNF	Coarse	Yes	Yes	4/20/90	0.4	8.6	6	1.9	206
California	CA	DNF	Coarse	Yes	Yes	4/25/92	0.8	6.9	5	2.1	1591
Colorado	CO	DF	Fine	Yes	Yes	10/3/91	0.1	7.8	8	1.9	438
Florida	FL	WNF	Coarse	Yes	Yes	4/5/95	0.6	2.4	2	1.2	N/A
Georgia	GA	WNF	Coarse	Yes	No	6/7/93	2.9	5.9	2	1.0	N/A
Maine	ME	WF	Coarse	Yes	Yes	6/20/95	2.2	3.0	2	1.2	N/A
Manitoba	MB	DF	Fine	No	Yes	9/1/89	0.1	9.9	9	N/A	N/A
Maryland	MD	WF	Fine	Yes	Yes	4/1/92	0.2	6.4	6	1.6	N/A
Minnesota	MN	WF	Fine	Yes	Yes	9/15/90	0.8	8.0	6	2.8	57
Mississippi	MS	WNF	Fine	Yes	No	9/24/90	0.1	8.6	5	2.3	676
Montana	MT	DF	Coarse	Yes	Yes	9/11/91	0.2	7.7	9	1.4	N/A
New Jersey	NJ	WF	Coarse	Yes	Yes	8/18/92	0.2	6.0	5	1.9	347
New Mexico	NM	DNF	Coarse	No	No	9/11/96	0.5	0.5	1	N/A	N/A
Oklahoma	OK	WNF	Fine	Yes	No	7/8/97	0.5	0.5	1	1.9	N/A
Texas	TX	WNF	Fine	Yes	No	9/1/91	0.4	5.8	4	1.5	N/A

Note 1: DF - Dry Freeze, DNF - Dry No-Freeze, WF - Wet Freeze, WNF - Wet No-Freeze

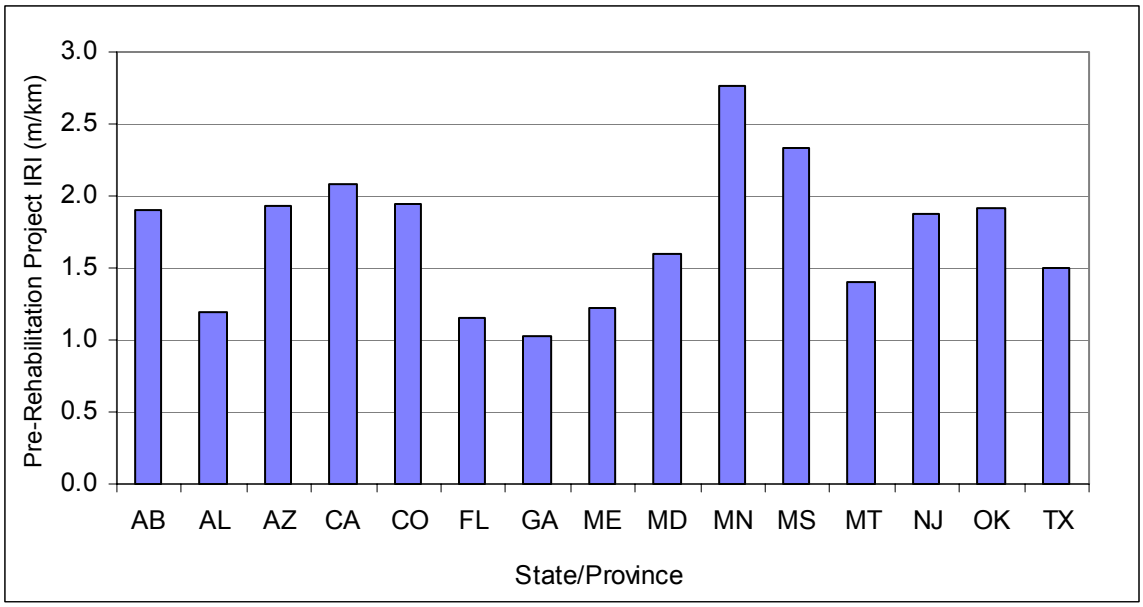

Figure 32. Pre-rehabilitation project IRI of SPS-5 projects.

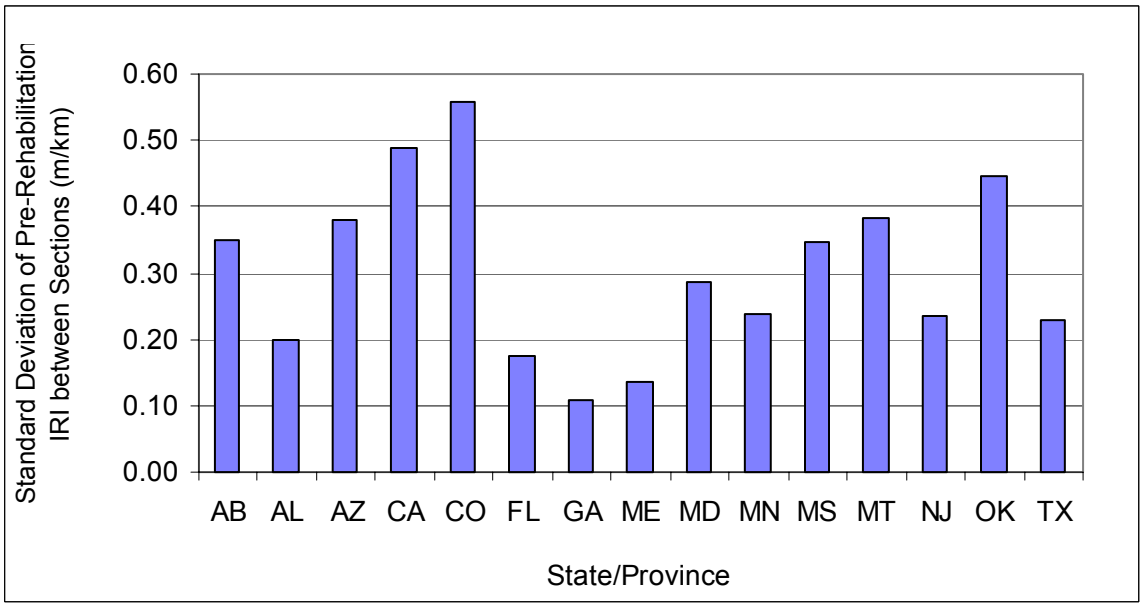

Figure 33. Standard deviation of pre-rehabilitation IRI of test sections in SPS-5 projects.

presents the average pre-rehabilitation IRI for each project. The project in Florida has a very low IRI, but is exhibiting a significant amount of distress. Table 31 presents the standard deviation of distress for the test sections in each project for fatigue cracking, block cracking, longitudinal

Table 30. Average distress and pre-rehabilitation IRI for SPS-5 projects.

State	Average Value For a Section							
	Pre-Rehab. IRI (m/km)	Fatigue Cracking (m^2)	Block Cracking (m^2)	Longitudinal Cracking (m)	Transverse Cracks (No)	Transverse Cracks (m)	Patches (No)	Patches (m^2)
Alabama	1.2	24	0	0	0	0	3	1
Alberta	1.9	1	0	1	0	1	0	0
Arizona	1.9	74	0	142	130	277	0	0
California	2.1	37	0	87	70	117	0	0
Colorado	1.9	12	0	144	16	20	1	8
Florida	1.2	183	156	138	66	34	0	0
Georgia	1.0	N/A	N/A	N/A	N/A	N/A	N/A	N/A
Maine	1.2	0	0	275	20	6	0	0
Manitoba	N/A	5	0	11	2	3	1	41
Maryland	1.6	73	5	51	11	33	1	3
Minnesota	2.8	0	0	152	37	129	0	0
Mississippi	2.3	N/A	N/A	N/A	N/A	N/A	N/A	N/A
Montana	1.4	131	10	46	44	72	0	0
New Jersey	1.9	77	179	19	11	19	2	5
New Mexico	N/A	N/A	N/A	N/A	N/A	N/A	N/A	N/A
Oklahoma	1.9	N/A	N/A	N/A	N/A	N/A	N/A	N/A
Texas	1.5	N/A	N/A	N/A	N/A	N/A	N/A	N/A

Note: N/A – Data not available.

cracking and transverse cracking. The data shows that there is variability in the amount of distresses present at the test sections in a specific project. The largest standard deviation in distress was observed for the projects in Florida and New Jersey. The large standard deviation in block cracking and fatigue cracking observed in these two projects may have been caused by inconsistent classification of these two distress types between the sections.

IRI After Rehabilitation

The average IRI of the SPS-5 projects after rehabilitation is presented in figure 34, while the standard deviation of IRI values for the test sections within a project is presented in figure 35. The average and the standard deviation values were computed using the IRI values for sections 2 through 9, all of which received an AC overlay. The post-rehabilitation project IRI ranged from

Table 31. Standard deviation of pre-rehabilitation distress for test sections in SPS-5 projects.

State	Average Pre-Rehab. IRI (m/km)	Standard Deviation of Distress				
		Fatigue Cracking (m^2)	Block Cracking (m^2)	Longitudinal Cracking (m)	Transverse Cracks (No)	Transverse Cracks (m)
Alabama	1.2	11	-	-	-	-
Alberta	1.9	4	-	1	1	1
Arizona	1.9	60	-	87	50	118
California	2.1	13	-	63	45	85
Colorado	1.9	16	-	17	10	13
Florida	1.2	207	208	235	114	59
Georgia	1.0	N/A	N/A	N/A	N/A	N/A
Maine	1.2	-	-	35	22	6
Manitoba	N/A	13	-	16	2	4
Maryland	1.6	48	11	43	3	9
Minnesota	2.8	-	-	9	7	28
Mississippi	2.3	N/A	N/A	N/A	N/A	N/A
Montana	1.4	51	28	20	23	34
New Jersey	1.9	150	119	25	6	12
New Mexico	N/A	N/A	N/A	N/A	N/A	N/A
Oklahoma	1.9	N/A	N/A	N/A	N/A	N/A
Texas	1.5	N/A	N/A	N/A	N/A	N/A

Note: N/A Data not available
- Distress type not present

0.49 m/km (New Mexico) to 1.50 m/km (Mississippi). The project in New Mexico had the lowest standard deviation in IRI (0.04 m/km) with the project in Manitoba having the highest standard deviation in IRI (0.26 m/km). The post-rehabilitation IRI values for each test section in the SPS-5 projects are shown in table 32.

Relationship Between IRI Before and After Rehabilitation

Figure 36 shows the relationship between IRI prior to overlay and after overlay for the test sections in the SPS-5 experiment, differentiated according to the overlay thickness. Data from fifteen SPS-5 projects are shown in this figure. As there are 8 test sections in each SPS-5 project that received an overlay, in figure 36 there are 60 data points each for 50 mm and 125

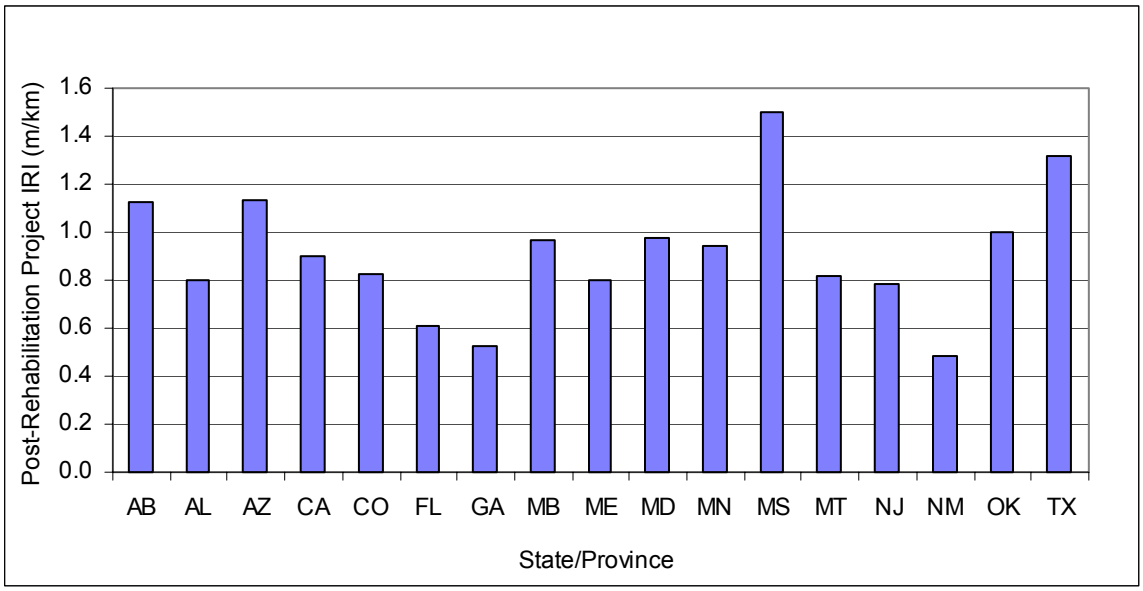

Figure 34. Post-rehabilitation project IRI for SPS-5 projects.

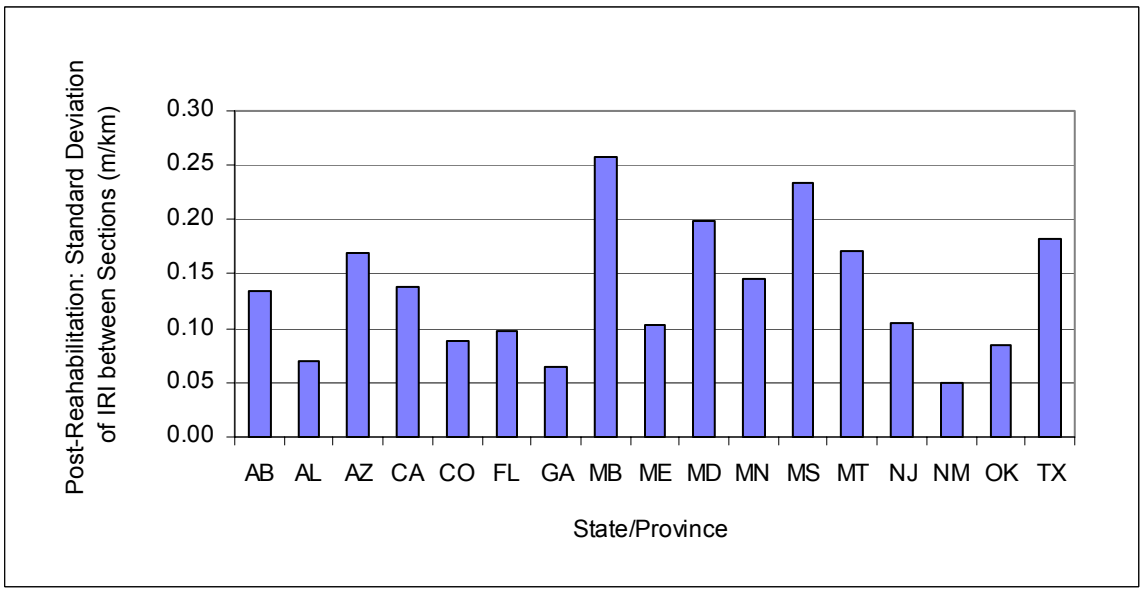

Figure 35. Post-rehabilitation standard deviation in IRI for SPS-5 projects.

mm overlays. As shown in this figure, there were several test sections that had low IRI values (i.e., close to 1.0 m/km) prior to rehabilitation. The IRI of these sections generally reduced by a small amount after rehabilitation. For sections that had an IRI of less than 1.5 m/km prior to overlay, the IRI after overlay was less than 1.0 m/km for approximately 80 percent of the

Table 32. Post-rehabilitation IRI values for test sections in SPS-5 projects.

State	Pre-Rehab IRI of Project (m/km)	IRI After Rehabilitation (m/km)								
		Test Section								Average (m/km)
		2	3	4	5	6	7	8	9	
Alabama	1.2	0.76	0.77	0.83	0.85	0.82	0.70	0.93	0.81	0.81
Alberta	1.9	1.04	1.05	1.29	1.14	1.06	1.38	1.04	1.01	1.12
Arizona	1.9	1.36	0.95	1.20	1.27	1.02	1.30	0.94	1.03	1.13
California	2.1	0.95	1.08	1.02	0.72	0.81	0.83	0.75	1.01	0.90
Colorado	1.9	0.94	0.78	0.83	0.78	0.93	0.70	0.78	0.91	0.83
Florida	1.2	0.68	0.74	0.64	0.49	0.50	0.55	0.72	0.57	0.61
Georgia	1.0	0.52	0.53	0.48	0.56	0.47	0.47	0.66	0.52	0.53
Maine	1.2	1.39	0.68	0.88	0.84	0.67	0.79	0.82	0.75	0.85
Manitoba	N/A	1.20	0.79	0.79	1.08	1.45	0.69	0.81	0.99	0.97
Maryland	1.6	1.39	1.03	0.91	1.00	0.74	0.88	0.79	1.03	0.97
Minnesota	2.8	0.85	0.76	1.12	1.08	1.08	0.85	1.00	0.78	0.94
Mississippi	2.3	1.41	1.80	1.20	1.72	1.41	1.26	1.41	1.78	1.50
Montana	1.4	0.89	1.00	0.69	0.68	0.69	1.14	0.75	0.71	0.82
New Jersey	1.9	0.99	0.67	0.72	0.89	0.73	0.78	0.74	0.75	0.78
New Mexico	N/A	0.45	0.59	0.45	0.44	0.47	0.44	0.51	0.49	0.48
Oklahoma	1.9	1.32	1.14	1.01	1.07	1.02	1.00	0.88	0.94	1.05
Texas	1.5	1.23	1.11	1.54	1.36	1.52	1.45	1.06	1.24	1.32
Average		**1.02**	**0.91**	**0.92**	**0.94**	**0.91**	**0.89**	**0.86**	**0.90**	

projects. Figure 36 shows that the IRI after overlay for most projects that had an IRI prior to overlay of greater than 1.5 m/km fell within a relatively narrow band of between 0.8 and 1.2 m/km. The data shows that overlays that are 50 mm thick are capable of reducing the IRI by a large amount. For example, such overlays were capable of achieving an IRI of less than 1.0 m/km for sections that had an IRI of 2.5 m/km prior to overlay.

A statistical analysis was conducted to determine if there was a relationship between the pre-rehabilitation IRI and the IRI after rehabilitation. The effect of overlay thickness, milling and AC type were also investigated in this analysis. The statistical analysis was performed by fitting a linear model to predict the IRI after rehabilitation by considering the following factors as independent variables: State, pre-rehabilitation IRI, overlay thickness (two levels), milling (yes or no), and AC type (virgin or recycled). The interaction terms between pre-rehabilitation IRI, overlay thickness, milling and AC type were also considered in the model. The factors State,

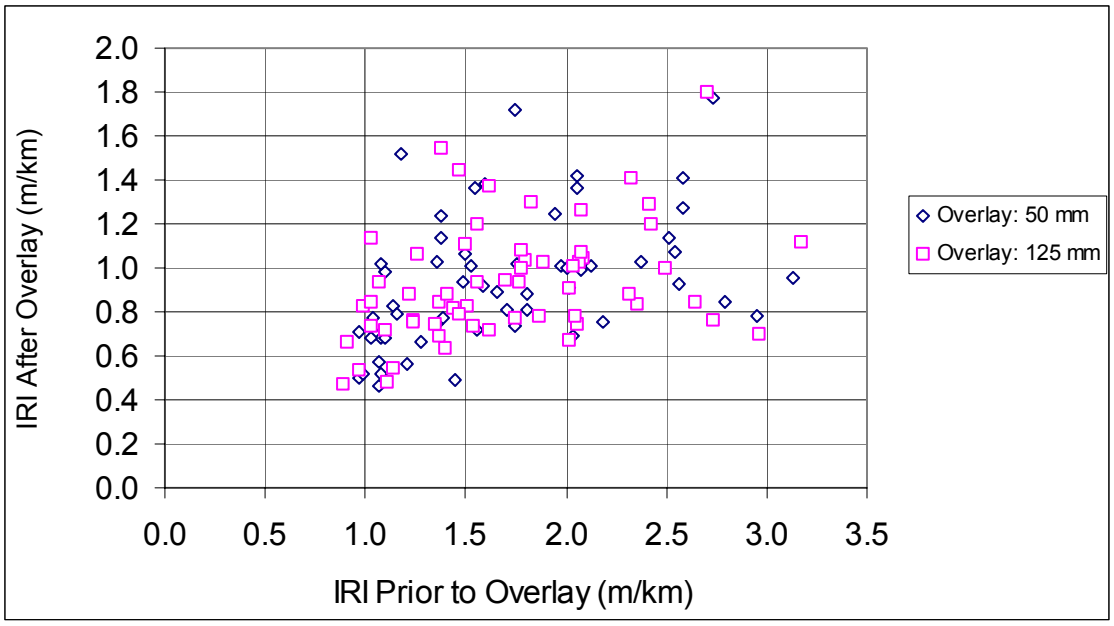

Figure 36. Relationship between IRI prior to overlay and IRI after overlay.

overlay thickness, milling and AC type are qualitative variables, while IRI after rehabilitation and pre-rehabilitation IRI are quantitative variables. The linear model function in S-plus software was used to fit the model. After fitting a model an ANOVA was performed and the main effects and the interactions were checked for significance. Only the factor State was significant, although there was evidence of a weak effect of milling (p-value = 0.07). The results from the statistical analysis indicated that the IRI after overlay did not depend on pre-rehabilitation IRI, overlay thickness, if milling was performed or not prior to overlay, or on the type of AC (virgin or recycled). These results are in agreement with the average IRI value for each section shown in table 32, where the average IRI of the sections are close to each other.

As many of the SPS-5 projects had pre-rehabilitation project IRI values that were less than 1.5 m/km, a similar analysis as described previously was performed to see if a different result would be obtained if only the projects that had an IRI greater than 1.5 m/km were considered. The projects considered for this analysis were: Alberta, Arizona, California, Colorado, Maryland, Minnesota, Mississippi, New Jersey and Oklahoma. This analysis indicated that factors State and milling were significant. Therefore, the analysis indicated for projects that

have an IRI of greater than 1.5 m/km, milling of the surface prior to overlay does result in a smoother pavement.

Figure 37 shows the relationship between IRI prior to overlay and IRI after overlay for sections that received a 50 mm overlay, with data points differentiated between sections that did and did not receive milling prior to overlay. Figure 38 shows a similar plot for sections that received a 125 mm overlay. For sections that had an IRI of greater than 1.5 m/km, the sections with milling prior to overlay generally had a lower IRI than sections that were not milled, which confirms the results of the statistical analysis.

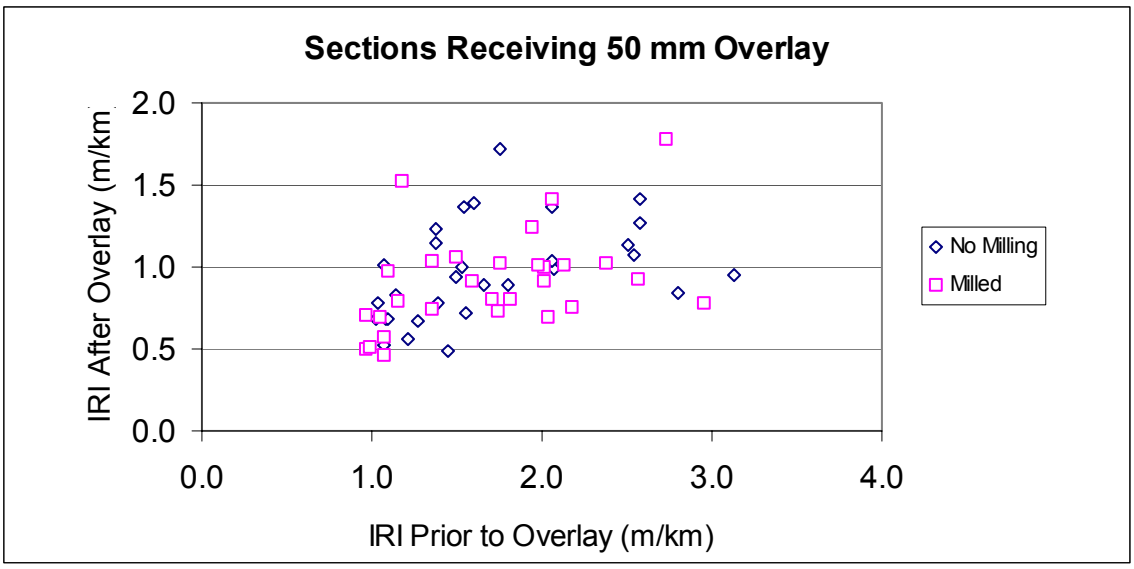

Figure 37. Relationship between IRI prior to and after overlay for 50 mm overlays.

The cumulative frequency distribution of IRI after rehabilitation for test sections in the projects that had an IRI greater than 1.5 m/km is presented in figure 39. This figure shows an IRI of less than 1.0 m/km was obtained for 50 percent of sections that received either a 50 mm or 125 mm overlay, but were not milled prior to overlay. For sections that were milled prior to overlay, 60 percent of sections with 50 mm overlays and 70 percent of sections with 125 mm overlays obtained IRI values that were less than 1.0 m/km.

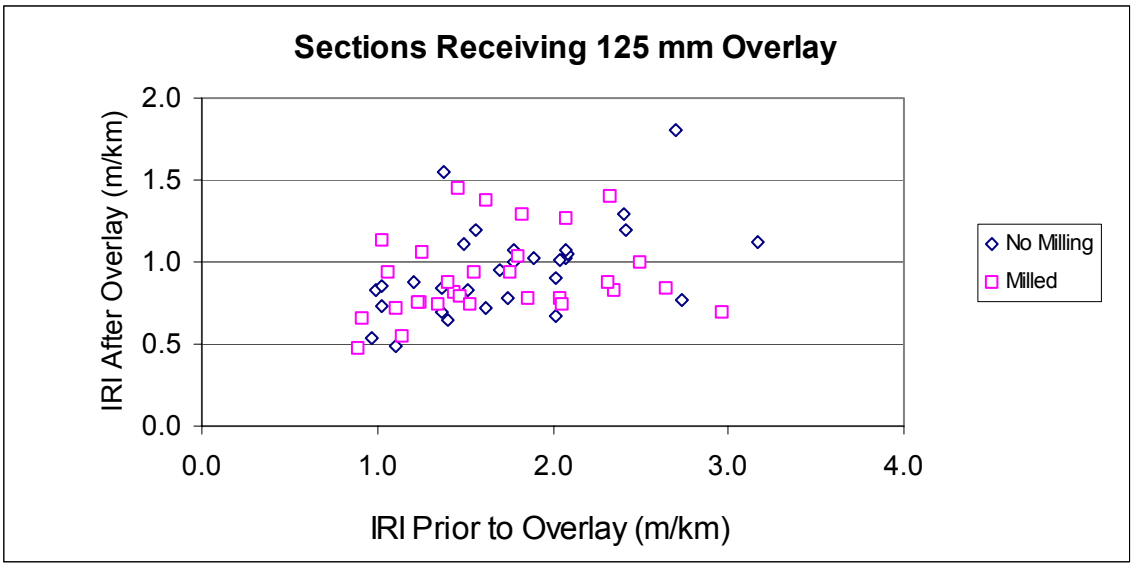

Figure 38. Relationship between IRI prior to and after overlay for 125 mm overlays.

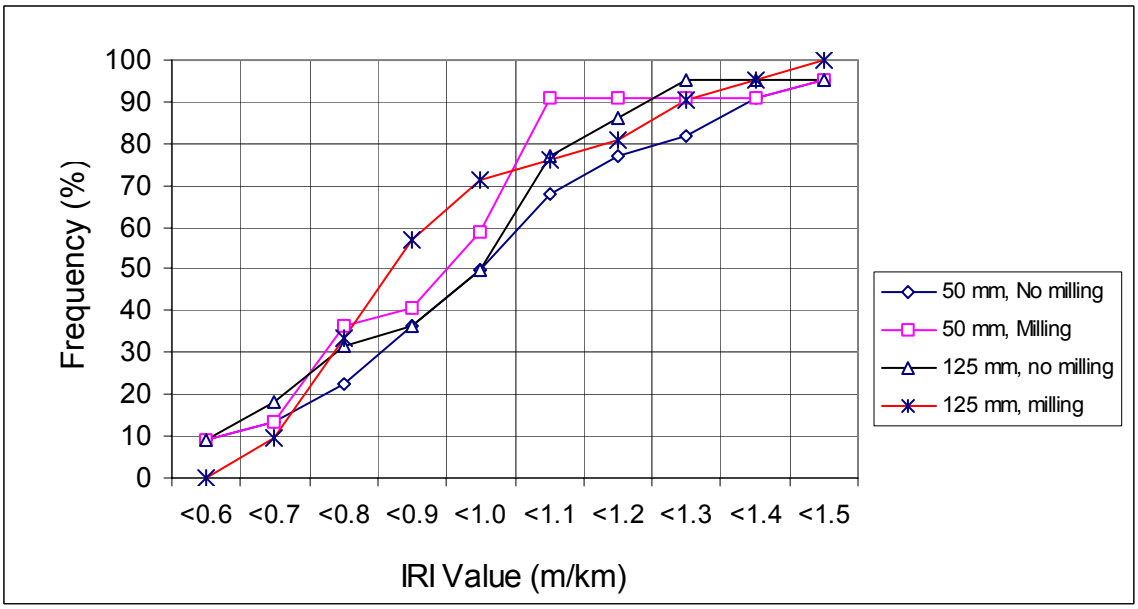

Figure 39. Cumulative frequency distribution of IRI after overlay – Projects with pre-rehabilitation IRI > 1.5 m/km.

The average IRI values obtained for several different scenarios are presented in table 33. When projects that have a pre-rehabilitation IRI of greater than 1.5 m/km are considered, the sections that received milling prior to overlay had an IRI that was 0.07 m/km less than the IRI obtained for projects that did not receive milling prior to overlay. Although statistically it was

shown that milling does make a difference in IRI values for projects that have a pre-rehabilitation IRI of greater than 1.50 m/km, as shown in table 33 in terms of magnitude the difference in IRI values for the two cases is small.

Table 33. Average IRI values for different scenarios.

Case	Overlay Thickness (mm)	Milled Prior to Overlay ?	IRI After Overlay (m/km)	
			Average	Standard Deviation
All Projects	50	No	0.98	0.30
All Projects	50	Yes	0.91	0.31
All Projects	125	No	0.91	0.29
All Projects	125	Yes	0.88	0.26
Pre-Rehabilitation IRI > 1.5 m/km	50	No	1.11	0.25
Pre-Rehabilitation IRI > 1.5 m/km	50	Yes	1.04	0.27
Pre-Rehabilitation IRI > 1.5 m/km	125	No	1.06	0.27
Pre-Rehabilitation IRI > 1.5 m/km	125	Yes	0.99	0.24

The cause for the milled sections to have a lower IRI can be attributed to two reasons. Milling the surface prior to placing the surface provides a more uniform surface for paving, which will result in a lower IRI. Also, as the milled thickness is replaced in addition to placing the overlay, the number of lifts used in placing the AC thickness for milled sections may have been more when compared to non-milled sections.

The relationship between pre and post-overlay IRI values for test sections in three SPS-5 projects are shown in figure 40. The pre-overlay project IRI, which is the average IRI of the eight test sections in the project that received an overlay is shown on top of each graphs. The pre-overlay project IRI for the three projects shown in figure 40 is 1.8, 2.3 and 1.9 m/km. These figures also show that there appears to be no relationship between pre and post overlay IRI values. It can be seen that for a specific SPS-5 project, the IRI values for all the test sections in the project tend to fall within a relatively narrow band of IRI values, irrespective of the IRI value prior to overlay of the test sections. This observation was generally noted for all SPS-5 projects.

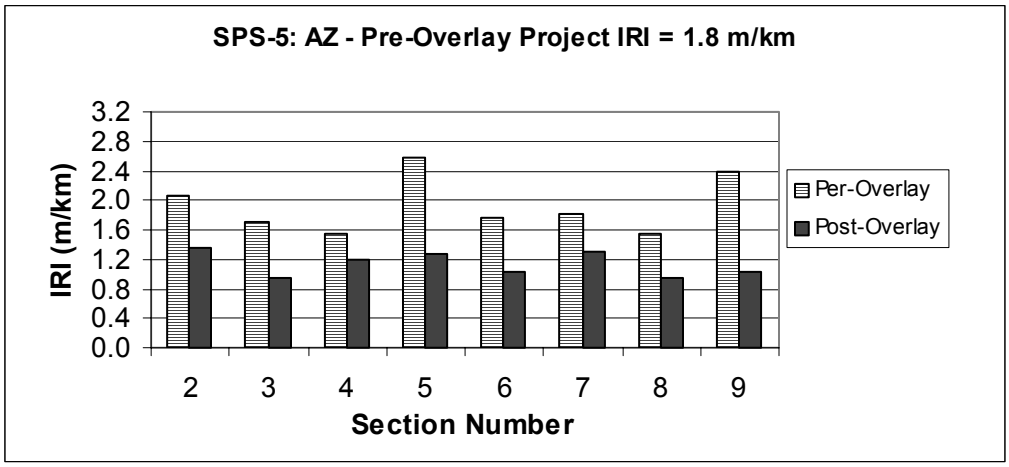

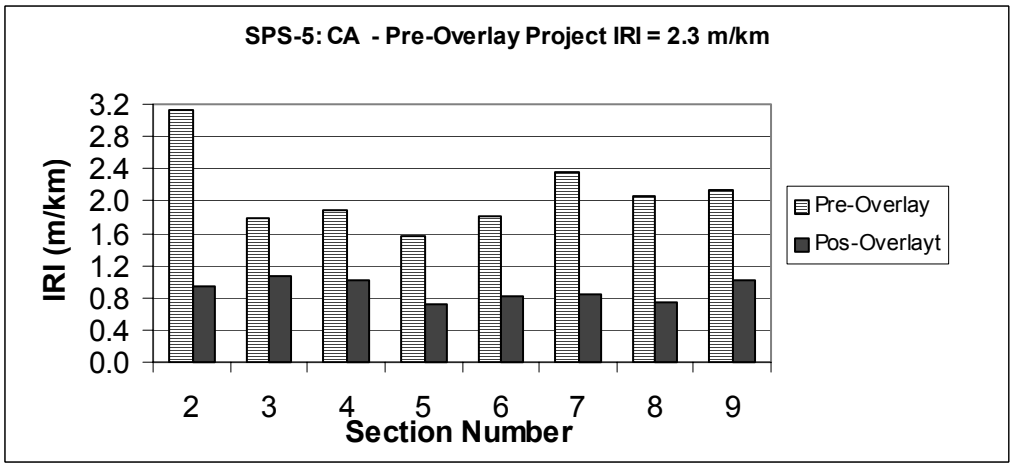

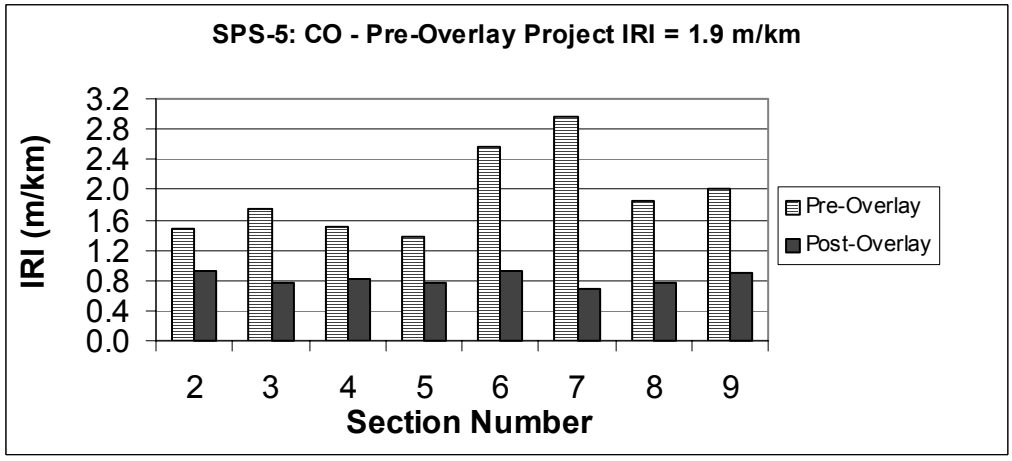

Figure 40. Relationship between pre and post overlay IRI values for three SPS-5 projects.

Changes in IRI for SPS-5 Projects

The changes in IRI over time for the SPS-5 projects in Arizona and Minnesota are shown in figure 41. Similar plots for all SPS-5 projects are included in Appendix C.

For SPS-5 projects that had at least three time-sequence IRI values, a linear regression was performed between IRI and time for each section to obtain the rate of development of roughness. Projects in Florida, Georgia and Maine had two time sequence IRI values after rehabilitation, but the time duration between these two profile dates was approximately 1, 2, and 3 years, respectively. Based on the review of IRI values, it was determined that a realistic rate of development of roughness could not be obtained from two time-sequence IRI values that were less than 2 years apart. The project in Georgia had two time-sequence IRI values that were approximately 3 years apart, and a rate of development of roughness was computed for sections in this project based on the two IRI values.

Figure 42 shows a box plot of the distribution of the rate of development of roughness at the test sections in the SPS-5 projects. The sections that received a 50 mm overlay without milling (sections 2 and 5) show a higher range between the first and third quartile ranges as well as for the overall range when compared to the two sections that received a 50 mm overlay after milling (sections 6 and 9). When compared to sections that received a 50 mm overlay, all sections that received a 125 mm overlay had lower ranges for rate of development of roughness between the first and third quartile, as well as a lower overall range.

The rate of development of IRI values that were computed for the test sections in each project were used to compute an average rate of development of roughness for each test section. That is for a specific test section, the rate of development of IRI obtained for that test section in all projects was averaged. The computed average rate of development of roughness values for the eight treatment types are shown in table 34.

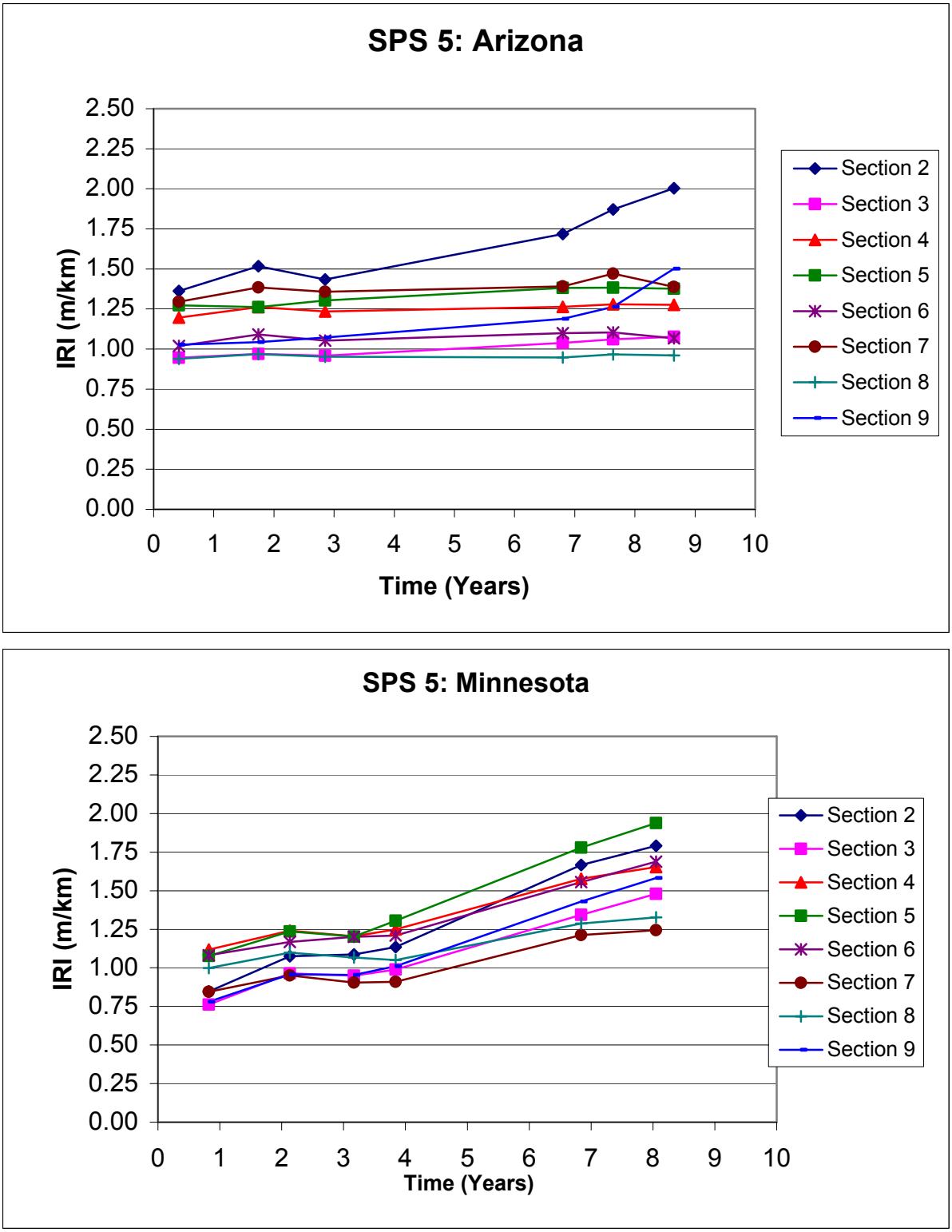

Figure 41. Change in IRI at SPS-5 projects in Arizona and Minnesota.

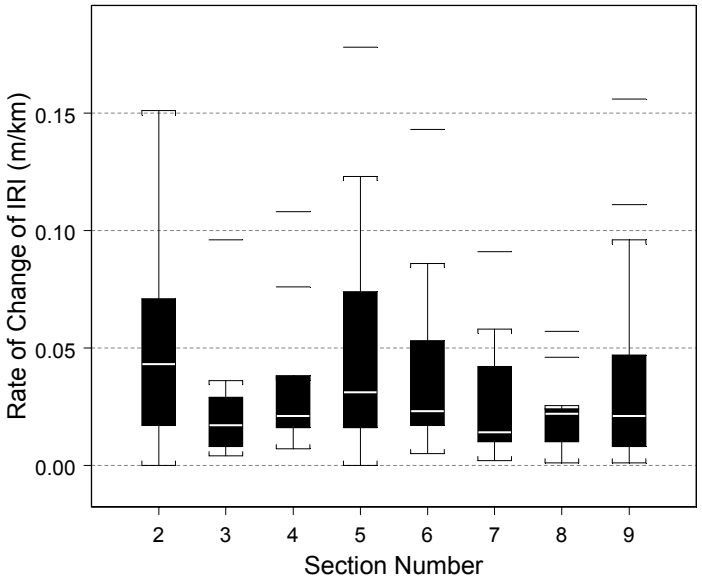

Figure 42. Box-plot of rate of development of IRI

Table 34. Average rate of development of IRI

Section Number	Surface Preparation	Type of AC	Overlay Thickness (mm)	Rate of Change of IRI (m/km)
2	Minimum	Recycled	50	0.049
3	Minimum	Recycled	125	0.023
4	Minimum	Virgin	125	0.032
5	Minimum	Virgin	50	0.051
6	Intensive	Virgin	50	0.039
7	Intensive	Virgin	125	0.028
8	Intensive	Recycled	125	0.022
9	Intensive	Recycled	50	0.044

The percent change in IRI for each test section in all SPS-5 projects is shown in table 35. The age of the projects shown in table 35 range from 2.4 to 9.9 years, with an average age of 7 years. Generally, projects that had higher pre-rehabilitation IRI show a higher increases in IRI. A statistical analysis was performed to investigate the factors that affect the increase of roughness

Table 35. Percent change in IRI at SPS-5 sections.

State	Pre-Overlay Project IRI (m/km)	Age of Project at First Profile Date (Yrs)	Age of Project at Last Profile Date (Yrs)	Time Difference for IRI Change (Years)	Percent Change in IRI (Note 1)								
					Section Number								Average
					2	3	4	5	6	7	8	9	
Alabama	1.2	0.3	4.3	4.0	6	5	9	11	13	22	8	11	11
Alberta	1.9	0.0	8.6	8.6	39	25	24	10	1	4	21	42	21
Arizona	1.9	0.4	8.6	8.2	47	14	7	8	5	7	2	46	17
California	2.1	0.8	6.9	6.1	107	11	10	162	42	40	43	103	65
Colorado	1.9	0.1	7.8	7.7	32	7	10	8	118	53	10	17	32
Florida	1.2	0.6	2.4	1.8	0	3	1	11	-2	0	0	-5	1
Georgia	1.1	2.9	5.9	3.0	8	4	13	4	13	13	11	4	9
Maine	1.2	2.2	3.0	0.8	0	-1	-2	-1	-5	0	-3	-2	-2
Manitoba	N/A	0.1	9.9	9.8	36	40	44	59	13	39	20	35	36
Maryland	1.6	0.2	6.4	6.2	-23	13	68	41	23	14	7	17	20
Minnesota	2.8	0.8	8.0	7.2	111	94	48	80	56	47	33	103	72
Mississippi	2.3	0.1	8.6	8.5	20	-3	20	2	26	4	11	-7	9
Montana	1.4	0.2	7.7	7.5	72	18	22	77	45	2	23	99	45
New Jersey	1.9	0.2	6.0	5.8	9	8	11	0	15	8	4	7	8
Texas	1.5	0.4	5.8	5.4	9	14	1	10	4	-3	11	3	6
AVERAGE		0.6	6.7	6.0	32	17	19	32	24	17	13	31	23

Note 1: Percent Change in IRI = 100 X (IRI Last Profile Date - IRI First Profile Date)/(IRI at First Profile Date)
N/A - Data not available.

by considering the following factors: pre-overlay IRI, milling (yes or no), overlay thickness (two levels), AC type (virgin or recycled), and time.

This analysis was performed by fitting a model to the time-sequence IRI values for all sections, and testing for significance of factors. The fitted model was of the following form:

$Log(IRI_{tij})$ = $State_j$ + Log (Pre-Overlay IRI_{ij}) + Main effects and interaction with time for Milling, Overlay Thickness, AC Type appropriate for $Section_{ij}$ + Time * Log (Pre-Overlay IRI_{ij})

Where,

IRI_{tij} = IRI at time t for section i in State j

Pre-Overlay IRI_{ij} = Pre-Overlay IRI for section i in State j

$Section_{ij}$ = Section i in State j, where I ranges from 2 to 9

In this model Milling (Yes or No), Overlay thickness (50 mm and 125 mm) and AC type (Virgin or Recycled) are qualitative factors. The model was fitted using the mixed model function of S-plus, and then the main effects and interactions were tested for significance. The test indicated State, interaction of time and overlay thickness, and interaction of time and Pre-overlay IRI were significant. The analysis indicated that the factors that are related to the future roughness of a section are pre-overlay IRI of section, overlay thickness, and time.

Figures 43 and 44 show the relationship between the rate of change of IRI and the pre-rehabilitation IRI for sections with 50 mm and 125 mm thick overlays, respectively. These figures confirm the result of the statistical analysis, which is that sections that had higher pre-overlay IRI show a higher rate of development of roughness.

The IRI vs. time plots of the different test sections in each SPS-5 project were generally parallel to each other (see figures in Appendix C). When we consider each overlay thickness separately, for a specific SPS-5 project the sections that had a lower initial IRI show a trend of maintaining a lower IRI value over time when compared to sections that had a higher initial IRI

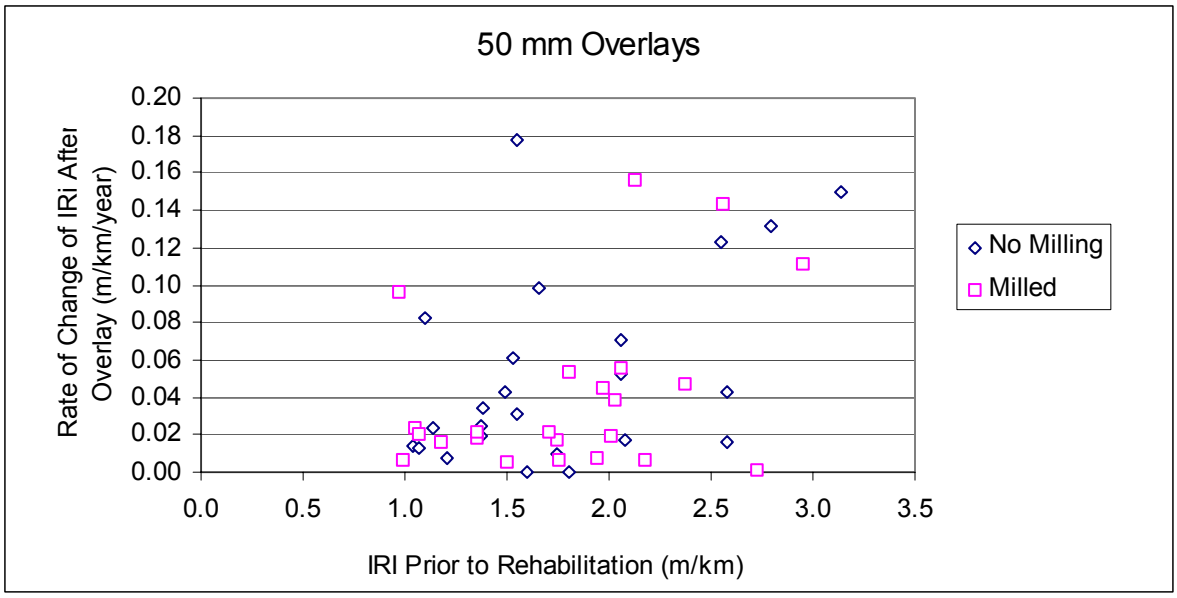

Figure 43. Rate of change of IRI vs. IRI prior to rehabilitation - 50 mm overlay sections.

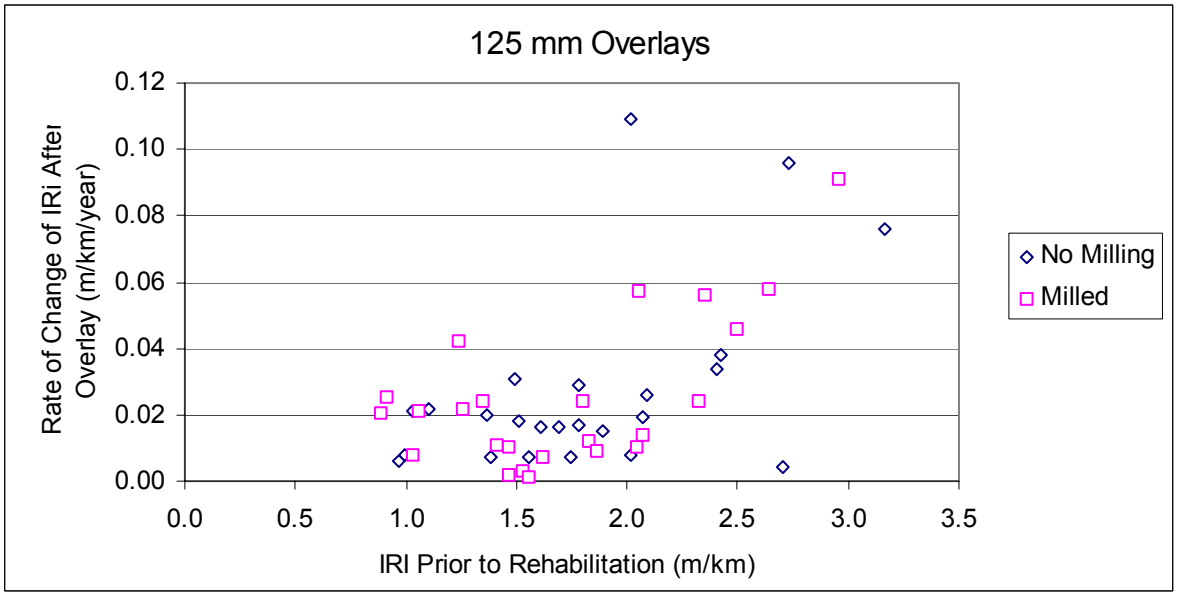

Figure 44. Rate of change of IRI vs. IRI prior to rehabilitation – 125 mm overlay sections.

value. The rate of change of IRI values shown in table 34 show the average value of the rate of change of IRI for sections that received a 125 mm overlay (sections 3, 4, 7, 8) were close to each other. Based on this data it can be seen that a section that has a lower initial IRI will maintain a lower IRI over time when compared to a section that had a higher initial IRI. These results are

based on observations and analysis that were made on projects that had an average age of seven years. The milled and non-milled sections that received a 125 mm overlay do not show a difference in the rate of change of IRI yet. However, as the pavements age, these trends may change. For sections that received a 50 mm overlay, the milled sections show a lower rate of change of IRI when compared to non-milled sections. If a comparison of roughness values over time is made between a non-milled and a milled section, where the non-milled section has a lower initial IRI, at some point in time the roughness values of these two sections will become equal (because the rate of change of IRI of non-milled section is higher that that of the milled section).

The three projects that had the highest lengths for transverse cracking were Arizona, California and Minnesota (see table 30). The highest average increase in roughness for SPS-5 projects are seen for the California and Minnesota projects (see table 35). The Arizona site also had a high number of transverse cracks, but did not show a higher percent change in IRI. This data indicates there may be a relationship between changes in roughness after overlay and transverse cracking at a section prior to overlay, but factors such as environment, subgrade conditions and traffic may have interaction effects with transverse cracking on the development of roughness.

Traffic data as well as key material testing data are not available yet in the LTPP database for many SPS-5 projects. Also, the age of the SPS-5 projects vary from 2.4 to 9.9 years, and the younger projects are not yet showing much change in IRI. Because of these limitations, a comprehensive analysis of the data to build models to predict development of roughness cannot be carried out yet. Because of the non-availability of traffic data, the influence of traffic on changes in roughness cannot be studied. It was also seen that the pre-rehabilitation IRI as well as pavement distress prior to rehabilitation varied between the test sections in many projects. This introduces an additional confounding factor to the analysis. In spite of these limitations, the existing data does reveal trends in roughness development at the SPS-5 projects.

Summary of Findings

Pre-rehabilitation IRI values of test sections were available for 15 SPS-5 projects. The pre-rehabilitation project IRI, which is the average IRI of all the test sections in the project, was less than 1.5 m/km for 7 of the projects. Considering that an IRI of 1.5 m/km corresponds to a serviceability rating of 3.4 (22), 7 of the analyzed SPS-5 projects were in a fairly good condition from a roughness point of view when rehabilitation was performed.

For sections that had an IRI of less than 1.5 m/km prior to overlay, the IRI after overlay was less than 1.0 m/km for 80 percent of the sections. For sections that had an IRI of over 1.5 m/km prior to overlay, the IRI after overlay for most sections fell between 0.8 and 1.2 m/km. It was seen that 50 mm overlays were capable of achieving a large reduction in roughness, with some of the 50 mm overlays reducing the IRI of the pavement from 2.5 m/km to 1.0 m/km

An analysis of all the data for the SPS-5 projects indicated that the IRI after overlay did not depend on the pre-rehabilitation IRI, overlay thickness, if milling was performed or not prior to overlay, or the type of AC. An analysis of the data from the projects that had an IRI of greater than 1.5 m/km indicated that milling prior to placing an overlay results in a smoother pavement. For projects having an IRI greater than 1.5 m/km, milling prior to placing an overlay resulted in a pavement that on average had an IRI of less than 0.07 m/km when compared to a non-milled section. Generally, for each SPS-5 project, the IRI of all test sections in the project fell within a relatively narrow band of IRI values, irrespective of the IRI prior to overlay of the test sections.

A statistical analysis indicated that the progression of the roughness over time of the overlaid pavements depend on the pre-overlay IRI of the section and overlay thickness. The statistical analysis did not indicate milling prior to overlay or AC type as being significant factors that affect the progression of roughness of overlaid pavements.

When all projects were considered, the following average rate of increase of roughness were observed: 50 mm overlays with milling prior to overlay – 0.042 m/km/year, 50 mm overlays without milling prior to overlay – 0.050 m/km/year, 125 mm overlays with milling prior

to overlay – 0.025 m/km/year, 125 mm overlays without milling prior to overlay – 0.028 m/km/year. It should be noted that these results are based on analysis that were made on projects that that had an average age of seven years. These results as well as observation of time-sequence data for the SPS-5 projects indicate that for a specific overlay thickness, a lower initial IRI results in a lower IRI over the service life of the pavement

SPS-6 EXPERIMENT: REHABILITATION OF JOINTED CONCRETE PAVEMENTS

Introduction

The SPS-6 experiment was developed to investigate the effect of different rehabilitation techniques performed on jointed concrete pavements. In this experiment, preparation and/or restoration of the existing pavement are classed into three levels: minimal, intensive, crack and seat or break and seat. The treatments minimal and intensive are applied with and without an AC overlay. The rehabilitation treatments applied to the test sections in the SPS-6 test sections are presented in table 36.

Table 36. Treatments applied to SPS-6 test sections.

Section Number	Surface Preparation	AC Overlay Thickness (mm)
1	Routine Maintenance	0
2	Minimum Restoration	0
3	Minimum Restoration	100
4	Minimum Restoration (saw and seal joints inn AC)	100
5	Intensive Restoration	0
6	Intensive Restoration	100
7	Crack/Break Seat	100
8	Crack/Break Seat	200
Note: In Section 4, after the placement of the AC overlay, the AC surface is sawed and sealed over the joints and working cracks of the PCC		

A detailed description of the surface preparation that is applied to the test sections is presented in table 37. Each SPS-6 project consists of seven test sections and a control section.

The control section designated as section 1 receives only maintenance activities that are needed to keep the section in a safe and functional condition in accordance with the standard procedure of the State agency where the project is located. The monitored portion of test sections 2 and 5 is 305 m, while that of the other sections is 152 m.

Table 37. Surface preparation activities for SPS-6 test sections.

	Surface Preparation							
Test Section Details and Treatment Options		Minimal			Intensive		Crack & Seat	
Section number	1	2	3	4	5	6	7	8
Section length (m)	152	305	152	152	305	152	152	152
Overlay thickness (mm)	0	0	100	100	0	100	100	200
Joint sealing	X	X	N	N	R&R	N	N	N
Crack sealing	X	X	N	N	R&R	N	N	N
Partial depth patch	N	X	X	X	R&R	R&R	N	N
Full depth patch/joint repair	N	X	X	X	R&R	R&R	N	N
Load transfer restoration	N	N	N	N	B	B	N	N
Full surface diamond grinding	N	X	N	N	A	N	N	N
Undersealing	N	N	N	N	X	X	N	N
Subdrainage	N	N	N	N	A	A	A	A
Crack/break and seat	N	N	N	N	N	N	A	A
Saw and seal	N	N	N	A	N	N	N	N

X - Apply treatment as warranted
R&R - Remove and replace existing and apply additional as warranted
N - Do not perform
B - Full depth doweled patch or retrofit dowels in slots.
A - Apply treatment regardless of condition or need.

Analyzed Projects

A review of the IMS database indicated profile data were available for ten SPS-6 projects. Table 38 presents the following information for each SPS-6 project: state located, climatic zone, subgrade type, if pre-rehabilitation IRI and distress data are available for the project, rehabilitation date, age of project at first profile date, age of project at last available profile date, number of times the project has been profiled after rehabilitation, pavement type (plain or reinforced), pre-rehabilitation IRI of the project, and the estimated annual ESALs at the

Table 38. SPS-6 projects.

State	State Code	Climatic Zone (Note 1)	Subgrade Type	Availability of Pre-Rehabilitation Data		Rehab. Date	Age of Pavement After Rehabilitation at First Profile Date (Yr)	Age of Project at Last Profile Date (Yr)	Number of Times profiled After Rehabilitation	Pavement Type	Pre-Rehab Project IRI (m/km)	Estimated Traffic KESAL (per year)
				IRI	Distress							
Arizona	AZ	DNF	Coarse	Yes	Yes	8/5/90	1.1	8.6	8	JPCP	1.9	1591
California	CA	WNF	Coarse	Yes	Yes	8/10/92	0.7	5.7	3	JPCP	3.2	N/A
Illinois	IL	WF	Fine	Yes	Yes	6/11/90	1.5	7.7	4	JRCP	2.3	723
Indiana	IN	WF	Fine	Yes	Yes	8/15/90	0.3	8.3	6	JPCP	1.8	317
Iowa	IA	WF	Fine	No	No	8/16/89	0.8	9.9	8	JRCP	N/A	490
Michigan	MI	WF	Fine	Yes	Yes	5/15/90	0.6	8.9	7	JRCP	2.1	360
Missouri	MO	WF	Fine	Yes	Yes	8/10/92	0.6	6.5	5	JRCP	2	N/A
Oklahoma	OK	WNF	Fine	Yes	No	8/27/92	0.6	6.8	3	JRCP	1.8	731
Pennsylvania	PA	WF	Fine	Yes	Yes	9/30/92	0.2	5.7	5	JRCP	2.5	N/A
South Dakota	SD	DF	Fine	Yes	No	9/25/92	1.1	6.6	5	JPCP	2.8	59

Note 1: DF - Dry Freeze, DNF - Dry No-Freeze, WF - Wet Freeze, WNF - Wet No-Freeze
N/A - Data not available

site. The pre-rehabilitation IRI of the project was computed by averaging the pre-rehabilitation IRI of the test sections in the SPS-6 project.

Figure 45 shows the pre-rehabilitation IRI for the nine SPS-6 projects for which pre-rehabilitation IRI values were available. The values shown in figure 45 were computed by averaging the pre-rehabilitation IRI of the test sections for each project. Six projects had a pre-rehabilitation IRI that was between 1.5 and 2.5 m/km, and three projects had IRI values exceeding 2.5 m/km.

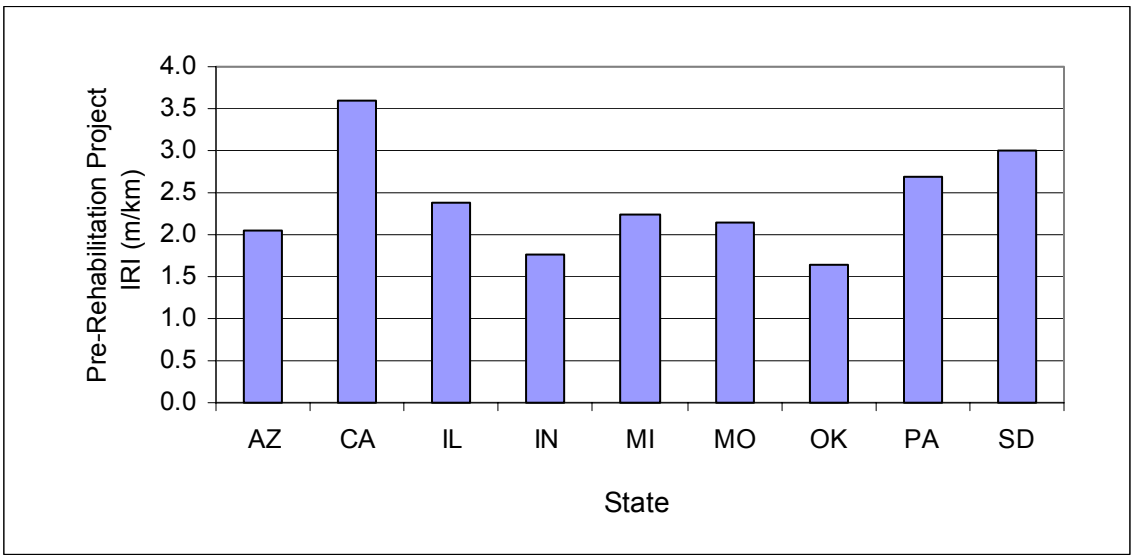

Figure 45. Pre-rehabilitation project IRI of SPS-6 projects.

Figure 46 presents the pre-rehabilitation standard deviation of IRI of the test sections that are contained in each SPS-6 project. There were large differences in the variability of IRI values between the test sections for the different projects. The sections in Indiana showed the lowest variability (standard deviation of IRI = 0.2 m/km), while the sections in Arizona showed the largest variability (standard deviation of IRI = 0.6 m/km).

Table 39 presents the average distress per section prior to rehabilitation for the seven projects for which pre-rehabilitation distress data were available. The average distress per section for a specific distress type in a SPS-6 project was computed by averaging the distresses (all

severity levels) present in all test sections for that SPS-6 project. Table 39 also presents the pre-rehabilitation IRI for the project.

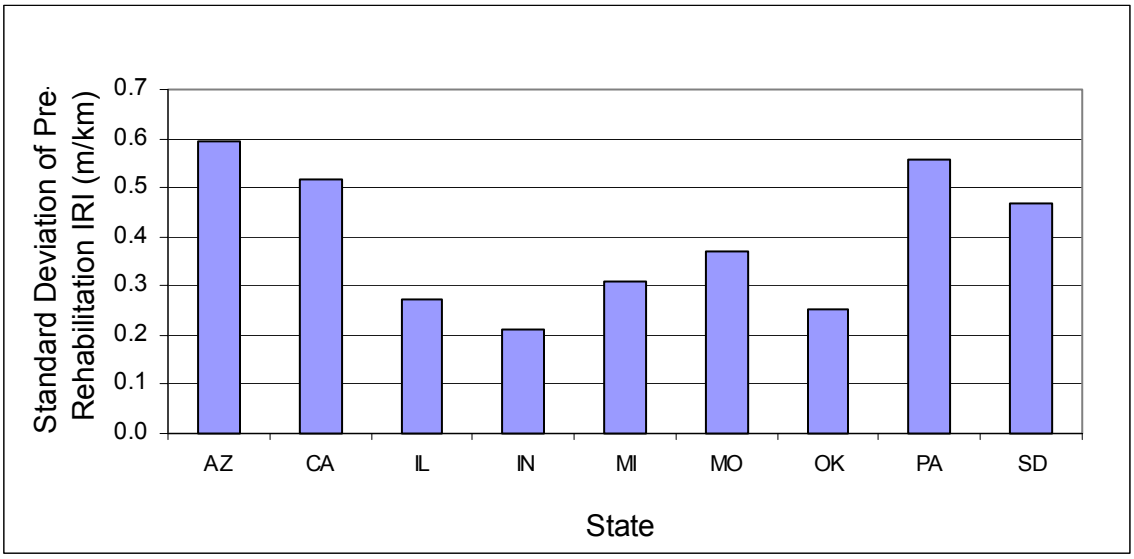

Figure 46. Standard deviation of pre-rehabilitation IRI of test sections in SPS-6 projects.

Table 39. Average distress per section and pre-rehabilitation IRI for SPS-6 projects.

Distress Type	Average Value per Section						
	State						
	AZ	CA	IL	IN	MI	MO	PA
Corner Breaks, Number	0	7	1	0	0	0	1
D. Cracking, Area (m^2)	0	0	0	0	0	6	0
Longitudinal Crackling, Length (m)	28	35	0	0	0	0	3
Transverse Cracks, Number	14	33	17	2	27	17	4
Transverse Cracks, Length (m)	46	89	56	9	112	45	13
Longitudinal Spalling, Length (m)	2	0	3	13	16	0	2
Transverse Spalls, Number	31	6	3	22	2	0	1
Transverse Spalls, Length (m)	98	2	2	52	6	0	1
Flexible Patches, Number	0	1	0	39	9	0	7
Flexible Patches, Area (m^2)	0	3	0	19	6	0	3
Rigid Patches, Number	0	0	1	0	3	3	1
Rigid Patches, Area (m^2)	0	0	13	0	28	45	10
Pre-Rehabilitation IRI (m/km)	1.9	3.2	2.3	1.8	2.1	2.0	2.5
Note: Pre-rehabilitation distress data not available for IA, OK and SD							

IRI After Rehabilitation

The post-rehabilitation IRI value for each test section in the SPS-6 projects is shown in table 40. Section 5 for projects in Michigan and Indiana were not diamond ground after repairs and the post-rehabilitation IRI values for these two sections are not shown in table 40.

Table 40. Post-rehabilitation IRI values for SPS-6 projects.

State	Pre-Rehab Average IRI of Project (m/km)	IRI After Rehabilitation (m/km) Test Section						
		2	3	4	5	6	7	8
Arizona	1.9	3.5	0.9	0.9	1.5	1.0	0.8	0.9
California	3.2	1.4	0.9	0.8	1.1	0.9	1.0	0.9
Illinois	2.3	2.2	1.0	1.1	0.8	1.1	1.2	1.1
Indiana	1.8	3.6	0.9	0.9	N/A	0.9	1.0	0.9
Iowa	N/A	1.2	0.9	1.1	1.5	0.9	1.0	1.2
Michigan	2.1	2.1	1.3	1.2	N/A	0.9	1.1	0.9
Missouri	2.0	N/A	1.1	1.1	N/A	1.1	1.3	1.3
Oklahoma	1.8	1.1	0.7	0.9	0.8	0.9	1.1	1.3
Pennsylvania	2.5	2.1	1.1	1.1	1.4	1.1	1.0	1.0
South Dakota	2.8	1.0	1.1	1.3	0.9	1.0	1.0	0.8
Average (m/km)		**1.9**	**1.0**	**0.9**	**1.1**	**1.0**	**1.1**	**1.0**
Standard Deviation (m/km)		**1.0**	**0.2**	**0.4**	**0.3**	**0.1**	**0.1**	**0.2**
N/A - IRI values not available. For section 5 in Michigan and Indiana values are omitted because the sections were not diamond ground								

The pre- and post-rehabilitation IRI values for section 2 that received minimal surface preparation are shown in table 41. Some states diamond ground this section, while others did not (Table 37 indicates that the States were given the option of carrying out diamond grinding of this section.) As shown in table 41, the IRI value after rehabilitation for sections that were diamond ground ranged from 1.03 to 1.36 m/km. The post-rehabilitation IRI values for section 2 in Arizona and Indiana (that were not diamond ground) showed a large increase in IRI after repairs. The increase in IRI value for section 2 in Arizona and Indiana after repairs was 1.03 m/km and 2.00 m/km, respectively from the pre-rehabilitation IRI. The repairs performed on the Arizona section consisted of joint sealing, crack sealing and partial depth patches, while at the section in Indiana full depth patches were performed. These repair activities resulted in an increase in IRI.

Table 41. Pre- and post-rehabilitation IRI values for section 2.

State	IRI (m/km)		Diamond
	Pre-Rehabilitation	Post-Rehabilitation	Ground ?
Arizona	2.43	3.46	No
California	3.44	1.36	Yes
Illinois	2.05	2.17	No
Indiana	1.64	3.64	No
Iowa	N/A	1.22	Yes
Michigan	2.04	2.08	No
Missouri	1.94	1.09	Yes
Oklahoma	2.10	1.09	Yes
Pennsylvania	2.22	2.05	No
South Dakota	3.05	1.03	Yes
Note: N/A - Value not available			

Section 3 through 8 in the SPS-6 projects received AC surface, except for section 5 that was diamond ground. The post-rehabilitation average IRI value for sections 3 through 8 for each SPS-6 project is shown in figure 47, while the standard deviations of IRI for test sections 3 through 8 for each project is presented in figure 48. The post-rehabilitation project IRI ranged from 0.93 m/km (Indiana) to 1.12 m/km (Pennsylvania). The project in Indiana had the lowest standard deviation in IRI (0.04 m/km) with the project in Arizona having the highest standard deviation in IRI (0.24 m/km).

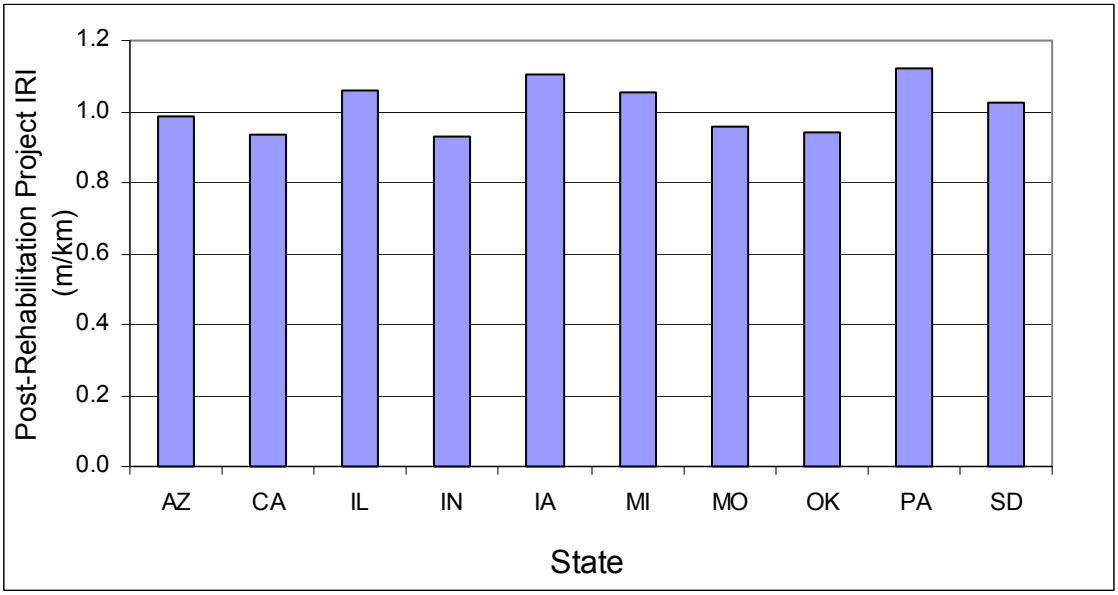

Figure 47. Average post-rehabilitation IRI of sections 3 through 8.

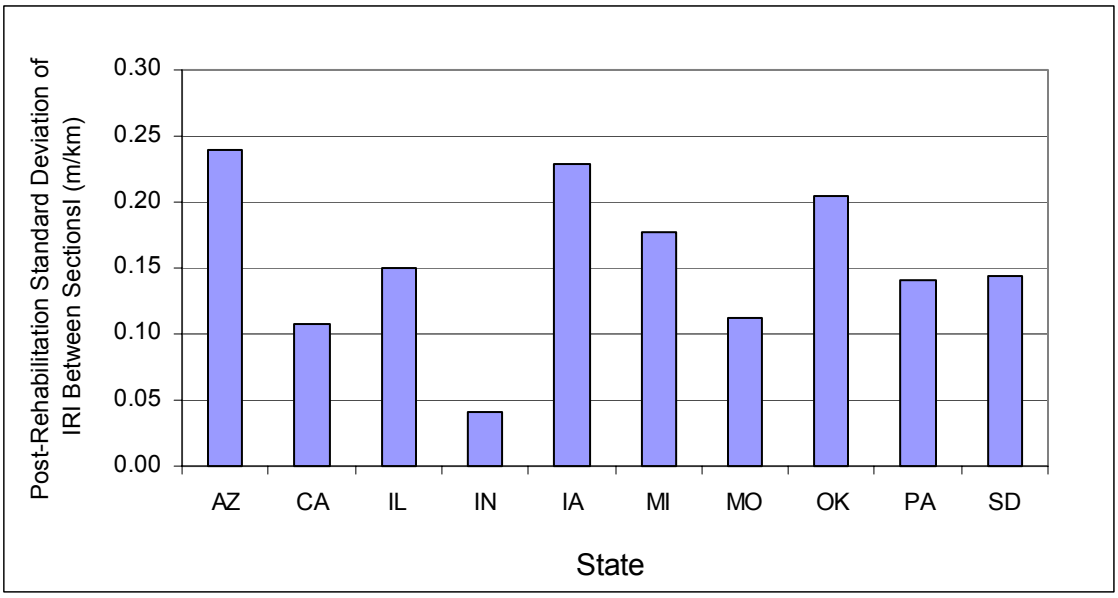

Figure 48. Post-rehabilitation standard deviation in IRI for sections 3 to 8.

Relationship Between IRI Before and After Rehabilitation

Figure 49 shows the relationship between IRI prior to rehabilitation and IRI after rehabilitation for section 2, which received minimum restoration. For section 2 (minimum restoration), the construction guidelines gave the States the option of diamond grinding the section if warranted (see table 37). In some SPS-6 projects, the minimum restoration section was diamond ground, while in others it was not. In figure 49, the sections that have post-rehabilitation values of less than 1.40 m/km are the projects that received diamond grinding. The data show in this figure show that diamond grinding can reduce the IRI of a pavement by a significant amount. As shown in figure 49, the pre-rehabilitation IRI of sections that were diamond ground ranged from 1.5 to 3.5 m/km, while the post-rehabilitation IRI ranged from 0.8 to 1.4 m/km. Generally, the sections that had lower pre-rehabilitation IRI values obtained lower IRI values after diamond grinding.

Figure 50 shows the relationship between IRI prior to rehabilitation and IRI after rehabilitation for section 5 that received intensive surface preparation followed by diamond

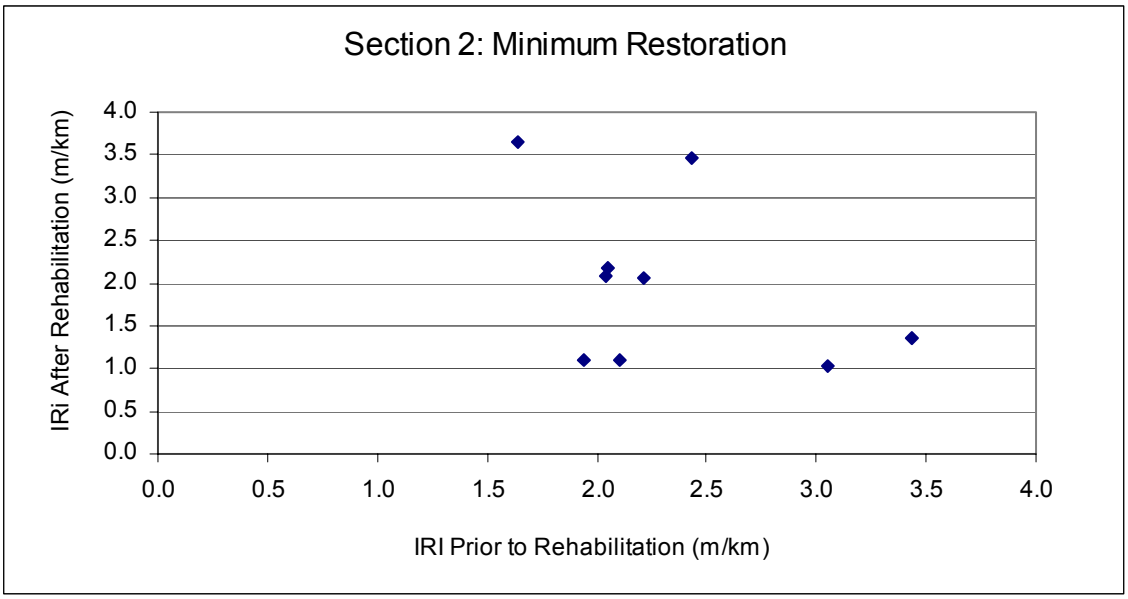

Figure 49. Relationship between IRI prior to and after rehabilitation for section 2 (minimal surface preparation).

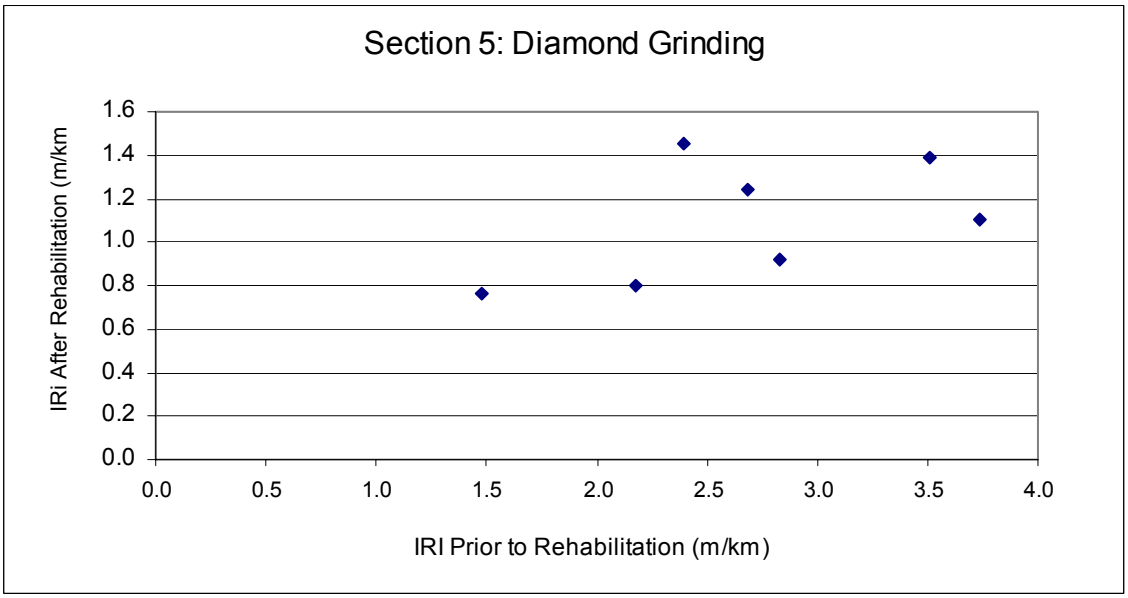

Figure 50. Relationship between IRI prior to and after rehabilitation for section 5 (intensive surface preparation followed by diamond grinding)

grinding. The pre-rehabilitation IRI of sections that were diamond ground ranged from 1.5 to 3.7 m/km, while the post-rehabilitation IRI ranged from 0.8 to 1.5 m/km. Generally, the sections that had lower pre-rehabilitation IRI values obtained lower IRI values after diamond grinding.

Figure 51 shows the relationship between IRI prior to rehabilitation and IRI after rehabilitation for sections 3, 4 and 5 all of which received a 100 mm AC overlay, with section 3 and 4 receiving minimum restoration prior to overlay, and section 5 receiving intensive surface preparation prior to overlay. Figure 51 show that AC overlays can reduce the roughness of a section significantly. There are several sections that had pre-rehabilitation IRI values that ranged from 2.9 to 3.8 m/km, but after the 100 mm AC overlay, the IRI of these sections ranged from 0.8 to 1.3 m/km.

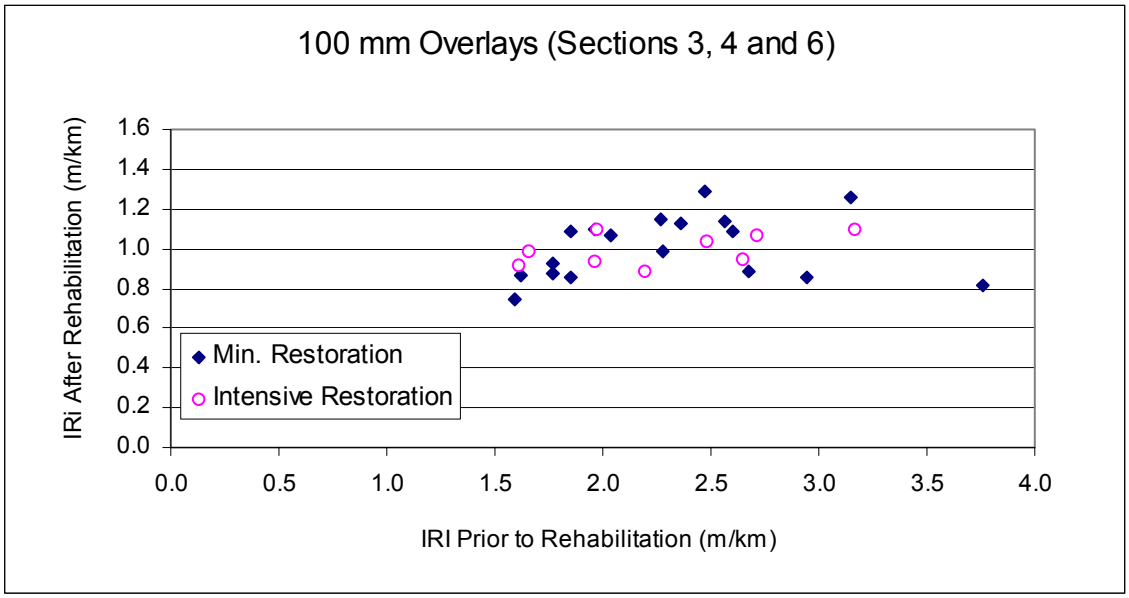

Figure 51. Relationship between IRI prior to and after rehabilitation for Sections 3, 4 and 6 (100 mm overlay)

Figure 52 shows the relationship between IRI prior to rehabilitation and IRI after rehabilitation for sections 7 and 8, that were crack/break seated and received a 100 mm and a 200 mm AC surface, respectively. As shown in figure 52, the post-rehabilitation IRI of crack/break seat sections ranged from 0.8 to 1.3 m/km.

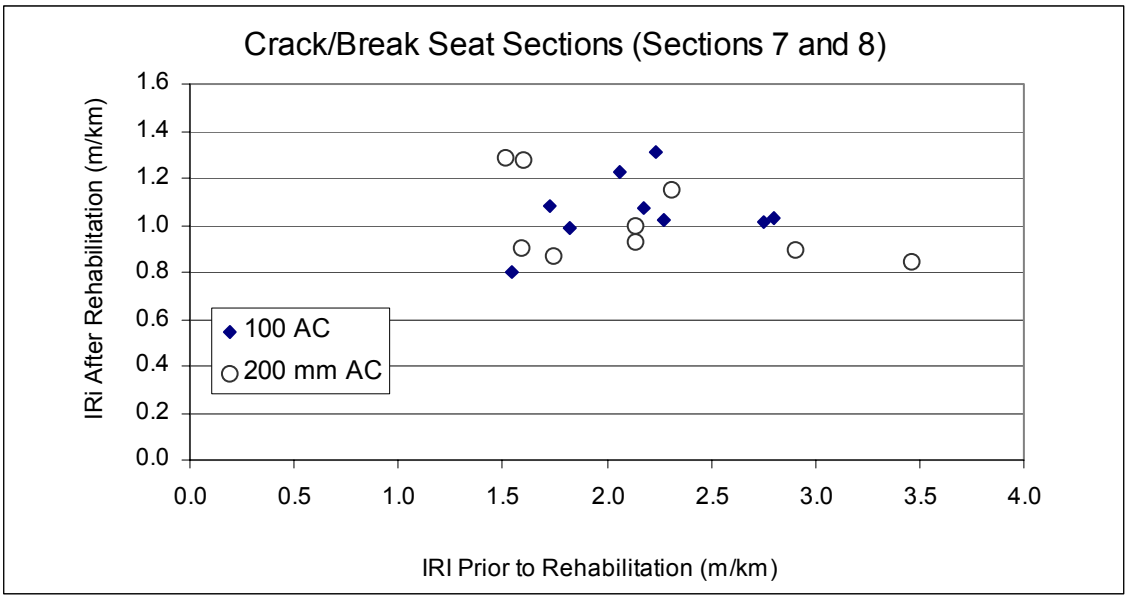

Figure 52. Relationship between IRI prior to and after rehabilitation for sections 7 and 8 (crack/break seated)

The relationship between pre and post-overlay IRI values for test sections in three SPS-6 projects (Arizona, Illinois and California) are shown in figure 53. The pre-rehabilitation project IRI, which is the average pre-rehabilitation IRI of the test sections in the project is shown on top of each graph. The pre-rehabilitation project IRI for the three projects shown in figure 53 range from 1.9 to 3.2 m/km. Data shown in figure 53 indicate that for a specific SPS-6 project, the IRI for all test sections except for section 2, tends to fall within a relatively narrow band of IRI values, irrespective of the IRI prior to rehabilitation of the test sections. This observation was generally noted for all SPS-6 projects that were analyzed. The pre- and post-rehabilitation IRI for test section 2 for the three projects shown in figure 53 show different trends. For the section in California, the IRI showed a large reduction, which was because the section was diamond ground. The section in Arizona showed a large increase in IRI after repairs, while section 2 in Illinois showed a small increase in IRI after repairs.

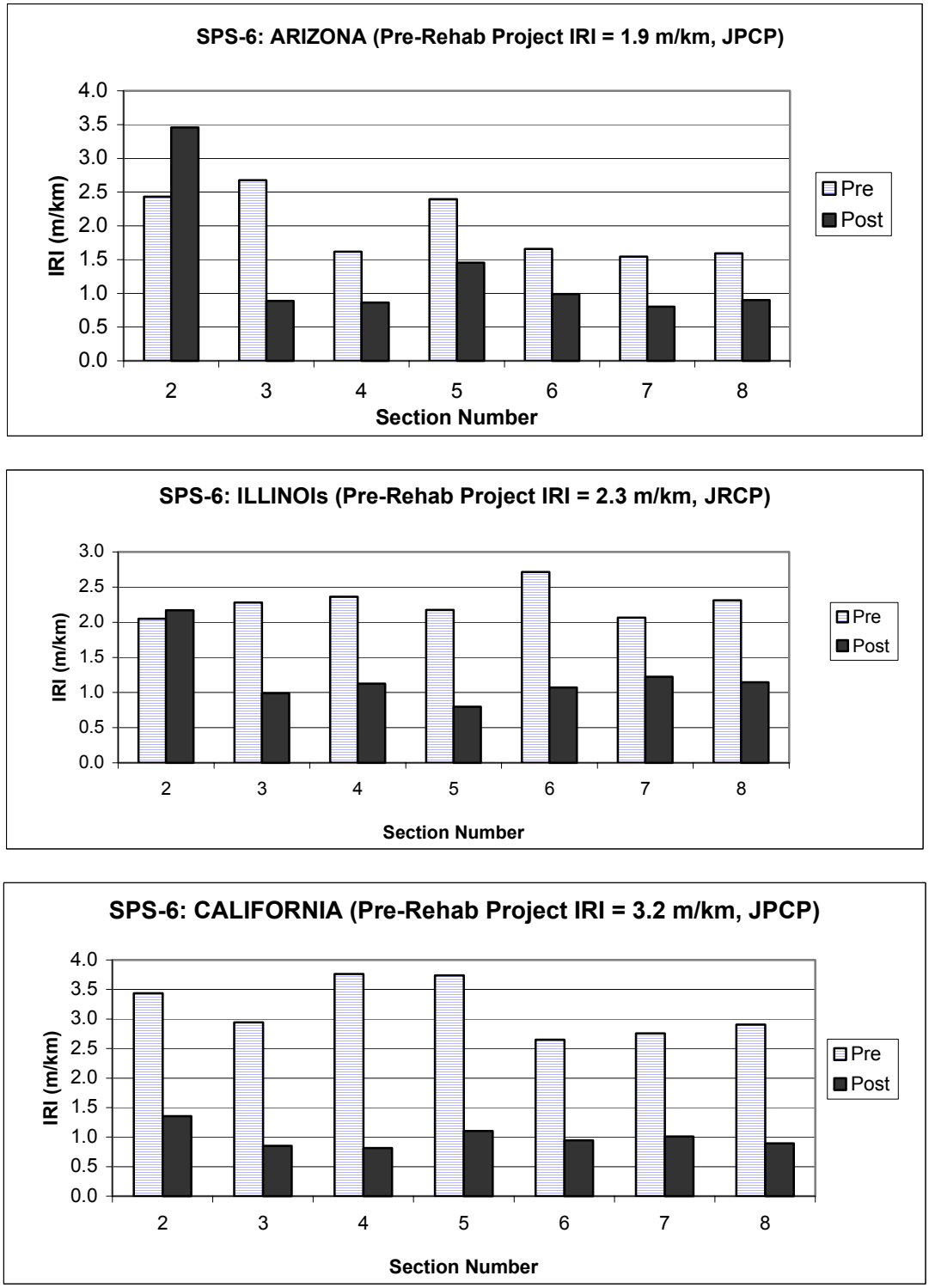

Figure 53. IRI before and after overlay for the different treatment factors for three SPS-6 projects.

An ANOVA was performed to see if the IRI values after rehabilitation for the seven different treatment methods were different from each other. The ANOVA indicated there were differences in IRI values between the sections (p-value < 0.001). A multiple comparison using statistical analysis indicated section 2 was different from other sections. In some SPS-6 projects section 2 had been diamond ground, while in others it had not been diamond ground. The cause for this section being significantly different than other sections was due to the higher IRI values for sections that had not been diamond ground. Another ANOVA was performed by considering sections 3 through 8, which indicated that there was no significant difference in IRI values between the sections. The interpretation of this result is that the IRI values that are obtained after diamond grinding, and AC overlay of 100 mm (minimal and intensive surface preparation), and crack/break seat and an AC surface (100 mm and 200 mm), were similar.

An analysis similar to that performed for SPS-5 by fitting a model to see if the post-rehabilitation IRI values depended on pre-rehabilitation IRI values was not carried out for the SPS-6 projects. This was because the post-rehabilitation IRI values for the sections that were subjected to crack/break seat are not expected to depend on the pre-rehabilitation IRI value. Elimination of these sections, as well as elimination of section 2 that had different treatments in different States from a model fitting analysis would not leave an adequate data set to carry out such an analysis.

Change in IRI for SPS-6 Projects

The change in IRI over time for the SPS-6 projects in California and Oklahoma are shown in figure 54. Similar plots for all SPS-6 projects are included in Appendix D.

For SPS-6 projects that had at least three time-sequence IRI values, a linear regression was performed to obtain the rate of development of roughness. An ANOVA was performed to determine if there was a difference in rate of development of roughness between the seven different rehabilitation types. The rate of development of roughness was taken as the dependant variable, and State and treatment type was taken as the independent variables. The ANOVA

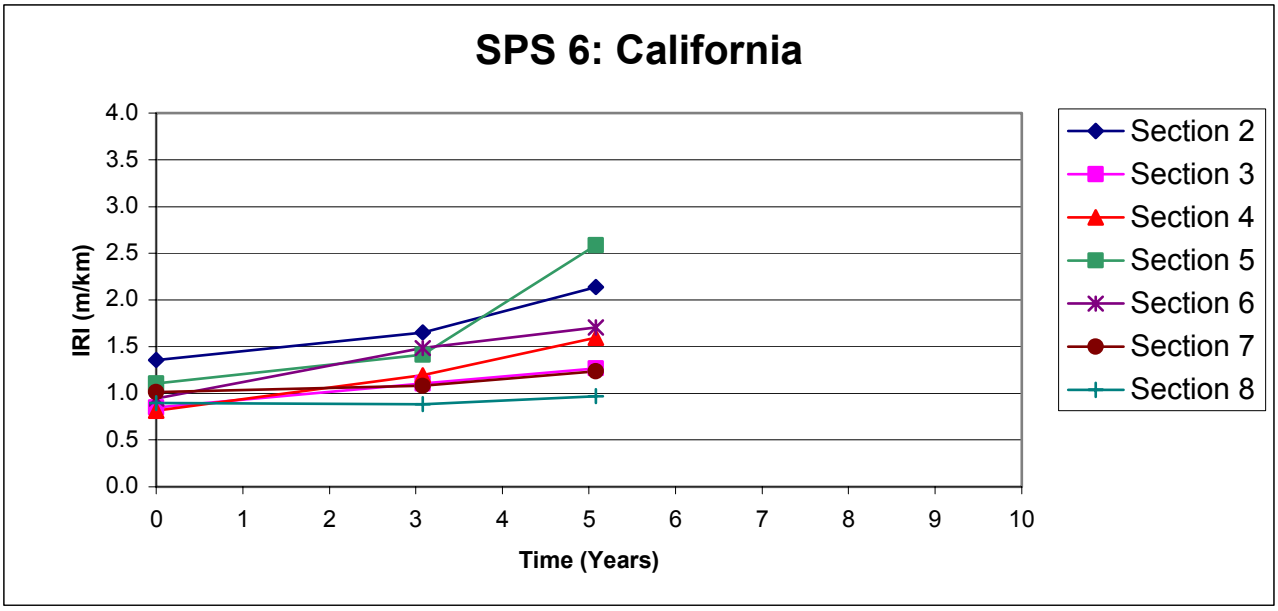

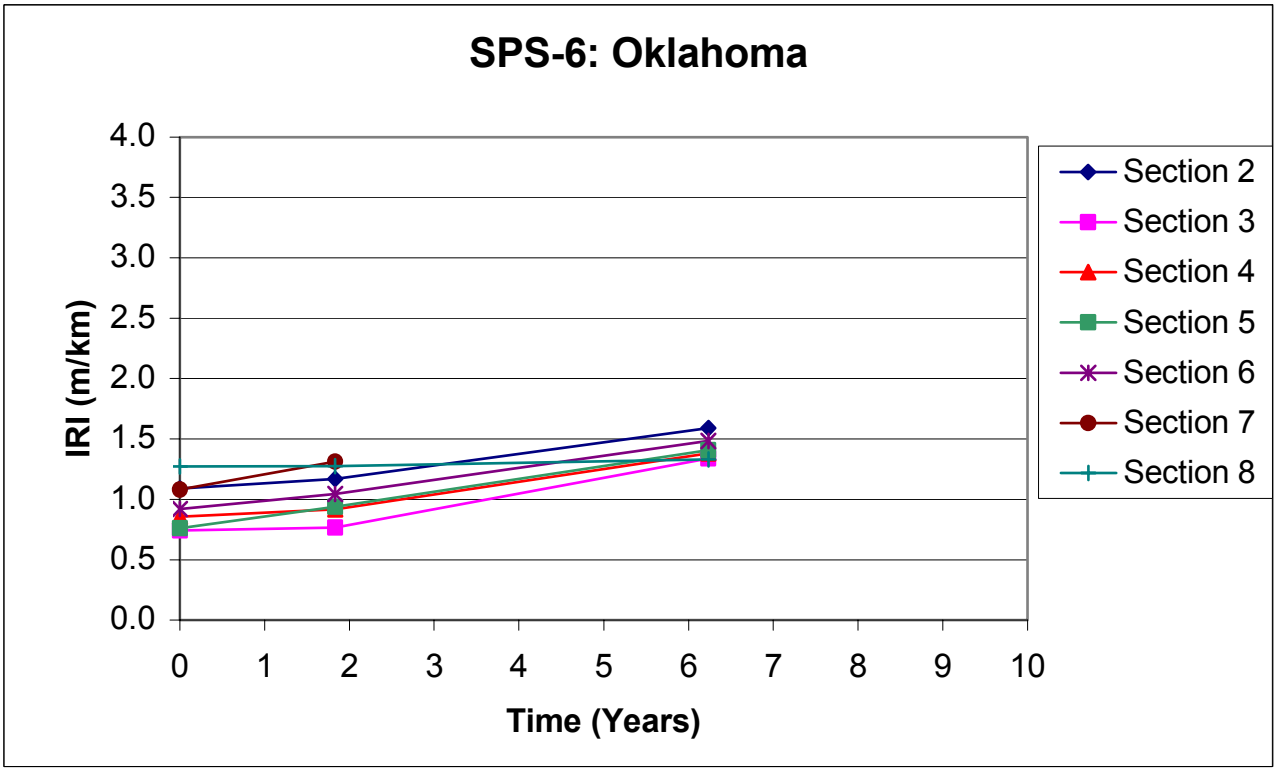

Figure 54. Changes in IRI for SPS-6 projects in California and Oklahoma.

indicated that the rehabilitation type was significant ($p < 0.001$). A multiple comparison analysis showed that the rate of change of roughness for section 5 (diamond grinding) was statistically different from all other types of treatment, and also section 2 (minimum restoration) was different from section 8 (crack/break seat and 200 mm AC surface). As different treatment types were performed at section 2 for different projects, another ANOVA was performed by omitting the data for section 2. This analysis also indicated that rate of change of IRI for section 5 (diamond grinding) was statistically different from all other sections.

Figure 55 shows a box-plot that shows the distribution of the rate of change of IRI at the different sections. This figure shows the highest values for the rate of change of roughness was obtained at section 5, which received diamond grinding.

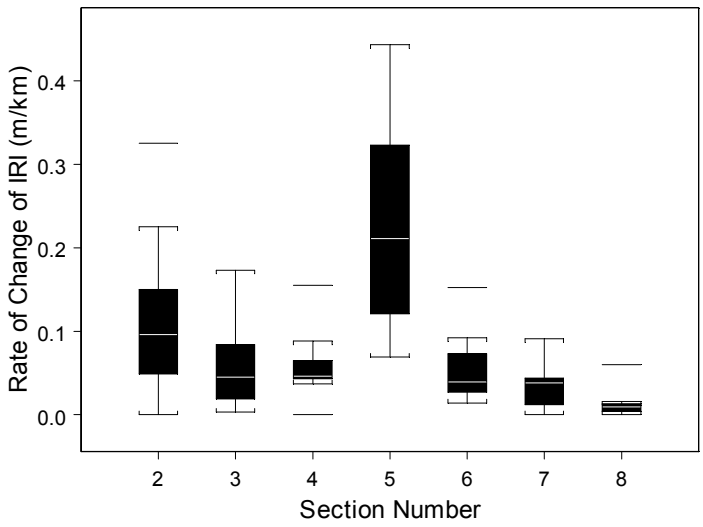

Figure 55. Box plot of rate of development of IRI.

The average and the standard deviation values for the rate of development of roughness for each treatment type are presented in table 42. The values shown in this table for a specific treatment type was obtained by using the rate of change of IRI values obtained for each project.

Table 42. Average and standard deviation of rate of change of IRI

Section Number	Surface Preparation	AC Overlay Thickness (mm)	Rate of Change of IRI (m/km/yr)	
			Average	Std. Dev.
2	Minimum Restoration	0	0.114	0.101
3	Minimum Restoration	100	0.058	0.051
4	Minimum Restoration (saw and seal joints)	100	0.057	0.042
5	Intensive Restoration	0	0.200	0.137
6	Intensive Restoration	100	0.054	0.042
7	Crack/Break Seat	100	0.032	0.033
8	Crack/Break Seat	200	0.013	0.017

The relationship between the rate of change of IRI and pre-rehabilitation IRI are shown in figures 56 through 59 for the different rehabilitation types. For the minimum restoration sections (see figure 56), the sections that received diamond grinding generally show a high rate of change of IRI. A clear relationship between rate of change of IRI and pre-rehabilitation IRI cannot be observed in figure 57, that shows the data for sections that received a 100 mm overlay. For sections that received diamond grinding (see figure 58), sections that had higher IRI prior to rehabilitation have a higher rate of change of IRI. Figure 59 shows that the majority of crack/break seat sections that received a 100 mm AC surface have a higher rate of change of IRI than the sections that received a 200 mm AC surface.

The percent change in IRI for the test sections (from the IRI value after rehabilitation) for all SPS-6 projects are shown in table 43. The values presented in this table are consistent with the results obtained from the ANOVA. The lowest changes in IRI values were observed at section 8, but two States had percent changes in IRI that exceeded 20 percent for this section.

An evaluation of the distresses observed on the diamond ground section (section 5) was performed to see if the distresses that were contributing to the high rate of increase of roughness seen at this section could be identified. Section 5 in projects shown in table 44 were selected for analysis. Table 44 gives the following information for the diamond ground section: IRI before diamond grinding, IRI after diamond grinding, IRI at last profile date, if pre-rehabilitation

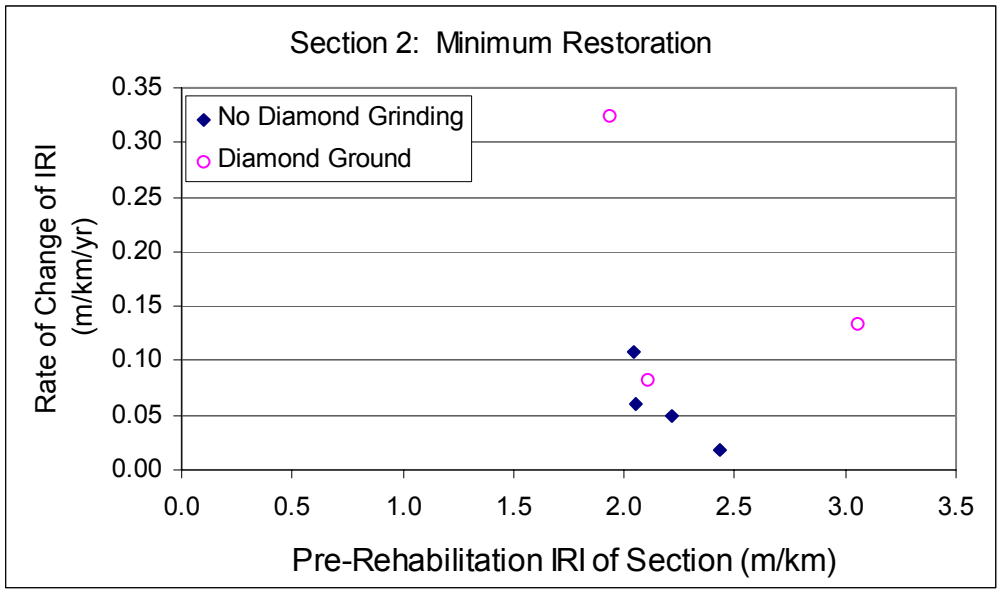

Figure 56. Relationship between rate of change of IRI and pre-rehabilitation IRI: Section 2 (minimum restoration)

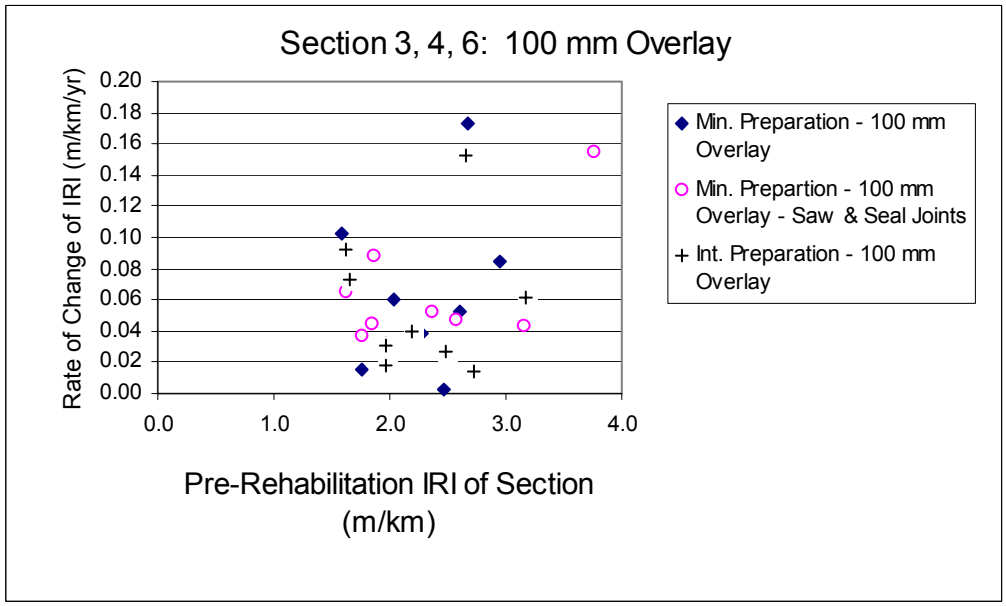

Figure 57. Relationship between rate of change of IRI and pre-rehabilitation IRI: Section 3, 4 and 6 (sections receiving 100 mm overlay)

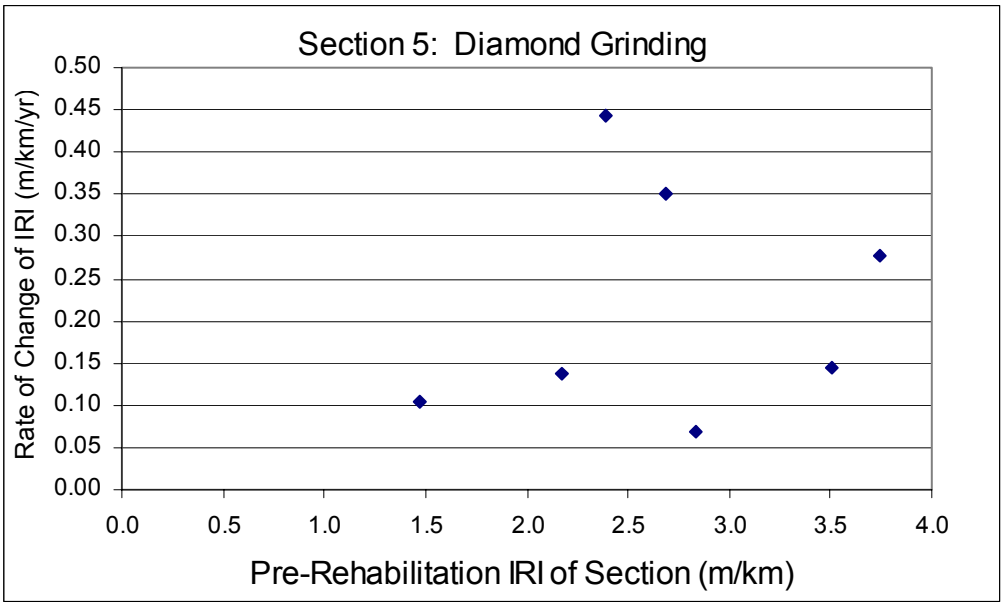

Figure 58. Relationship between rate of change of IRI and pre-rehabilitation IRI; Section 5 (diamond grinding)

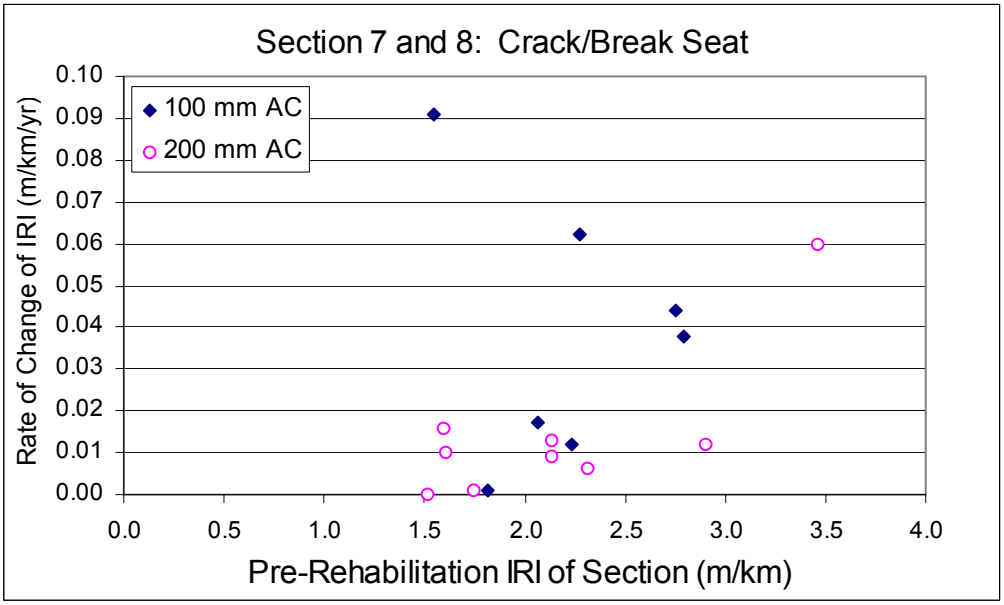

Figure 59. Relationship between rate of change of IRI and pre-rehabilitation IRI; Section 7 and 8 (crack/break seat and AC surface)

Table 43. Percent change in IRI at sections in SPS-6 projects.

State	Age When Project at First Profile Date (Yrs)	Age of Project at Last Profile Date (Yrs)	Time Difference for IRI Change (Years)	Percent Change in IRI (Note 1)						
				Section Number						
				2	3	4	5	6	7	8
Arizona	1.1	8.6	7.5	3	146	49	43	56	92	21
California	0.7	5.7	5.1	58	49	96	134	80	22	8
Illinois	1.5	7.7	6.2	17	23	27	103	9	8	4
Indiana	0.3	8.3	8.0	-1	17	35	N/A	18	4	8
Iowa	0.8	9.9	9.1	64	18	44	68	38	45	1
Michigan	0.6	8.9	8.3	37	-1	-9	N/A	37	-10	-2
Missouri	0.6	6.5	5.9	223	15	22	242	15	15	-4
Oklahoma	0.6	6.8	6.2	46	81	61	85	61	21	4
Pennsylvania	0.2	5.7	5.5	13	31	23	57	34	20	7
South Dakota	1.1	6.6	5.6	70	21	17	47	13	33	31
Average	0.7	7.5	6.7	53	40	37	97	36	25	8

Note 1: Percent Change in IRI = 100 X (IRI Last Profile Date - IRI First Profile Date)/(IRI at First Profile Date)
N/A - Data not available.

Table 44. Diamond ground sections evaluated.

SPS-6 Project	IRI (m/km)			Last Profile Date	Distress Survey Date (Note 1)	Pre-Rehabilitation Distress Available ?	Comment
	Before Diamond Grinding	After Diamond Grinding	Last Profile Date				
Arizona	2.39	1.45	2.08	2/12/93	9/25/91	Yes	Note 2
California	3.74	1.10	2.58	5/6/98	7/28/99	No	Note 3
Illinois	2.18	0.80	1.62	3/4/98	9/14/98	Yes	
Iowa	N/A	1.51	2.53	11/30/93	4/21/93	No	Note 2
Missouri	2.68	1.24	3.01	2/10/99	10/6/98	Yes	
Oklahoma	1.47	0.76	1.41	6/9/99	11/18/98	No	
Pennsylvania	3.51	1.39	2.18	5/28/98	7/21/99	Yes	
South Dakota	2.83	0.92	1.35	5/15/99	8/6/98	No	

N/A - Data not available
Note 1: Distress survey date that is closest to last profile date
Note 2: Appears to be rehabilitated after last profile date
Note 3: Pre-rehabilitation distress data available for most sections in SPS-6, but no data for section 5

distress data were available for the project, and the distress survey date that was closest to the last profile date.

Table 45 shows the distresses noted at the diamond ground section prior to rehabilitation, as well as the distresses for the date closest to the last profile date. The distress quantities shown in table 45 for each distress type is the sum of the distresses for all severity levels. The distress survey type is also indicated in this table. For the Pasco distress surveys, the distresses are obtained from photographic images, while in the manual surveys the distresses are recorded by a surveyor. An evaluation of the data tables in the IMS was performed to obtain the total faulting at the section corresponding to the distress survey date, or at a date closest to this date. However, the faulting data available was for much earlier survey dates, and therefore were not included in the analysis. The most prevalent distress noted at the diamond ground sections was transverse cracking. It is not known if faulting occurring at these cracks, in addition to faulting occurring at the joints are contributing to the increase in roughness. Some of the sections have large number of rigid patches. It is not clear how these patches have performed, and if these patches have tilted or are rocking under traffic and are contributing to the increase in roughness.

Table 45. Distresses at diamond ground sections.

State	Distress Survey Date	Distress Survey Type	Case (Note 1)	IRI (m/km) (Note 2)	Corner Breaks (No)	Long. Cracking Length (m)	Trans. Cracks (No)	Trans. Crack Length (m)	Long. Spalling Length (m)	Trans. Spalls (No)	Trans. Spall Length (m)	Flexible Patches (No)	Flexible Patches Area (m2)	Rigid Patches (No)	Rigid Patches Area (m2)
Arizona	11/21/89	Pasco	Pre-Rehab	2.39	0	8	12	41	0	33	111	0	0	0	0
Arizona	9/25/91	Manual	Last Profile	2.08	5	16	24	80	49	14	18	9	3	52	17
California	7/28/99	Manual	Last Profile	2.58	2	0	33	82	0	0	0	2	35	0	0
Illinois	5/6/90	Pasco	Pre-Rehab	2.18	0	0	13	48	1	1	1	0	0	4	54
Illinois	9/14/98	Manual	Last Profile	1.62	0	0	46	215	5	3	4	1	1	9	68
Iowa	4/21/93	Pasco	Last Profile	2.53	0	1	34	144	9	2	5	57	47	36	242
Missouri	8/7/91	Manual	Pre-Rehab	2.68	0	0	24	0	0	1	0	0	0	6	130
Missouri	10/6/98	Manual	Last Profile	3.01	0	7	34	215	1	21	11	3	1	27	389
Oklahoma	11/18/98	Manual	Last Profile	1.41	0	26	13	33	0	8	14	1	0	7	40
Pennsylvania	7/24/90	Manual	Pre-Rehab	3.51	1	4	5	12	4	0	0	9	5	3	33
Pennsylvania	7/21/99	Manual	Last Profile	2.18	0	3	10	25	147	12	8	27	8	9	145
South Dakota	8/6/98	Manual	Last Profile	1.35	4	24	4	4	5	1	0	2	1	25	62

Note 1: Pre-Rehab: Distresses recorded prior to rehabilitation.
Last Profile - Distresses recoded at a date that was closess to the date the section was last profiled

Traffic data as well as material testing data are not yet available in the LTPP database for many SPS-6 sections. Because of these limitations, a comprehensive analysis of the data to build models to predict development of roughness cannot be carried out yet. It was also seen that the pre-rehabilitation IRI as well as the pavement distress prior to rehabilitation varied between the test sections in individual SPS-6 projects. This introduces an additional confounding factor to the analysis. In spite of these limitations, the existing data does reveal trends in roughness development at SPS-6 sections.

Summary of Findings

Section 2 in a SPS-6 project was subjected to minimum restoration. Minimum restoration consisted of joint sealing, crack sealing, partial depth patching, and full depth patching. Each agency was also allowed to diamond grind this section as warranted. In some projects this sections was diamond ground, while in others it was not. At section 2 in Arizona, joint sealing, crack sealing and partial depth patching was performed, that resulted in the IRI of the section increasing from 2.43 to 3.46 m/km. Full depth patches were performed at section 2 in Indiana, that caused the roughness to increase from 1.64 m/km to 3.64 m/km. These results show that if repairs are not performed correctly in PCC pavements, they can result in an increase in roughness of the pavement. For the sections that were subjected to minimal restoration, and were diamond ground, the post-rehabilitation IRI of the sections ranged from 1.03 to 1.36 m/km.

A statistical analysis indicated there were no differences in IRI values obtained immediately after rehabilitation for sections 3 through 8. That is the analysis indicated applying the following treatments on a PCC pavement result in similar IRI levels: (1) minimum restoration of existing pavement followed by a 100 mm AC overlay (section 3), (2) minimum restoration of existing surface followed by a 100 mm AC surface, with sawing and sealing over joints (section 4), (3) Intensive restoration of existing surface that includes diamond grinding (section 5), (4) Intensive restoration of existing surface followed by a 100 mm AC overlay

(section 6), (5) crack/break seat of PCC with a 100 mm AC surface (section 7), (6) crack/break seat of PCC with a 200 mm AC overlay (section 8). An investigation of the IRI before and after rehabilitation for the SPS-6 projects indicated that for a specific SPS-6 project, the IRI after rehabilitation for sections 3 through 8 all fell within a relatively narrow band.

An analysis of the rate of increase of IRI for the different treatment types indicated the following average values for rate of increase of roughness: (1) Section 3, minimum restoration and 100 mm overlay: 0.058 m/km/year, (2) Section 4, minimum restoration and 100 mm overlay with sawing and sealing of joints: 0.057 m/km/year, (3) Section 5, intensive restoration with diamond grinding: 0.200 m/km/year, (4) Section 6, intensive restoration with 100 mm overlay: 0.054 m/km/year, (5) Section 7, crack/break seat with 100 mm AC surface: 0.032 m/km/year, and (6) Section 8, crack/break seat with 200 mm AC surface: 0.013 m/km/year. A statistical analysis indicated the rate of increase of IRI of section 5 (diamond grinding) was statistically different from the rate of increase of IRI of the other sections. Generally, the rate of change of IRI at diamond ground sections was higher for sections that had higher IRI values prior to rehabilitation.

This page left intentionally blank.

CHAPTER 7

ANALYSIS OF GPS SECTIONS IN THE FIRST DESIGN PHASE

ANALYSIS APPROACH

There are five GPS experiments that study pavements in the first design phase. These experiments are: GPS-1, AC pavements on granular base; GPS-2, AC pavements on stabilized base; GPS-3, jointed plain concrete pavements; GPS-4, jointed reinforced concrete pavements, and GPS-5, continuously reinforced concrete pavements. The analysis approach that was followed in analyzing the data from each of these experiments was similar. Initially, the test sections in each experiment were categorized by environmental zone and subgrade type to see the distribution of the test sections according to environmental zone and subgrade type. A distribution of the sections according to pavement age at the first and last profile dates was developed to obtain information on the age distribution of the pavements. Thereafter an evaluation of the magnitude of the change in roughness that had occurred at the test sections over the monitored period was performed. This was accomplished by computing the change in roughness, which is the difference in IRI between the last profile date and the first profile date. The change in roughness that occurred over the monitored period was then classified according to different IRI ranges and environmental zones to evaluate the distribution of the change in roughness between environmental zones. The time difference in which this change in roughness occurred is different for the test sections. This is because the date when the section was first profiled as well as the last available profile date are not the same for the test sections. For each test section, a linear regression was performed to obtain the rate of change of IRI. Thereafter, the distribution of the rate of change of IRI was classified according to different ranges and according to different environmental zones to examine trends. For each of the evaluated experiments, the time-sequence data were then plotted separately for each environmental zone. Depending on the experiment, more detailed plots were prepared. For example, for jointed plain concrete pavements, time-sequence plots were prepared separately for pavements with and without dowels, as a distinct difference in roughness progression was noted between the two pavement types. Thereafter, scatter plots between IRI and/or the rate of change of IRI and parameters that could have an effect on roughness development (e.g., climatic and subgrade

parameters) was performed. For experiment types where an appreciable change in IRI occurred over the monitored period (e.g., GPS-1), relationships between the rate of change of IRI and the evaluated parameters were studied. For experiment types where not much change in IRI occurred over the monitored period (e.g. GPS-5), relationships between median IRI over the monitored period and evaluated parameters were studied. Thereafter, models for predicting roughness were developed.

GPS-1: ASPHALT CONCRETE PAVEMENTS ON GRANULAR BASE

Test Sections

There are 219 GPS-1 sections in the LTPP database for which IRI data are available. However, subgrade information is available for only 202 sections. The distribution of these sections according to the environmental zone and subgrade type is shown in table 46. The percentage distribution of sections according to the environmental zones are: dry-freeze – 16 percent, dry no-freeze – 12 percent, wet freeze – 36 percent and wet no-freeze – 36 percent. Seventy one percent of the GPS-1 sections are located on coarse grained soil, while 29 percent are located on fine grained soil.

Table 46. Distribution of GPS-1 sections.

Subgrade Type	Number of Sections				
	Environmental Zone				Total
	Dry-Freeze	Dry No-Freeze	Wet Freeze	Wet No-Freeze	
Coarse	20	24	53	46	143
Fine	13	1	19	26	59
Total	33	25	72	72	202

Figure 60 shows the distribution of GPS-1 sections according to their age at the time they were first profiled and at the last available profile date. On average, the GPS-1 sections have so far been profiled six times, over a six-year period. Over 50 percent of the sections have been monitored between a period of seven to ten years.

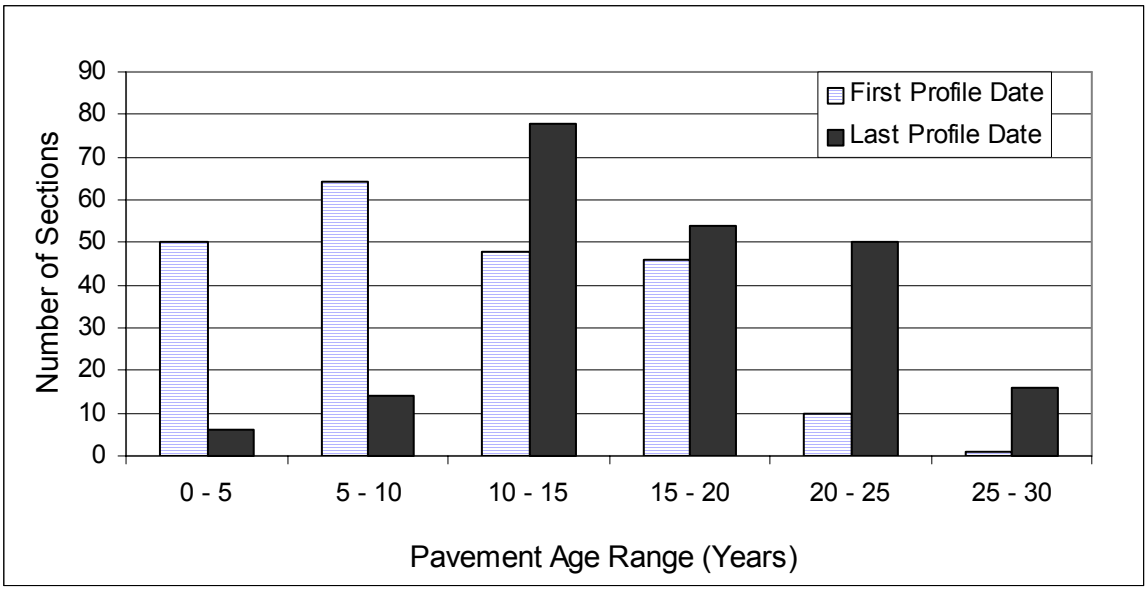

Figure 60. Distribution of GPS-1 sections according to age at first and last profile dates.

Changes in IRI

The difference in IRI between the last profile date and first profile date, classified according to different IRI ranges when all environmental zones are considered, as well as for each environmental zone is presented in table 47. The data presented in table 47 provides an overview of the magnitude of changes in IRI that have occurred at the GPS-1 sections over the monitored period.

The percent distribution for all regions show that at 13 percent of the sections, the IRI at last profile date was less than the IRI at the first profile date, while at 15 percent of the sections the difference in IRI between the last and first profile date was less than 0.1 m/km. A change in IRI of 0.1 m/km is a very small change in IRI, and these types of differences can easily occur due to variations in the profiled path. The decrease in roughness that is seen at 13 percent of the sections is attributed to variations in profiled path or changes in pavement profile due to changes in the subsurface layers (i.e., swelling or shrinkage). Therefore, it can be concluded that at 28 percent of the GPS-1 sections, the roughness has not changed or showed negligible change over the monitored period. Similar observations are noted when the changes in IRI in individual

Table 47. Percent distribution of GPS-1 sections according to change in IRI.

Change in IRI Over the Monitored Period (m/km)	Percent Sections				
	Environmental Zone				
	All Zones	Dry Freeze	Dry No-Freeze	Wet Freeze	Wet No-Freeze
<0	13	11	12	17	11
0.0 - 0.1	15	9	8	17	19
0.1 - 0.2	16	20	8	13	19
0.2 - 0.3	13	11	12	14	13
0.3 - 0.4	8	11	8	6	9
0.4 - 0.5	6	9	20	2	4
0.5 - 0.6	5	6	4	6	3
0.6 - 0.7	3	3	8	2	3
0.7 - 0.8	2	0	4	2	3
0.8 - 0.9	4	3	8	2	4
0.9 - 1.0	2	6	0	1	3
> 1.0	13	11	8	18	9
Total	100	100	100	100	100

environmental zones are examined. When evaluating the changes in roughness shown in table 47, it should be noted that the monitored period varies between the sections.

Roughness progression between test sections can be evaluated by obtaining a rate of change of roughness for each section. A regression analysis was performed on the time-sequence IRI values to obtain a rate of change of IRI at each section. Table 48 presents the rate of change of IRI at the test sections classified according to different ranges for all environmental zones, as well as for individual environmental zones. Table 49 presents the percent test sections that have a rate of change of roughness that is less than a specified level. Pavements in the wet-freeze zone have the most potential for the roughness to be affected by environmental factors. However, as the data show, 51 percent of the test sections in the wet-freeze zone have a rate of change of IRI of less than 0.04 m/km, when compared to 33 percent for dry-freeze zone, 36 percent for dry no-freeze zone, and 53 percent for wet no-freeze zone. Environmental effects do have an influence on the rate of change of IRI, but if the pavement is designed to take these factors into account, the effect on the rate of change of IRI may not be seen.

Table 48. Percent distribution of GPS-1 sections according to rate of change of IRI

Rate of Change of IRI (m/km/yr)	Percent Sections				
	Environmental Zone				
	All Zones	Dry Freeze	Dry No-Freeze	Wet Freeze	Wet No-Freeze
< 0	11	3	9	18	8
0.00 - 0.02	22	19	13	19	28
0.02 - 0.04	14	10	13	14	18
0.04 - 0.06	17	27	14	13	17
0.06 - 0.08	7	7	14	7	6
0.08 - 0.10	4	7	9	1	3
0.10 - 0.12	4	7	9	1	3
0.12 - 0.14	7	7	5	10	6
0.14 - 0.16	3	3	5	4	2
> 0.16	11	10	9	13	9
Total	100	100	100	100	100

Table 49. Cumulative distribution of GPS-1 sections according to rate of change of IRI

Rate of Change of IRI (m/km/yr)	Percent Sections				
	All Zones	Dry Freeze	Dry No-Freeze	Wet Freeze	Wet No-Freeze
< 0	11	3	9	18	8
<0.02	33	23	23	37	36
< 0.04	47	33	36	51	53
< 0.06	64	60	50	63	70
< 0.08	71	67	64	70	77
< 0.10	75	73	73	72	80
< 0.12	79	80	82	73	83
< 0.14	86	87	86	83	89
< 0.16	89	90	91	87	91

Figure 61 shows the relationship between the rate of change of IRI and the average age of the pavement over the monitored period. No clear relationship between rate of change of IRI and the pavement age is observed. There are several very old pavements that are still showing very low rates of increase in IRI, while there are some pavements that are between 10 and 15 years old that show a very high rate of increase of roughness.

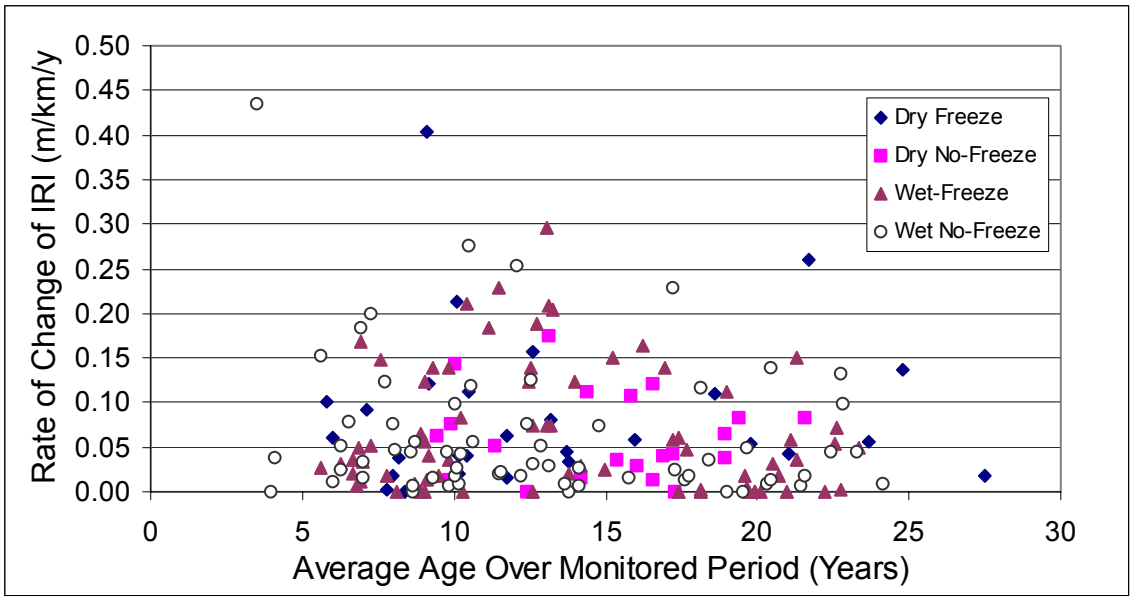

Figure 61. Relationship between rate of change of IRI and pavement age for GPS-1 sections.

Trends in Roughness Development

The time-sequence IRI plots for the GPS-1 sections classified according to the environmental zones, and then further subdivided according to the percent material in subgrade that is passing the No. 200 sieve were plotted to examine trends in IRI development. The ranges of percent material passing the No. 200 sieve that were considered are: less than 20 percent, between 20 and 50 percent, more than 50 percent. These plots are shown in figures 62 through 65. An examination of these plots show that the overall trend of roughness progression to be a linear trend followed by an exponential increase in roughness. Generally, pavements that are of similar age show a parallel trend in roughness progression.

Forty percent of the test sections in the GPS-1 experiment have been deasssigned, that is monitoring activities at these sections have been stopped because the sections were rehabilitated. The deassigned sections are also included in the plots shown in figures 62 through 65. The average IRI at the last profile date for the deassigned sections was 1.7 m/km, which is a rather low IRI value. However, the average age of the deassigned sections was 15 years, and the cause

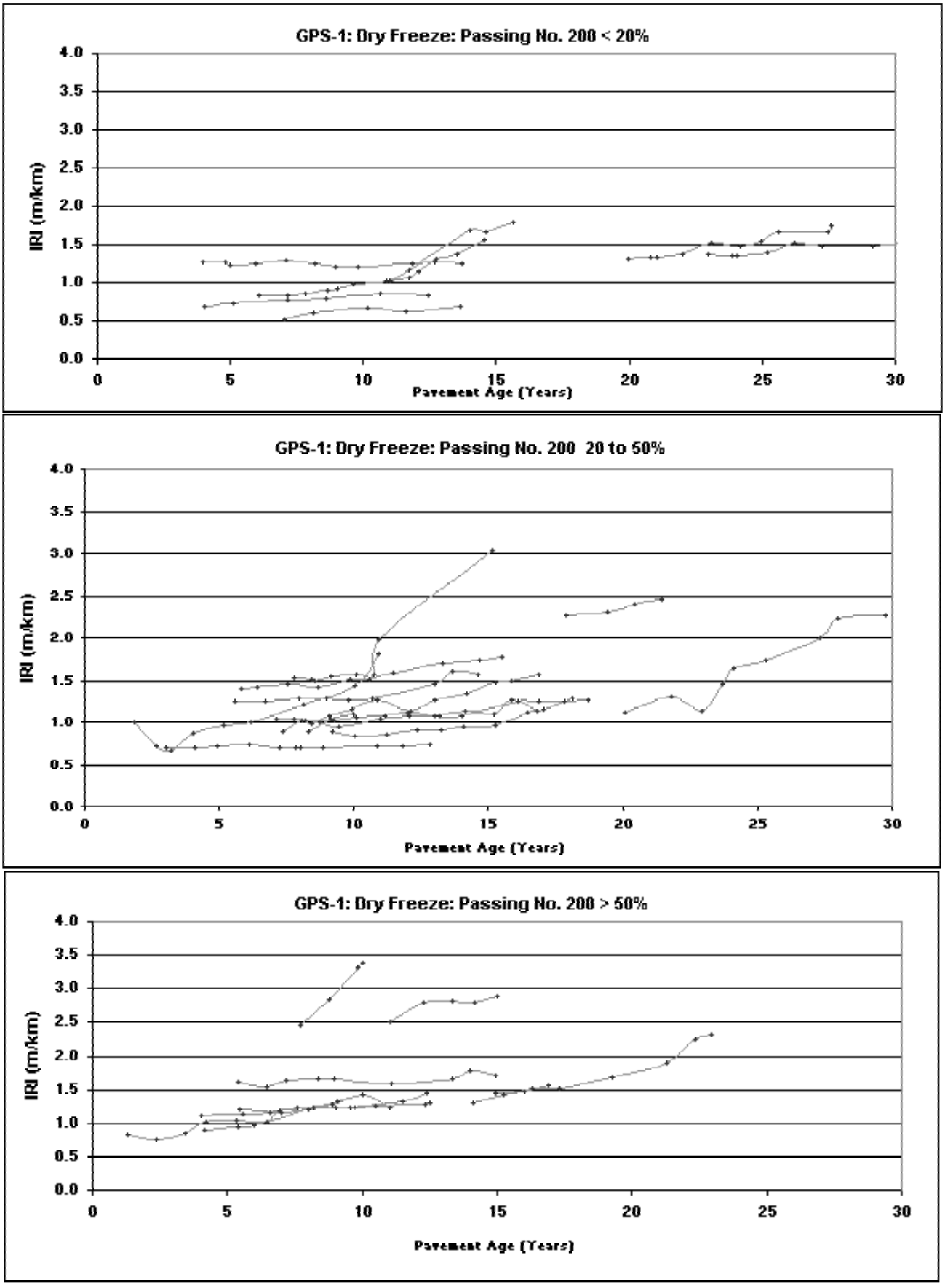

Figure 62. IRI trends for GPS-1 sections in the dry freeze zone

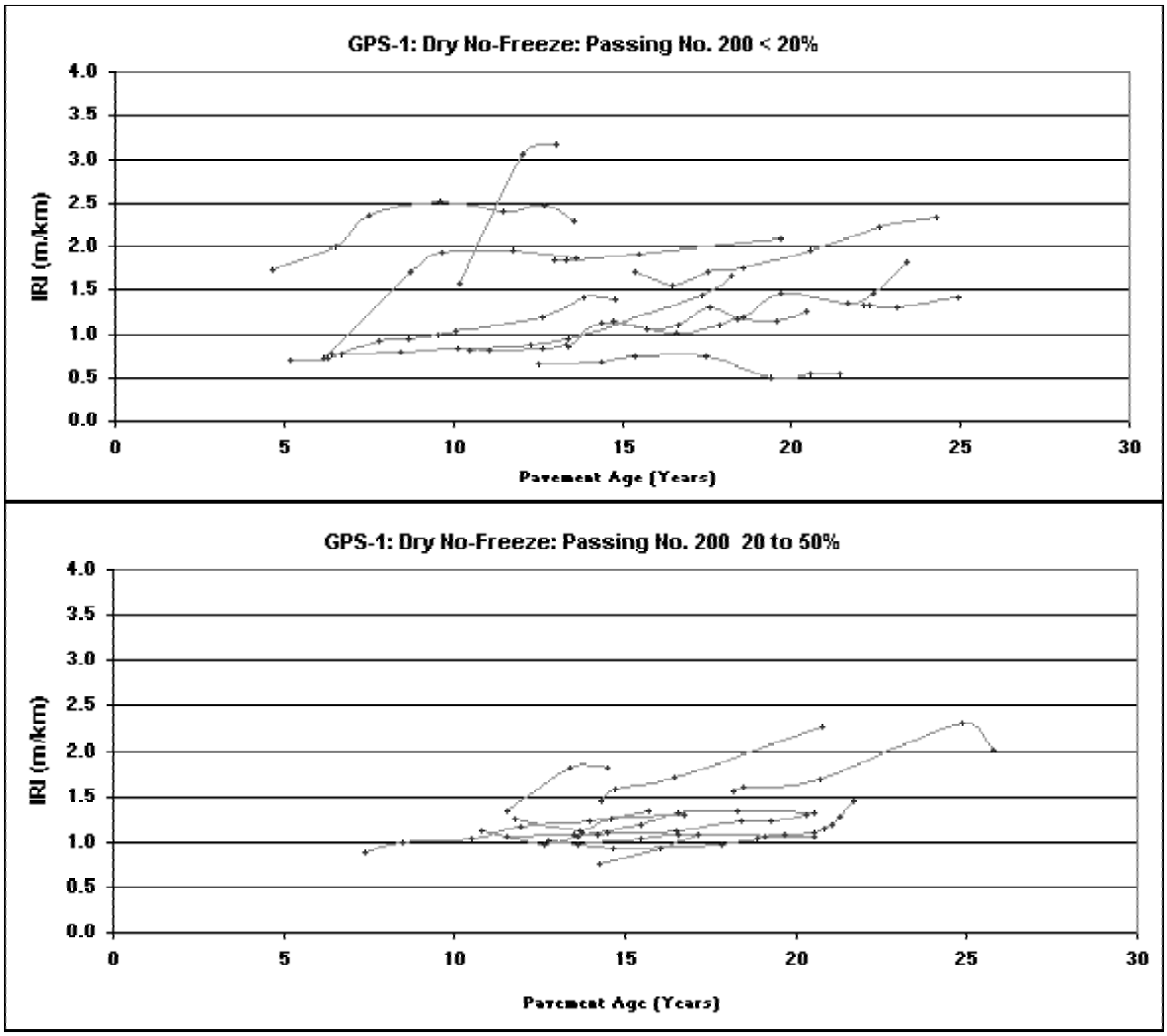

Figure 63. IRI trends for GPS-1 sections in the dry no-freeze zone

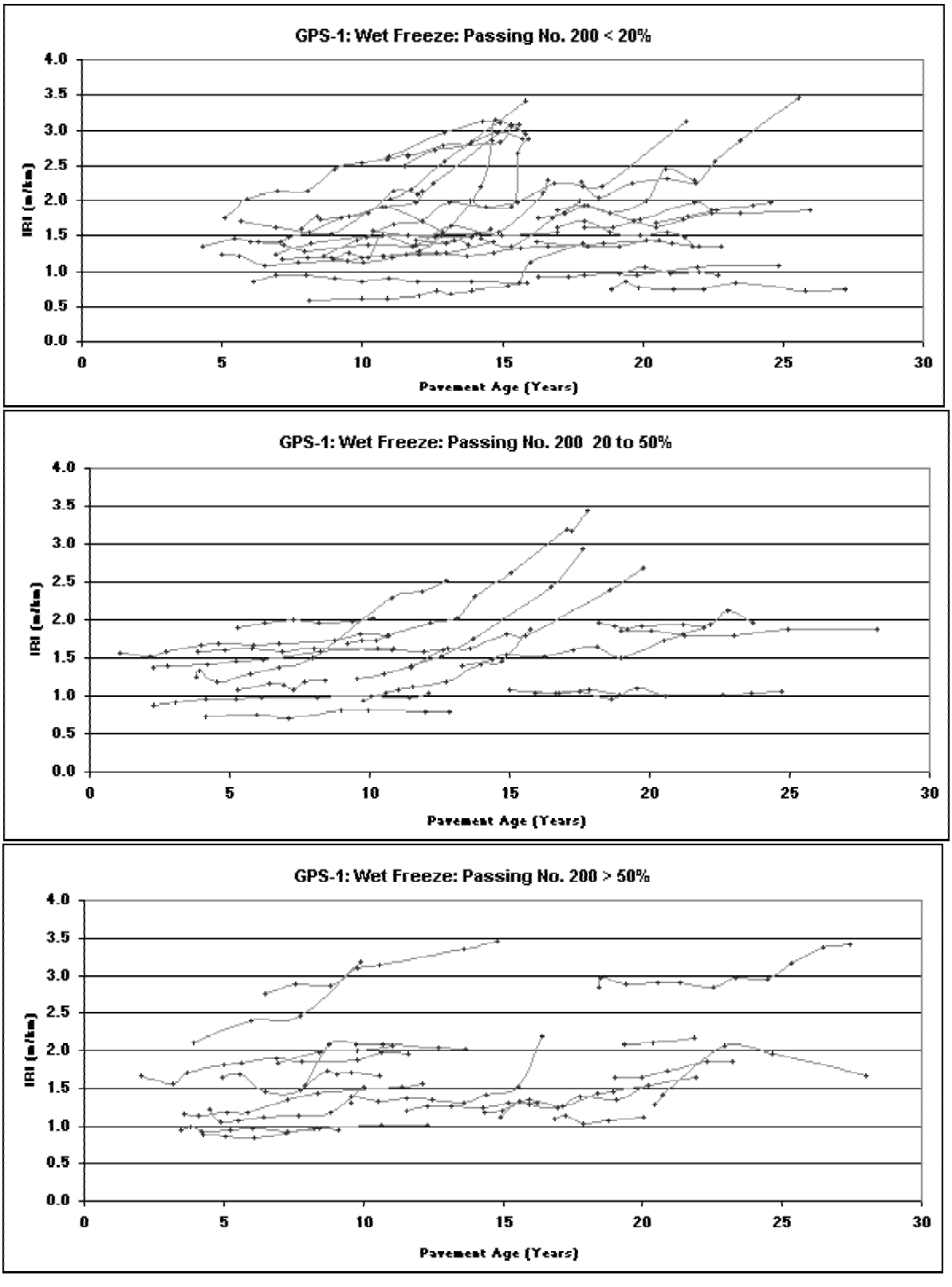

Figure 64. IRI trends for GPS-1 sections in the wet no-freeze zone

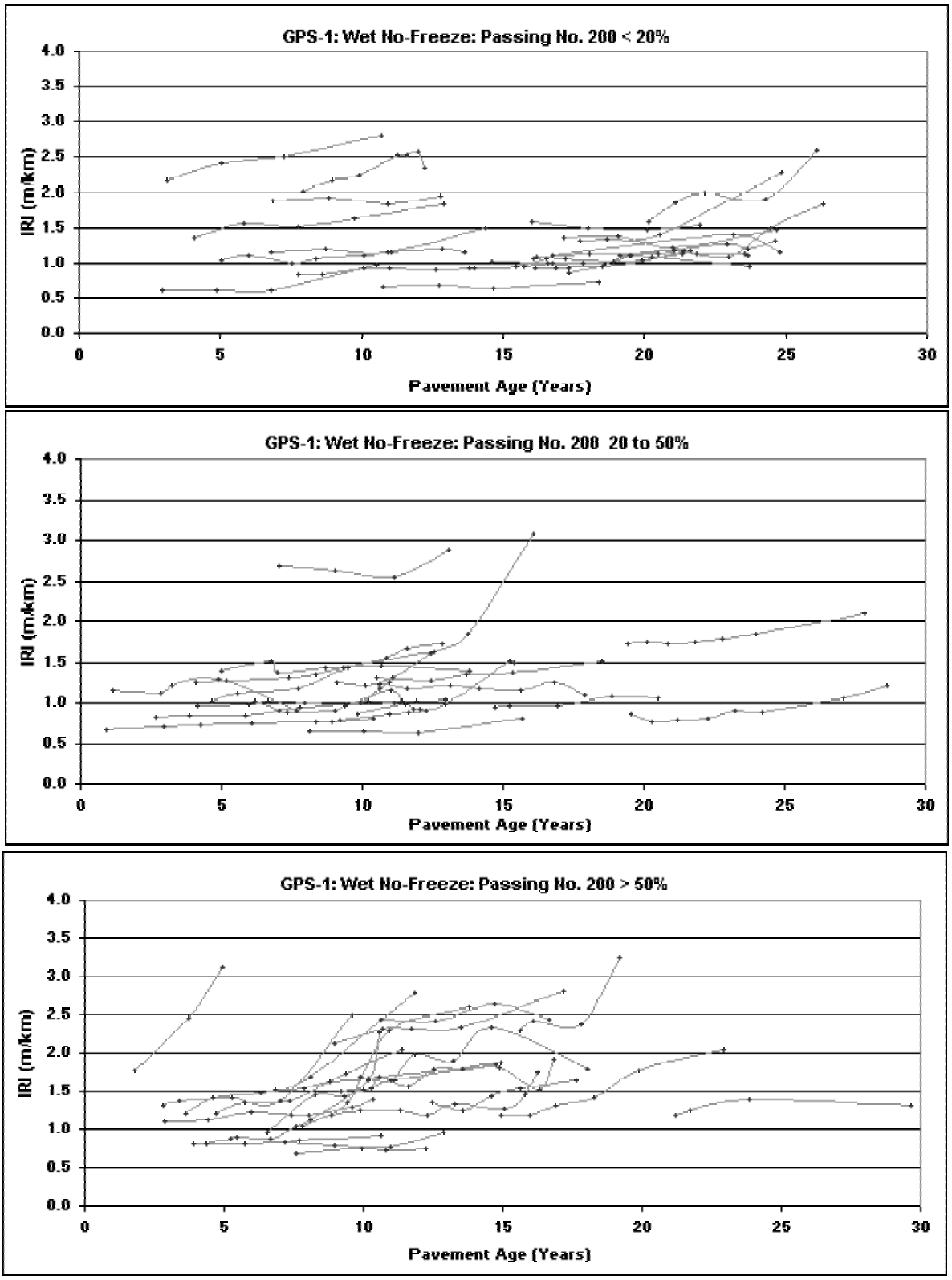

Figure 65. IRI trends for GPS-1 sections in the wet freeze zone

of rehabilitation of many of the deassigned sections may not have been excessive roughness. The fact that only a few sections show an exponential increase in roughness at the latter stages of the pavement life in figures 62 through 65 is because State highway agencies appear to be rehabilitating pavements before they reach such a stage. As figures 62 through 65 show, there are only a few sections that have IRI values of over 2.5 m/km at their last profile date.

The plots for the wet freeze zone show that some sections located on subgrade that has less than 20 percent material passing the No, 200 sieve show large increases in roughness. The silt content in such material can have a significant effect on the frost heave potential of the subgrade. The sections that are showing large increases in roughness generally have a silt content between 5 and 20 percent. The plots for the wet no-freeze zone show the highest increases in roughness generally occur on sections located on subgrades containing greater than 50 percent material passing the No. 200 sieve. In the wet no-freeze zone, pavements located on subgrades having less than 20 percent material passing the No. 200 sieve are performing well.

Factors Affecting Changes in IRI

An analysis was performed to identify the factors that have an influence on the increase in IRI. Scatter plots between the rate of increase in IRI and parameters that were selected for analysis (see table 5) were examined to observe data trends. This analysis was initially performed by considering all GPS-1 sections, and thereafter separate analyses were performed for individual environmental zones. There were only a few cases where a relationship between the rate of increase of IRI and an evaluated parameter was observed

When the analysis was performed for the entire data set, the strongest relationships between the rate of increase of IRI and an evaluated parameter existed for the percentage of base material passing the No. 200 sieve, freezing index, and plasticity index of subgrade. Higher rates of increase of roughness were observed with increasing values for each of these parameters. Plots showing the relationship between rate of change of IRI and each of these parameters are shown in figures 66 though 68.

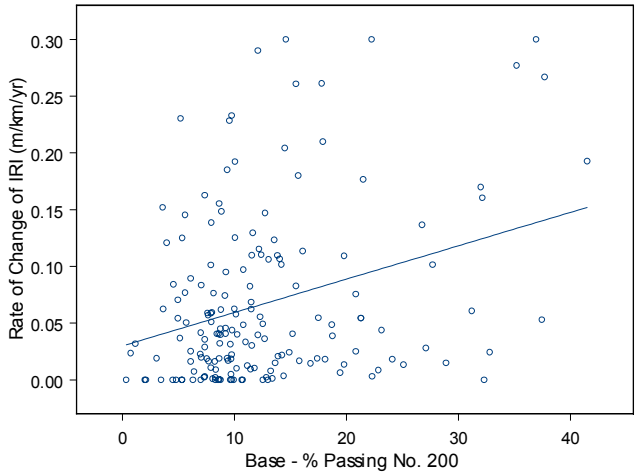

Figure 66. Relationship between rate of change of IRI and percent material in base passing No. 200 sieve.

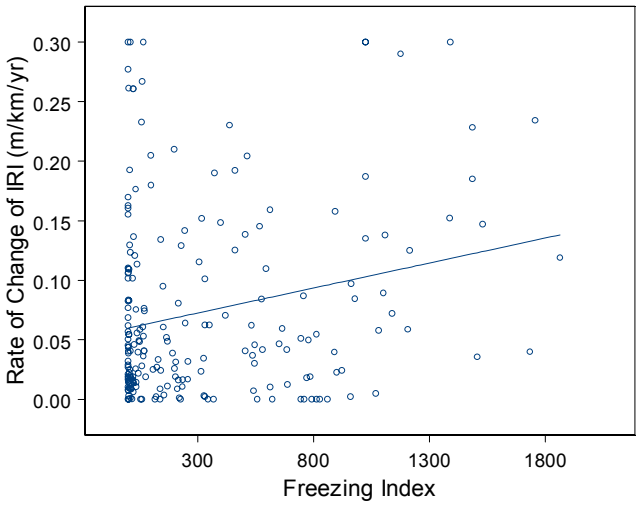

Figure 67. Relationship between rate of change of IRI and freezing index.

Excess amounts of fine material in the base layer results in a weaker base, increases the frost heave potential of the base, and increases the pumping potential of the base. Moisture infiltrating a base containing an excess amount of fine material can substantially reduce the strength of the base. Some of the largest rates of increase of roughness were observed for sections that had very high fines content in the base. Higher freezing indexes will result in

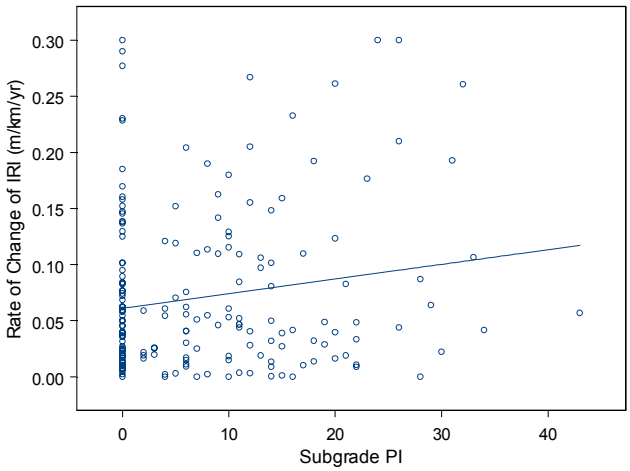

Figure 68. Relationship between rate of change of IRI and plasticity index of subgrade.

greater frost heave if frost susceptible layers are present below the pavement surface. In areas that have high freezing indices and frost susceptible subsurface layers, the pavements must be adequately designed to minimize the frost heave of the pavement. A trend of a higher rate of increase of roughness with higher plasticity index of the subgrade was also observed. Subgrades having high plasticity indices are more susceptible to volume changes with changes in moisture content, and this can result in an increase in roughness of the pavement.

A comparison between the IRI and cumulative traffic on the pavement was performed to see if there was a relationship between the two parameters. No relationship between the two parameters was observed.

The previously described relationships were observed when the relationships between rate of change of IRI and the evaluated parameters were examined for the entire data set. Relationships between the rate of change of IRI and the evaluated parameters were then carried out separately for each environmental zone to see if trends specific to each environmental zone could be identified. The following are the observations noted for each environmental zone.

Dry-Freeze Zone

Pavements subjected to higher annual precipitation showed higher increases in roughness. In the dry-freeze zone, the range of annual precipitation range from 200 to 500 mm. Higher precipitation will increase the moisture content of the subsurface layers, and this will increase the frost heave potential of frost susceptible layers. Higher rates of increase of IRI were observed for higher freezing indices, increasing plasticity index of subgrade and higher amounts of fine material in the base layer.

Dry No-Freeze Zone

Sections having asphalt contents of less than 4.5 percent showed a higher rate of increase of roughness than sections with asphalt contents that were greater than 4.5 percent. Pavements in areas having a higher mean annual temperatures, and higher number of days above 32 °C had higher increase in roughness. High temperatures increase the potential for increase in rutting, and this can lead to an increase in roughness. Pavements on subgrades that had higher plastic limits had higher rates of increase of roughness.

Wet-Freeze Zone

Pavements with higher total pavement thickness (i.e., sum of surface, base and subbase) had lower rates of increases in roughness. A higher total pavement thickness reduces the frost heave potential of pavements located on frost susceptible subgrades. Some sections that had low asphalt contents had high rates of increases of roughness. Sections with lower annual precipitations or lower number of wet days per year had higher increases in roughness. Subgrades in areas having a higher number of wet days would tend to have more stable moisture content of the subgrade when compared to areas that have less number of wet days. Therefore, the shrink-swell potential of subgrades in areas having higher number of wet days would be less than the areas that have a lower number of wet days. Increasing potential for swelling or shrinkage of subgrade can cause deformations on the pavement surface, and result in higher roughness. Some sections on coarse subgrades, that had the percentage material passing No. 200 sieve of less than 20 percent, had high rates of increase of roughness. Generally, these sections had a silt content between 5 and 15 percent. The high rate of increase of IRI at these sections is

attributed to the frost heave potential of the subgrade, due to the silt in the subgrade. In the wet freeze zone, sections experiencing higher freezing indices and sections that had high amounts of fine materials in the base layer showed higher rates of increase of roughness.

Wet No-Freeze Zone

There were several sections in the wet no-freeze zone that had a structural number of less than 2, and these sections were showing a high rate of roughness development. A number of these sections had a surface thickness of approximately 50 mm. A trend of a higher rate of increase of roughness with increasing number of days above 32 °C was observed. High temperatures increase the rutting potential of the AC layer, if the AC mix has not been adequately designed. Higher rates of increases in roughness were observed with higher plasticity index of subgrade, higher moisture content of subgrade, and for sections located on subgrades with high fines content. Pavements on bases that had a high percentage of fine material (generally in excess of 15%) had higher increases in roughness.

Comparison Between Good and Poorly Performing Sections

A subset of GPS-1 sections in the wet no-freeze zone were evaluated to see if the factors contributing to their performance from a roughness point of view could be identified. Figure 69 shows the time-sequence IRI values of five sections, three of which are showing an increase in IRI with time, and two that have provided good performance.

The following observations were noted for sections 48-1178, 37-1802 and 48-1169 that have shown high rates of increase in IRI: (1) Section 48-1178: This section is located in the wet no-freeze zone, on a fine grained subgrade that has 72 percent material passing the No. 200 sieve. The plasticity index of the subgrade is 26, and the subgrade has a moisture content of 28 percent. The base has a fines content (passing No. 200) of 22 percent, and the number of days with temperature greater than 32 °C at this location is 100. The combination of poor subgrade and base conditions, and the high temperature at this location is attributed to the high rate of increase of IRI observed at this section, which is less than 5 years old. (2) Section 37-1802: This

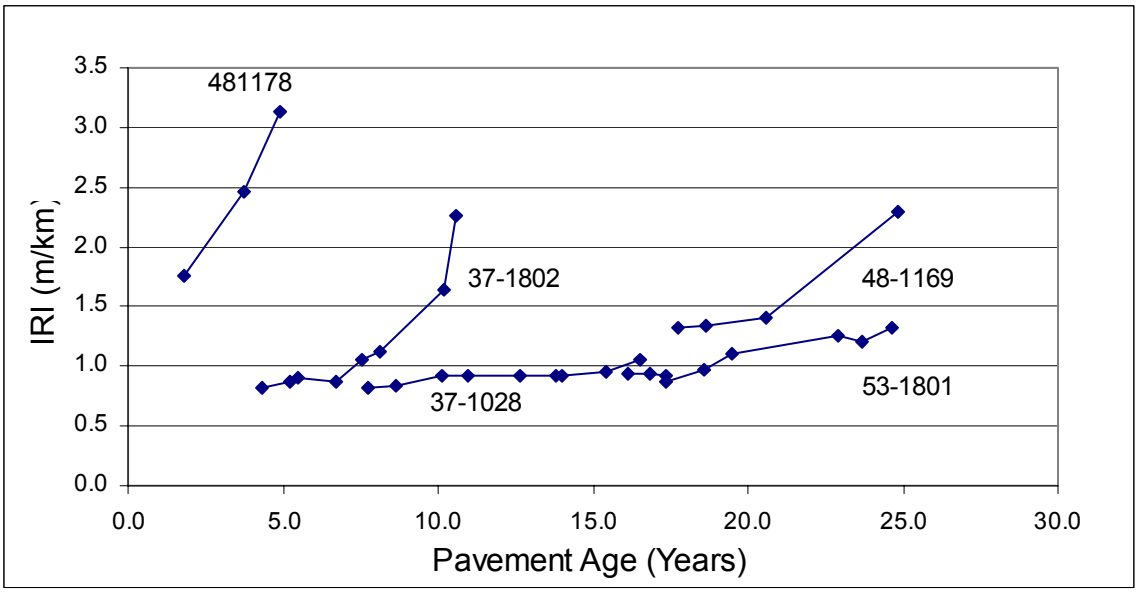

Figure 69. Good and poorly performing GPS-1 sections

section is located in the wet no-freeze zone has shown a rapid increase in roughness. The fine grained subgrade has 57 percent material passing the number 200 sieve, and a moisture content of 24 percent. This section has an estimated structural number of 3.3, and it appears this section may have exceeded its design traffic volume. (3) Section 48-1169: This section is located in the wet no-freeze zone, and has shown a rapid increase in IRI. This section has a very thin surface of 48 mm, and a base layer that is 287 mm thick, which has a fines content (passing No. 200) of 26 percent. It is likely that when distresses appeared on the surface layer, water infiltrated into the base and caused a very weak base layer because of the high fines content in the base layer. This can cause the roughness to increase rapidly.

Two sections that have performed well over the years are section 37-1028 and 53-1801. The following observations were noted at these two sections: (1) Section 37-1028: This section is in the wet no-freeze zone, and is located on a coarse grained subgrade, which has 9 percent material passing the No. 200 sieve. The good subgrade condition is one factor that is likely to have caused its good performance. (2) Section 53-1801: This section is 25 years old, and has an IRI of 1.3 m/km. This section is located in the wet no-freeze zone on a coarse grained subgrade, that has 19 percent material passing the No. 200 sieve. This section has a high structural number, and it appears that the cumulative traffic that has been applied to this section is much less than its

theoretical traffic capacity. The good subgrade conditions, as well as the low traffic volume this section has carried when compared to its theoretical traffic capacity are likely to have contributed to the good performance of this section.

As these examples show, for sections that are showing either a good performance or a poor performance, an in-depth analysis of the test section can identify the factors that are affecting its performance.

Models to Predict Roughness

The initial IRI of the GPS-1 sections are not known. An estimate of the initial IRI value of a pavement section can be obtained by backcasting the time-sequence IRI values, and then obtaining the IRI value corresponding to zero value of pavement age. An examination of the time sequence IRI plots shown in figures 62 through 65 show that a reasonable initial IRI may be obtained for relatively young pavements that are showing a linear increase in IRI by backcasting the IRI growth curve. This procedure assumes that the roughness increases linearly over time. However, some of the IRI plots, particularly sections that are over 10 years old show an exponential trend in the increase of roughness. For pavements showing such a behavior, backcasting will result in low IRI values. A linear regression was performed on the time-sequence IRI values to obtain the backcasted initial IRI value. An examination of the backcasted IRI values showed that for older pavements that are showing high rates of increase of roughness, backcasting resulted in low IRI values. One way of resolving the issue of low initial IRI values would be to assign an initial IRI based on IRI values that are typically obtained on new pavements for sections that had an initial IRI that was lower than a specified minimum cut-off value. An evaluation of the data indicated such a procedure would have to be used for many of the GPS-1 sections. The use of such a procedure can force a pavement to have an initial IRI that may not be correct, and any modeling performed using an incorrect initial IRI values will result in erroneous models.

Because of these limitations, it was decided to model the IRI development of GPS-1 sections by using an incremental modeling approach, where the time-sequence IRI values at a

section were used as the dependant variable, with the first IRI measured at the section being treated as the initial IRI. A mixed model analysis was performed on the GPS-1 data using the S-Plus software. The following model was developed to predict the IRI development:

$IRI_{Last} = -0.143 + 1.0765(IRI_{First}) + 0.0424(\Delta Time) + 0.0094(Traffic^{0.5}/SN^5) + 0.0012(\Delta Time \times PL) + 0.006(\Delta Time \times Base_{200})$

Section effects standard deviation = 0.20, residual standard deviation = 0.20,
No. of sections = 168

IRI_{Last} = IRI at time = ΔTime after first IRI, m/km
IRI_{First} = IRI at first profile date, m/km
ΔTime = Change in time from first profile date, years
Traffic = Cumulative traffic on section in KESALs
SN = Structural number
PL = Plastic limit of subgrade
$Base_{200}$ = Percentage material of base passing number 200 sieve

In a previous research study, Perera et al [(1)] used an optimization approach to model IRI development. This analysis method was applied to the GPS-1 data set, and the results of this analysis are presented in Appendix E.

Summary for GPS-1

When roughness progression of all GPS sections were evaluated, the factors that had the strongest relationship to the rate of increase of roughness were percent material in base passing the No. 200 sieve, freezing index and plasticity index of subgrade. Higher rates of increase of roughness were observed for higher values of these parameters. Thereafter, separate analyses were performed for each environmental zone to identify factors in each environmental zone that had an influence on the increase of roughness. In the dry-freeze zone, higher rates of increase of roughness were associated with higher annual precipitation, higher freezing indices and higher amounts of fine material in the base layer. In the dry no-freeze zone, higher rates of increase of

roughness were associated with higher mean annual temperatures, higher days above 32 °C, and higher plastic limits of subgrade. In the wet freeze zone, higher rates of increase of roughness were associated with low total pavement thickness (sum of surface, base and subbase), lower annual precipitation, lower number of wet days, high freezing indices, and high amounts of fine material in base layer. Pavements located on subgrades that had a silt content between 5 and 15 percent also showed high rates of increase of roughness. This is attributed to the frost heave potential of such subgrade. In the wet no-freeze zone, higher rate of increase of roughness were associated with higher number of days above 32 °C, higher plasticity index of subgrade, higher moisture content of subgrade, higher fines content in the subgrade, and for sections with base layers that had a high content of fine material (passing No. 200 sieve > 50 percent).

GPS-2: ASPHALT CONCRETE PAVEMENTS ON STABILIZED BASE

Test Sections

There are 128 GPS-2 sections in the LTPP database, but subgrade information is available for only 118 of these sections. The distribution of these sections according to the environmental zone and subgrade type is shown in table 50. The percentage distribution of the GPS-2 sections according to the environmental zones is: dry-freeze – 14 percent, dry no-freeze – 9 percent, wet-freeze 25 percent, and wet no-freeze – 52 percent. Sixty six percent of the GPS-2 sections are on coarse grained subgrade, while 34 percent of sections are on fine grained subgrade.

Table 50. Distribution of GPS-2 sections.

Subgrade Type	Number of Sections				
	Environmental Zone				Total
	Dry-Freeze	Dry No-Freeze	Wet Freeze	Wet No-Freeze	
Coarse	14	11	16	38	79
Fine	3	-	14	22	39
Total	17	11	30	60	118

The distribution of the sections according to the stabilized base type, classified according to the environmental zones is shown in table 51. There are only a few cement stabilized bases in the wet freeze zone, while there is an equal distribution of asphalt and cement stabilized bases in the wet no-freeze zone.

Table 51. Distribution of GPS-2 sections according to base type and environmental zone.

Stabilized Base Type	Number of Sections				
	Environmental Zone				Total
	Dry-Freeze	Dry No-Freeze	Wet-Freeze	Wet No-Freeze	
Asphalt	6	4	23	27	60
Cement	11	7	7	33	58

Figure 70 shows the distribution of pavement sections according to their age at the time they were first profiled, and at the last available profile date. On average, the GPS-2 sections have so far been profiled six times, over a six-year period. Fifty percent of the sections have been profiled for a period between 7 and 10 years.

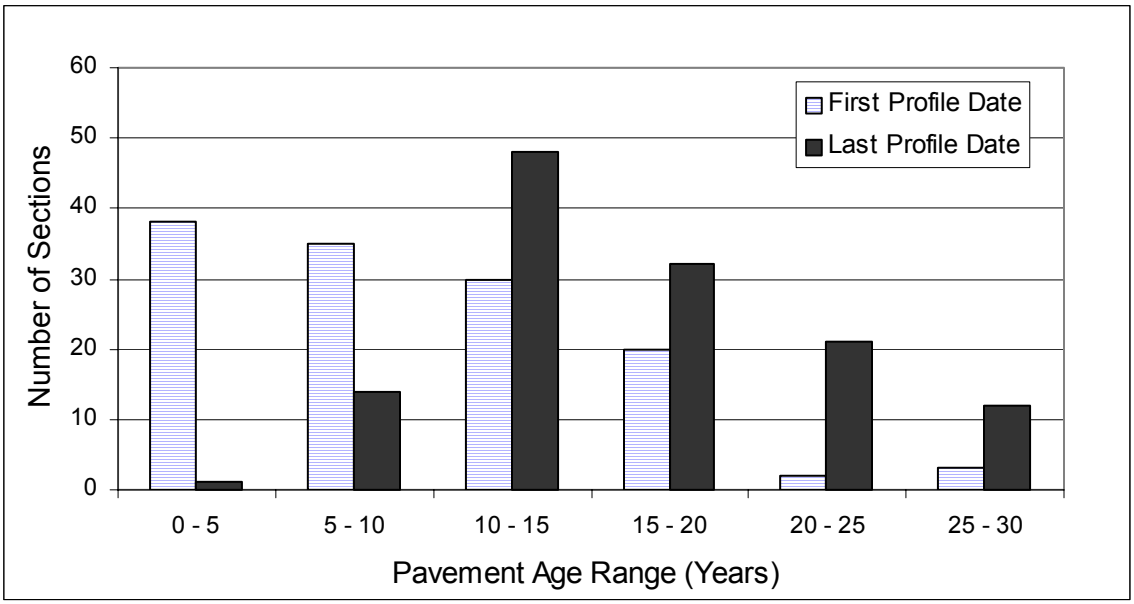

Figure 70. Distribution of GPS-2 sections according to age at first and last profile dates.

Changes in IRI

The difference in IRI between the last profile date and first profile date, classified according to different IRI ranges when all environmental zones are considered, as well as for each environmental zone is presented in table 52. The data presented in table 52 gives an overview of the magnitude of changes in IRI that have occurred at the GPS-2 sections over the monitored period.

Table 52. Percent distribution of test sections according to change in IRI.

Change in IRI Over Monitored Period (m/km)	Percent Sections				
	Environmental Zone				
	All Zones	Dry Freeze	Dry No-Freeze	Wet Freeze	Wet No-Freeze
<0	11	6	33	18	5
0.0 - 0.1	11	21	8	6	11
0.1 - 0.2	20	27	0	18	22
0.2 - 0.3	21	6	18	24	22
0.3 - 0.4	14	11	25	13	13
0.4 - 0.5	4	6	0	3	5
0.5 - 0.6	3	0	0	3	5
0.6 - 0.7	3	6	8	3	2
0.7 - 0.8	2	6	0	0	2
0.8 - 0.9	2	0	0	3	3
0.9 - 1.0	3	0	0	3	5
> 1.0	6	11	8	6	5
Total	100	100	100	100	100

The percent distribution of test sections for all environmental zones show that at 11 percent of the sections, the IRI at last profile date was less than the IRI at the first profile date, while at 11 percent of the sections the difference in IRI between the last and first profile date was less than 0.1 m/km. A change in IRI of 0.1 m/km is a very small change in IRI, and these types of differences can easily occur due to variations in the profiled path. The decrease in roughness that is seen at 11 percent of the sections is attributed to variations in profiled path or changes in pavement profile due to changes subsurface layers (i.e., swelling or shrinkage). Therefore, it can be concluded that at 22 percent of the sections, the roughness has not changed or showed

negligible change over the monitored period. When evaluating the changes in roughness shown in table 52, it should be noted that the monitored period varies between the sections.

Roughness progression between test sections can be compared by observing the rate of change of roughness at each section. A regression analysis was performed on the time-sequence IRI values to obtain a rate of change of IRI at each section. Table 53 presents the rate of change of IRI at the test sections, classified according to different ranges for all environmental zones as well as for individual environmental zones.

Table 53. Percent distribution of GPS-2 sections classified according to rate of change of IRI.

Rate of Change of IRI (m/km/yr)	Percent Sections				
	Environmental Zone				
	All Regions	Dry Freeze	Dry No-Freeze	Wet Freeze	Wet No-Freeze
< 0	10	6	20	18	5
0.00 - 0.02	20	27	10	21	20
0.02 - 0.04	22	28	20	12	26
0.04 - 0.06	12	6	20	6	15
0.06 - 0.08	8	11	0	10	8
0.08 - 0.10	9	6	10	9	8
0.10 - 0.12	2	0	0	0	5
0.12 - 0.14	4	6	0	3	5
0.14 - 0.16	2	0	0	6	0
> 0.16	11	11	20	15	8
Total	100	101	100	100	100

Figure 71 shows the relationship between the rate of change of IRI and the average age of the pavement over the monitored period. No clear relationship between rate of change of IRI and the pavement age is observed. There are several very old pavements that are still showing a very low rate of increase of IRI, while there are some pavements that are between 10 and 15 years old that show a very high rate of increase of roughness.

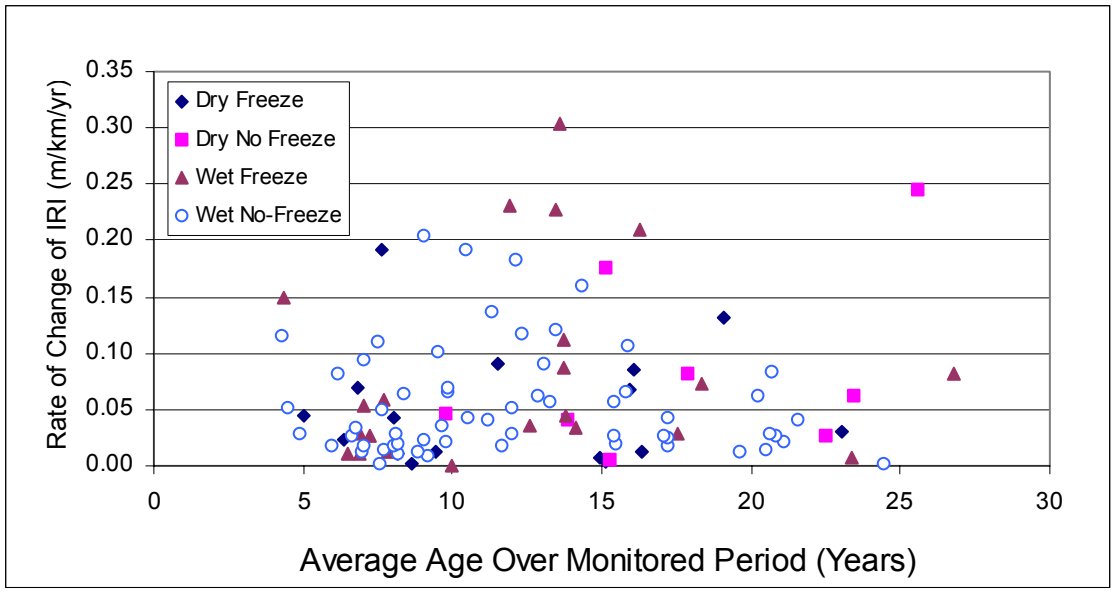

Figure 71. Relationship between rate of change of IRI and pavement age for GPS-2 sections.

Trends in Roughness Development

The types of stabilized bases that are used in the GPS-2 experiment can be broadly divided into asphalt stabilized or cement stabilized. However, a variety of material types have been used for each of these stabilized base types. For the asphalt stabilized bases, the material types that have been used were: hot mix AC, asphalt treated mixture, sand asphalt, mixed in place cold-laid mixtures, and central plant mix cold-laid mixtures. For cement stabilized bases, the material types used were: cement aggregate mixtures, soil cement, and lean concrete. For each stabilized base type (i.e., asphalt or cement), the properties of the different material types that have been used as the base material are very different from each other. Therefore, in order to accurately analyze the data, each of the different base types in the asphalt and cement stabilized base types should be analyzed separately. However, if each base type was further subdivided into different subcategories, some of these subcategories would not have a sufficient sample size for analysis. Therefore, for the purpose of this study, the stabilized base types were treated simply to be either asphalt stabilized or cement stabilized.

The time-sequence IRI values of GPS-2 sections classified into the four environmental zones are shown separately for asphalt stabilized and cement stabilized bases in figures 72 and 73. The sections generally show a linear increase in roughness with some sections showing an exponential increase in roughness in the latter part of the life. No clear differences in roughness progression can be noted between the asphalt stabilized and cement stabilized bases. Forty five percent of the GPS-2 sections whose roughness trends are shown in figure 72 and 73 have been deassigned from the GPS-2 experiment (i.e., they are no longer monitored), because they were rehabilitated. The median age of the deassigned pavements was 15 years, and their median IRI was 1.3 m/km. As the median IRI of the deassigned pavements were very low, the cause for the rehabilitation on the majority of these sections is obviously not the roughness level. However, as the sections that were deassigned had a median age of 15 years, some of these sections are old and were likely to be exhibiting pavement distress. Only a few sections in figures 72 and 73 show an exponential increase in roughness at the end of the service life. It appears that the State highway agencies are rehabilitating pavements before they reach this stage, as indicated by the number of deassigned sections. In both figures 72 and 73, very few sections have IRI levels that exceed 2.0 m/km.

Factors Affecting Changes in IRI

An analysis was performed to identify the factors that have an influence on the increase in IRI. Scatter plots between rate of increase of IRI and parameters that were selected for selected for analysis (see table 5) were examined to observe data trends. This analysis was initially performed by considering all GPS-2 sections, and thereafter separate analyses were performed for asphalt stabilized and cement stabilized sections. In addition, for each base type, data analyses were performed separately for each environmental zone. There were very few cases where a relationship between the rate of increase of IRI and an evaluated parameter was observed. The variety of different base types that are used for asphalt and cement treated bases may be a reason why no clear trends were seen, even when each of the base types were evaluated separately.

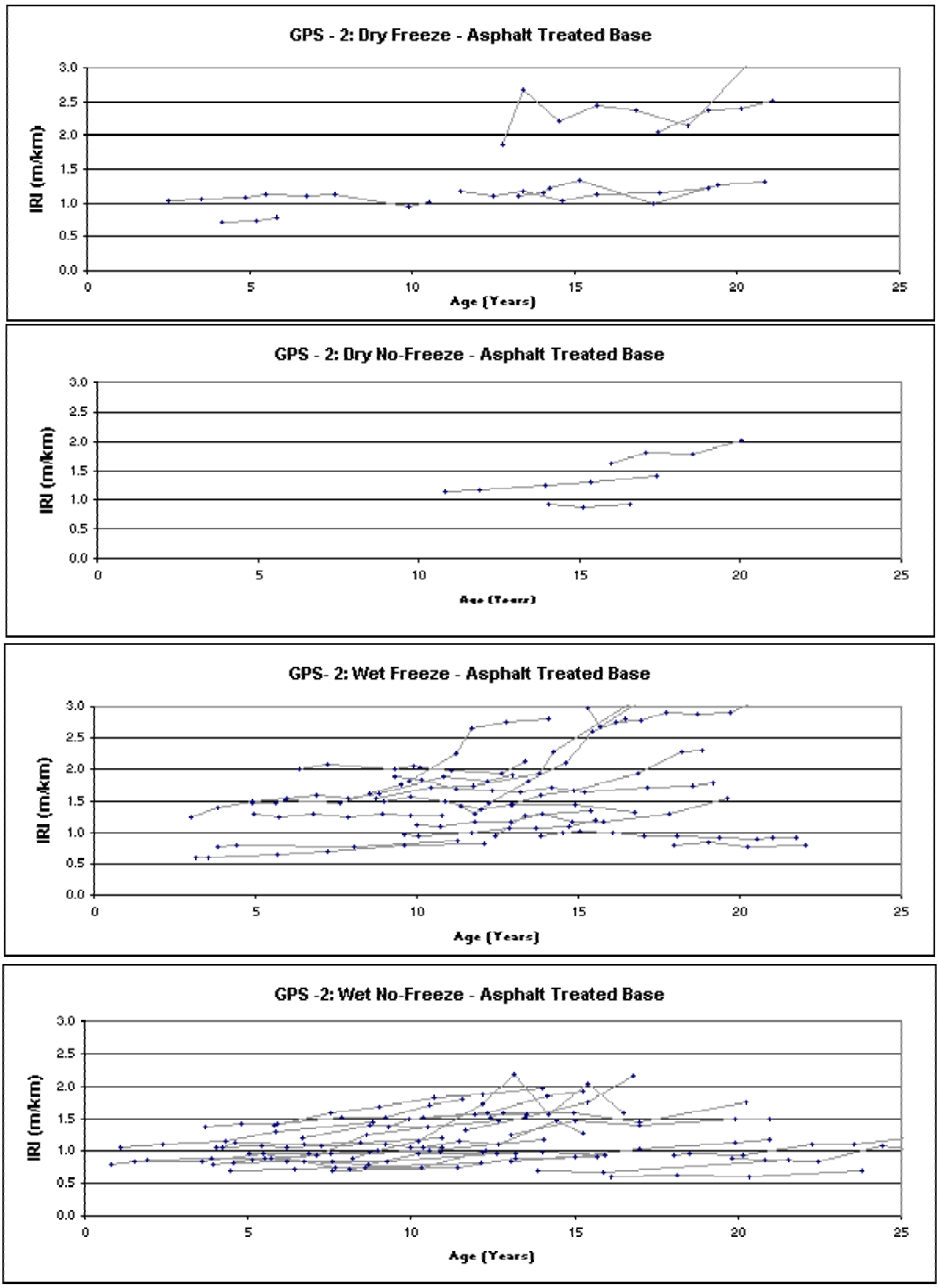

Figure 72. IRI trends for GPS-2 sections on asphalt stabilized bases

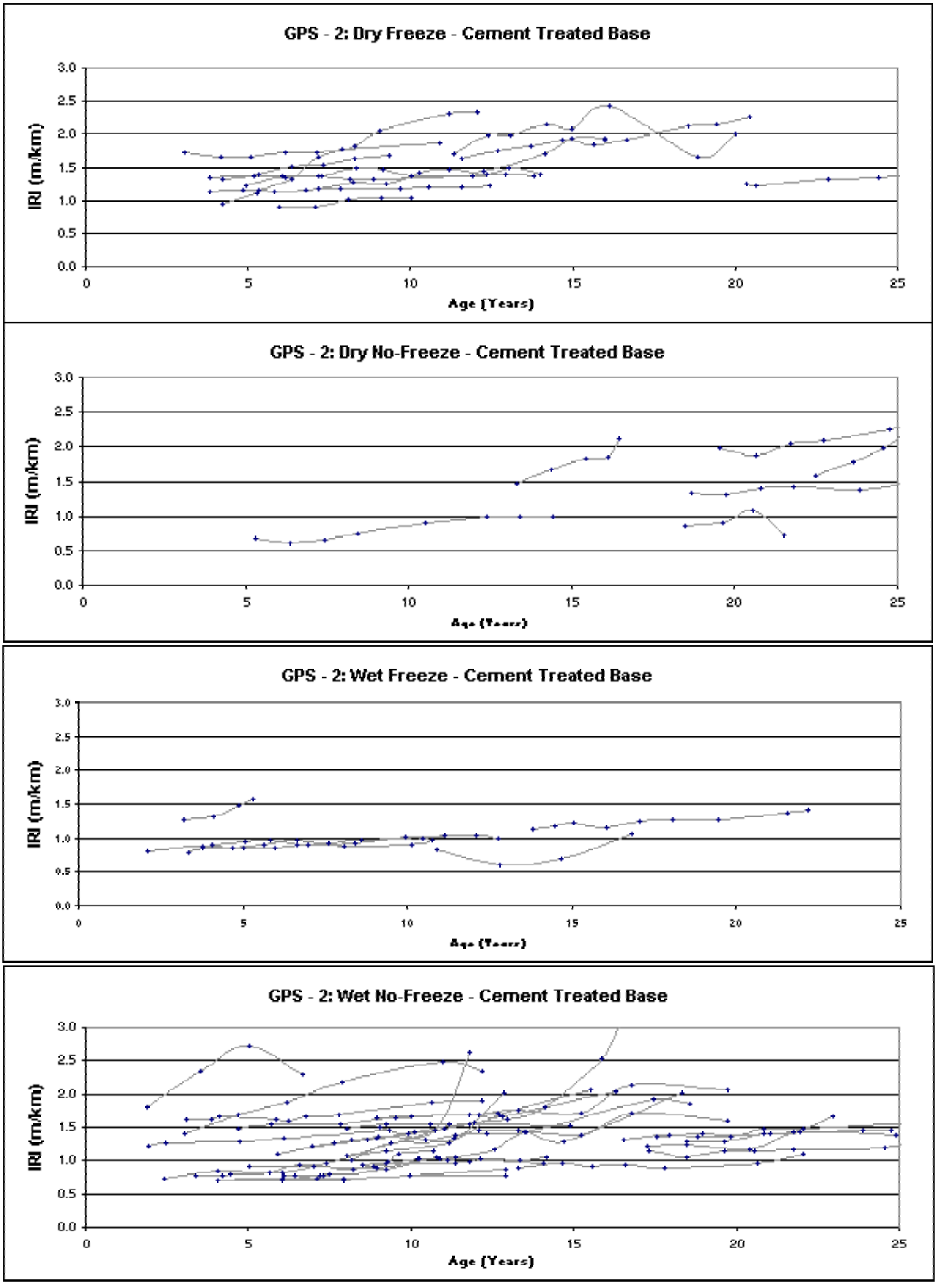

Figure 73. IRI trends for GPS-2 sections on cement stabilized bases

When all GPS-2 sections were considered, a weak trend of a higher rate of change of IRI with increasing air voids in AC was observed. This relationship was strongest in the wet freeze zone. Figure 74 shows the relationship between the rate of change of IRI and air voids for all GPS-2 sections. High air voids in pavements subjected to heavy traffic will lead to rutting and cause an increase in roughness.

For sections with cement treated bases, a high rate of increase of IRI was observed for sections in warmer climates. Figure 75 shows the relationship between the rate of change of IRI and the number of days per year that have a temperature greater than 32 °C. The cement treated bases that are rigid may be resisting vertical deformations, and a lateral movement of AC may be occurring at these sections leading to rutting and therefore causing an increase in roughness. A relationship between the rate of increase of IRI and the number of days per year with temperatures exceeding 32 °C was not observed for pavements on asphalt stabilized bases. No relationship between cumulative traffic and roughness level was observed when all sections were considered, and also when the two base types were analyzed separately.

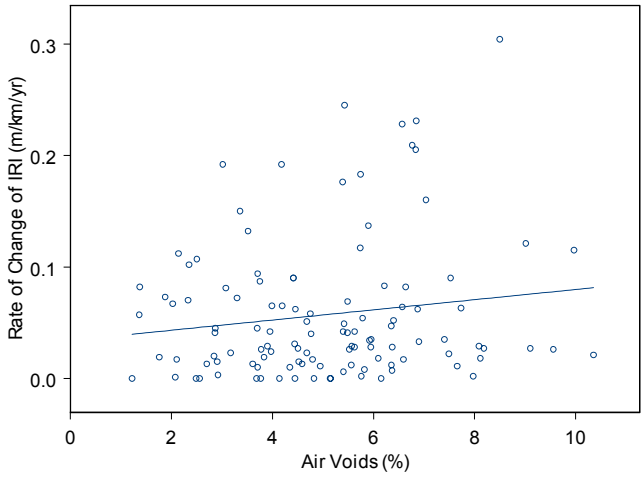

Figure 74. Relationship between rate of increase of IRI and air voids.

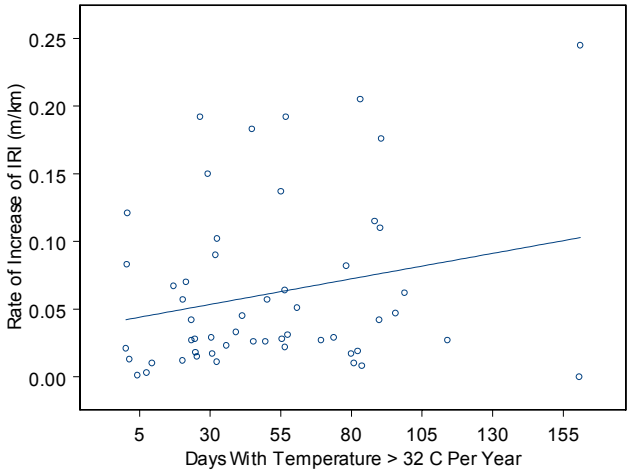

Figure 75. Relationship between days with temperature greater than 32 °C and rate of increase of IRI

Comparison Between Good and Poorly Performing Sections

Figure 76 shows the time-sequence IRI values of five sections, three of which are showing an increase in IRI with time, and two that have remained smooth over a long period of time.

Figure 76. Good and poorly performing GPS-2 sections.

The following observations were noted for sections 36-1643, 28-3091, and 6-7491 that have shown high increases in IRI with time: (1) Section 36-1643: This section is a AC stabilized section that is located in the wet freeze zone on a coarse grained subgrade. This section has been subjected to a high traffic volume and the AC core samples indicated the air voids to be 8.5 percent. The high air voids in AC in combination with the high traffic volume may have been a factor that caused a high rate of increase of IRI to occur at this section. (2) Section 28-3091: This section is an AC stabilized section that is located in the wet no-freeze zone. The annual days with temperature greater than 32 °C at this location is 65 days, and the air voids in the AC is 7 percent at the time the core samples were obtained. Although this section has been subjected to a relatively low traffic volume, the high temperatures and high air voids is a possible cause for the high IRI values seen at this section, (3) Section 6-7491: This is a cement stabilized section located in the dry no-freeze zone, and has carried the highest cumulative traffic volume of all the cement stabilized sections. The rapid increase in IRI at this section is likely because it has reached the end of its design life.

Two sections that have shown good performance are sections 6-2053 and 24-1634. The following observations were noted at these two sections. (1) Section 24-1634: This section has an asphalt stabilized base. It is located in a zone bordering the wet freeze and wet no-freeze zone, and is on a silty subgrade. This section has been subjected to a very low traffic volume, and the good performance of this section is attributed to this cause. (2) Section 6-2053: This section is located in the wet no-freeze zone on a subgrade that has 49 percent material passing the No. 200 sieve. The pavement section comprises of a 100 mm AC surface, placed over a 75 mm lean concrete base, that is on a 150 mm thick cement aggregate base, that is on a 325 mm thick cement treated subbase. This section has been subjected to a relatively low traffic volume compared to its structural capacity, and the cause for the excellent performance of this section is attributed to this fact.

As these examples show, for sections that are showing either a good performance or a poor performance, an in-depth analysis of the test section can identify the factors that are affecting its performance.

Models for Roughness Development

The initial IRI of the GPS-2 sections is not available. A modeling approach similar to that used for GPS-1 sections was used to analyze the GPS-2 data. The roughness development of GPS-2 sections was modeled by using an incremental roughness increase approach, where the time-sequence IRI values at a section were used as the dependant variable, with the first IRI measured at the section treated as the initial IRI. A mixed model analysis was performed on the GPS-2 data using the S-Plus software. The following model was developed to predict roughness:

$IRI_{Last} = -0.16584 + 1.11253(IRI_{First}) + 0.00004(Traffic/SN) + 0.00466(\Delta Time \times AV) + 0.0018(\Delta Time \times MC_{Subg})$

Section effects standard deviation = 0.18, residual standard deviation = 0.18

IRI_{Last} = IRI at time = ΔTime after IRI_{First} , m/km
IRI_{First} = IRI at first profile date, m/km
ΔTime = Change in time from first profile date, years
Traffic = Cumulative traffic on section in KESALs
SN = Structural number of pavement
AV = Air Voids in AC, percent
MC_{Subg} = Moisture content of subgrade, percent

Summary for GPS-2

The types of stabilized bases that are used in the GPS-2 experiment can be divided into asphalt stabilized or cement stabilized. However, a variety of material types have been used for each of the stabilized base types. For asphalt stabilized bases, the material types that have been used are: hot mix AC, asphalt treated mixtures, sand asphalt, mixed in place cold-laid mixtures, and central plant mix cold-laid mixtures. For cement stabilized bases, the material types that have been used are: cement aggregate mixtures, soil cement and lean concrete. For each stabilized base type, the properties of the different material types that have been used as base material are very different from each other. Therefore, in order to accurately analyze the data,

each of the different base types in the asphalt and cement stabilized base types should be analyzed separately. However, sufficient sections were not available to do this type of analysis. Only a few causes that contribute to increase in roughness of GPS-2 sections could be found. This may be because of the variety of base types that have been used. A higher rate of increase of IRI was noted for sections with high AC void ratios. For sections on cement treated bases, a high rate of increase of IRI was observed for sections in warmer climates.

GPS-3: JOINTED PLAIN CONCRETE PAVEMENTS

Test Sections

There are 127 GPS-3 sections in the LTPP database for which IRI data are available, but subgrade information is available for only 115 of those sections. Dowels are present in forty five percent of the GPS-3 sections. The distribution of the GPS-3 sections according to environmental zone, subgrade type and load transfer type is shown in table 54. The percentage of sections in each environmental zone that have dowels are, dry-freeze: 16 percent, dry no-freeze: 18 percent, wet-freeze: 50 percent, and wet no-freeze: 54 percent. As these data indicate, there are only a few sections in the dry regions (dry-freeze and dry no-freeze) that have dowels.

Table 54. Distribution of GPS-3 sections.

Load Transfer	Environmental Zone & Subgrade Type								Total
	Dry Freeze		Dry No-Freeze		Wet-Freeze		Wet No-Freeze		
	Coarse	Fine	Coarse	Fine	Coarse	Fine	Coarse	Fine	
Non-Doweled	14	2	8	1	11	14	14	2	66
Dowels		3	2		14	11	11	8	49
Total	14	5	10	1	25	25	25	10	115
Total	19		11		50		35		115

Figure 77 shows the distribution of the pavement sections according to their age at the time they were first profiled and at the last available profile date. On average, the GPS-3 sections

have been profiled seven times over a seven-year period. Over 50 percent of the sections have been monitored between a period of eight to ten years.

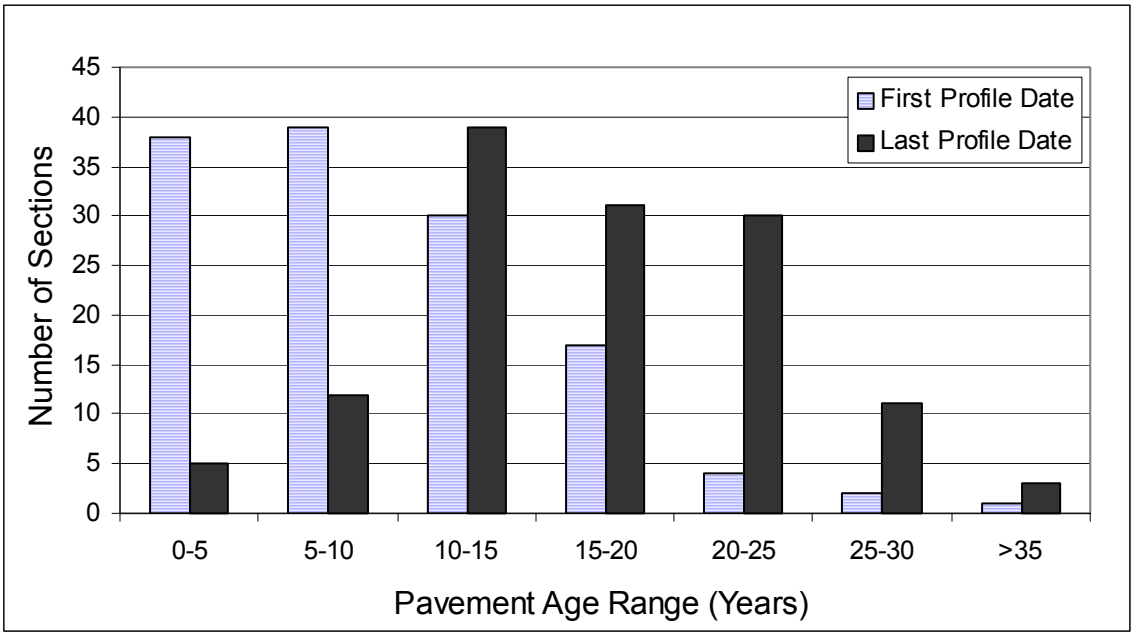

Figure 77. Distribution of GPS-3 sections according to age at first and last profile dates.

Changes in IRI

The difference in IRI between the last profile date and first profile date, classified according to different IRI ranges is presented in table 55 for the different environmental zones and load transfer types. In table 55, the sections for dry-freeze and dry no-freeze zones were combined into one region called the dry-region. This procedure was adopted, as there were 19 sections in the dry-freeze zone and 11 sections in the dry no-freeze zones, and it was considered that sufficient sections were not available to look at changes that occur in each zone separately. The data presented in table 55 gives an overview of the magnitude of changes in IRI that have occurred at the GPS-3 sections over the monitored period. There were many sections that had an IRI at last profile date that was less than the IRI at the first profile date. Also, there were many sections that had an IRI change of less than 0.1 m/km between the last and the first profile date.

Table 55. Percent distribution of GPS-3 sections according to change in IRI.

Change in IRI (m/km)	Percent Sections					
	Environmental Zone and Load Transfer Type					
	Dry		Wet-Freeze		Wet No-Freeze	
	Dowel	Non-Doweled	Dowel	Non-Doweled	Dowel	Non-Doweled
< 0	0	31	36	4	11	19
0.0 - 0.1	40	15	24	14	31	6
0.1 - 0.2	0	16	22	21	26	19
0.2 - 0.3	40	8	9	14	11	19
0.3 - 0.4	0	8	3	4	11	0
0.4 - 0.5	20	12	0	7	5	6
0.5 - 0.6	0	0	0	14	5	6
0.6 - 0.7	0	4	0	0	0	13
0.7 - 0.8	0	0	0	4	0	0
0.8 - 0.9	0	0	0	0	0	6
0.0- 1.0	0	4	3	7	0	0
> 1.0	0	4	3	11	0	6
Total	100	100	100	100	100	100
No. Sections	5	26	29	28	19	16

An IRI change of 0.1 m/km can occur due to changes in the profiled path or due to curling or warping effects in PCC slabs. The reason for some sections to have an IRI at last profile date that was less than the IRI at the first profile date is also attributed to these causes. In the wet-freeze zone, 60 percent of the sections that had dowels had an IRI change of less than 0.1 m/km between the first and last profile dates compared to 18 percent for sections that did not have dowels. In the wet no-freeze zone, 42 percent of the sections with dowels had an IRI change of less than 0.1 m/km between the last and first profile dates, compared to 25 percent for sections that did not have dowels.

The changes in IRI that are shown in table 55 were observed over the monitored period of the sections, but the monitored period varied between the sections. Roughness progression between test sections can be evaluated by obtaining a rate of change of roughness at each section. A regression analysis was performed on the time-sequence IRI values to obtain a rate of change of IRI at each section. Table 56 presents the rate of change of IRI at the test sections classified according to different ranges for the three environmental zones that were considered in the analysis. In the dry zone, meaningful comparisons between sections with and without dowels cannot be performed, as there are only five sections with dowels when compared to 26 sections

Table 56. Percent distribution of GPS-3 sections according rate of change of IRI.

Rate of Change of IRI (m/km/yr)	Percent Sections					
	Environmental Zone and Load Transfer Type					
	Dry		Wet-Freeze		Wet No-Freeze	
	Dowel	Aggregate	Dowel	Aggregate	Dowel	Aggregate
< 0	0	31	31	4	11	19
0.0 - 0.01	40	12	24	11	21	6
0.01 – 0.02	0	15	18	21	26	13
0.02 – 0.03	40	7	8	4	15	24
0.03 – 0.04	0	7	3	13	5	0
0.04 – 0.05	20	12	0	4	11	6
0.05 – 0.06	0	0	0	4	0	0
0.06 – 0.07	0	4	3	7	11	13
0.07 – 0.08	0	0	0	7	0	0
0.08 – 0.09	0	4	3	0	0	6
0.09 – 0.10	0	0	0	0	0	0
> 0.10	0	8	10	25	0	13
Total	100	100	100	100	100	100
No. Sections	5	26	29	28	19	16

that do not have dowels. In the wet-freeze zone, a rate of change of IRI of less than 0.02 m/km/yr was noted at 72 percent of sections with dowels, and at 36 percent of sections without dowels. In this zone, a rate of increase in IRI of over 0.05 m/km/year was seen for 16 percent of sections with dowels and at 43 percent of the sections without dowels. In the wet no-freeze zone, a rate of change of IRI of less than 0.02 m/km/yr was noted for 58 percent of sections with dowels and at 38 percent of sections without dowels. In this zone, a rate of increase of IRI of greater than 0.05 m/km/yr was seen for 11 percent of sections with dowels, and for 26 percent of sections without dowels. A t-test performed on the combined data set from wet-freeze and wet no-freeze regions indicated that the sections without dowels had a higher rate of increase of IRI when compared to doweled sections.

Figure 78 shows the relationship between the rate of change of IRI and the average age of the pavement over the monitored period. No clear relationship between rate of change of IRI and the pavement age can be observed. There are several pavements that are doweled and are over 15

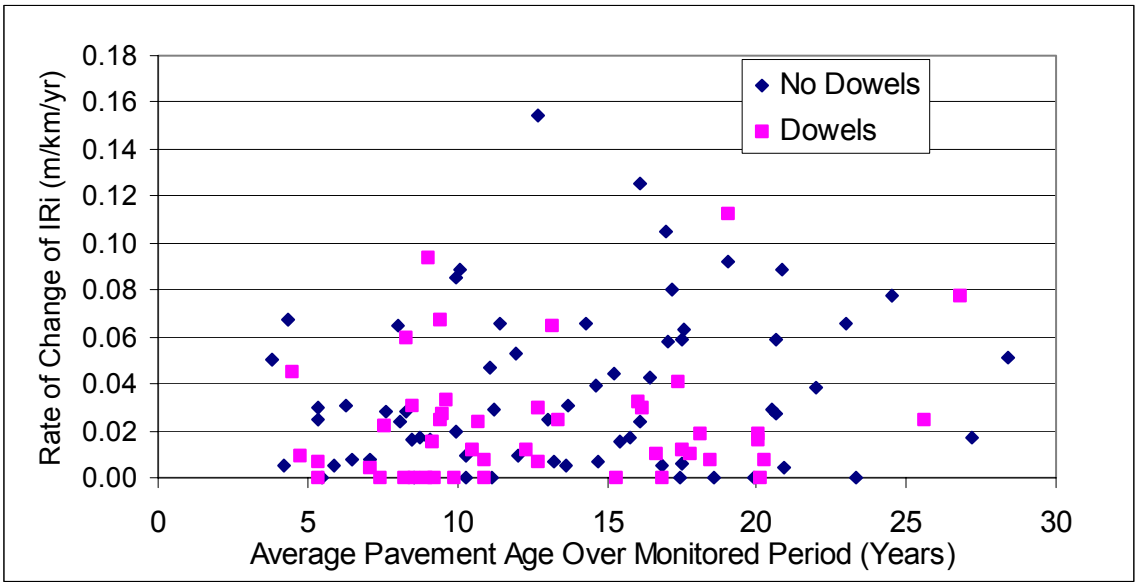

Figure 78. Relationship between rate of change of IRI and pavement age for GPS-3 sections.

years that are showing very low rates of increases in IRI. However, most of the pavements that are over 15 years old, and do not have dowels are showing very high rates of increase in IRI.

Trends in Roughness Development

Figures 79 and 80 show the time-sequence IRI values that were obtained for sections with and without dowels classified according to environmental zones. These plots reflect the trends in roughness development that were noted earlier, where the majority of the non-doweled sections show more increase in roughness when compared to doweled sections. In the non-doweled sections, higher rates of increase of IRI were observed for pavements that reached a roughness level of between 2.0 to 2.5 m/km. The time-sequence IRI values for some sections show varying IRI values between the years. The roughness of jointed concrete pavements is affected by curling and warping that occurs in the PCC slabs. Generally, curling effects due to temperature occur in the early morning hours. The variability in time-sequence IRI values that are seen for some of the GPS-3 sections is attributed to curling and warping effects. Sections without dowels show much more variation in IRI when compared to doweled sections.

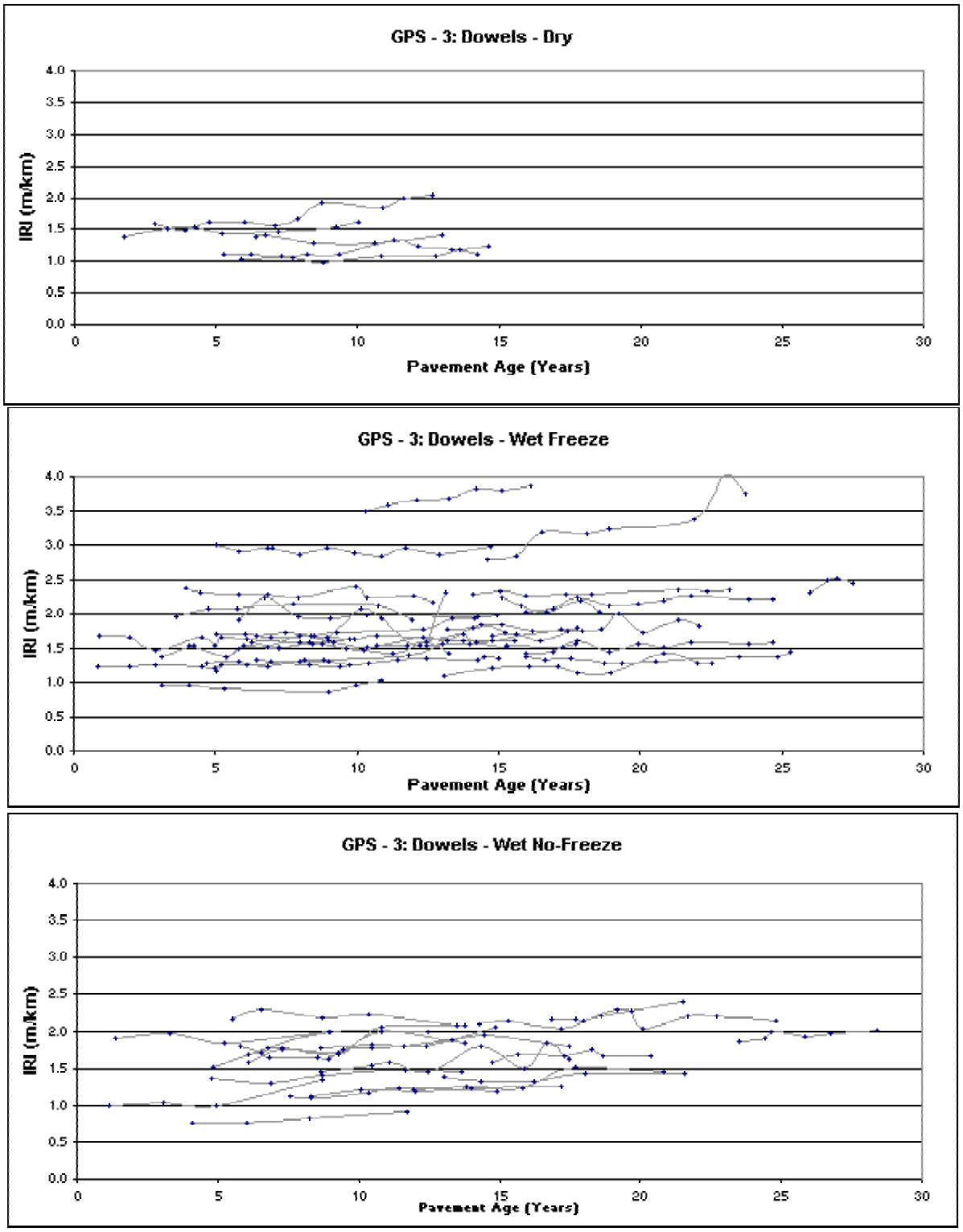

Figure 79. IRI trends for GPS-3 sections with dowels as load transfer.

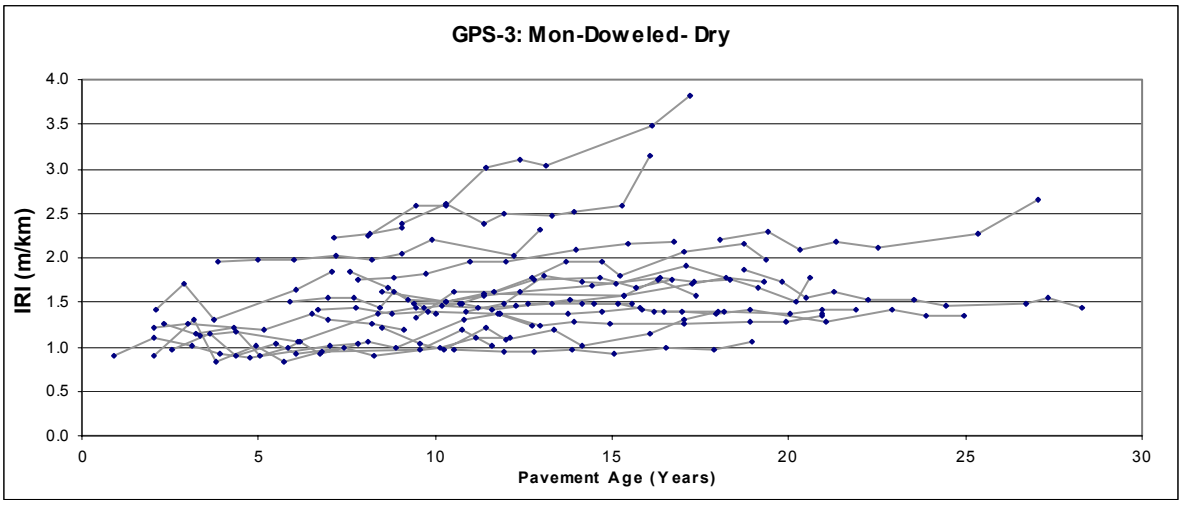

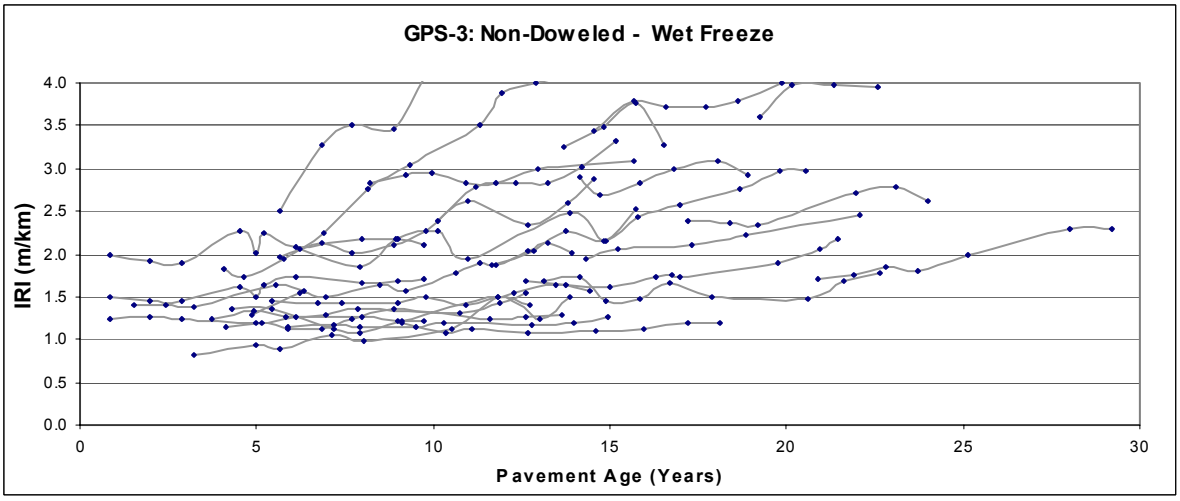

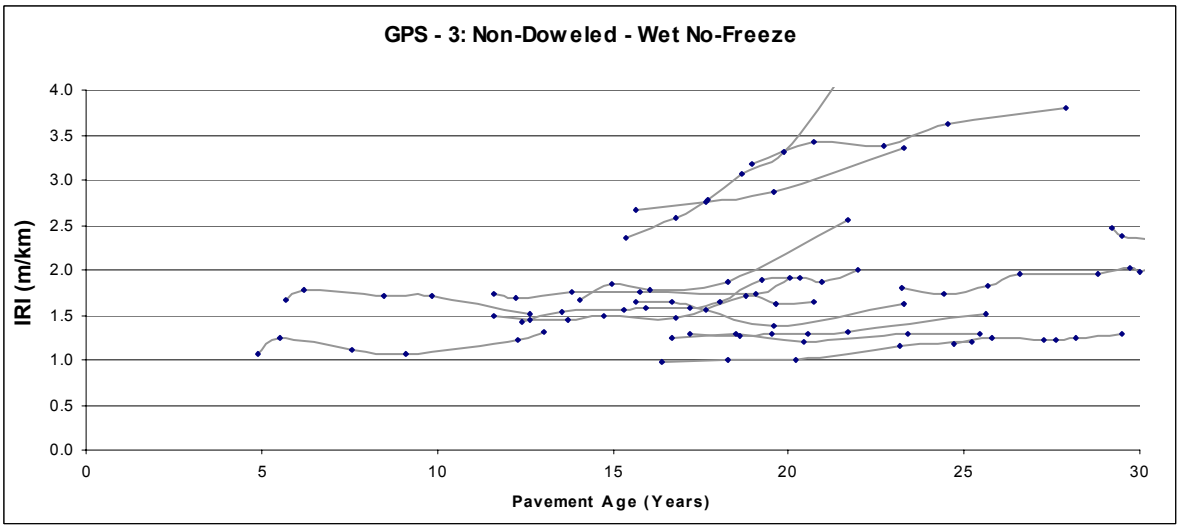

Figure 80. IRI trends for GPS-3 sections without dowels.

This is because the dowels provide some restraint against curling and warping, and this minimizes variations in the profile.

The time-sequence IRI values of GPS-3 sections were separated according to load transfer type, and then subdivided into base types of gravel and treated base to observe if differences in IRI trends could be identified. No distinct differences in trends in roughness development could be noted between the base types. However, the time-sequence IRI values of sections on treated bases appeared to be less variable between the years when compared to sections that were on gravel bases. This may be related to the effect of the base type on the curling and warping behavior of the PCC slabs.

Factors Affecting IRI

An analysis was performed to investigate the factors that have an effect on the roughness of JPC pavements. The factors that were considered in the analysis are shown in table 5 in chapter 4. This analysis was performed by studying relationships between median IRI of the section over the monitored period as well as the rate of change of IRI and the parameters selected for analysis. The relationships between median IRI and the selected parameters will indicate parameters that have an influence on the IRI value, while the relationship between rate of change of IRI and the data parameters will identify parameters that have an influence on the change in IRI. This analysis approach was selected in analyzing GPS-3 data, as there was many sections that had extremely low rates of roughness development, especially for doweled sections. If only the rate of change of IRI was selected for analysis, relationships between rate of change of IRI and the evaluated parameters may not be seen because of the very low rates for rate of change of IRI. Scatter plots between rate of change in IRI as well as the median IRI with the evaluated parameters that were selected for analysis were examined to observe data trends. The noted observations are presented separately for non-doweled and doweled pavements.

Non-doweled Pavements

PCC Strength Parameter:

When the data for all non-doweled GPS-3 sections were examined, higher IRI values were observed with increasing values of PCC elastic modulus, PCC compressive strength, and Poisson's ratio. There is a strong correlation between PCC elastic modulus and PCC compressive strength, with higher compressive strengths of PCC resulting in higher values of PCC elastic modulus. A strong relationship was also observed between IRI and ratio between PCC elastic modulus and PCC tensile strength. However, when the data was separated into the dry (dry freeze and dry no-freeze) and wet (wet freeze and wet no-freeze) environmental zones, no relationship between PCC elastic modulus and IRI was seen for the dry regions while a strong relationship was noted in the wet regions. Figure 81 and 82 shows the relationship between IRI and PCC elastic modulus for the wet and dry regions, respectively. In the dry regions there were only two sections that had a PCC elastic modulus that was greater than 35,000 Mpa, while in the wet regions there were many sections that had PCC elastic moduli exceeding these values. Generally, sections in the wet regions that had PCC elastic modulus greater than 35,000 Mpa had high IRI values.

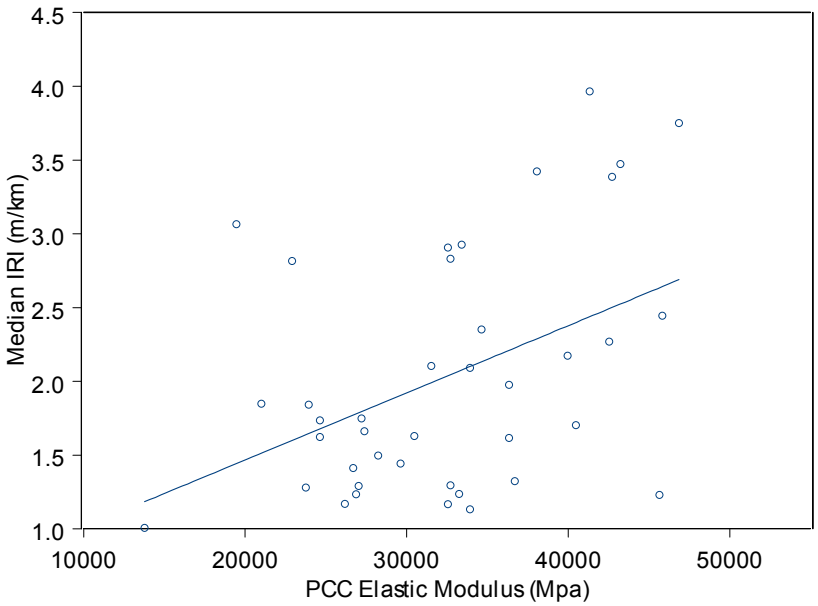

Figure 81. Relationship between IRI and PCC elastic modulus – wet regions (non-doweled sections).

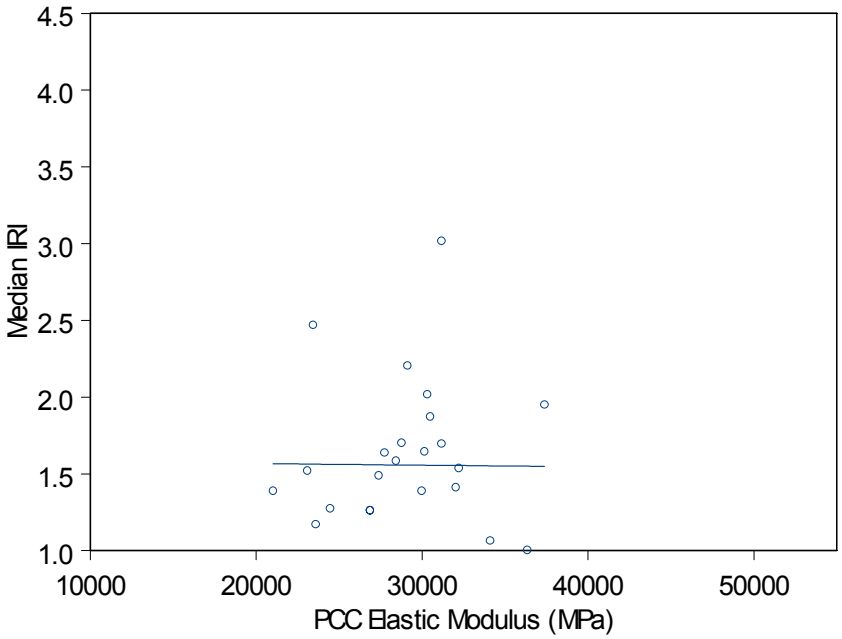

Figure 82 Relationship between IRI and PCC elastic modulus – dry regions (non-doweled sections).

A relationship similar to that observed between median IRI and PCC elastic modulus was observed between compressive strength of PCC and median IRI for each of these regions. Such a relationship is to be expected, as there was a strong correlation between PCC compressive strength and PCC elastic modulus. The relationship between IRI and the ratio between PCC elastic modulus and PCC tensile strength showed a very strong relationship in the wet regions, as shown in figure 83. There was no relationship between these two parameters for the data in the dry regions as shown in figure 84. In the dry regions, only 15 percent of the sections had a value for this ratio that was greater than 8000, while in the wet regions 45 percent of the sections had a value for this ratio that was greater than 8000. Several sections that had high values for the ratio between PCC elastic modulus and PCC tensile strength had high rates of increase of roughness.

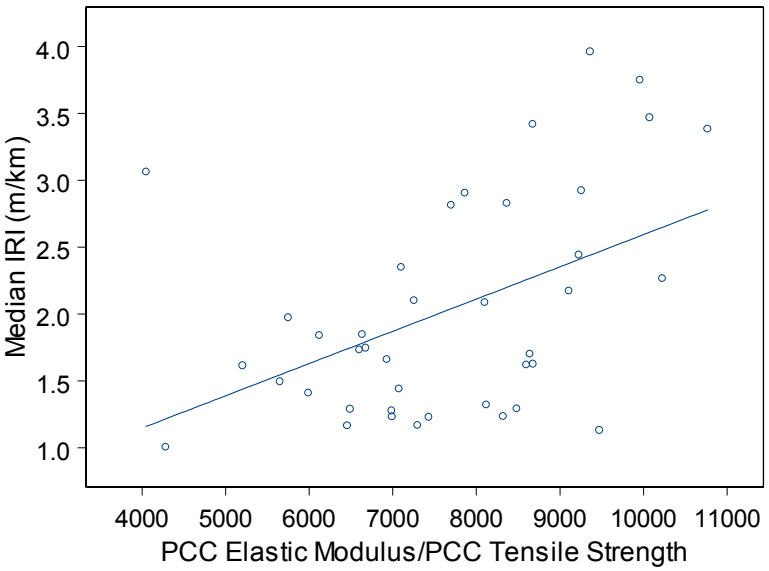

Figure 83. Relationship between IRI and ratio between PCC elastic modulus and tensile strength: wet regions (non-doweled sections).

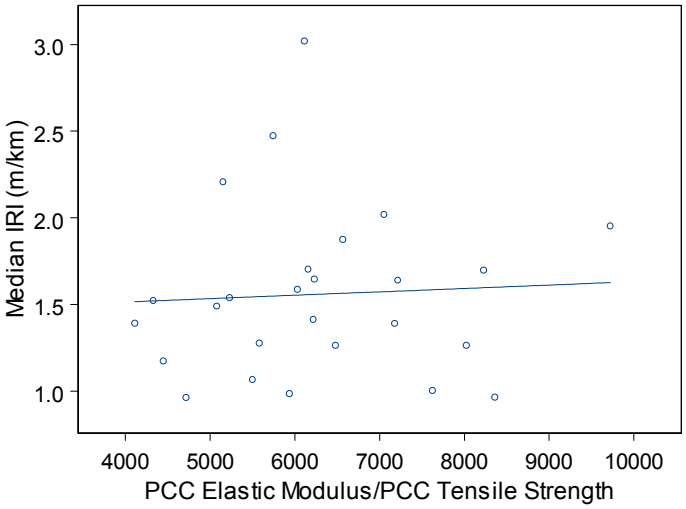

Figure 84. Relationship between IRI and ratio between PCC elastic modulus and tensile strength: dry regions (non-doweled sections).

PCC Mix Parameters

No relationships between IRI and PCC mix parameters such as coarse aggregate content, fine aggregate content, cement content, ratio between coarse and fine aggregate, and water cement ratio were observed in the dry region. In the wet regions, some sections that had low water cement ratios had high IRI values. In the wet regions, a general trend of higher IRI values were noted for sections that had high amount of coarse aggregate and higher coarse to fine aggregate ratios. There were several sections that had low water cement ratios that were less than 0.35 that were showing a high rate of increase of IRI.

Subgrade Properties

Pavements located on subgrades having higher moisture contents had higher roughness. Higher roughness levels were observed for pavements on subgrades that had high clay contents, and for subgrades with higher plasticity indices, with these relationships being stronger for the pavements in the wet zones. The subgrade at a majority of the sections in the dry zone is coarse grained, and these relationships are therefore weak in the dry zone. Higher rates of increase of roughness were noted with increasing moisture content of the subgrade.

Environmental Conditions

Pavements in areas subjected to higher precipitation had higher IRI values, and figure 85 shows the relationship between the two parameters. This relationship was stronger for the pavements in the wet regions. The rate of change of IRI was higher in regions that had a higher number of wet days.

Pavements in areas where the mean annual temperature was low had higher IRI values. Pavements in areas that had a high number of days above 32 °C had low IRI values when compared to pavements in areas that had a low number of days above 32 °C. The rate of increase of IRI generally decreased with higher mean temperatures. A similar trend was noted between rate of increase of IRI and the number of days above 32 °C. The relationship between IRI and mean annual temperature as well as the relationship between rate of change of IRI and mean annual temperature are shown in figures 86 and 87, respectively. The reason for this relationship

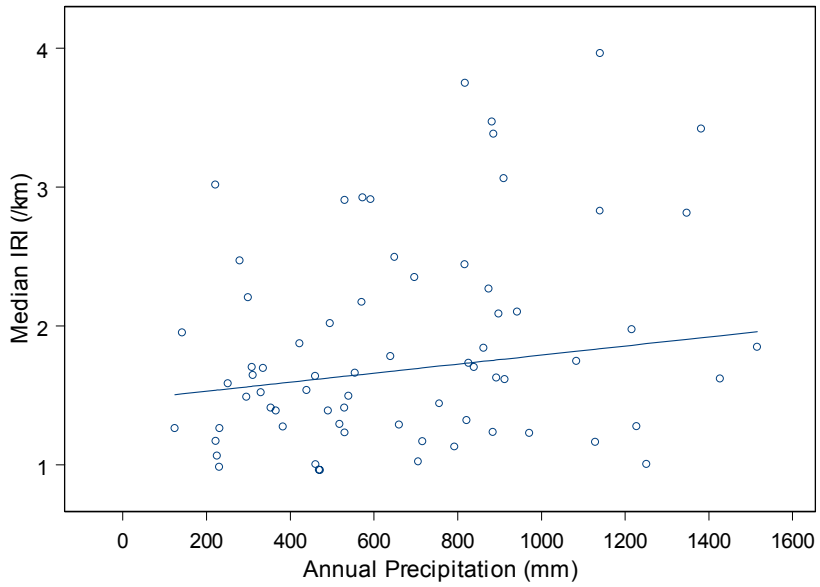

Figure 85. Relationship between IRI annual precipitation (non-doweled sections).

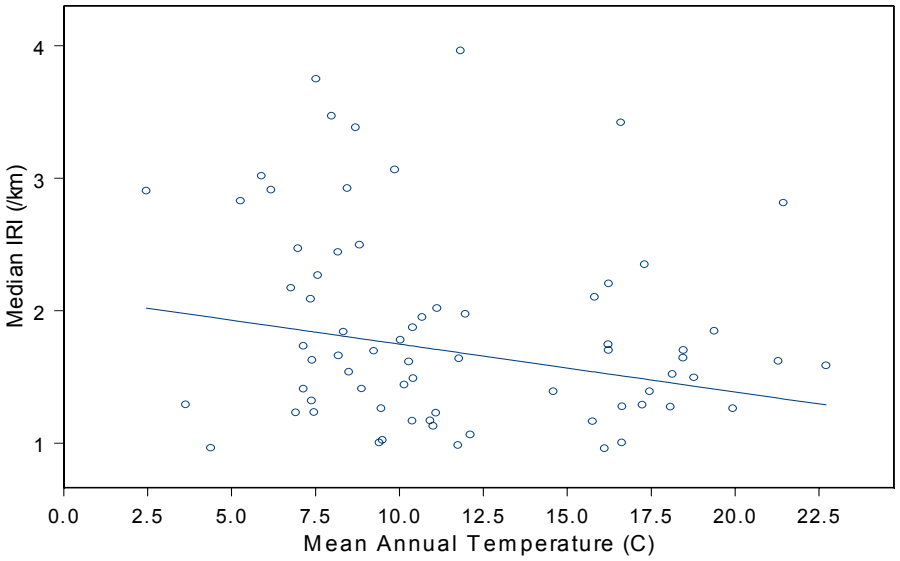

Figure 86. Relationship between IRI and mean annual temperature (non-doweled sections).

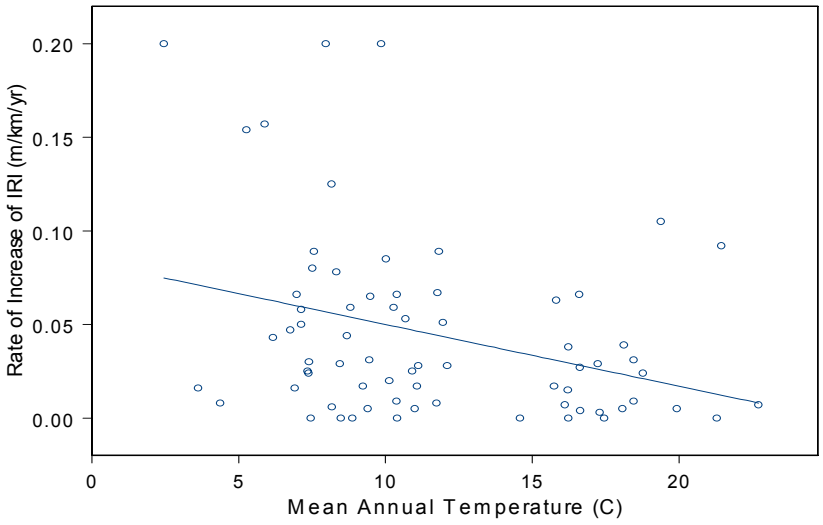

Figure 87. Relationship between rate of change of IRI and mean annual temperature (non-doweled sections).

may have two causes. The load transfer of non-doweled JPC pavements is affected by the ambient temperature. When the temperatures are high, PCC slabs expand and provide better load transfer, and when the temperatures are low, the load transfer is reduced. When there is low load transfer, stresses on the subsurface layer are greater and this increases the potential for faulting.

The second cause for this phenomenon may be because in areas where there are low mean temperatures the freezing index values are high, and the roughness of the pavement can increase because of frost heave effects.

Time and Traffic

No relationship between cumulative traffic and IRI was observed. However, a trend of higher IRI values with increasing pavement age was observed, and this relationship is shown in figure 88.

Faulting

A clear relationship was observed between IRI and total faulting at a section as shown in figure 89. The IRI value shown in figure 89 is the IRI corresponding to the last available profile

date. The total faulting is the sum of faulting measured along the outer wheel path at joints and cracks.

Figure 88. Relationship between IRI and pavement age for non-doweled sections.

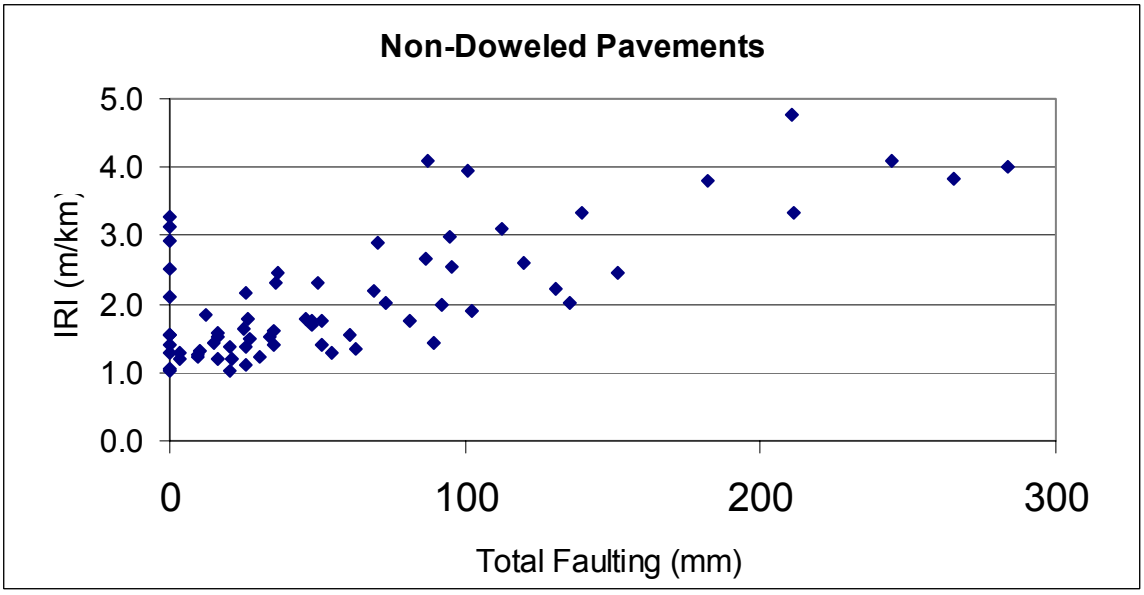

Figure 89. Relationship between IRI and faulting for non-doweled sections.

Doweled Pavements

Generally the relationship between IRI and the evaluated parameters that were observed for doweled pavements were weak. The reason for a lack of relationships between rate of change of IRI and the evaluated parameters is attributed to very low changes in roughness that had occurred over the monitored period at the doweled sections.

PCC Strength Parameters:

A relationship between IRI and PCC elastic modulus was not seen for the doweled pavements. Figure 90 shows the relationship between these two parameters. Non-doweled sections in the wet regions that had a PCC elastic modulus of over 35,000 Mpa generally had high IRI values. There were only four doweled sections that had a PCC elastic modulus of over 35,000 Mpa. This is likely to be the reason why no relationship was seen. The range of PCC elastic modulus of the doweled pavements was similar to the range that was observed for non-doweled sections in the dry regions, which also showed no relationship between IRI and PCC elastic modulus (see figure 82). A trend between IRI and the ratio between PCC elastic modulus

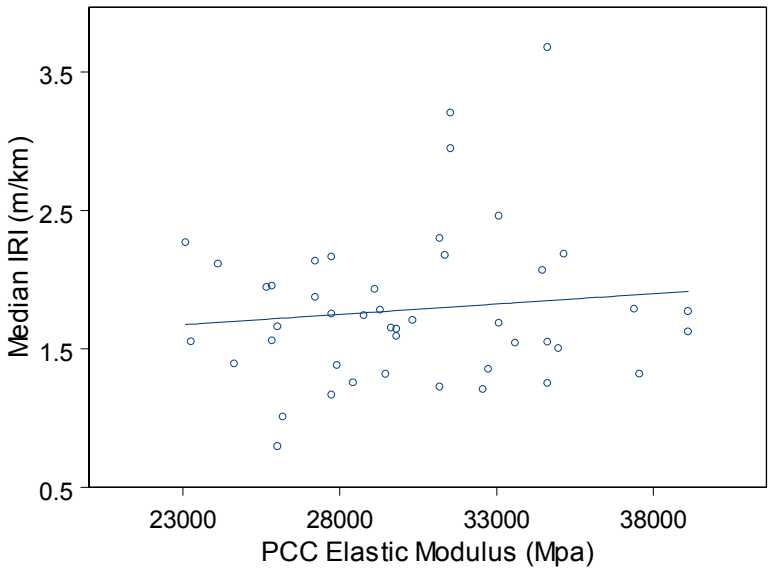

Figure 90. Relationship between IRI and PCC elastic modulus for doweled pavements.

and tensile strength was also not observed for the doweled sections. Some sections with low split tensile strengths (less than 3.6 Mpa) had high rates of increase of IRI.

Environmental Conditions

A weak trend of higher IRI with high wet days was observed. Higher wet days tend to keep the moisture content of the subsurface layers at a high level, and can increase the potential for pumping at the joints. Several sections in areas having high freezing indices showed high rates of increases of IRI.

Time and Traffic

No relationship between IRI and cumulative traffic was observed. The IRI was related to pavement age, with older pavements having higher IRI values, and this relationship is shown in figure 91. Older pavements generally had higher rates of increase of roughness.

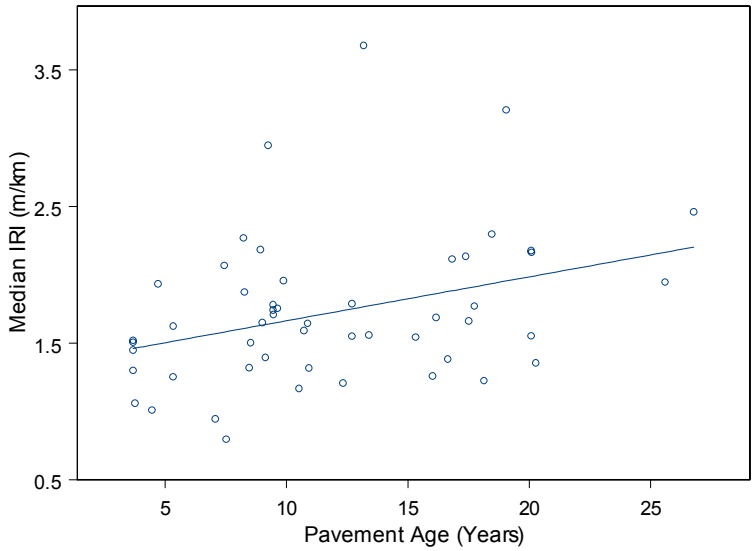

Figure 91. Relationship between IRI and pavement age – doweled sections.

Faulting

No relationship between faulting and IRI was observed for the doweled pavements. The relationship between these two parameters is shown in figure 92. A total faulting greater than 50 mm was observed at 7 percent of the doweled sections compared to 41 percent for non-doweled sections. Theses results show that having dowels in the pavement reduces faulting in pavements, which in turn results in a lower IRI value.

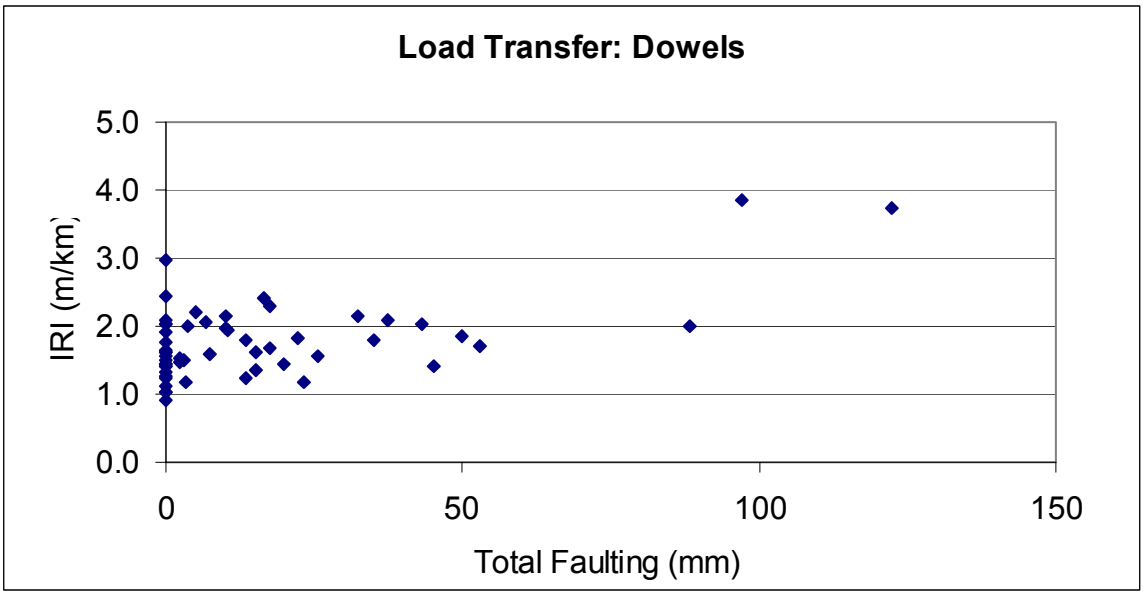

Figure 92. Relationship between IRI and faulting for doweled sections.

Comparison Between Good and Poorly Performing Sections

An evaluation of the good and poorly performing non-doweled GPS-3 sections was performed to identify the factors contributing to their performance. Figure 93 shows the time-sequence IRI values of five sections, three of which are showing an increase in IRI with time, and two pavements that have remained smooth over a long period of time.

The following observations were noted for sections 83-3802, 56-3027, and 55-3015 that have shown high increases in IRI with time: (1) Section 83-3802: This section is located on a

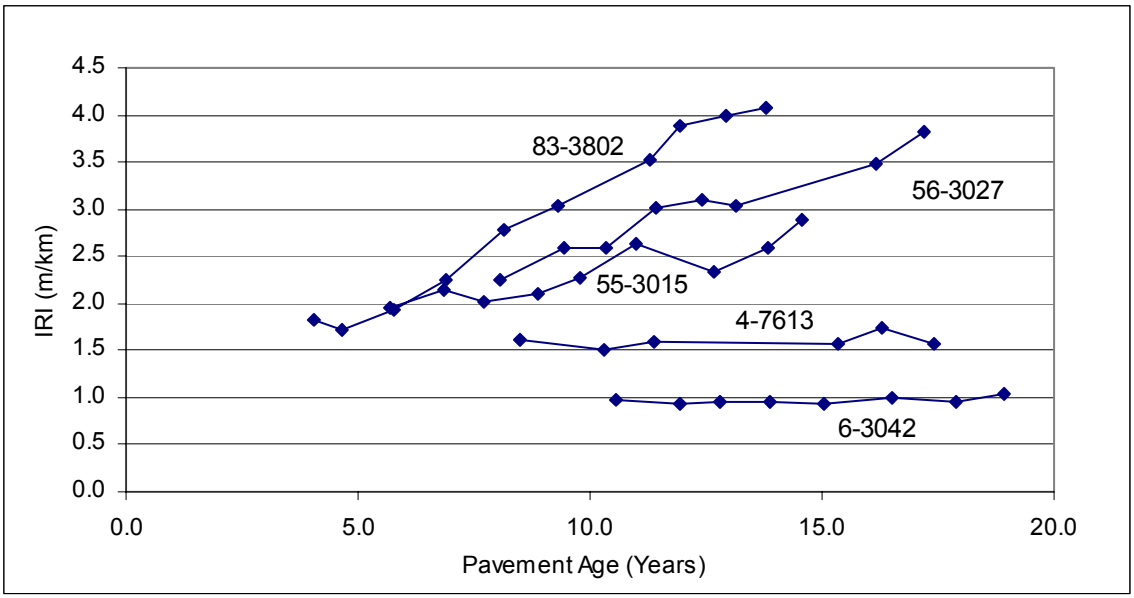

Figure 93. Good and poorly performing non-dowelled GPS-3 sections.

fine grained subgrade that has 92 percent material passing No. 200 sieve, a moisture content of 34 percent, and a plastic limit of 32. The mean annual ambient temperature at this location is 2.5 °C with a freezing index of 1862 °C days. This section has carried a relatively low traffic volume. However, the poor subgrade conditions and harsh environmental conditions are attributed to the poor performance of this section. (2) Section 56-3027: This section is located in the dry-freeze zone at a location where the mean annual ambient temperature is 5.9 °C. This section is subjected to a fairly high traffic level. The high traffic volume in combination with the poor load transfer due to the low mean temperature is attributed to the increase in roughness at this section. (3) Section 55-3015: This section has carried a low traffic volume, but this section has a high PCC modulus relative to the PCC split tensile strength resulting in a ratio between these two values of 10,224 (which is the second highest value for the GPS-3 data set). The increase in roughness at this section is attributed to this fact.

Sections 4-7613 and 6-3042 have both maintained low IRI values over their service lives, and the following observations were noted for these two sites: (1) Section 4-7613: This section has 177 days per year with temperatures greater than 32 °C. This section is resting on a coarse

grained subgrade and has carried a relatively low traffic volume. The low traffic volume in combination with the good load transfer provided by high temperature is attributed to the good performance of this section. (2) Section 6-3042: This section is located in the dry no-freeze zone on a fine grained subgrade that has a plasticity index of 9. The thickness of the PCC slab of this section is 224 mm, and the combined base and subbase thickness is 260 mm. The mean annual ambient temperature at this location is 16 °C, with 66 days with temperatures greater than 32 °C. This section has carried a high traffic volume. The low precipitation in combination with the good load transfer provided by high temperatures is attributed to the excellent performance of this section.

As these examples show, for sections that are showing either a good performance or a poor performance, an in-depth analysis of the test section can identify the factors that are affecting its performance.

Models for Roughness Prediction

Doweled Sections

The change in IRI over the monitored period for doweled sections tabulated in table 55 as well as the time-sequence IRI plots shown in figure 79 show most of the doweled sections have shown little change in IRI. The time-sequence IRI values were backcasted to obtain the initial IRI of the pavement by fitting a linear regression equation for each GPS-3 section. Reasonable IRI values were obtained for initial IRI by this approach.

Thereafter, a mixed model analysis was carried out on the data to develop a model to predict roughness. The mixed model analysis in the S-Plus software was used to carry out this analysis. The following model was developed to predict IRI:

$IRI_t = 0.12284 + 0.94229IRI_0 + 0.05009(\text{Time}) - 0.00733(\text{Time X } PCC_{ten})$

Section effects standard deviation = 0.26, residual standard deviation = 0.11

where,

IRI_t = IRI at time t, m/km
IRI_0 = IRI at time = 0, m/km
Time = Time, years
PCC_{ten} = PCC tensile strength, Mpa

Non-doweled Sections

Some of the non-doweled sections are showing large increases in roughness, with the IRI increasing in an exponential pattern. The initial IRI of these sections cannot be backcasted to get an accurate estimate of initial roughness. Therefore, it was decided to model the IRI development of non-doweled sections by using an incremental modeling approach, where the time-sequence IRI at a section was used as the dependant variable. A mixed model analysis was performed on the GPS-3 data using the S-Plus software. The following model was developed to predict the IRI development:

$IRI_{Last} = -0.33172 + 1.15383(IRI_{First}) + 0.00436(Traffic/PCCthick) + 0.00418(\Delta Time \text{ X } MCSubg) – 0.00178(\Delta Time \text{ X } Meantemp)$

Section effects standard deviation = 0.26, residual standard deviation = 0.18

No. of sections = 63

IRI_{Last} = IRI at time = ΔTime after first available IRI, m/km
IRI_{First} = First available IRI value, m/km
ΔTime = Change in time from first profile date, years
Traffic = Cumulative traffic on section in KESALs
PCCthick = Thickness of PCC layer, mm
MCSubg = Moisture content of subgrade, percent
Meantemp= Mean annual ambient temperature, °C

Summary for GPS-3

In both the dry freeze and dry no-freeze environmental zones, nearly 85 percent of the sections were non-doweled. Therefore, for the dry zone, a comparison of performance between doweled and non-doweled pavements could not be made. In the wet zones (wet-freeze and wet

no-freeze), doweled sections showed a lower rate of increase of roughness compared to non-doweled sections. In the wet-freeze zone, a rate of change of IRI of less than 0.02 m/km/yr was noted at 72 percent of the sections with dowels, and for 36 percent of the sections without dowels, while a rate of change of IRI of over 0.05 m/km/yr was seen for 16 percent of the sections with dowels and 43 percent of sections without dowels. In the wet no-freeze zone, a rate of change of IRI of less than 0.02 m/km/yr was noted at 58 percent of the sections with dowels and at 38 percent of the sections without dowels, while a rate of change of IRI greater than 0.05 m/km/yr was seen for 11 percent of sections with dowels and 26 percent of sections without dowels. These results indicate in the wet zone, the rate of increase of roughness of doweled pavements is much less than that of non-doweled pavements.

For non-doweled pavements, higher IRI values were associated with higher moisture content of subgrade, high clay content in the subgrade, high plasticity index of subgrade, higher annual precipitation, and pavement age. Lower IRI values and lower rate of increase of IRI was noted for pavements that are located in areas that have a high number of days above 32 °C. Non-doweled pavements in areas where the mean annual temperature was low had high rates of increase of roughness. This is attributed to the higher load transfer that occurs when the temperatures are higher. There was a strong relationship between IRI and the total faulting at the section. For non-doweled sections in the wet zone, higher IRI values were observed for high values of PCC elastic modulus (greater than 35,000 Mpa), for sections that had high PCC modulus relative to the tensile strength (ratio between PCC elastic modulus and PCC tensile strength > 8000), high compressive strength and high Poisson's ratio. These relationships were not seen for the sections in the dry zones, as nearly all sections in the dry-zones had PCC elastic modulus values of less than 35,000 Mpa, and a ratio between PCC elastic modulus and tensile strength that was less than 8000.

For doweled pavements in both the wet and dry zones, a relationship between IRI and PCC elastic modulus was not seen. For non-doweled pavements, higher IRI values were associated with sections that had PCC moduli in excess of 35,000 Mpa. But, for the doweled pavements, there were only four sections that had a PCC elastic modulus of over 35,000 Mpa, and this is likely to be the reason why such a relationship was not seen. For doweled pavements,

higher IRI values were associated with high number of wet days. There were several doweled sections with low PCC split tensile strength (less than 3.6 Mpa) that had high rates of increase of roughness. No relationship between total faulting and IRI was observed for doweled pavements. A total faulting greater than 50 mm was observed at 7 percent of the doweled sections compared to 41 percent for non-doweled sections. These results show that having dowels in pavements reduces faulting in pavements, which in turn results in lower IRI values.

GPS-4: JOINTED REINFORCED CONCRETE PAVEMENTS

Test Sections

There are 61 GPS-4 sections in the LTPP database that have IRI data. The distribution of these sections according to the environmental zone and subgrade type is shown in table 57. All GPS-4 sections are located either in the wet-freeze or wet no-freeze zones, with 76 percent of the sections being in the wet-freeze zone and 24 percent of the sections being in the wet no-freeze zone.

Table 57. Distribution of GPS-4 sections.

Subgrade Type	Number of Sections		
	Environmental Zone		Total
	Wet Freeze	Wet No-Freeze	
Coarse	22	6	28
Fine	24	9	33
Total	46	15	61

Figure 94 shows the distribution of the pavement sections according to their age at the time they were first profiled and at the last available profile date. On average, the GPS-4 sections have so far been profiled six times, over a seven-year period. Sixty percent of the sections have been monitored for a period between 8 and 10 years.

Changes in IRI

The difference in IRI between the last profile date and first profile date, classified according to the different IRI ranges is presented in table 58. Table 58 presents the percent distribution of sections when both wet-freeze and wet no-freeze zones are combined, as well as separately for each environmental zone. Data in table 58 shows that when all GPS-4 sections are considered, 8 percent of the sections had an IRI at last profile date that was less than the IRI at first profile date, while the difference in IRI between last and first profile dates was less than 0.1 m/km for 27 percent of the sections. A change in IRI of 0.1 m/km is a very small change in IRI, and differences of this magnitude can easily occur due to variations in the profiled path or temperature effects. Therefore, it can be concluded that at 35 percent of the GPS-4 sections the roughness has not changed or showed negligible change over the monitored period. The decrease in roughness

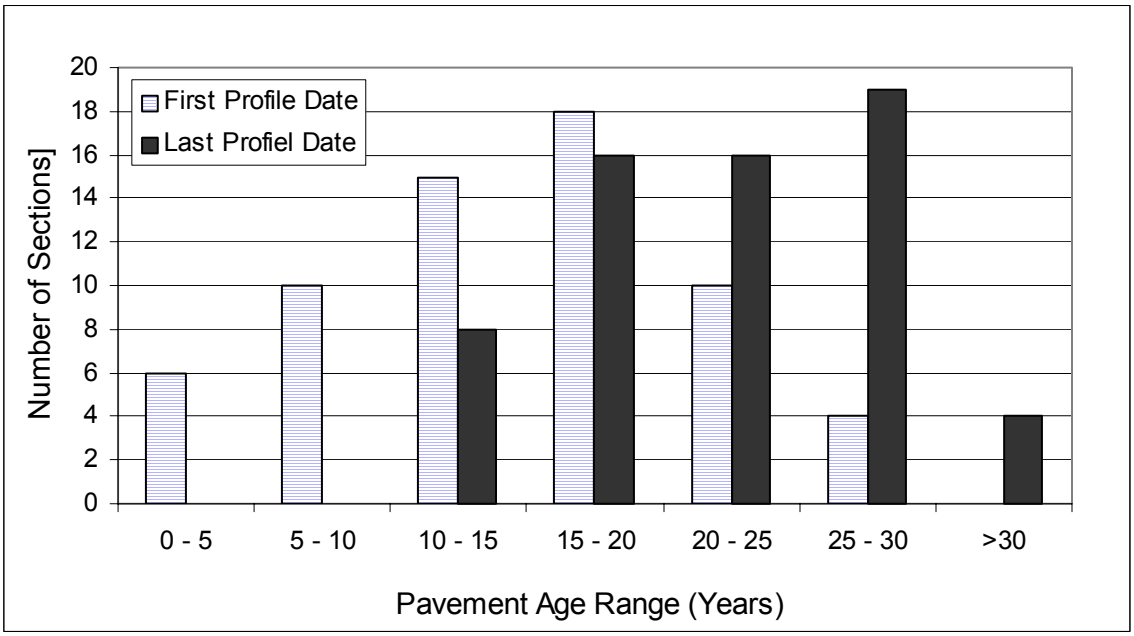

Figure 94. Distribution of GPS-4 sections according to age at first and last profile dates.

that is seen in 8 percent of the sections is attributed to variations in profiled path or changes in pavement profile due to temperature changes.

Table 58. Percent distribution of GPS-4 sections according to change in IRI.

Rate of Change of IRI (m/km/yr)	Percent Sections		
	Environmental Zone		
	Both Zones	Wet-Freeze	Wet No-Freeze
< 0	9	5	20
0.00 - 0.01	20	18	27
0.01 - 0.02	20	22	13
0.02 - 0.03	12	12	13
0.03 - 0.04	7	10	0
0.04 - 0.05	4	3	7
0.05 - 0.06	9	12	0
0.06 - 0.07	4	5	0
0.07 - 0.08	2	0	7
0.08 - 0.09	2	3	0
0.09 - 0.10	0	0	0
> 0.10	11	10	13
Total	100	100	100

The changes in IRI that are shown in table 58 were observed over the monitored period of the sections, but the monitored period varied between the sections. Roughness progression between test sections can be compared by obtaining a rate of change of roughness at each section. A rate of change of IRI at each test section was computed by performing a linear regression on the time-sequence IRI values. Table 59 presents the distribution for the rate of change of IRI when both environmental zones are combined, as well as for each environmental zone. A rate of change of IRI of less than 0.01 m/km was observed for 47 percent of the sections in the wet no-freeze zone, and 23 percent of the sections in the wet freeze zone. This shows that the GPS-4 sections in the wet-freeze zone are showing higher rate of increase of roughness than the sections in the wet no-freeze zone.

Figure 95 shows the relationship between the rate of change of IRI and the average age of the pavement over the monitored period. Generally, pavements that are over 20 years old are showing a higher rate of change of IRI.

Table 59. Percent distribution of GPS-4 sections according to rate of change of IRI.

Rate of Change of IRI (m/km/year)	Percent Sections		
	All Zones	Wet-Freeze	Wet No-Freeze
< 0	9	5	20
0.00 - 0.01	20	18	27
0.01 - 0.02	20	23	13
0.02 - 0.03	13	13	13
0.03 - 0.04	7	10	0
0.04 - 0.05	4	3	7
0.05 - 0.06	9	13	0
0.06 - 0.07	4	5	0
0.07 - 0.08	2	0	7
0.08 - 0.09	2	3	0
0.09 - 0.10	0	0	0
> 0.10	11	10	13
Total	100	100	100

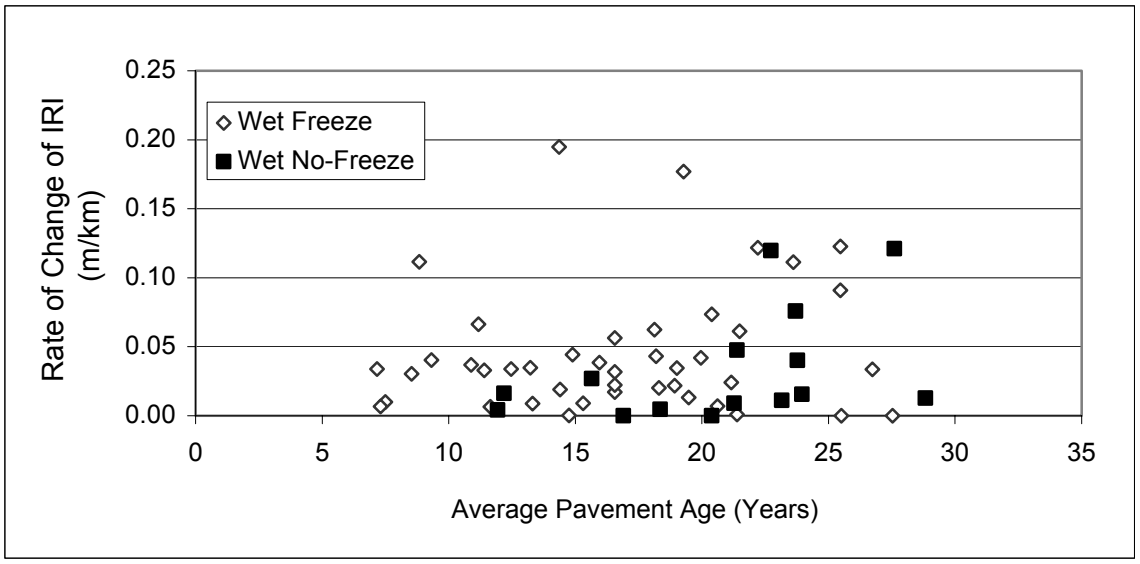

Figure 95. Relationship between rate of change of IRI and pavement age for GPS-4 sections

Trends in Roughness Development

The time-sequence IRI plots for the GPS-4 sections in the wet freeze zone and wet no-freeze zone differentiated according to the base type are shown in figures 96 and 97. Many GPS-4 sections, especially in the wet-freeze zone show variability in the time-sequence IRI values. This variability is likely related to curling and warping effects in the PCC slabs, or due to frost heave effects.

Several GPS-4 sections in the wet-freeze zone are showing an exponential trend in the increase of IRI. Twenty percent of the sections in the GPS-4 experiment have been deassigned from the experiment because they were rehabilitated (i.e., they are no longer being monitored). The time-sequence IRI plots for these sections are also included in figures 96 and 97. The median IRI at the time these sections were deassigned was 2.1 m/km, with the median age of these sections being 22 years.

Factors Affecting Changes in IRI

An analysis was performed to investigate the factors that have an effect on the roughness of GPS-4 pavements. The factors that were considered in the analysis are shown in table 5 in chapter 4. This analysis was performed by studying relationships between median IRI of the section over the monitored period as well as the rate of change of IRI with the parameters considered in the analysis. The relationships between median IRI and evaluated parameters will indicate parameters that have an influence on the IRI value, while the relationship between rate of change of IRI and the evaluated parameters will identify parameters that have an influence on the change in IRI. The following observations were noted from this analysis.

PCC Strength Parameters

The observed trends between IRI and PCC strength parameters were generally weak. There was a trend of lower IRI for higher compressive strength of PCC and higher unit weights of PCC. A trend of higher IRI values with higher PCC elastic modulus, higher PCC Poisson's

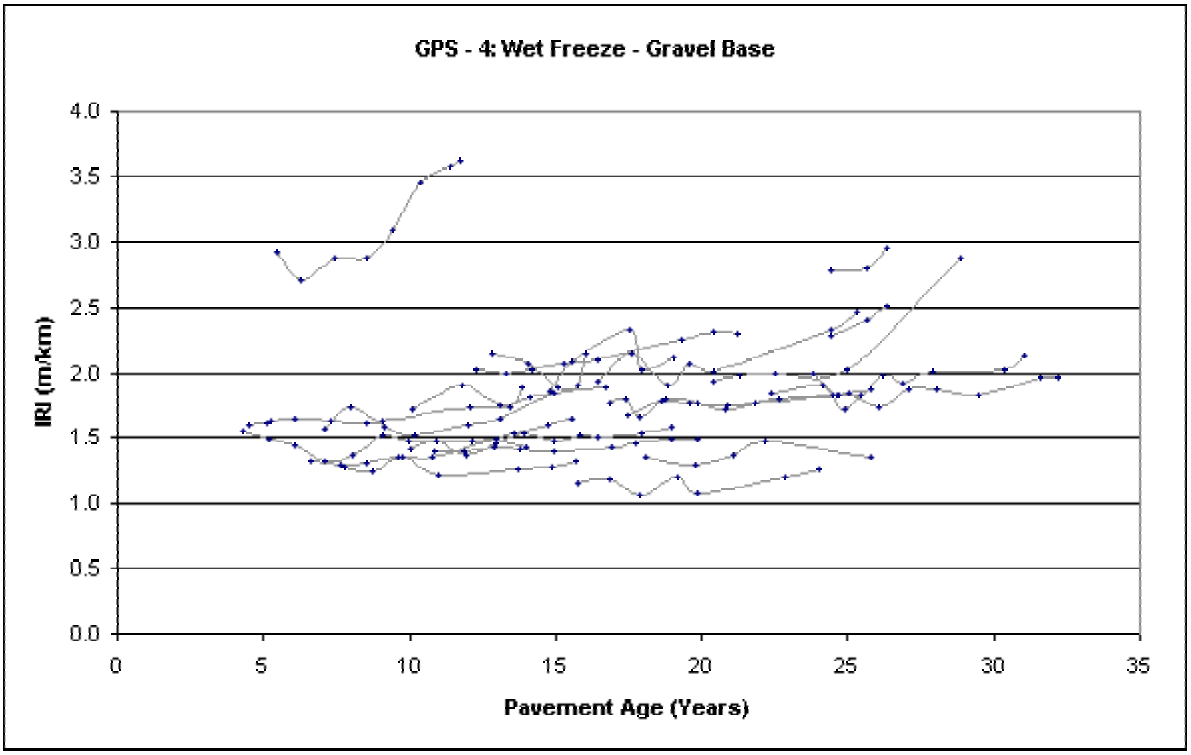

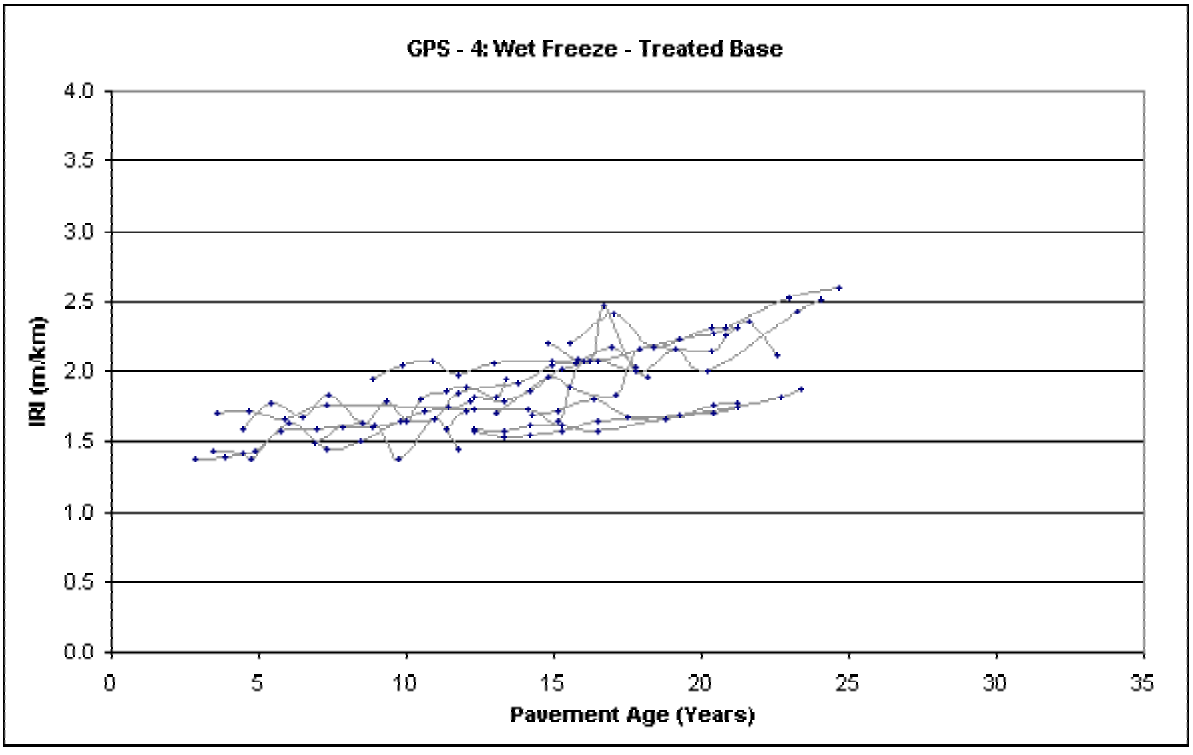

Figure 96. IRI trends for GPS-4 sections in the wet freeze zone.

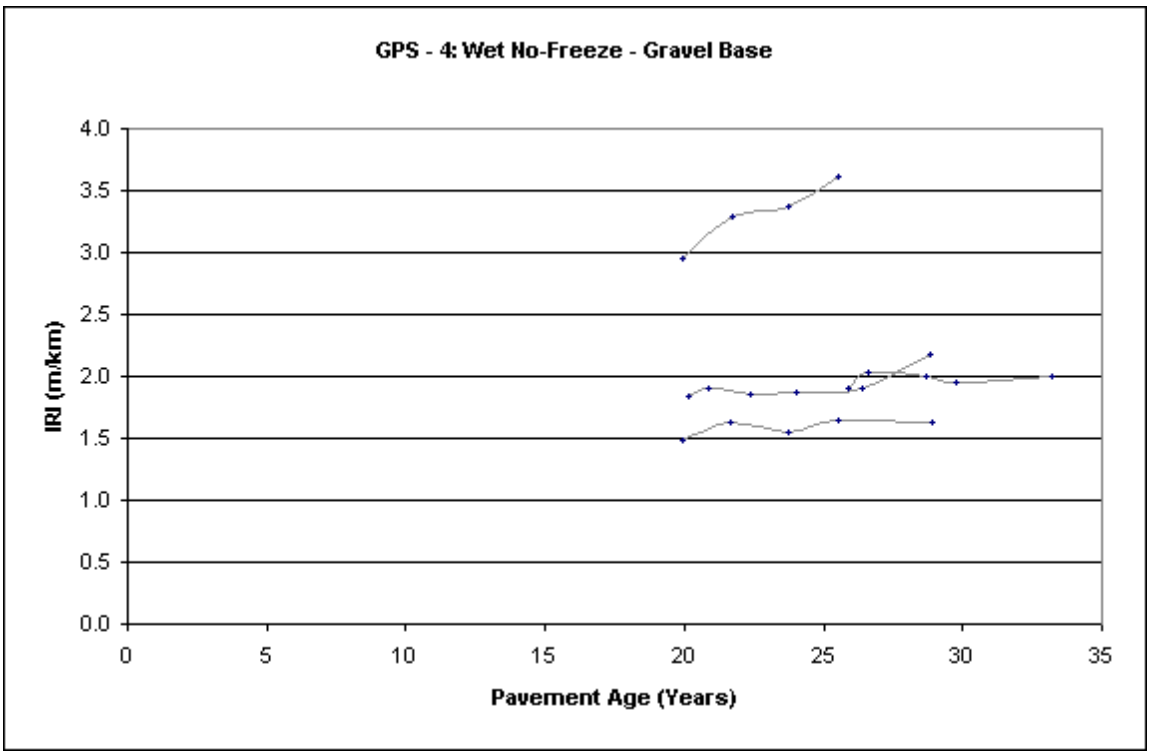

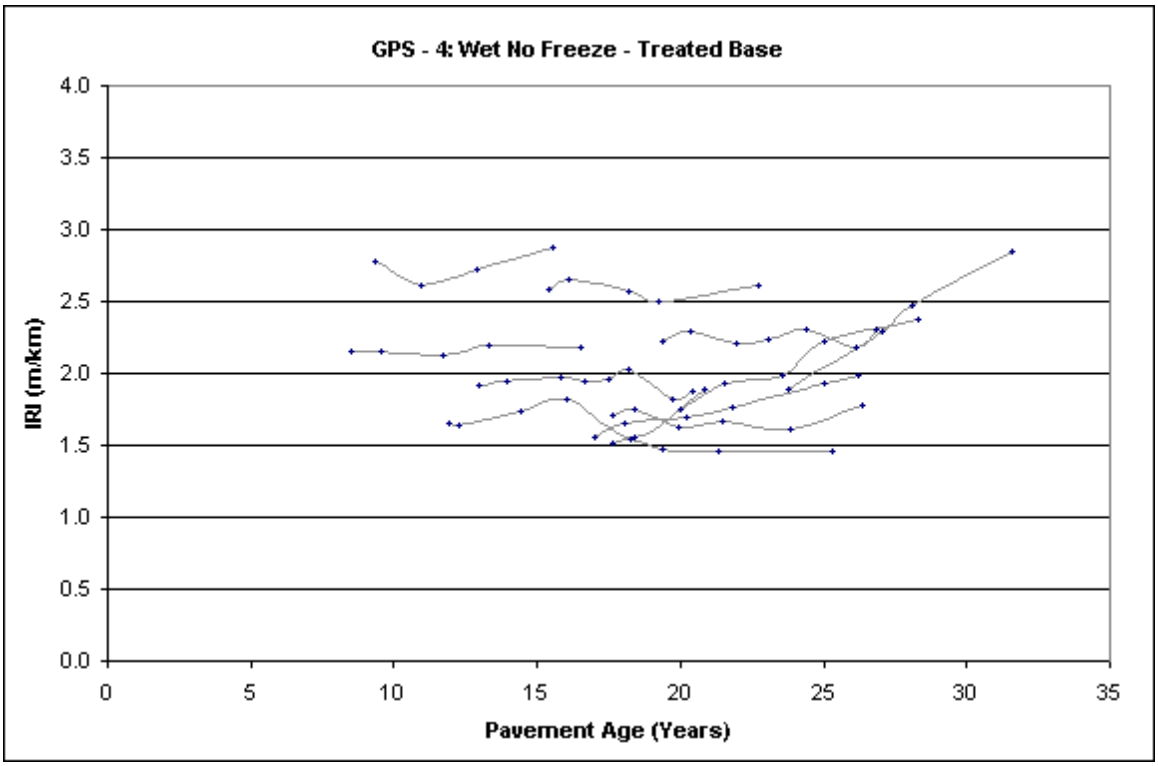

Figure 97. IRI trends for GPS-4 sections in the wet no-freeze zone.

ratios, and higher ratios between PCC elastic modulus and PCC tensile strength was observed. The relationship between rate of change of IRI and ratio between PCC elastic modulus and tensile strength is shown in figure 98.

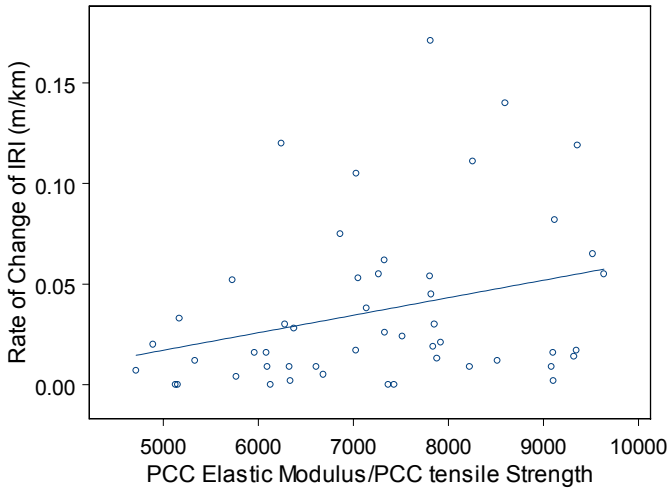

Figure 98. Relationship between rate of change of IRI and ratio between PCC elastic modulus and tensile strength.

PCC Mix Parameters

There were several sections that had low cement contents (less than 300 kg/m^3) that had high IRI values. Several sections that had water cement ratios in excess of 0.50 had high rates of increase of IRI.

Subgrade Properties

Higher IRI values were seen with increasing moisture content of the subgrade, higher clay content in the subgrade, and for sections on subgrades having high plastic limits. Figure 99 shows the relationship between IRI and clay content of the subgrade. Potential for pumping is greater on pavements that are located on fine grained soils. Higher rates of increase of IRI were noted for pavements on subgrades having higher plastic limits, higher clay contents, and higher moisture content of subgrade.

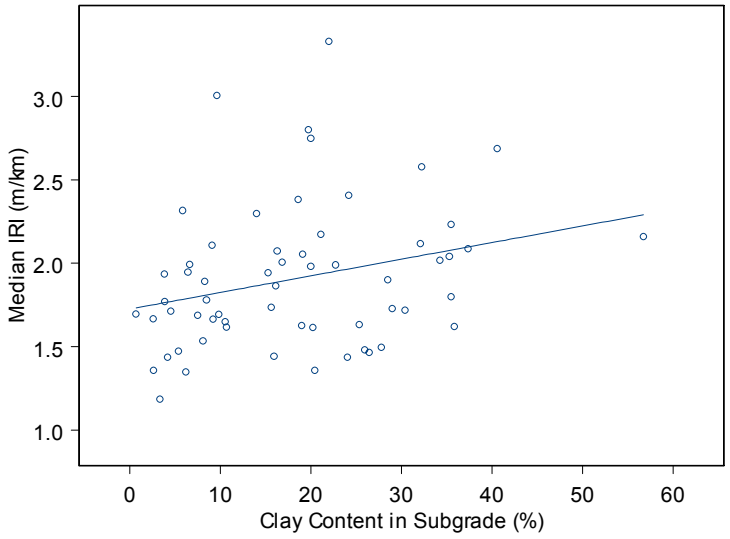

Figure 99. Relationship between IRI and clay content of subgrade.

Environmental Conditions

Higher IRI values were observed with higher annual precipitation and higher mean temperatures, and these relationships are shown in figures 100 and 101. Higher rates of increase of IRI were noted for pavements in areas that had a higher number of wet days. Higher precipitation can increase the pumping susceptibility of the pavement, if it is not adequately designed to prevent pumping. Higher mean temperatures increase the potential for expansion of the pavement, and can lead to spalling that will increase the roughness of the pavement.

Time and Traffic

Higher IRI values were seen with increasing age of pavement and higher cumulative traffic. The relationship between pavement age and IRI is shown in figure 102.

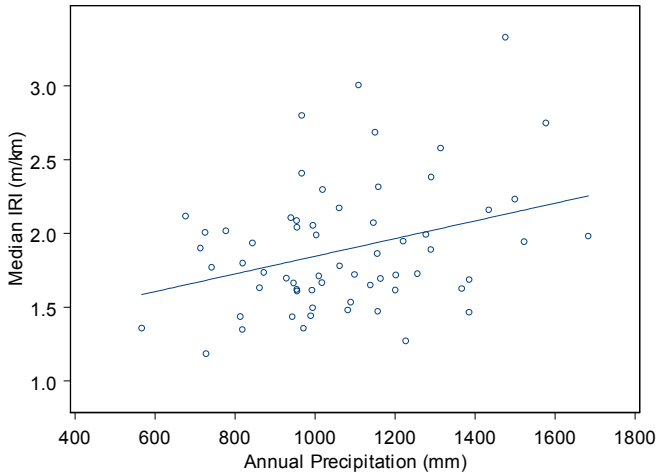

Figure 100. Relationship between IRI and annual precipitation.

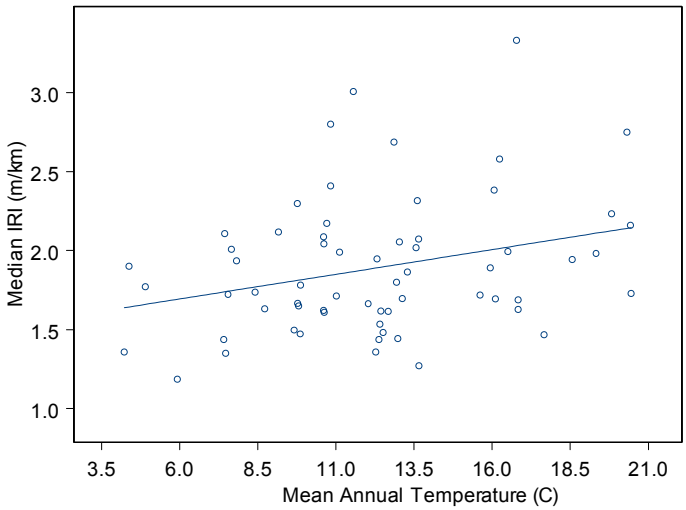

Figure 101. Relationship between IRI and mean annual temperature.

Pavement Design Parameters

Higher IRI values were observed for thicker PCC slabs, and for higher joint spacing. An increased joint spacing would likely result in a greater number of transverse cracks, and therefore increase the spalling and faulting potential of the pavement. Higher rates of increase of IRI were noted for pavements with higher joint spacing. The relationship between joint spacing and the median IRI over the monitored period is shown in figure 103.

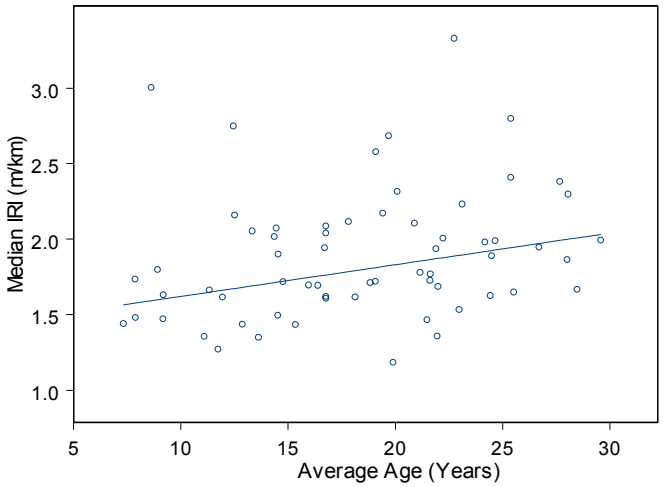

Figure 102. Relationship between IRI and pavement age.

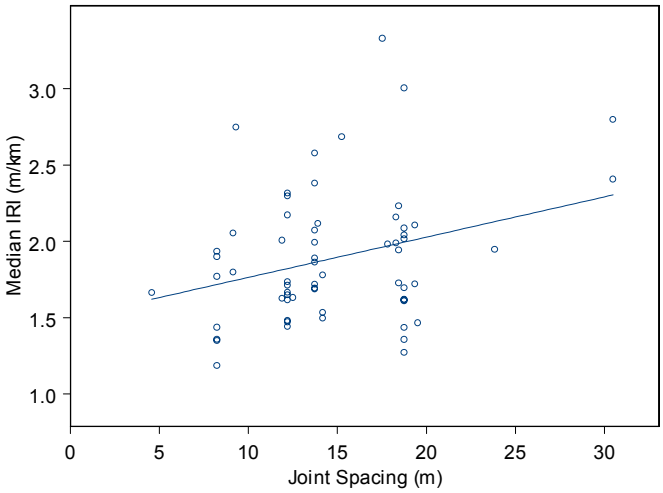

Figure 103. Relationship between IRI and joint spacing.

Good or Poorly Performing Sections

Figure 104 shows the time-sequence IRI values of five sections, three of which are showing an increase in IRI with time, and two pavements that have remained smooth over a long period of time.

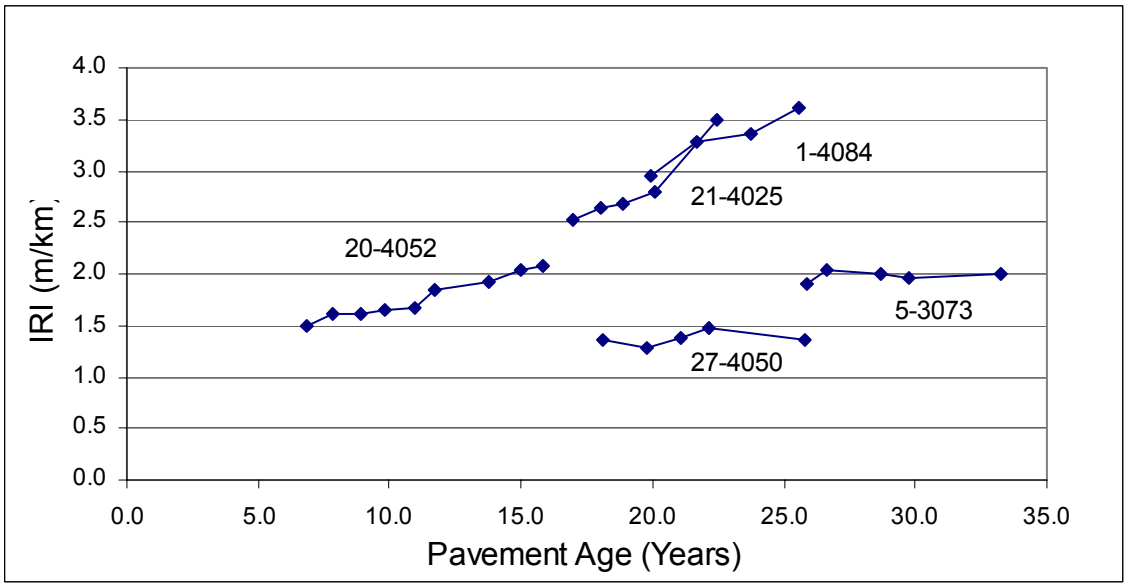

Figure 104. Good and poorly performing GPS-4 sections.

The following observations were noted for sections 20-4052, 21-4025, and 1-4084 that have shown high increases in IRI with time: (1) Section 20-4052: This section has the second lowest value of PCC split tensile strength in the database for GPS-4 sections (3.2 Mpa), and this low value is likely to be contributing factor for the high increase in IRI. (2) Section 1-4084: This section has carried a high cumulative traffic volume over its life, and the high increase in roughness that is seen at this section is attributed to the high traffic level. (3) Section 21-4025: This section is in the wet-freeze zone and us located on a fine grained subgrade with 82 percent material passing the No. 200 sieve, with the subgrade having a moisture content of 26 percent, and a plastic limit of 24. The poor subgrade condition maybe contributing to the poor performance of this section.

The following observations were noted for sections 27-4050 and 5-3073, that have both performed well over the years: (1) Section 27-4050: This section has a carried a very low traffic volume and is located on a coarse grained subgrade that has 11 percent material passing the No. 200 sieve. The low traffic volumes and good subgrade conditions are attributed to the good performance of this section. (2) Section 5-3073: This section is located in the wet no-freeze zone

has carried a high traffic volume. This section has a surface thickness of 231 mm, and a total pavement thickness of 683 mm (i.e., surface, base and subbabse), and is located on a coarse grained subgrade. The high total pavement thickness and good subgrade conditions are likely to be factors that are contributing to the excellent performance of this section.

As these examples show, for sections that are showing either a good performance or a poor performance, an in-depth analysis of the test section can identify the factors that are affecting its performance.

Models for Roughness Prediction

The time-sequence IRI values were backcasted to obtain the initial IRI of the pavement by fitting a regression equation for each GPS-4 section. The regression was performed by using logarithm of IRI as the dependant variable and time as the independent variable. Generally, reasonable IRI values could be obtained by using this approach.

Thereafter, a mixed model analysis was carried out on the data to develop a model to predict roughness. The mixed model analysis in the S-Plus software was used to carry out this analysis. The following model was developed to predict IRI:

$Log_e(IRI_t) = -0.1875633 + 0.3967905IRI_0 + 0.0000081(Traffic) + 0.0003266(Time\ X\ MC) + 0.0000002(Time\ x\ PCCEmod)$

Section effects standard deviation = 0.15, residual standard deviation = 0.05

No. of sections = 52.

where,

IRI_t	=	International Roughness Index at time t, m/km
IRI_0	=	IRI at time = 0, m/km
Traffic	=	Cumulative traffic, KESAL
Time	=	Time, years
MC	=	Moisture content of subgrade, percent
PCCEmod	=	Elastic modulus of PCC, Mpa

Summary for GPS-4

All GPS-4 sections are located either in the wet freeze or the wet no-freeze zone. Higher IRI values were associated with higher PCC elastic modulus, high ratios between PCC elastic modulus and split tensile strength (greater than 8000), higher moisture content of subgrade, higher clay contents in the subgrade, higher plastic limits of subgrade, higher annual precipitation, higher mean temperatures, higher joint spacing, pavement age and cumulative traffic. Several sections that had low cement contents (less than 300 kg/m3) had high IRI values. Some sections that had water cement ratios in excess of 0.50 also had high rates of increase of IRI.

GPS-5: CONTINUOUSLY REINFORCED CONCRETE PAVEMENTS

Test Sections

There are 82 GPS-5 sections in the LTPP database. The distribution of these sections according to the environmental zone and subgrade type is shown in table 60. Forty nine percent of the GPS-5 sections are in the wet freeze zone, 41 percent in the wet no-freeze zone, and the remaining 10 percent are in the dry regions (dry-freeze and dry no-freeze). Approximately equal numbers of sections are located on fine grained and coarse grained subgrade.

Figure 105 shows the distribution of the pavement sections according to their age at the time they were first profiled and at the last available profile date. On average, the GPS-5 sections have so far been profiled six times, over a seven-year period. Fifty percent of the GPS-5 sections have been monitored over a period between 8 and 9.5 years.

Table 60. Distribution of GPS-5 sections.

Subgrade Type	Number of Sections				
	Environmental Zone				Total
	Dry-Freeze	Dry No-Freeze	Wet Freeze	Wet No-Freeze	
Coarse	4	1	17	18	40
Fine	1	3	22	16	42
Total	5	4	39	34	82

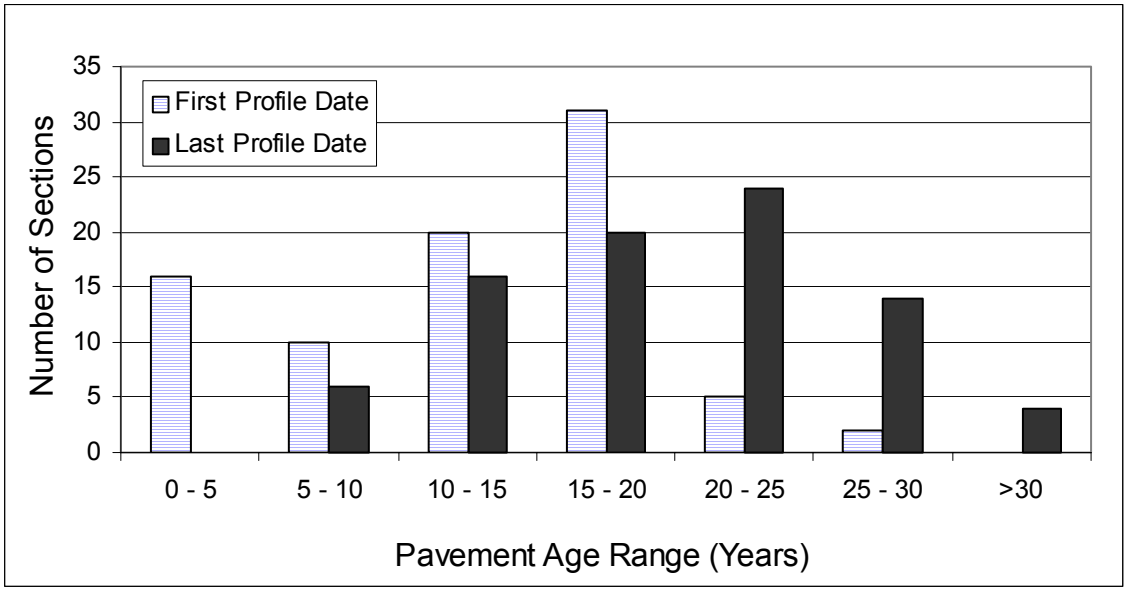

Figure 105. Distribution of GPS-5 sections according to age at first and last profile dates.

Changes in IRI

The difference in IRI between the last profile date and first profile date, classified according to different IRI ranges is presented in table 60. Table 61 presents the percent distribution of sections when all regions are considered, as well as for distributions for each environmental zone. The sections in the dry-freeze and dry no-freeze zones were combined into one zone, called the dry-zone, as the number of sections in these two zones was low. The values presented in table 61 provides an overview of the magnitude of changes in IRI that have occurred at the GPS-5 sections over the monitored period.

Table 61. Percent distribution of GPS-5 sections according to change in IRI.

Change in IRI Over Monitored Period (m/km)	Percent Sections			
	Environmental Zone			
	All Zones	Wet-Freeze	Wet No-Freeze	Dry
<= 0.00	31	31	42	22
0.00 – 0.10	37	33	33	44
0.10 – 0.20	19	22	13	22
0.20 – 0.30	5	3	6	12
0.30 – 0.40	4	3	6	0
0.40 – 0.50	0	0	0	0
>0.50	4	8	0	0
Total	100	100	100	100

An examination of the percent distribution of sections for all environmental zones show that 31 percent of the sections had an IRI at last profile date that was equal to less than the IRI at first profile date. Also, 37 percent of the section had a change in IRI that was less than 0.1 m/km over the monitored period. A change in IRI of 0.1 m/km is a very small change in IRI, and differences of this magnitude can easily occur due to variations in the profiled path or temperature effects. The cause for 37 percent of the sections to have an IRI at last profile date that was less than the IRI at the first profile date is attributed to variations in the profiled path between the two dates, and environmental effects that may cause variations in the surface shape. As the data shows 68 percent of the test sections had an IRI change of less than 0.1 m/km over the monitored period. Therefore, it can be concluded that the change in roughness was negligible over the monitored period at 68 percent of the sections. For the sections that showed a change in IRI that was greater than 0.1 m/km, 20 percent of sections had an IRI change between 0.10 and 0.20 m/km, which still is a very small change in IRI and the other 13 percent showed an increase in IRI of over 0.20 m/km over the monitored period. The data shown in table 61 indicate pavement sections in each environmental zone generally exhibited similar trends.

A rate of change of IRI was computed for each section by dividing the difference between the last and first IRI values by the time change between the two observations. Table 62

presents the distribution for the rate of change of IRI for all regions as well as for individual regions classified according to different rate of changes. As seen from this table, the rates of change of IRI for majority of sections was extremely small, with similar trends being seen for the different environmental zones.

Table 62. Percent distribution of GPS-5 sections according to rate of change of IRI

Range for Rate of Change of IRI (m/km/yr)	Percent Sections			
	Environmental Zone			
	All Zones	Wet-Freeze	Wet No-Freeze	Dry
<0.00	35	22	29	45
0.00 - 0.01	25	44	22	22
0.01 - 0.02	21	23	25	15
0.02 - 0.03	7	0	9	9
0.03 - 0.04	4	11	0	6
0.04 - 0.05	3	0	3	3
0.05 - 0.06	0	0	0	0
0.06 - 0.07	1	0	3	0
0.07 - 0.08	1	0	3	0
>0.08	3	0	6	0
Total	100	100	100	100

Figure 106 shows the relationship between the rate of change of IRI and the average age of the pavement over the monitored period. No distinct difference in the rate of change of IRI with the pavement age can be observed in this plot.

Trends in Roughness Development

The time-sequence IRI plots for the GPS-5 sections, differentiated according to the environmental zones are presented in figure 107. These plots show the data trends that were discussed previously, that is for most sections the IRI remained relatively constant over the monitored period. Some sections showed variability in IRI over the years, with the IRI for a specific year being either higher or lower than the previous and subsequent years. The cause for

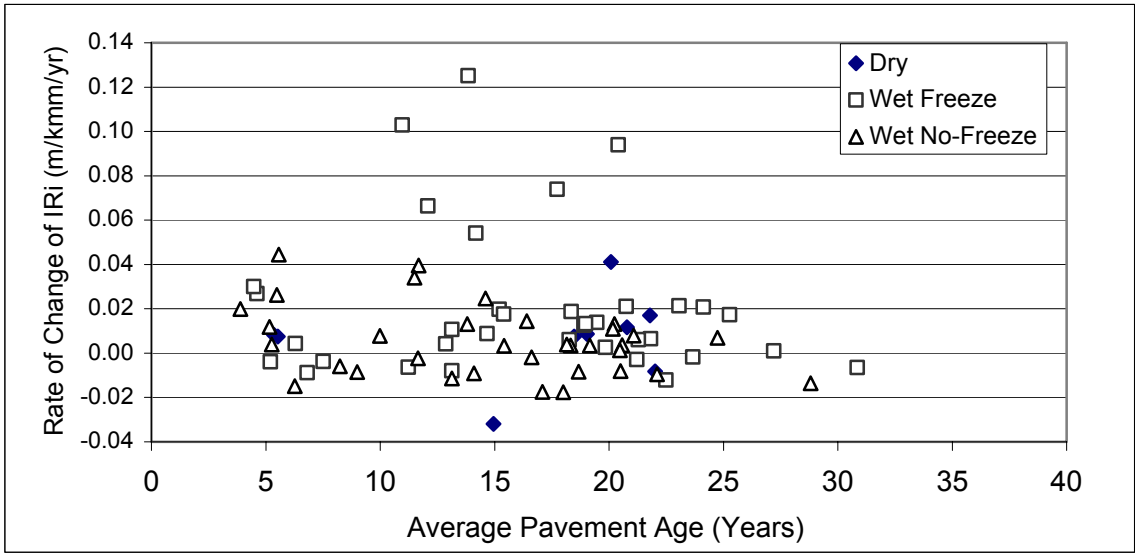

Figure 106. Relationship between rate of change of IRI and pavement age for GPS-5 sections.

these differences may be variations in the profiled paths between the years, or changes in the pavement profile that is caused by temperature variations or subgrade effects. Generally, the pavements that were young (less than 5 years) as well as pavements that were old (over 20 years) showed the same IRI behavior pattern across all environmental zones. These observations indicate that the majority of the CRCP pavements are maintaining their IRI value over time. Eighteen percent of the test sections in the GPS-5 experiment have been deassigned, that is they are no longer being monitored as they were rehabilitated. The time-sequence IRI values of these sections are also shown in figure 107. The average IRI value of the deassigned sections was 1.4 m/km, with the average age of the deassigned sections being 20 years. As the average IRI of the deassigned sections was 1.4 m/km, it appears that many sections were not rehabilitated because of excessive roughness.

Factors Affecting IRI

An analysis was performed to investigate the factors that have an effect on the roughness at GPS-5 sections. The list of factors that were considered in the analysis is shown in table 5 (in

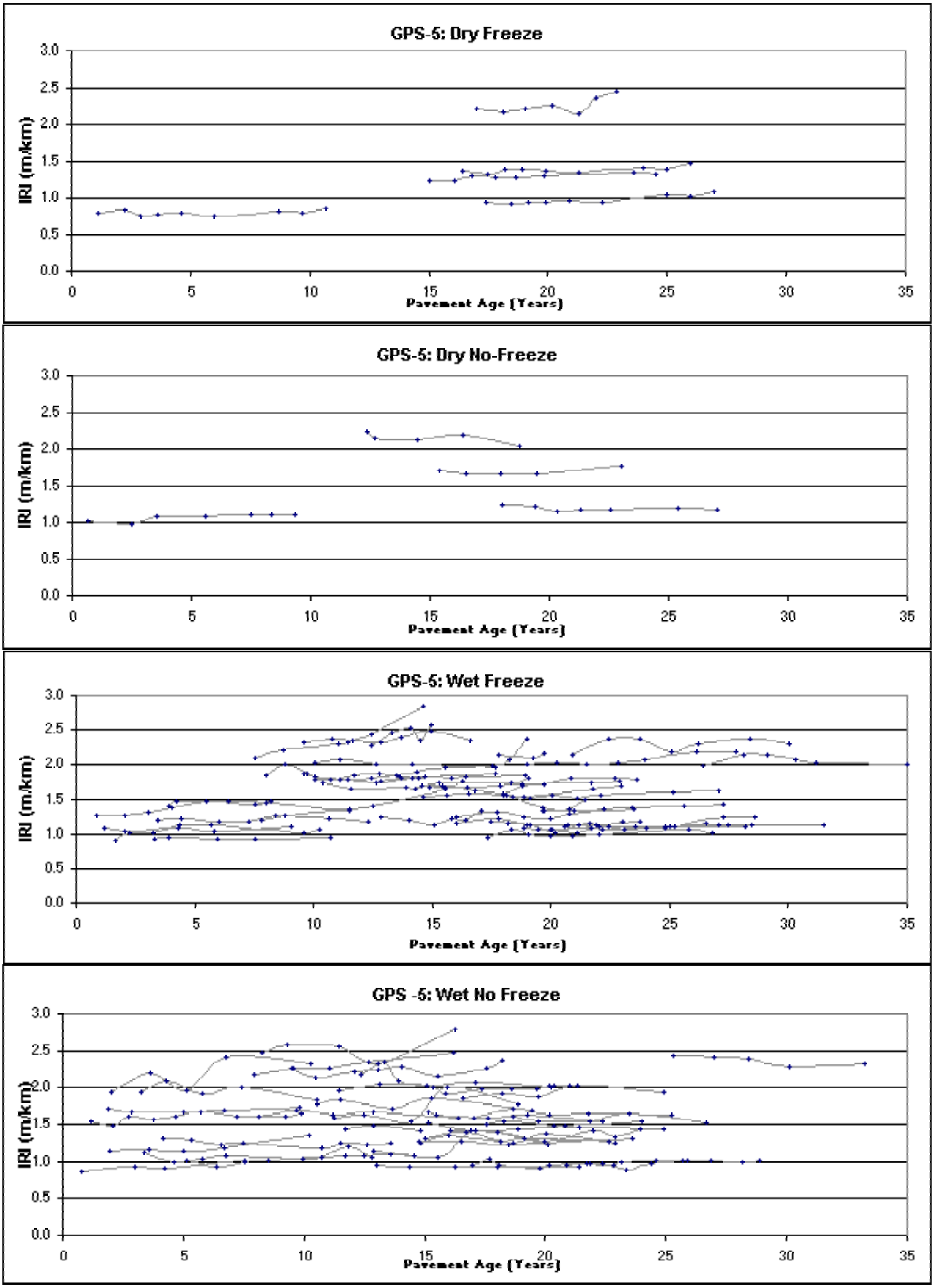

Figure 107. IRI trends for GPS-5 sections.

chapter 4). The analysis was performed by analyzing the relationship between the last IRI value available at a section and each of the selected parameters. Correlation coefficients between the parameters and the IRI, as well as scatter plots that show the relationship between the parameters and IRI were used in this analysis. Initially data trends between IRI and the selected parameters were carried out by considering the data for all environmental zones, and thereafter the data for each environmental zone were examined separately. The observed data trends are presented separately for pavement section parameters, time and traffic, subgrade parameters, environmental parameters, PCC strength parameters, and PCC mix design parameters.

PCC Section Parameters

No relationships between IRI and surface thickness or base thickness, or between IRI and base type was observed. In the GPS-5 sections, 17 percent of sections have a granular base, while 83 percent of the sections have a treated base, where approximately equal number of sections have asphalt treated and cement treated bases. No relationship between the IRI values and base types was found. A weak trend of lower IRI values with higher total pavement thickness (i.e, sum of surface, base and subbase thickness) was observed. In the wet no-freeze zone, lower IRI values were associated with higher steel contents, and this relationship is shown in figure 108.

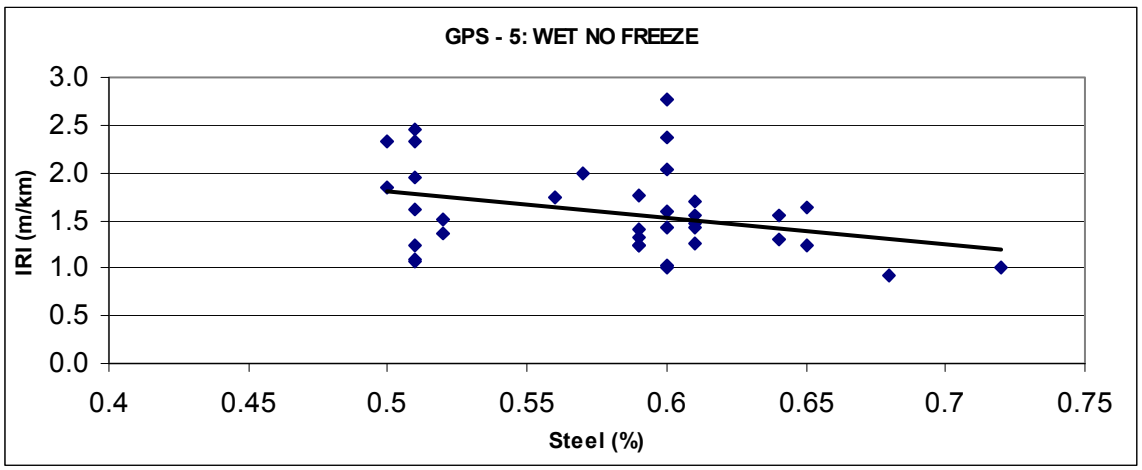

Figure 108. Relationship between IRI and steel content – wet no-freeze zone.

Time and Traffic

No relationship between IRI and pavement age or IRI and cumulative traffic was observed.

Subgrade Properties

In the wet-freeze zone, a weak trend of higher IRI with increasing percentage of subgrade passing No. 200 sieve and higher moisture contents in the subgrade was noted. In both the wet freeze and wet no-freeze zone, a weak trend of increasing IRI with higher plasticity index of subgrade was also noted. High subgrade moisture contents increase the frost heave effects of the subgrade, and high plasticity index of subgrade will increase the swelling potential of the subgrade, both if which can cause higher roughness.

Environmental Conditions

In the wet freeze zone, a general trend of higher IRI values with higher number of wet days per year was observed, while in the wet no-freeze zone, a general trend of lower IRI values with higher wet days per year was observed. The relationship between IRI and wet days for the wet-freeze and wet no-freeze zones is shown in figures 109 and 110, respectively. Higher wet days result in higher moisture contents in the subsurface layers, and in the freezing regions this will increase the frost heave potential of the subgrade, and this can result in a higher roughness. In the wet no-freeze regions, higher wet days tends to keep the moisture content of the subsurface layers at a constant level, and therefore reducing the shrink and swell behavior in these layers. The lower IRI observed with higher wet days in the wet no-freeze regions might be caused by this factor.

In the wet no-freeze zone, higher annual mean temperatures and higher days above 32 °C were associated with higher IRI values. The relationship between IRI and days above 32 °C for the wet no-freeze zone is shown in figure 111. No clear trends between IRI and freezing index or days below 0 °C were observed in the wet-freeze zone. A weak trend of increasing IRI with increasing freeze-thaw cycles was observed for wet-freeze zones.

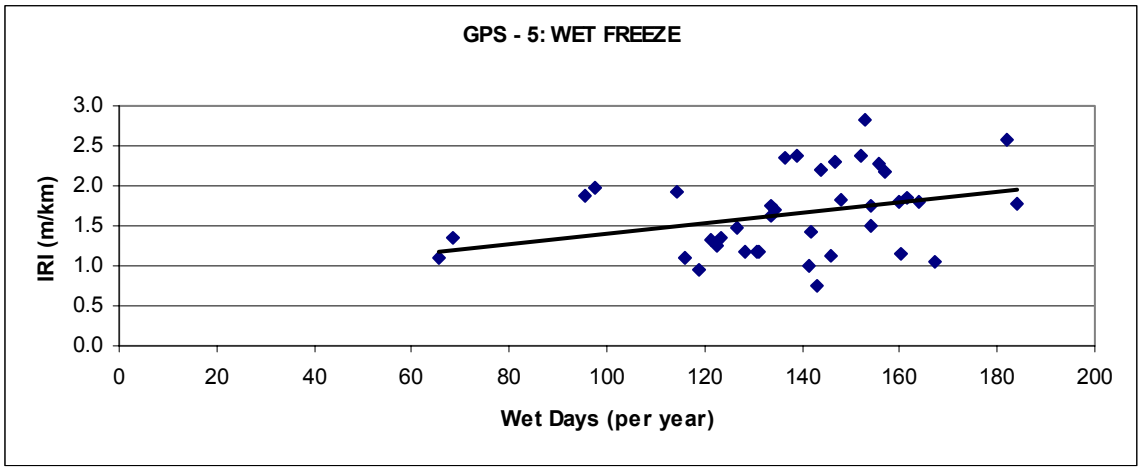

Figure 109. Relationship between IRI and wet days – wet freeze zone.

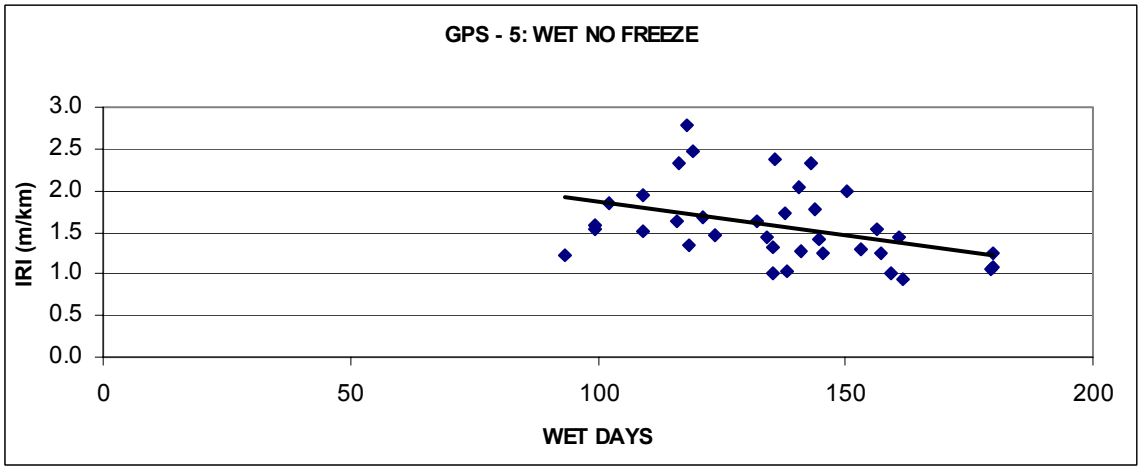

Figure 110. Relationship between IRI and wet days – wet no-freeze zone.

PCC Strength Parameters

When data for all GPS-5 sections were considered, an increase in IRI with an increase in elastic modulus of PCC was observed, and this relationship is shown in figure 112. A much stronger relationship was noted between the IRI and the ratio between elastic modulus and split tensile strength of PCC, and this relationship is shown in figure 113. PCC that has a high value of elastic modulus relative to its split tensile strength may exhibit more brittle behavior, and this may be the cause for the high IRI.

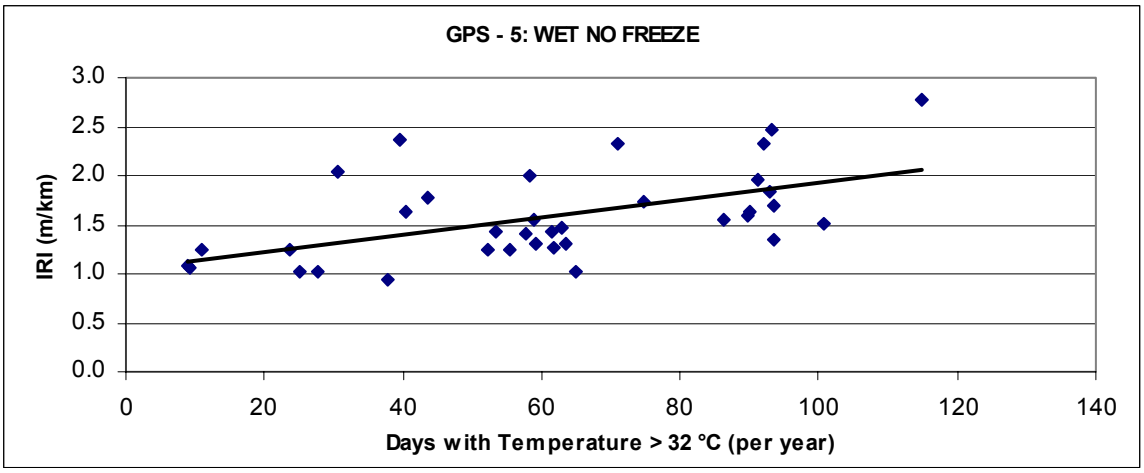

Figure 111. Relationship between IRI and days with temperature > 32 °C – wet no-freeze zone.

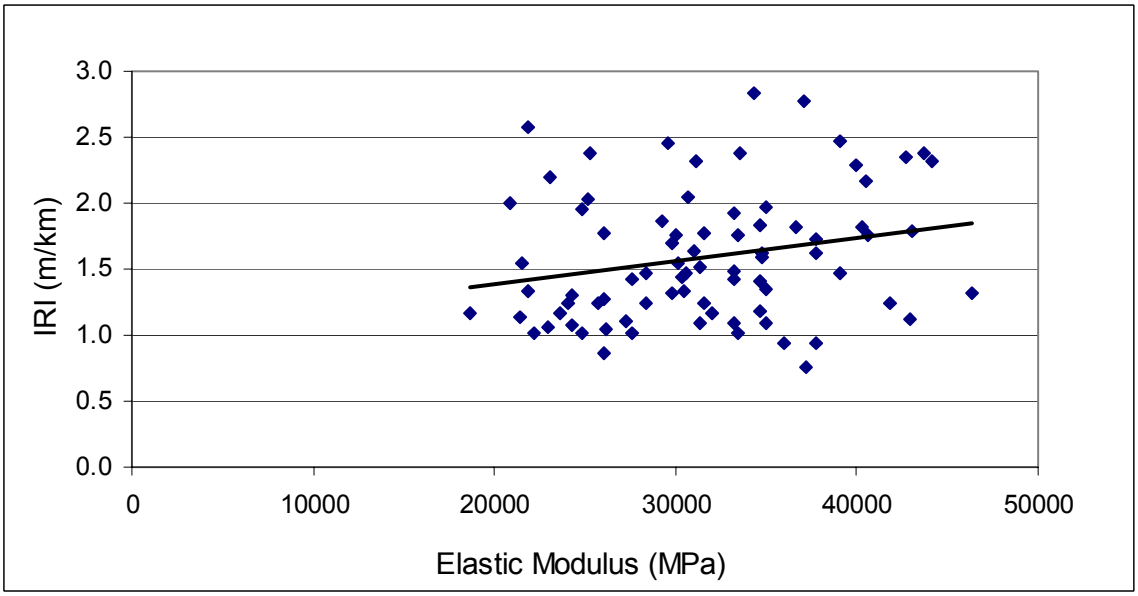

Figure 112 Relationship between IRI and PCC elastic modulus.

PCC Mix Parameters

Sections with higher water cement ratios had lower IRI values, with this relationship being the weakest for the wet no-freeze region. The relationship between IRI and water cement

ratios in PCC mix for all GPS-5 sections is shown in figure 114. Generally, the sections that have higher water cement ratios are located in the no-freeze zones.

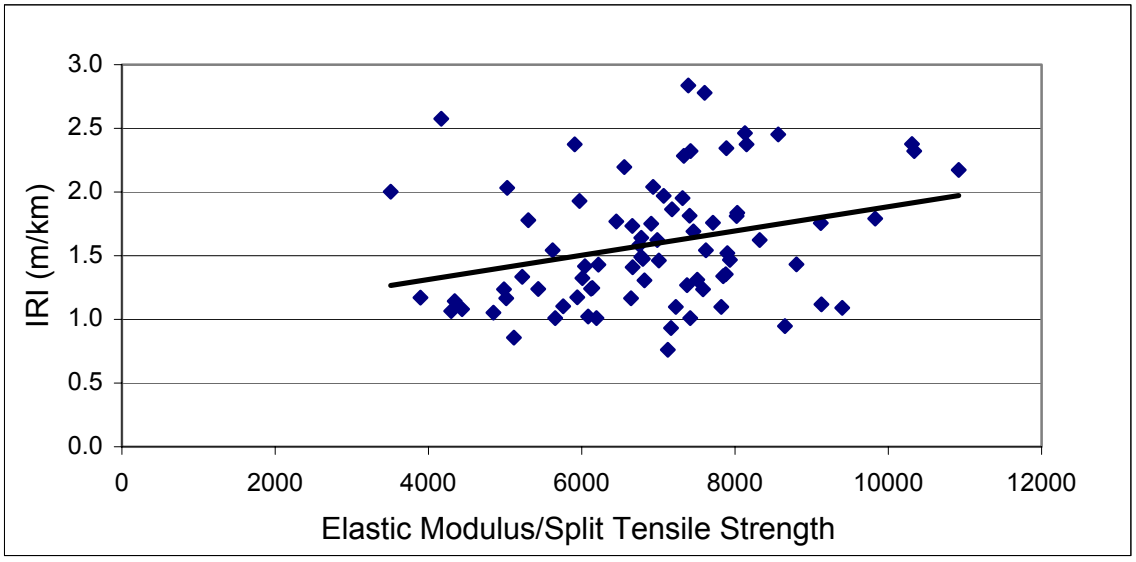

Figure 113. Relationship between IRI and ratio between PCC elastic modulus and split tensile strength.

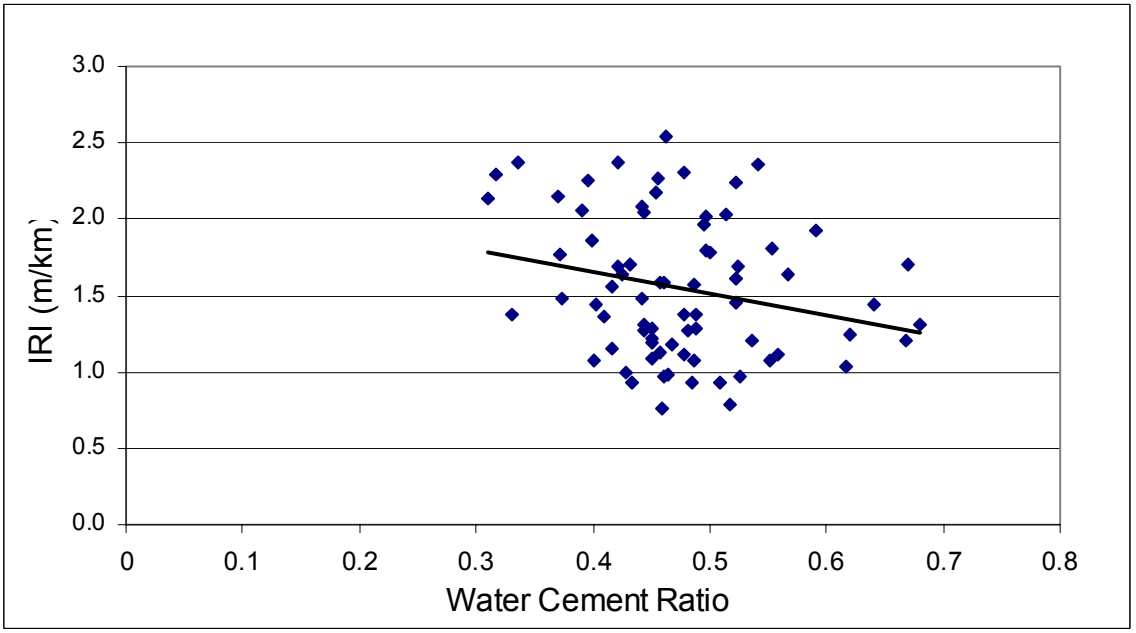

Figure 114. Relationship between IRI and water cement ratios in PCC mix.

Good and Poorly Performing Sections

As described previously, most GPS-5 sections were maintaining their IRI values with little change in IRI over the monitored period. The median IRI value of all GPS-5 sections at the last profile date was 1.5 m/km. An analysis was performed to see if differences between pavements that have an IRI of less than 1.5 m/km, and an IRI that is greater than 1.5 m/km could be identified. The GPS-5 sections were divided into two groups, with one group having an IRI less than 1.5 m/km and the other group having an IRI greater than 1.5 m/km. Thereafter, t-tests between mean values of selected parameters between these two groups were performed to identify parameters that are statistically different between the two groups. The analysis indicated the following factors contribute to higher IRI: (1) a low total pavement thickness where total pavement thickness is the sum of surface, base and subbase layers, (2) high PCC modulus, (3) high ratio between PCC elastic modulus and PCC tensile strength (i.e. PCC Elastic Modulus/PCC Tensile Strength), (4) high PCC Poisson's ratios, and (5) low water cement ratios.

Figure 115 shows the time-sequence IRI values of five sections, three of which are showing an increase in IRI with time, and two sections that have remained exceptionally smooth over a long period of time.

Figure 115. Good and poorly performing GPS-5 sections.

The following observations were noted for sections 42-5020, 17-5843, and 48-5317 that have shown an increase in IRI over time: (1) Section 42-5020: This section has a surface thickness of 236 mm, a PCC elastic modulus of 43,752 Mpa, and a ratio between PCC elastic modulus and PCC tensile strength of 10,308 which is the third highest value in the entire GPS-5 data set. The high rate of increase of IRI is attributed to the high value for the ratio between PCC elastic modulus and PCC tensile strength. (2) Section 17-5843: This section has a PCC surface thickness of 264 mm, a relatively high PCC elastic modulus of 40,651 Mpa, and a relatively high value for the ratio between PCC elastic modulus and PCC tensile strength of approximately 9000. The high rate of increase of IRI is attributed to the high value between PCC elastic modulus and PCC tensile strength. (3) Section 48-5317: This section has a surface thickness of 203 mm, and it is located in an area that has 93 days when the temperature is greater than 32 °C, and a relatively high value of 8130 for the ratio between PCC elastic modulus and PCC tensile strength. The high number of days greater than 32 °C and the high value for ratio between PCC elastic modulus and tensile strength is attributed to the high rate of increase of IRI observed at this section.

The following observations were noted for sections 55-5037 and 48-5334 that have remained exceptionally smooth over time: (1) Section 55-5037: This section has a PCC surface thickness of 208 mm, with 5 days in the year when the temperature is greater than 32 °C, and a ratio between PCC elastic modulus and PCC tensile strength of 5940, which is below the average for the entire data set. The low number of days when the temperature is greater than 32 °C and the relatively low value for the ratio between PCC elastic modulus and PCC tensile strength may have contributed to the good performance of this test section. (2) Section 48-5334: This section has a PCC surface thickness of 203 mm, and a high water cement ratio of 0.56, and a ratio between PCC elastic modulus and PCC tensile strength of 7229, which is close to the average for the entire data set. The high water cement ratio for this section resulted in a low IRI value, and this section has maintained this IRI over time.

As these examples show, for sections that are showing either a good performance or a poor performance, an in-depth analysis of the test section can identify the factors that are affecting its performance.

Models to Predict Roughness

Two approaches were used to develop models to predict roughness. In the first approach, the last IRI value that is available at a section was used as the dependant variable, and multiple regression analysis was used to predict the last IRI using the data parameters that are available for GPS-5 sections. In the second approach, the mixed model analysis was performed on the data by treating the IRI as the dependant variable. Initially modeling was performed for the entire data set. However, as the data elements that affect roughness values in the wet-freeze and wet no-freeze regions were different, better models were obtained when these data sets were analyzed separately. The developed models are presented separately for the two environmental zones.

Wet Freeze Zone

Multiple Regression Analysis:

IRI = -0.6433 + 0.0082(Wet_Days) + 0.0001(Emod/Tensile) + 0.0063(SG200)

R2 = 0.29, standard error = 0.47

Mixed-Model Analysis:

IRI = -0.4963 + 0.0064(Wet_Days) + 0.0001(Emod/Tensile) + 0.0054(SG200) + 0.0124(Time)

Section effects standard deviation = 0.44, residual standard deviation = 0.08

where,

IRI	=	International Roughness Index, m/km
Wet_Days	=	number of days per year with precipitation exceeding 0.25 mm
Emod	=	elastic modulus of PCC, Mpa
Tensile	=	tensile strength of PCC, Mpa
SG200	=	percentage of subgrade passing the No. 200 sieve
Time	=	time, years

Wet No-Freeze Zone

Multiple Regression Analysis:

IRI = 2.2106 + 0.008(Days32) –1.925(Long_Steel)

R2 = 0.34, standard error = 0.34

Mixed-Model Analysis:

IRI = 2.1952 + 0.0076(Days32) –2.015(Long_Steel) + 0.0042(Time)

Section effects standard deviation = 0.35, residual standard deviation = 0.08

where,

IRI	=	International Roughness Index, m/km
Days32	=	number of days per year with mean temperature greater than 32 °C
Long_Steel	=	longitudinal steel %
Time	=	time, years

As describe previously, the majority of the GPS-5 sections have shown very little change in IRI over the monitored period. Therefore, as expected the models built using regression analysis had very low R^2 values, and the standard deviation values for the mixed models were also very high.

Summary for GPS-5

Ninety percent of CRCP sections are located in the wet zone (wet freeze and wet no-freeze). The CRCP pavements have not shown much change in roughness over the monitored period, with 68 percent of sections showing an IRI change of less than 0.1 m/km over the monitored period (average monitored period of seven years). For pavements in both the wet freeze and wet no-freeze zones, higher IRI values were associated with higher plasticity index of subgrade, higher PCC elastic modulus, for sections that had a high PCC elastic modulus relative to its tensile strength, and for lower water cement ratios in the PCC mix.

In the wet no-freeze zone, lower IRI values were associated with higher steel contents and higher number of wet days, while higher IRI values were associated with higher number of days per year with temperatures greater than 32 °C. In the wet freeze zone, higher IRI values were associated with increasing percentage of subgrade material passing the no. 200 sieve, higher moisture content of the subgrade, and higher number of wet days per year.

DISCUSSION OF RESULTS

When pavements are designed by State agencies, they are designed based on existing subgrade conditions to carry the anticipated traffic loading over the design life of the pavement. The agencies in different parts of the country take into account the effect of environmental factors in their regions when designing pavements. If the pavements are designed "correctly" for the subgrade conditions, anticipated traffic loading, and environmental factors, an evaluation between roughness and the parameters that cause an increase in roughness may not yield any trends. The reason that there was no relationship between cumulative traffic volumes and roughness for most of the GPS experiments is attributed to the reason that the pavements are designed to carry the anticipated traffic, and therefore there should be no relationship between these two parameters. In the AASHO road test, pavement sections of varying cross sections were built and the same traffic was applied to all sections. As there were differences between the structural properties between the sections, differences in performance between the test sections was clearly seen. However, because the pavements in the GPS experiments are expected to be designed for the existing subgrade and environmental conditions, and anticipated traffic levels, the analysis carried out in this study found few strong relationships between roughness and parameters associated with these factors.

However, the scatter plots that were used in the evaluation did reveal sections that were showing very high rates of increase of roughness or very low rates of increase of roughness. A closer evaluation of some of the sections that were exhibiting high rates of increase of roughness

showed deficiencies in design or material properties. For example, the GPS-4 section that had the lowest split tensile strength of the entire data set was showing a high rate of increase of roughness. The relationship for GPS-1 sections between freezing index and rate of increase of roughness showed that there were sections located in areas that had high freezing indices that were showing very high rates of increases of roughness. An evaluation of these sections indicated they have not been adequately designed for the high freezing indices. There were sections located in areas that had high freezing indices that were not showing high rates of increase of roughness. These sections had high total pavement thickness (i.e., sum of surface, base and subbase) that provided adequate frost protection and therefore were not showing a high rate of increase in roughness. There were GPS-1 sections that had low structural numbers and have carried high traffic volumes that were showing high rates of increase of roughness. These sections are most likely to have reached the end of their design life. Some of the sections that have maintained their smoothness over relatively long periods of time appear to have carried low traffic volumes relative to their design traffic volumes, or had good subgrade conditions. These sections are most likely to be over designed based on a 20-year design life for the conditions at the site.

The investigations that were carried out at the GPS sections identified subgrade, climatic and pavement material parameters that contribute to higher roughness levels. Pavement designers should be aware of the factors that contribute to a higher rate of roughness development, and design the pavement structure so that the effect of these factors on the increase of roughness is minimized.

The roughness trends of each GPS experiment indicated that the roughness progression of test sections generally follow a parallel pattern. This indicates that pavements that are constructed smoother provide a smoother pavement to the traveling public over the pavement life when compared to a pavement that has a lower initial smoothness level (i.e., a higher initial roughness). However, achieving a high smoothness level after construction does not guarantee that the pavement will perform well over its service life. High rates of development of roughness can occur in a pavement even in its early life due to the following causes: (1) deficiencies in the material properties of pavement layers, (2) if the pavement is not adequately designed based on

the subgrade conditions, environmental conditions and anticipated traffic levels, (3) if the pavement was not constructed to meet the specified specifications, and (4) if construction problems were encountered during construction.

This page left intentionally blank.

CHAPTER 8
ANALYSIS OF OVERLAID PAVEMENTS

ANALYSIS APPROACH

The two overlaid pavement types that were studied in this project were AC overlays of AC pavements, and AC overlays of PCC pavements. The analysis approach that was followed in analyzing the data from each of these experiments was similar to the approach that was used in analyzing GPS sections in the first design phase, which was described in Chapter 7.

GPS-6: AC OVERLAY OF AC PAVEMENTS

Test Sections

The GPS-6 experiment is the study of AC pavements that are overlaid with AC. The GPS-6 sections can be divided into two categories: (a) sections that were established on in-service roadways and were at different periods in their service lives when monitoring activities began at these sections, and (b) sections that were overlaid after the LTPP program was started, and monitoring activities at these sections began immediately after the overlay. For the sections in the first category, the initial IRI of the pavement as well as the IRI prior to rehabilitation are not available. These sections are classified as belonging to the GPS-6A experiment. The IRI after overlay for the pavements that fall into the second category is available. The sections in the second category are classified into GPS-6B, -6C or –6S experiment. Sections where recycled AC was used as overlay material is classified to be GPS-6C sections, while sections on which milling was performed prior to overlay or a fabric was used prior to placing an overlay are classified to be GPS-6S sections. Sections that are classified to be GPS-6B sections received a conventional AC overlay. The number of sections falling into the different GPS-6 experiments is shown in table 63.

Table 63. Number of sections in GPS-6 experiments.

Experiment	Number of Sections
GPS-6A	58
GPS-6B	75
GPS-6C	11
GPS-6S	29

The specific type of rehabilitation strategy that was carried out at the GPS-6S sections (i.e., whether milled or fabric was placed prior to overlay) is available for only a very few sections in the rehabilitation tables of IMS. The behavior of sections that had a fabric placed before overlay or milled prior to overlay could be different than the performance of sections that received a conventional overlay. As the specific type of rehabilitation that was carried out for GPS-6S sections was not available for most sections, these sections were omitted from the analysis. The GPS-6C sections that had a recycled overlay were combined with the GPS-6B sections in the analysis. The distribution of the GPS-6A, -B and –C sections according to the environmental zones is shown in table 64.

Table 64. Distribution of GPS-6 sections.

Experiment	Environmental Zone				Total
	Dry Freeze	Dry No-Freeze	Wet Freeze	Wet No-Freeze	
6A	22	6	18	12	58
6B&C	17	3	36	30	86
Total	39	9	54	42	144

Figures 116 and 117 shows the distribution of pavement sections according to their age at the time they were first profiled and at the last available profile date for GPS-6A and GPS-6B&C sections, respectively. For 6-B&C sections, the IRI value after the overlay was obtained within one year of overlay for 63 percent of sections, between 1 and 2 years after overlay for 30 percent of sections, and after two years for 7 percent of the sections. For 70 percent of the GPS-6B and C sections, the IRI prior to overlay was available.

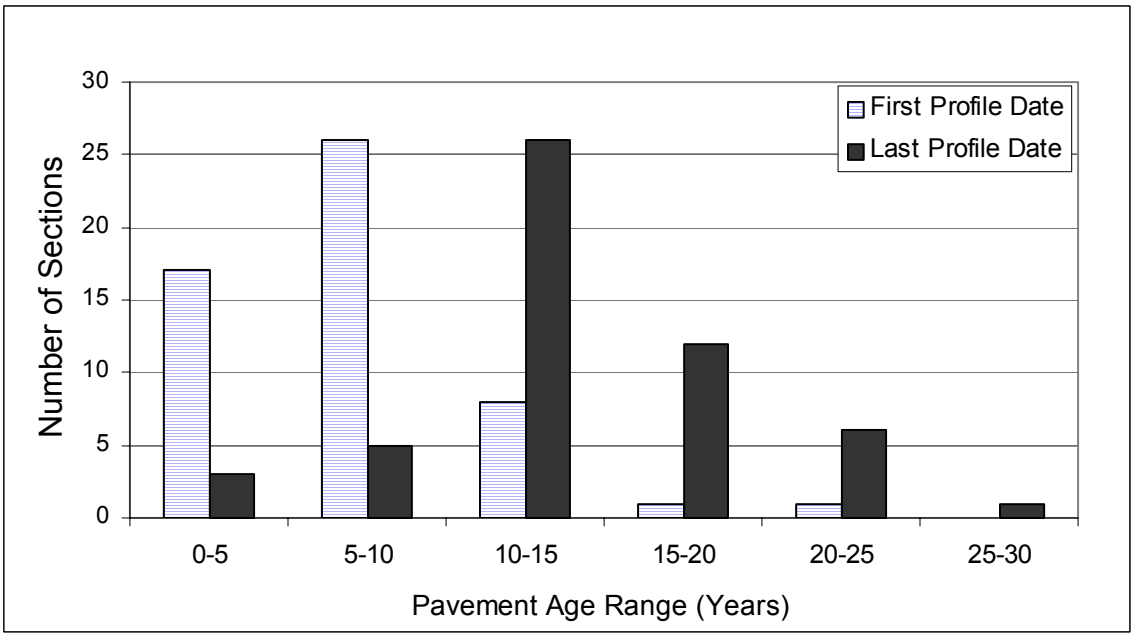

Figure 116. Distribution of GPS-6A sections according to age.

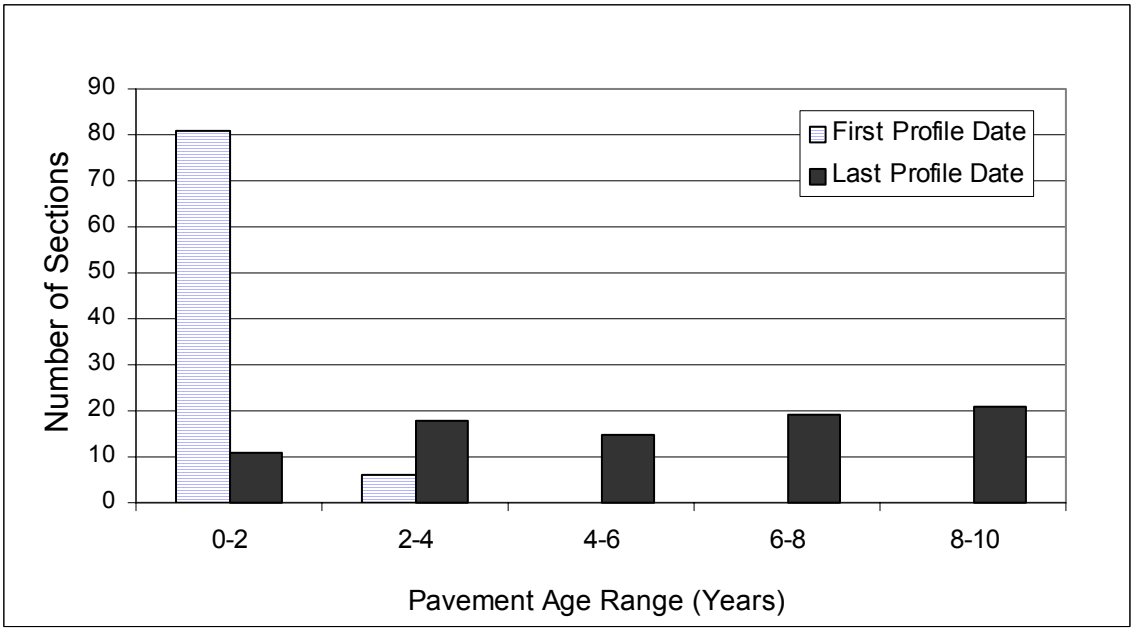

Figure 117. Distribution of GPS-6B&C sections according to age.

Relationship Between IRI Before and After Overlay

The IRI before and after overlay are available for 61 GPS-6B&C sections. Figure 118 shows the relationship between the IRI before and after overlay for these sections. This figure shows that many sections had low IRI values when they were overlaid.

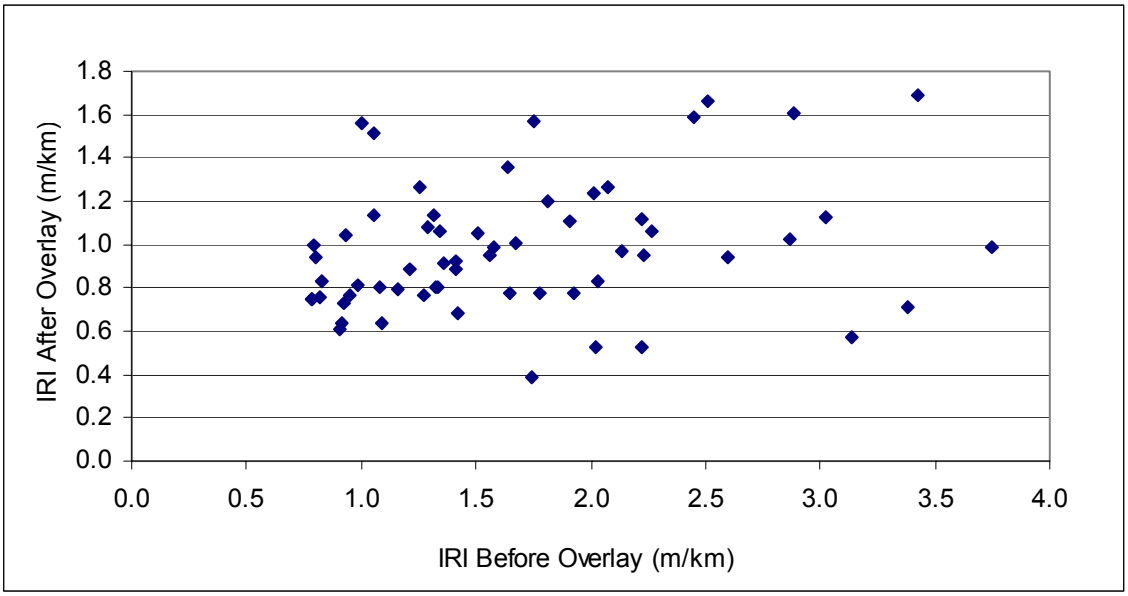

Figure 118. Relationship between IRI before and after overlay.

The frequency distribution of the IRI before overlay for GPS-6B&C sections is shown in table 65. Table 65 also shows the estimated PSI corresponding to the IRI ranges obtained from the relationship developed by Al-Omari and Darter (22). As shown in table 65, many of the pavements that were overlaid were still in a good condition from a roughness point of view, with 50 percent of the sections having a PSI greater than 3.5.

The overlay thickness was available for 41 sections for which the IRI before and after overlay was available. The overlay thicknesses ranged from 23 to 211 mm, with 32 percent of sections having a thickness between 23 and 38 mm, 46 percent of sections having a thickness between 38 and 76 mm, and the remaining 22 percent having a thickness greater than 76 mm.

Table 65. Frequency distribution of the IRI prior to overlay.

IRI Range (m/km)	Percent Sections (%)	Estimated PSI
< 1	20	> 3.9
1.0 - 1.5	30	3.5 - 3.9
1.5 - 2.0	20	3.1 - 3.5
2.0 - 2.5	15	2.7 - 3.1
> 2.5	15	< 2.7

Figure 119 shows the relationship between IRI before and after overlay separated according to the different overlay thickness ranges. Data in this figure shows that the IRI after overlay for most sections fall between the ranges of 0.8 to 1.2 m/km after the overlay.

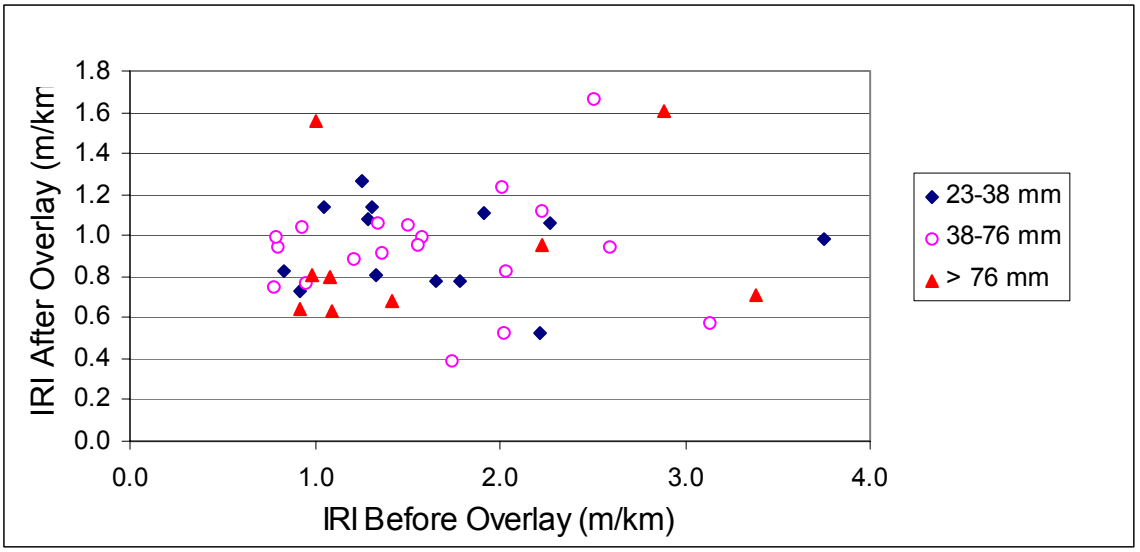

Figure 119. Relationship between IRI before and after overlay

The frequency distribution of IRI after overlay for the 61 sections that had IRI before and after overlay is shown in figure 120, while the cumulative frequency distribution is shown in figure 121. The cumulative frequency distribution shows that 80 percent of the sections achieved an IRI of less than 1.2 m/km after the overlay.

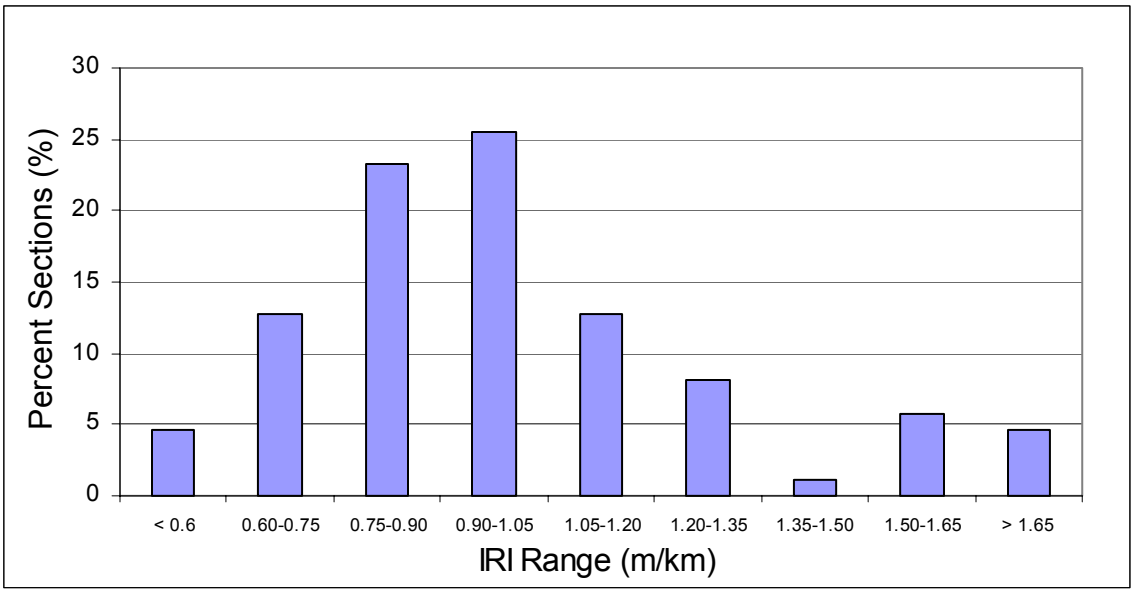

Figure 120. Frequency distribution of IRI after overlay.

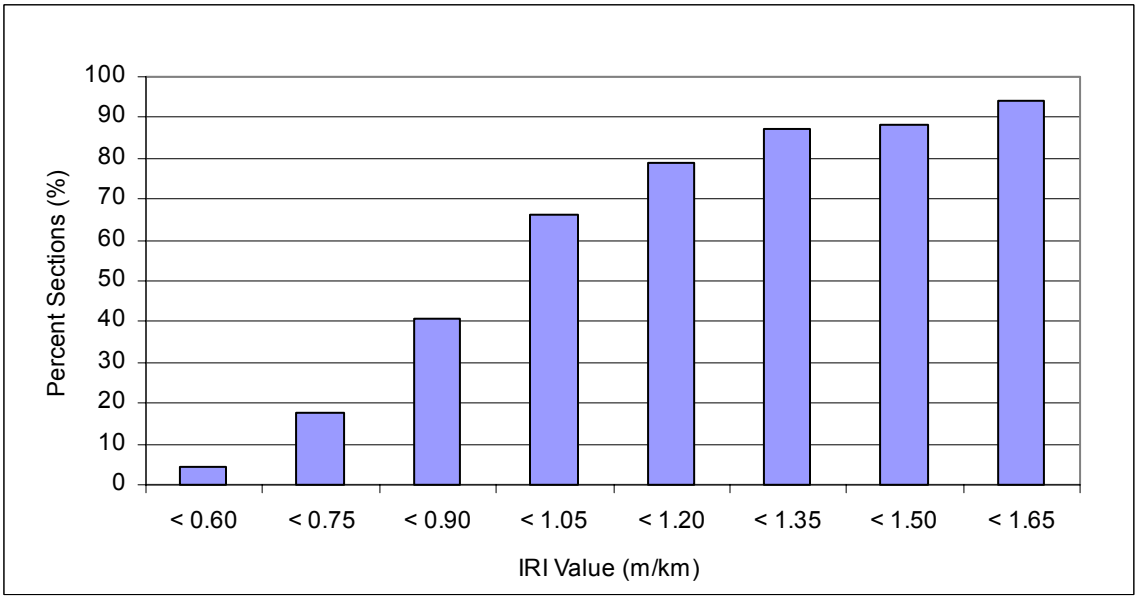

Figure 121. Cumulative frequency distribution of IRI after overlay.

Changes in IRI

A rate of change of IRI for each GPS-6 section was computed by performing a linear regression for the sections that had at least three time sequence IRI values. Table 66 presents the computed rate of change of IRI classified according to different ranges for GPS-6A and GPS-

6B&C experiments. The relationship between rate of change of IRI and average age of the pavement over the monitored period is shown in figure 122. As the data in this figure shows, the rate of increase of roughness is higher for older pavements. The rate of change of IRI was 0.02 m/km or less for 48 percent of the GPS-6B&C sections, compared to 29 percent of the GPS-6A sections. This is attributed to the lower age of the GPS-6B&C sections when compared to GPS-6A sections, as the rate of change of IRI increases as pavements get older.

Table 66. Rate of change of IRI.

Rate of Change of IRI (m/km/yr)	Percent Sections	
	GPS-6A	GPS-6A&C
< 0	6	14
0.00 - 0.02	23	33
0.02 - 0.04	15	20
0.04 - 0.06	15	9
0.06 - 0.08	7	3
0.08 - 0.10	7	5
0.10 - 0.12	6	2
0.12 - 0.14	4	3
0.14 - 0.16	6	0
> 0.16	11	11
Total	100	100

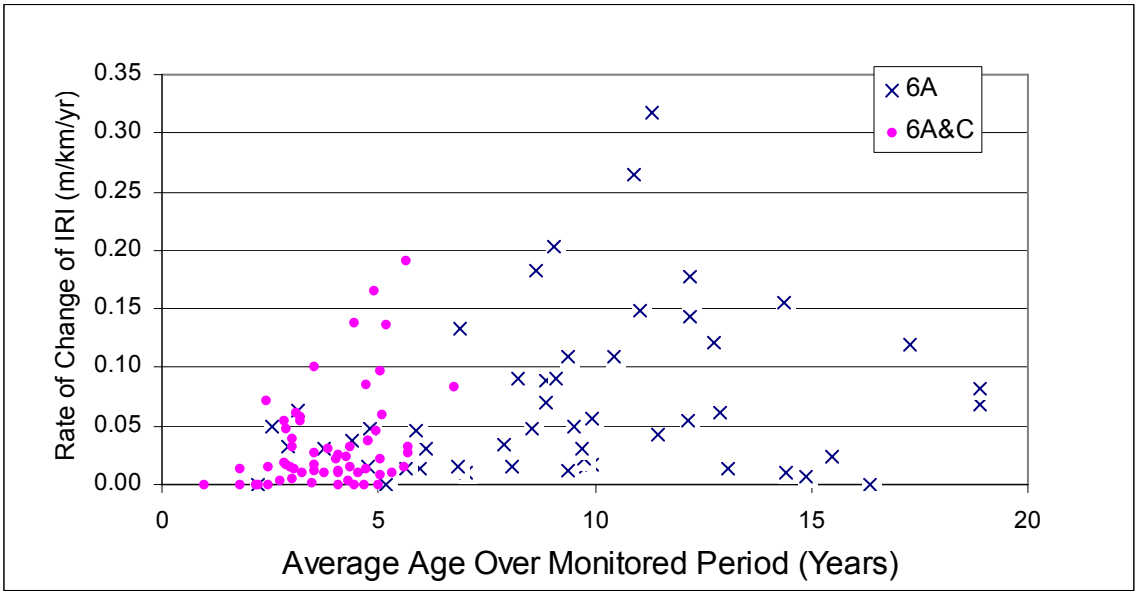

Figure 122. Relationship between pavement age and rate of change of roughness.

The time-sequence IRI plots for the GPS-6 sections classified according to the environmental zones are presented in figures 123 and 124 for GPS-6A and GPS-6B&C experiments, respectively. These plots show a general trend of a linear increase in roughness with some sections showing an exponential increase in roughness. The exponential increase in roughness for most sections appears to occur after 10 years of service. Generally, the IRI trends of GPS-6B sections show a parallel pattern in roughness progression.

Factors Affecting Changes in IRI

An analysis was performed to identify the factors that have an influence on the increase in IRI. Scatter plots between rate of increase in IRI and parameters that were selected for analysis (see table 5) were examined to observe data trends. This analysis was initially performed by considering all GPS-6 sections, and thereafter separate analyses were performed for individual environmental regions. There were only a few parameters for which a relationship was observed. The following are the results of this analysis.

Affect of IRI Before Overlay

The relationship between the rate of change of IRI and the IRI before overlay is shown in figure 125, for the GPS-6B&C sections for which the IRI prior to overlay was available. The sections that had a higher IRI prior to overlay are generally showing a higher increase in IRI.

Pavement Structure

The pavements that have a higher structural number are generally showing a lower rate of increase of IRI. The relationship between these two parameters is shown in figure 126. The rate of increase of IRI of an overlaid pavement will depend on the structural strength of the entire pavement section. An overlay that is placed on a pavement that has the structural capacity to carry the traffic will perform better than an overlay that is placed on a pavement that does not have the structural capacity to carry the traffic over the anticipated design life.

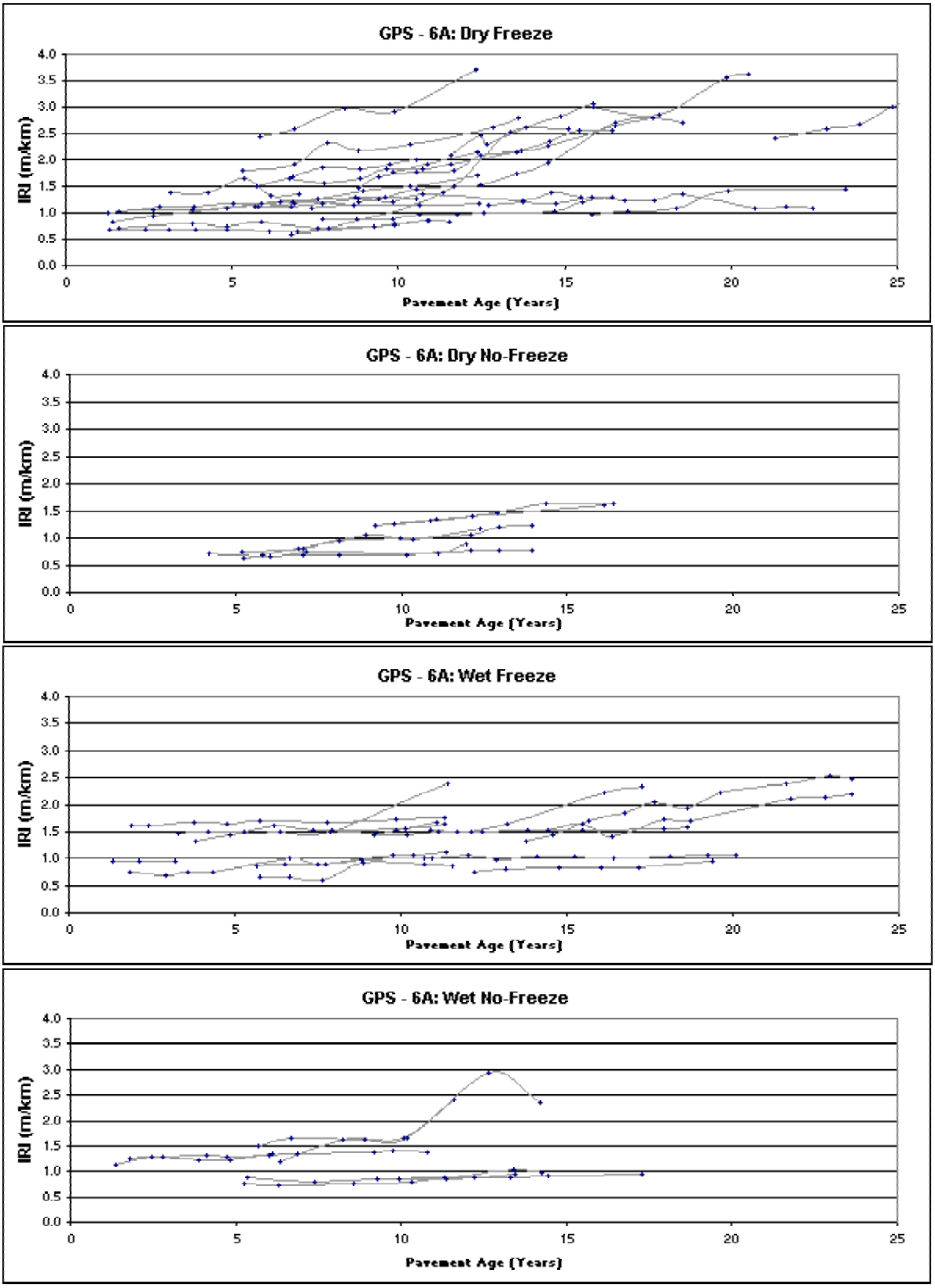

Figure 123. IRI trends for GPS-6A experiments

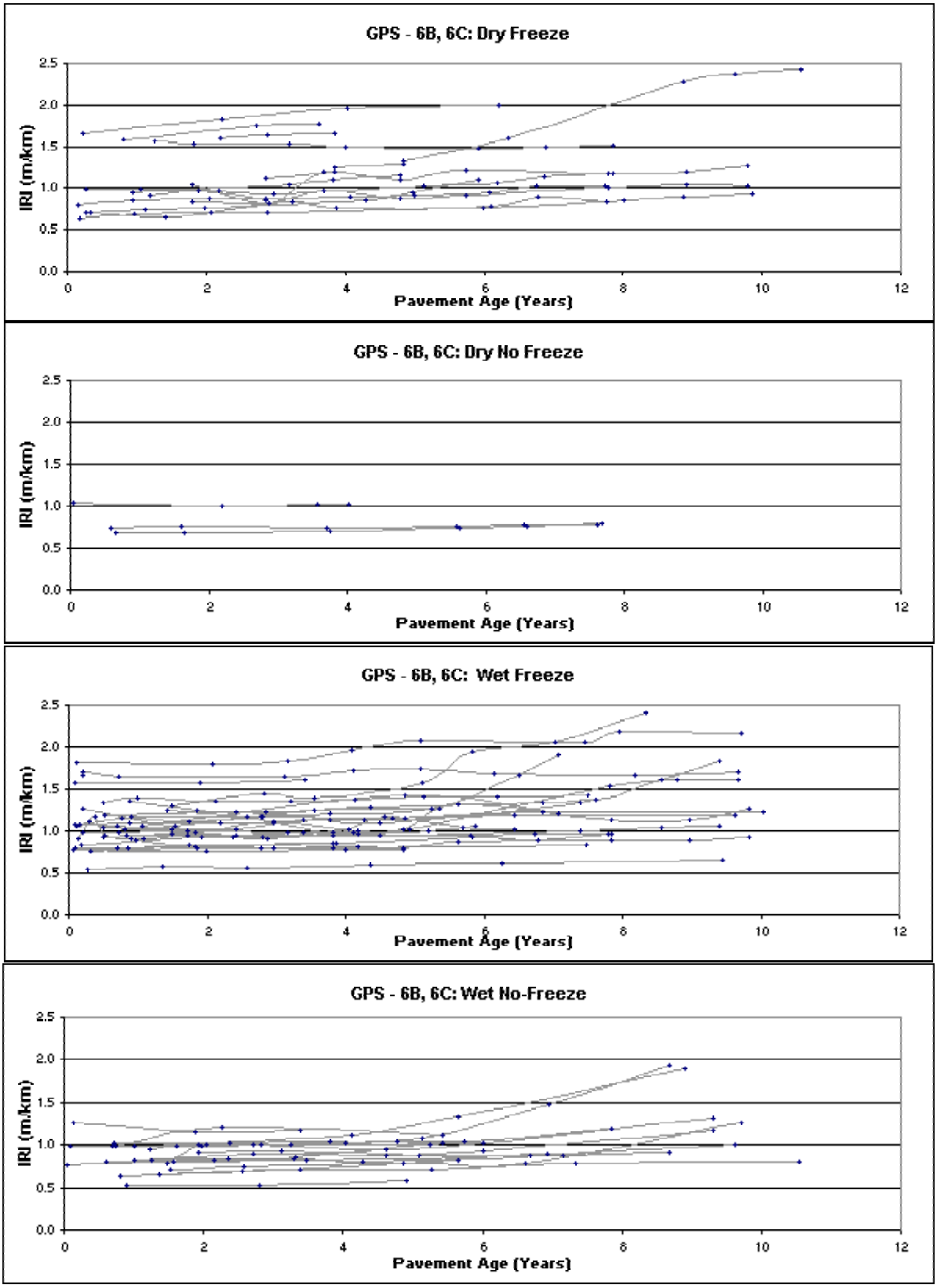

Figure 124 IRI trends for GPS-6B and –6C experiments

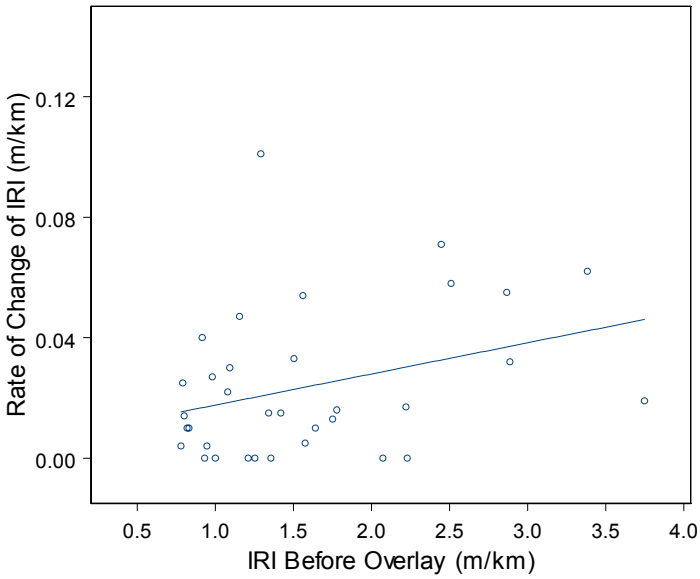

Figure 125. Relationship between rate of change of IRI and IRI prior to overlay.

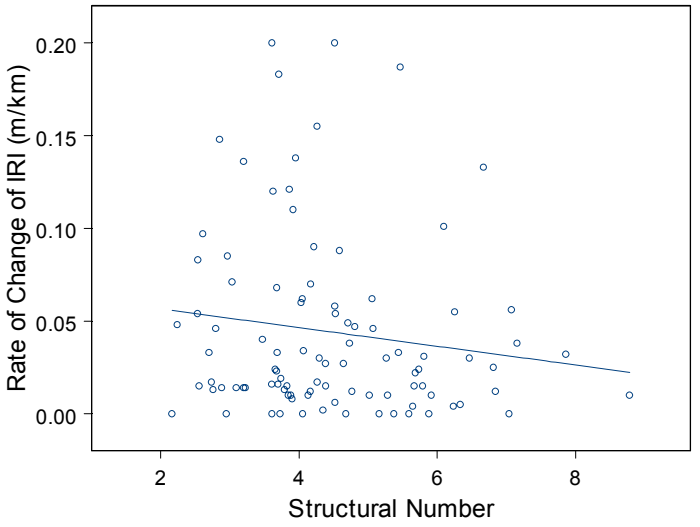

Figure 126. Relationship between rate of change of IRI and IRI prior to overlay.

AC Mix Design Properties

Some sections that had low AC bulk specific gravities and low air contents were showing high rates of increases of roughness. These observations indicate that deficiencies in the AC mix can lead to higher rates of increases of roughness.

Environmental Parameters

Overall a trend of a higher rates of increase of IRI were observed with higher freeze thaw cycles and higher number of days below 0° C. When all data were examined no trend was detected between the rate of change of IRI and mean temperature. However, when the data for each environmental zone was examined, it was observed that some sections in regions that had a high mean temperature showed high rates of increase of IRI. There are many regions in the wet freeze zones that have cold winters and warm summers. The AC mix must be adequately designed in these regions to withstand rutting that can occur during periods of warm temperature. Occurrence of rutting leads to higher increases in roughness. The relationship between the rate of increase of IRI and the mean temperature for the sections in the wet freeze zone is shown in figure 127.

Subgrade Parameters

A general trend of a higher increase in roughness with higher moisture content of subgrade, higher percent of material passing the No. 200 sieve in subgrade and higher plasticity index of subgrade was observed. Relationships between rate of increase of IRI and these parameters were strongest for the sections in the wet-freeze regions. Plots between rate of increase of IRI and moisture content in the subgrade and plasticity index of subgrade for the sections in the wet freeze zone are shown in figures 128 and 129, respectively. Higher moisture content in the subgrade and higher plasticity index of the subgrade in the wet freeze zone will increase the potential for frost heave and swelling of the subgrade.

Traffic

A trend of a higher rate of increase of IRI with higher cumulative traffic was generally observed.

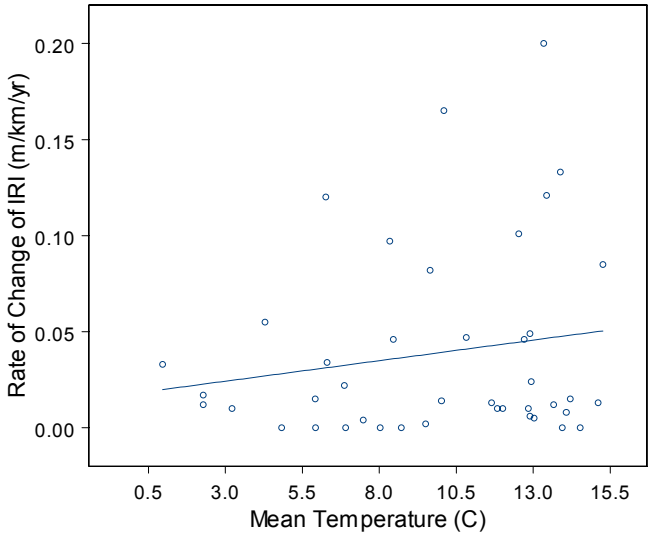

Figure 127. Relationship between rate of increase in IRI and mean annual ambient temperature – wet freeze zone

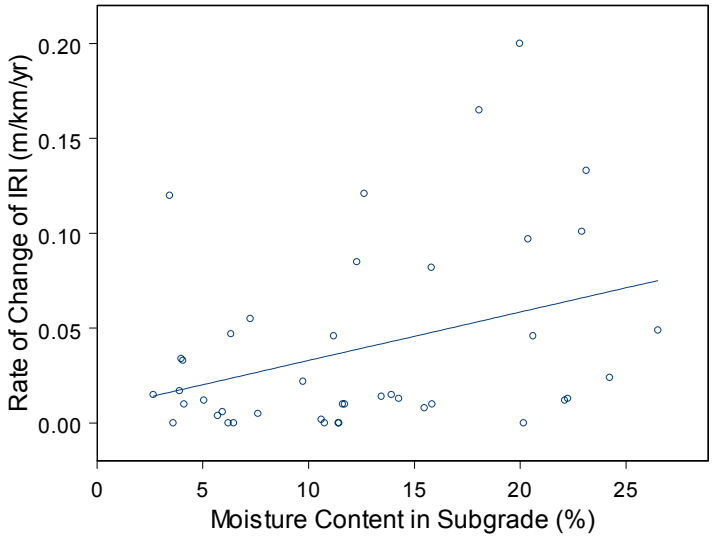

Figure 128. Relationship between rate of increase in IRI and subgrade moisture content – wet freeze zone

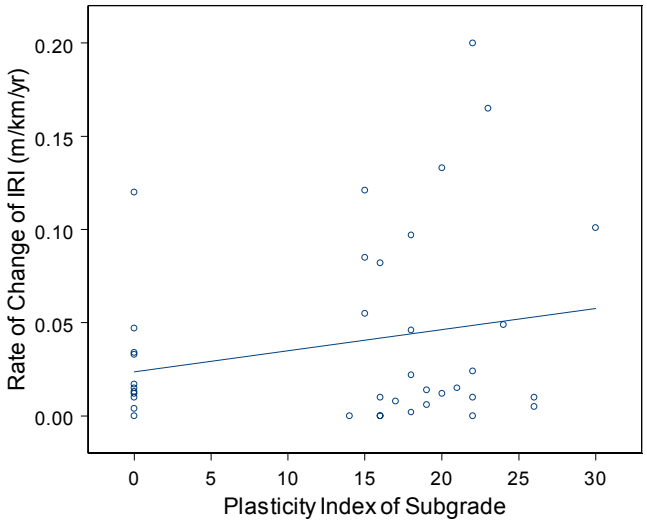

Figure 129. Relationship between rate of change in IRI and plasticity index of subgrade – wet freeze zone.

Models to Predict Roughness

Data from GPS-6B&C

The data available for the GPS-6B&C sections provides the best data to develop models to predict the increase in roughness for overlaid pavements. The initial IRI of these sections are known although the initial IRI was not generally obtained immediately after overlay. However, at 63 percent of the sections the IRI was obtained within one year of overlay, while for 30 percent of the sections the IRI was obtained between 1 and 2 years after overlay. The IRI before the overlay is available for 71 percent of the sections and overlay thickness is available for 65 percent of the sections. However, both IRI before overlay and overlay thickness are available for 48 percent of sections.

A mixed model analysis using the S-Plus software was carried out using the time-sequence data from the GPS-6B&C experiments. The following model was developed to predict the roughness:

$Log_e(IRI_t)$ = -0.06555 + 0.95559 (Log_e(IRIinit)) +0.04075(Time) + 0.01035(Time X IRIbefovl) – 00451(SN X Time)

Section effects standard deviation = 0.10, residual standard deviation = 0.08, groups = 54

sections = 54

where,

IRI_t = IRI at time t years, m/km

IRIinit = Initial IRI of pavement, m/km

Time = Time after construction, years
IRIbefovl = IRI before overlay, m/km
SN = Structural number of pavement

The model indicates that the roughness after overlay is affected by the roughness prior to overlay, and this verifies the relationship shown in figure 121 that showed there was a relationship between the rate of increase of IRI and the IRI prior to overlay.

Data from all GPS-6 sections

The distribution of the age of the GPS-6B&C sections at the last profile date is shown in figure 117, and shows that the age of the sections at the last profile date range from 2 to 10 years. The model to predict the development of roughness using data from this experiment reflect the increase in roughness that occur early in the life of the pavement. The roughness trends for GPS-6A sections that are shown in figure 123 indicate that a more rapid increase in roughness may occur in some sections after 10 years of service. Therefore, modeling was performed by combining the data from GPS-6B&C experiments with the data from GPS-6A experiment.

A major drawback in this modeling effort was the non-availability of IRI prior to overlay for the GPS-6A sections. The modeling performed for the GPS-6B&C sections showed that the IRI progression in pavements after overlay depends on the IRI prior to overlay. Another drawback was the non-availability of the initial IRI values for the GPS-6A sections, while this information was available for the GPS-6B&C sections. The initial IRI of the GPS-6A sections was backcasted by using a linear regression for each GPS-6A section, with the log of the IRI

used as the dependant variable. Using the logarithm of IRI as the dependant variable provided much more reasonable values for initial IRI than using the IRI as the dependant variable, as the log function is better able to handle the exponential nature of the increase of IRI. The backcasted initial IRI value for each section was compared with the time-sequence IRI plots of the section to assess the reasonableness of the backcasted IRI value. For cases where the backcasted IRI was deemed to be unreasonable, an initial IRI was assigned to the section. The IRI frequency distribution that was obtained for the GPS-6B&C sections (see figure 120) was used as a guide in assigning these values. Thereafter, a mixed model analysis on the combined data set of GPS-6A and GPS-6B&C sections was carried out. The following model was developed to predict roughness:

$Log_e(IRI_t) = -0.03578 + 0.86157(Log_e(IRIinit)) + 0.00011(Traffic/SN) + 0.00027(Time\ X\ Subg200) + 0.00017(Time\ X\ Freezethaw)$

Section effects standard deviation = 0.17, residual standard deviation = 0.10, groups = 128

Sections = 128

where,

IRI_t	=	IRI at time t years, m/km
IRIinit	=	Initial IRI of pavement, m/km
Traffic	=	Cumulative traffic, KESAL
Time	=	Time after construction, years
Subg200	=	Amount of material passing the No. 200 sieve, percent
Feezethaw	=	Freeze thaw cycles per year
SN	=	Structural number of pavement

Summary for GPS-6

For the overlaid pavements, no relationship between IRI before the overlay and the IRI immediately after the overlay was noted. The IRI after overlay for a majority of the sections fell between 0.8 and 1.2 m/km. Thin overlays were seen to be capable of reducing the roughness of a pavement substantially. For example, a 76 mm thick AC overlay was capable of achieving an IRI after overlay of 0.7 m/km for a pavement that had a roughness of 3.4 m/km prior to the overlay.

The IRI before overlay was seen to be a factor that affected the rate of roughness development in overlaid pavements. The sections that had an IRI greater than 2.0 m/km prior to overlay generally showed a higher rate of increase of IRI compared to sections that had an IRI of less than 2.0 m/km prior to overlay. Based on the roughness progression over the initial life of the pavement, the majority of pavements that had an IRI prior to overlay that were less than 2.0 m/km showed a rate of development of roughness that was less than 0.04 m/km. Placing overlays on pavements that have an IRI of less than 2.0 m/km appear to be an effective rehabilitation strategy in extending the life of the pavement. However, the section should have sufficient structural capacity to carry the anticipated traffic volume. Placement of the overlay will result in a smoother pavement for the traveling public. These pavements have generally shown a rate of development of roughness that was less than 0.04 m/km over the initial life of the overlay (5 to 10 years).

Higher rates of development of roughness in overlaid pavements were associated with low AC bulk specific gravities, high freezing indices, higher number of days below 0 °C, higher temperatures, higher subgrade moisture contents, higher fines content in subgrade, and higher plasticity index values for subgrade.

GPS-7: AC OVERLAY OF PCC PAVEMENTS

Test Sections

The GPS-7 experiment is the study of PCC pavements that are overlaid with AC. The GPS-7 sections can be divided into two categories: (a) sections that were established on in-service roadways and were at different periods in their service life when monitoring activities began at these sections, and (b) sections that were overlaid after the LTPP program was started, and monitoring activities at these sections began from the initial life of the overlay. The sections in the first category belong to the GPS-7A experiment, and the initial IRI of these pavements as well the IRI prior to rehabilitation are not available for these sections. The sections in the second

category belong to the GPS-7B experiment, and the initial IRI as well as the IRI prior to overlay are available for many sections. The distribution of the sections in the GPS-7 experiment classified according to the experiment type and the environmental zone is shown in table 67. As shown in table 67, most of the GPS-7 sections are located in the wet-freeze zone.

Table 67. Distribution of GPS-7 sections.

Experiment	Environmental Zone				Total
	Dry Freeze	Dry No-Freeze	Wet Freeze	Wet No-Freeze	
7A	2	0	24	9	35
7B	1	0	28	2	31
Total	3	0	52	11	66

The distribution of GPS-7A and –7B sections according to their age at the time they were first profiled and at the last available profile date is shown in figures 130 and 131, respectively.

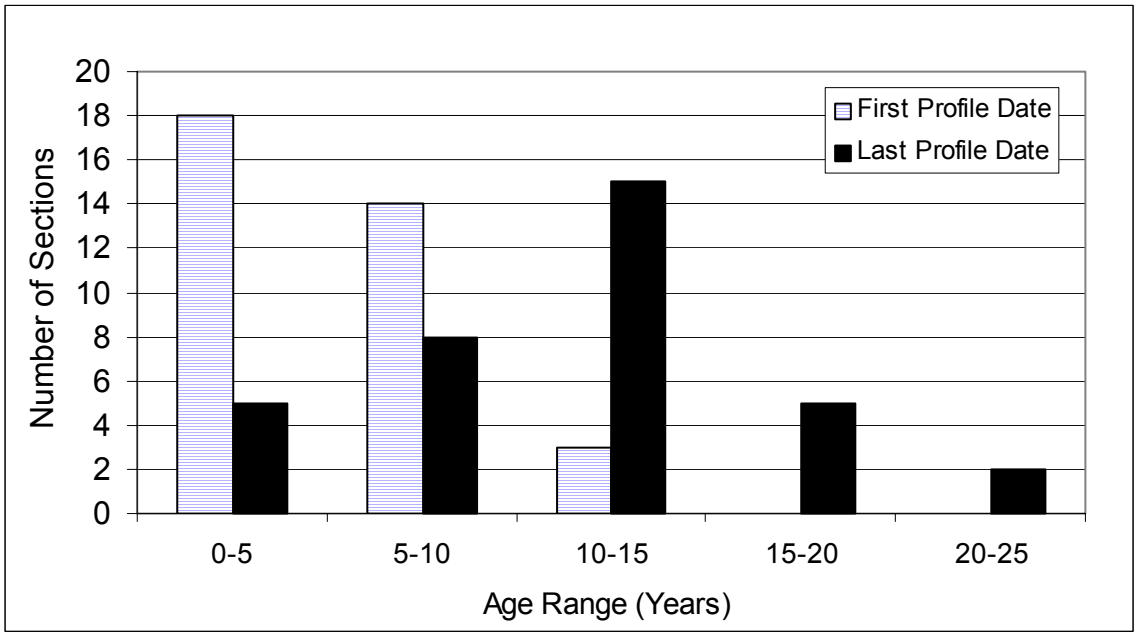

Figure 130. Distribution of age of GPS-7A sections according to age.

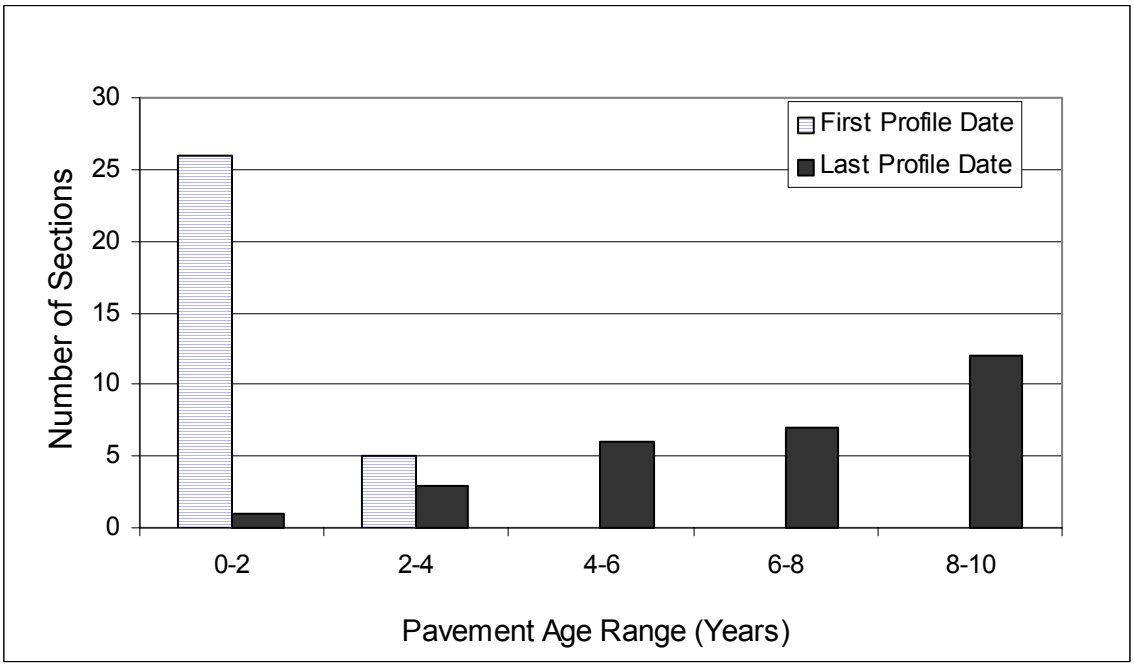

Figure 131. Distribution of GPS-7B sections according to age.

Relationship Between IRI Before and After Overlay

The IRI before and after overlay are available for 25 GPS-7B sections. Figure 132 shows the relationship between the IRI before and after overlay for these sections. The PCC pavement on which the overlay is placed includes JPC, JRC and CRCP. The distribution of the PCC pavement types is: JPC – 4 sections, JRC – 11 sections, and CRCP – 10 sections. As seen in figure 132, the IRI after overlay of the majority of the sections fell between 0.8 and 1.0 m/km, with seventy two percent of the sections having an IRI of less than 1.0 m/km after overlay. The data shown in figure 132 shows that some of the PCC sections that were overlaid had low IRI values, with 22 percent of sections having an IRI of less than 1.5 m/km, which is equivalent to a PSI greater than 3.5, at the time of overlay.

Changes in IRI

A rate of change of IRI for each GPS-7 section was computed by performing a linear regression for the sections that had at least three time sequence IRI values. Table 68 presents the

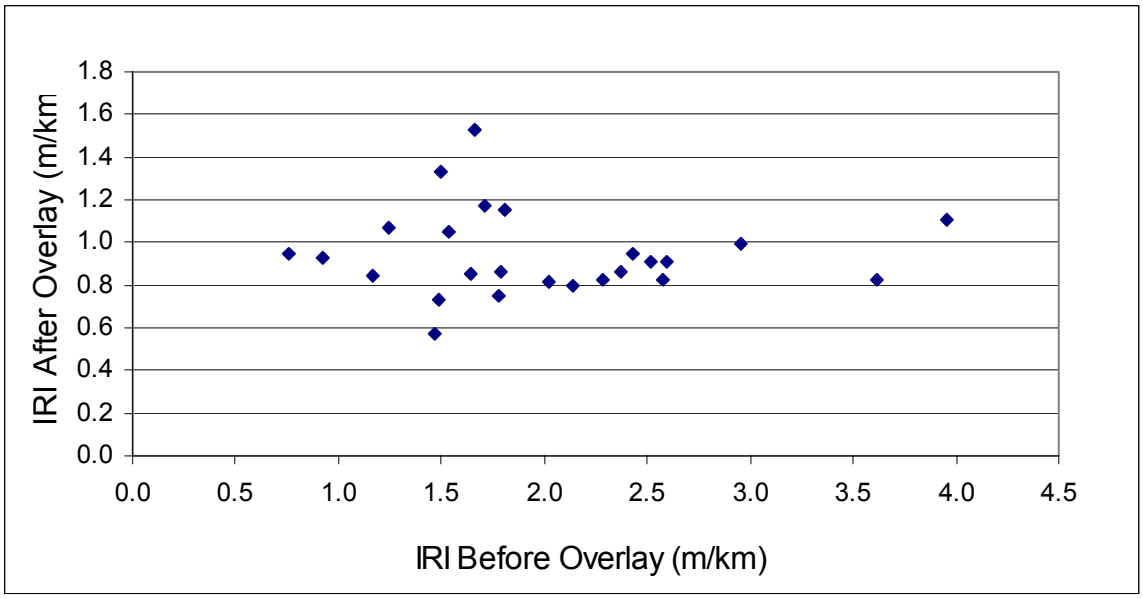

Figure 132. Relationship between IRI before and after overlay.

Table 68. Rate of change of IRI.

Rate of Change of IRI (m/km/yr)	Percent Sections	
	GPS-7A	GPS-7B
0.00 - 0.02	43	21
0.02 - 0.04	22	50
0.04 - 0.06	13	11
0.06 - 0.08	6	7
0.08 - 0.10	0	4
>0.10	16	7
Total	100	100

computed rate of change of IRI classified according to different ranges for GPS-7A and GPS-7B experiments.

The relationship between rate of change of IRI and average age of the pavement over the monitored period is shown in figure 133. A few sections are showing high rates of increase of IRI. However, a majority of the sections are showing a rate of increase of IRI that is less than

0.05 m/km/yr. There is no clear relationship between the rate of change of IRI and the average age of the pavement over the monitored period.

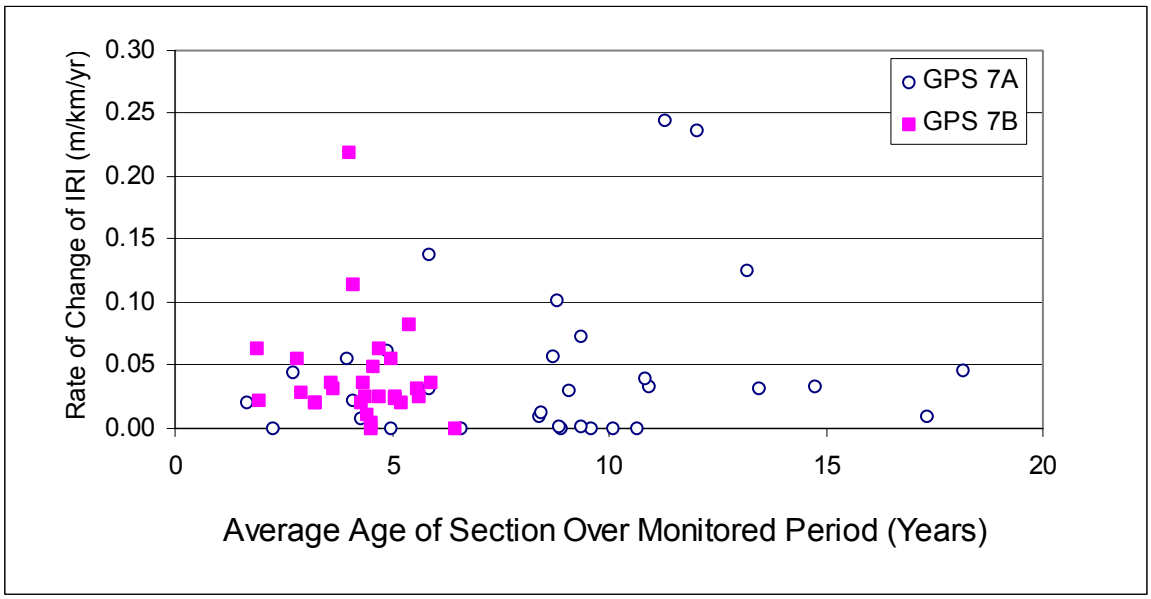

Figure 133. Relationship between pavement age and rate of change of roughness.

The time-sequence IRI values for the GPS-7A and –7B sections are shown in figures 134 and 135, respectively. Note that the x-axis and y-axis scales are different in these two figures. Some of the GPS-7A sections are showing large variations in the time-sequence IRI values, with only a very few GPS-7B sections exhibiting such a behavior. The GPS-7B sections are generally showing a linear increase in IRI, however the trend in increase in IRI is variable between the sections for the GPS-7A sections. Some of the GPS-7A sections are showing a linear increase in IRI, some showing an exponential increases in IRI, with others showing varying IRI between the years. The GPS-7B sections are generally showing a parallel pattern in roughness progression between the sections.

Factors Affecting Changes in IRI

The increase in IRI of the AC overlay will be influenced by the behavior of the PCC slab. As indicated previously, the AC overlays on PCC pavements were placed on JPC, JRC and

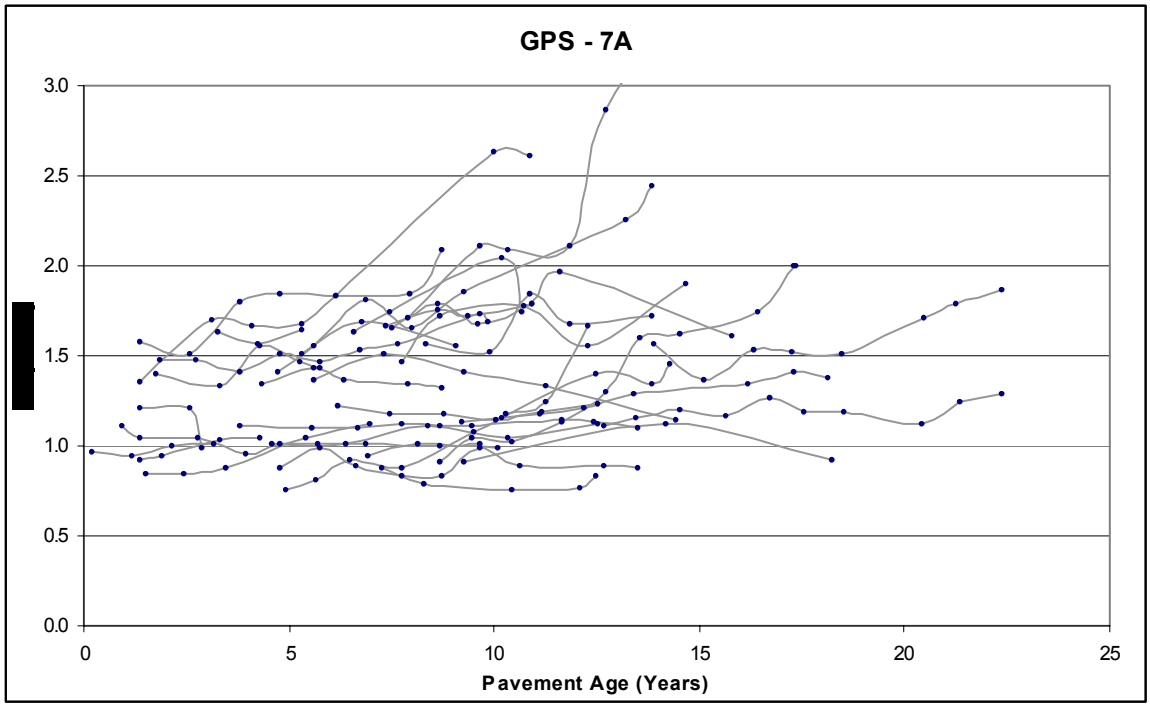

Figure 134. Time sequence IRI values for GPS-7A sections.

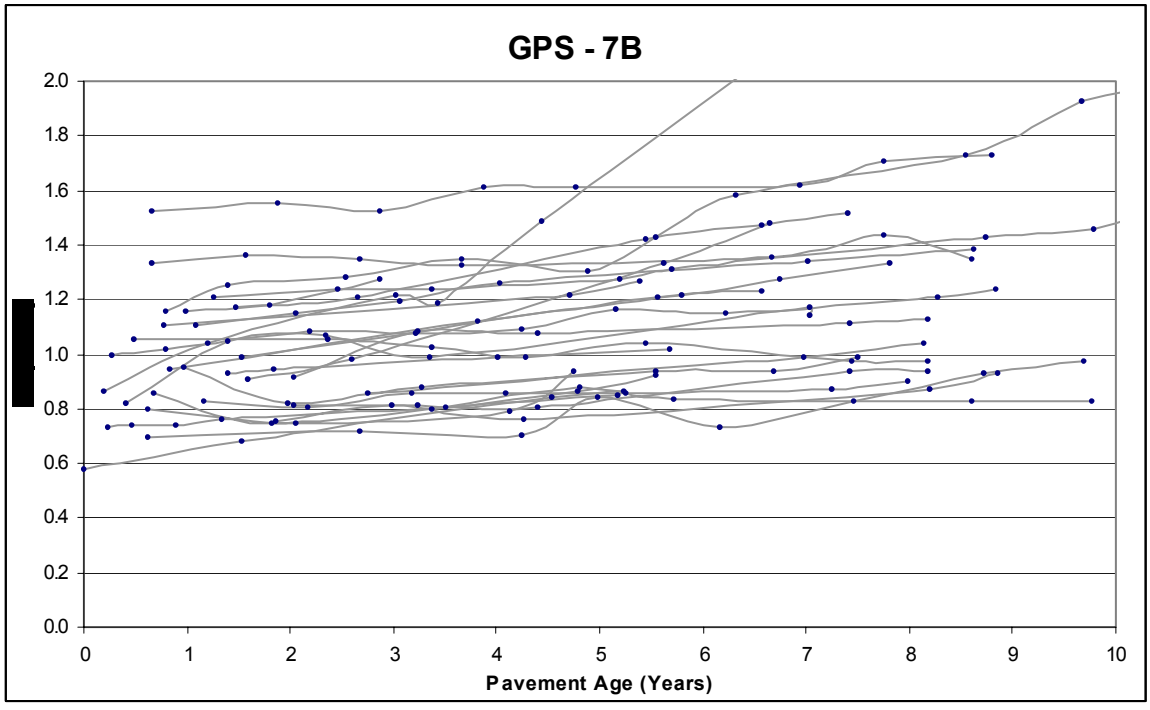

Figure 135. Time sequence IRI values for GPS-7B sections.

CRCP pavement. The factors that contribute to the increase in roughness of each of these pavement types is expected to contribute to the increase in roughness of the AC overlay. For example, it was shown that for JPC pavements, pavements with dowels had lower rates of increase in roughness than pavements without dowels. Therefore, AC overlays placed on PCC pavements that have dowels are expected to perform better than AC overlays that are placed on JPC pavements without dowels. However, because detailed information on the PCC pavements were not available for many GPS-7A sections, the behavior of the overlays classified according to the PCC pavement type could not be performed.

An analysis was performed to identify the factors that have an influence on the increase in IRI. Scatter plots between rate of increase in IRI and parameters that were selected for analysis were examined to observe data trends. Only a few weak relationships between the rate of change of IRI and the parameters considered in the analysis (see table 5) were found. The following are the results of this study.

Affect of IRI Before Overlay

The relationship between the rate of change of IRI and the IRI before overlay is shown in figure 136. There was no clear relationship between these two parameters.

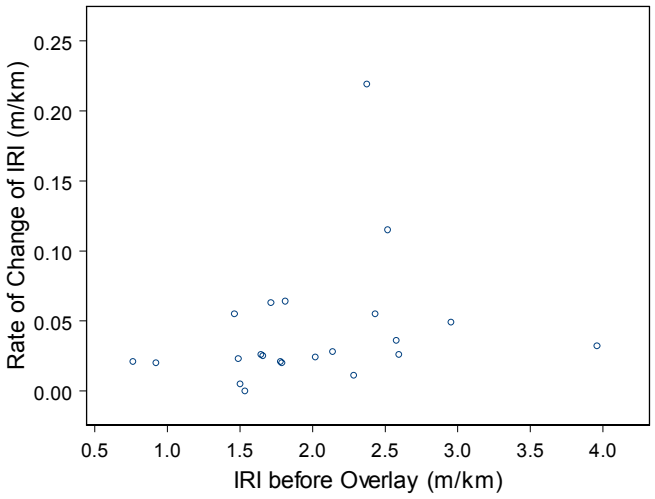

Figure 136. Relationship between rate of change of IRI and IRI before overlay.

Environmental Parameters

No relationships between rate of change of IRI and environmental parameters were observed, except that some sections in the freezing regions that showed a high rate of increase of IRI. The relationship between the rate of increase of IRI and the freezing index is shown in figure 137.

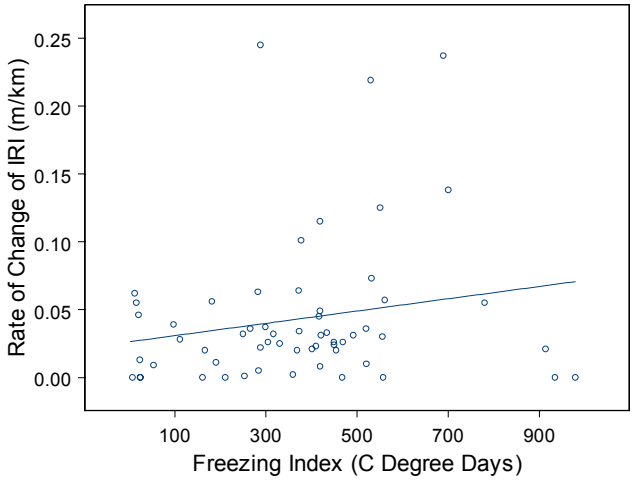

Figure 137. Relationship between rate of change of IRI and freezing index.

PCC Properties

A trend of a higher rate of increase of IRI with high values for PCC elastic modulus was observed. High rates of increase of IRI were observed for several sections that had a PCC elastic modulus of over 35,000 Mpa. The relationship between the rate of change of IRI and PCC elastic modulus is shown in figure 138.

Models to Predict Roughness

Data from GPS-7B Sections

There are 31 GPS-7B sections in the LTPP database, and the initial IRI of these sections have been obtained within two years of construction for most of the sections. The IRI prior to overlay is available for 25 of these sections. A mixed model analysis using the S-Plus software

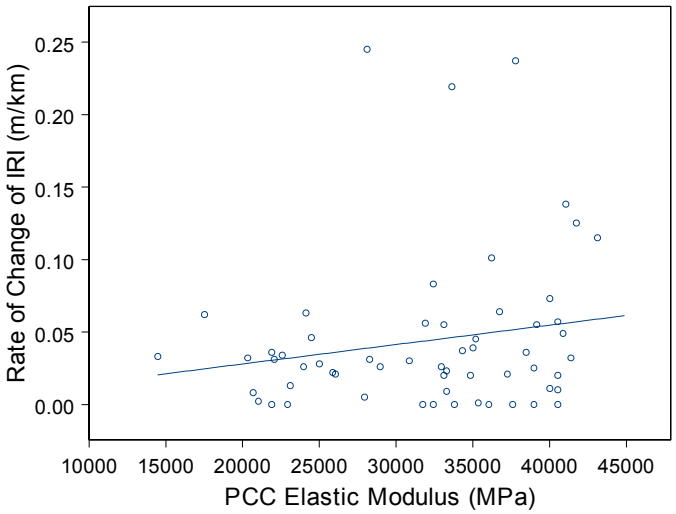

Figure 138. Relationship between rate of change of IRI and PCC elastic modulus.

was carried out using the time-sequence data from the GPS-7B experiment. The following model was developed to predict the roughness:

$Log_e(IRI_t) = -0.04368 + 0.87096\ (Log_e(IRIinit)) + 0.02822(Time) + 0.0000108(Traffic)$

Section effects standard deviation = 0.13, residual standard deviation = 0.09, groups = 30

where,

IRI_t = IRI at time t years, m/km

IRIinit = Initial IRI of pavement, m/km

Time = Time after construction, years

Traffic = Cumulative traffic after construction, KESAL

Data from all GPS-7 sections

The distribution of the age of the GPS-7B sections at the last profile date is shown in figure 131, and shows that the age of the sections at the last profile date range from 2 to 10 years.

The model to predict the development of roughness using data from this experiment reflects the increase in roughness that occurs early in the life of the pavement. The roughness trends for GPS-7A sections that are shown in figure 120 indicate that a more rapid increase in roughness may occur in some sections after 10 years of service. Therefore, a modeling effort was carried out by combining the data from GPS-7B experiments with the data from GPS-7A experiment.

Although the initial IRI value of the GPS-7B sections are known, the initial IRI value of GPS-7A sections are not known. The initial IRI of the GPS-7A sections was obtained by backcasting the time-sequence IRI values to obtain the initial IRI of the section. This was done by performing a linear regression on the on each section that had three or more time-sequence IRI values. The backcasted initial IRI value for each section was compared with the time-sequence IRI plots of the section to assess the reasonableness of the backcasted IRI value. For cases where the backcasted IRI was deemed to be unreasonable, an initial IRI was assigned to the section. The initial IRI values that were obtained in the GPS-7B sections were used as a guide when assigning the initial IRI. The following model was developed to predict roughness:

$$Log_e(IRI_t) = -0.03717 + 0.84441(Log_e(IRIinit)) + 0.01914(Time) + 0.00002(Time\ X\ FZI)$$

Section effects standard deviation = 0.17, residual standard deviation = 0.10, groups = 62

where,

IRI_t = IRI at time t years, m/km

IRIinit = Initial IRI of pavement, m/km

Time = Time after construction, years

FZI = Freezing Index, degree days (C)

Summary for GPS-7

The PCC pavement types on which the AC overlay has been placed included JPC pavements (with and without dowels), JRCP pavements and CRCP pavements. The roughness

progression for the different PCC pavement types is expected to be different. However, sufficient sections were not available to perform separate analysis for each of these PCC pavement types.

There was no relationship between IRI before the overlay and IRI immediately after overlay. The IRI after overlay for a majority of the sections fell between 0.8 and 1.0 m/km. The roughness progression in the AC overlays did not depend on the IRI prior to overlay. The majority of the overlaid pavements were showing a rate of increase of IRI that was less than 0.04 m/km. The factors that were influencing the roughness development of the PCC pavement are expected to control the roughness development in the AC overlay. An example of this is the high rates of increase of roughness that was observed for overlays that were placed on PCC sections that had high PCC elastic modulus.

DISCUSSION OF RESULTS

In the study of overlaid pavements, performance of AC overlays on AC pavements and AC overlays of PCC pavements were studied.

For AC overlays placed on AC pavements, no relationship between IRI before the overlay and after IRI immediately after the overlay was noted. The IRI after overlay for a majority of the sections fell between 0.8 and 1.2 m/km. Thin overlays were seen to be capable of reducing the roughness of a pavement by a large amount. For example, a 76 mm thick AC overlay was capable of achieving an IRI after overlay of 0.7 m/km, for a pavement that had a roughness of 3.4 m/km prior to the overlay.

The IRI before the overlay was seen to be a factor that affected the IRI development of the overlaid pavement. The sections that had an IRI greater than 2.0 m/km prior to overlay generally showed higher rates of increase of IRI compared to sections that had an IRI of less than 2.0 m/km prior to overlay. Based on the roughness progression over the initial life of the pavement, the majority of pavements that had an IRI prior to overlay that were less than 2.0 m/km showed a rate of development of roughness that was less than 0.04 m/km. Placing overlays on pavements that have an IRI of less than 2.0 m/km appears to be an effective rehabilitation

strategy in extending the life of the pavement. Overlays placed on such pavements have generally shown a rate of development of roughness that was less than 0.04 m/km over the initial life of the overlay (5 to 10 years). However, the section should have sufficient structural capacity to carry the anticipated traffic volume.

The PCC pavement types on which the AC overlay have been placed included JPC pavements (with and without dowels), JRCP pavements, and CRCP pavements. The roughness progression for the different PCC pavement types is expected to be different. However, sufficient information on the PCC pavement type prior to overlay was not available to perform separate analysis for each of these PCC pavement types.

There was no relationship between the IRI before overlay and IRI immediately after overlay for the PCC pavements. The IRI after overlay for a majority of the sections fell between 0.8 and 1.0 m/km. The roughness progression in the overlays did not depend on the IRI prior to overlay. The majority of the overlaid pavements were showing a rate of increase of IRI that was less than 0.04 m/km.

CHAPTER 9
CONCLUSIONS AND RECOMMENDATIONS FOR FUTURE RESEARCH

CONCLUSIONS

New AC Pavements: SPS-1

The data from SPS-1 projects indicated the average early-age IRI of the 100 mm thick AC surfaces to be 0.88 m/km, with a standard deviation of 0.21 m/km. For the 175 mm thick AC, the average early-age IRI was 0.82 m/km, with a standard deviation of 0.18 m/km. An IRI value of less than 0.8 m/km was achieved on 40 percent of the sections that received a 100 mm AC surface and 55 percent of the sections that received a 175 mm AC surface. An IRI of less than 1.0 m/km was obtained on 75 percent of the sections that received a 100 mm AC surface and 85 percent of the sections that received a 175 mm AC surface. The AC surfaces in SPS-1 projects have been placed on three different types of bases: DGAB, ATB, and PATB. The average early-age IRI of sections placed on DGAB, ATB and PATB surfaces were 0.94 m/km, 0.82 m/km, and 0.84 m/km. Increases in IRI have been observed at most sections in some projects at a relatively young pavement age. The cause for the increase in IRI at these projects is attributed to pavement distress such as transverse cracking, longitudinal cracking in the wheel path, fatigue cracking and rutting.

New PCC Pavements: SPS-2

The data from the SPS-2 projects indicated the average early-age IRI of the 200 mm thick PCC surfaces to be 1.27 m/km, with a standard deviation of 0.28 m/km. For the 275 mm thick PCC, the average IRI was 1.30 m/km, with a standard deviation of 0.30 m/km. The PCC surface in the SPS-2 projects has been placed on three different base types: DGAB, LCB and PATB. The average early-age IRI values for PCC pavements placed on DGAB, LCB, and PATB were 1.27 m/km, 1.40 m/km, and 1.25 m/km. The highest early-age IRI was obtained for PCC surfaces placed on LCB. Most of the sections in SPS-2 projects have not shown much change in

roughness. However, an evaluation of the sections did show changes in roughness at some sections and the following trends were observed: (1) some sections in some of the projects showed high increases in roughness, (2) some sections in some projects showed a reduction in roughness, (3) increase in roughness for a specific pavement design section was observed across all projects, and (4) some sections in some projects showed very high variability in roughness between the years. Most of these cases occurred on sections that had a 200 mm thick PCC slab. An investigation of the profile data at these sections found that the changes in roughness at these sections were related to changes in curvature of PCC slabs. In some cases, the changes in roughness were due to temperature associated curling of the slabs. But in many cases, the curling or warping had occurred over time and was not related to temperature effects. The section that showed an increase in roughness (greater than 10%) across all projects was the section with a 200 mm thick PCC surface, that had a slab width of 3.66 m, a 14-day flexural strength of 3.8 Mpa, and was resting on a DGAB surface. The changes in roughness that occurred at this section were related to changes in the curvature of the slab.

Rehabilitation of AC Pavements: SPS-5

A statistical analysis of data from all SPS-5 projects showed the IRI after overlay did not depend on the pre-rehabilitation IRI, overlay thickness, if milling was performed or not prior to overlay, or the type of AC. Generally, for each SPS-5 project, the IRI after overlay of all test sections in the project fell within a relatively narrow band of IRI values, irrespective of the IRI prior to overlay of the test sections. Statistical analysis of the data from the projects that had an IRI of greater than 1.5 m/km indicated that milling prior to placing an overlay results in a smoother pavement. For projects having an IRI greater than 1.5 m/km, milling prior to placing an overlay resulted in a pavement that on average had an IRI value that was 0.07 m/km lower than non-milled section. For sections that had an IRI of less than 1.5 m/km prior to overlay, the IRI after overlay was less than 1.0 m/km for 80 percent of the sections. For sections that had an IRI of over 1.5 m/km prior to overlay, the IRI after overlay for most sections fell between 0.8 and 1.2 m/km. It was seen that 50 mm overlays were capable of achieving a large reduction in roughness, with some of the 50 mm overlays reducing the IRI of the pavement from 2.5 m/km to 1.0 m/km.

The progression of roughness over time of the overlaid pavements was found to depend on the pre-overlay IRI of the section and the overlay thickness. When all projects were considered, the following average rate of increase of roughness were observed: 50 mm overlays with milling prior to overlay – 0.042 m/km/year, 50 mm overlays without milling prior to overlay – 0.045 m/km/year, 125 mm overlays with milling prior to overlay – 0.025 m/km/year, 125 mm overlays without milling prior to overlay – 0.028 m/km/year. These results as well as observation of time-sequence data for the SPS-5 projects indicate that for a specific overlay thickness, a lower initial IRI results in a lower IRI over the service life of the pavement

Rehabilitation of PCC Pavements: SPS-6

In some of the sections where joint sealing, crack sealing, partial depth patching, and full depth patching were performed, the roughness increased after repairs. These results show that if repairs are not performed correctly in PCC pavements, they can result in an increase in roughness of the pavement. A statistical analysis indicated that applying the following treatments on a PCC pavement result in similar IRI levels: (1) minimum restoration of existing pavement with a 100 mm AC overlay (section 3), (2) minimum restoration of existing surface with a 100 mm AC surface, with sawing and sealing over joints (section 4), (3) Intensive restoration of existing surface that includes diamond grinding (section 5), (4) Intensive restoration of existing surface followed by a 100 mm AC overlay (section 6), (5) crack/break seat of PCC with a 100 mm AC surface (section 7), (6) crack/break seat of PCC with a 200 mm AC overlay (section 8). An investigation of the IRI before and after rehabilitation for a specific SPS-6 project indicated that the IRI after rehabilitation for sections 3 through 8 all fell within a relatively narrow band. The analysis indicated the following average values for rate of increase of roughness: (1) Section 3, minimum restoration and 100 mm overlay: 0.058 m/km/year, (2) Section 4, minimum restoration and 100 mm overlay with sawing and sealing of joints: 0.057 m/km/year, (3) Section 5, intensive restoration with diamond grinding: 0.200 m/km/year, (4) Section 6, intensive restoration with 100 mm overlay: 0.054 m/km/year, (5) Section 7, crack/break seat with 100 mm AC surface: 0.032 m/km/year, and (6) Section 8, crack/break seat with 200 mm AC surface: 0.013 m/km/year. The section that received diamond grinding showed the highest rate of

increase of roughness, and a statistical analysis indicated the rate of increase of IRI at this section was statistically different from the other sections. Generally, diamond ground sections that had higher values of IRI prior to overlay are showing a higher rate of increase of IRI.

Factors Affecting Roughness Progression of AC Pavements

The two AC pavement types analyzed were AC pavements on granular base (GPS-1) and AC pavements on stabilized base (GPS-2). The effect of parameters presented in table 69 on the roughness level of these two pavement types was evaluated.

Table 69. Parameters evaluated for AC pavements.

Parameter
Surface Thickness
Base Thickness
Total Pavement Thickness
Structural Number
Overburden Pressure
AC Bulk Specific Gravity
AC Air Voids
Asphalt Content
Annual Precipitation
Intense Precipitation Days per year
Annual Wet Days
Mean Temperature
Days with Temperature > 32 °C, per year
Days with Temperature < 0 °C, per year
Annual Freezing Index
Freeze Thaw Cycles per Year
Plasticity Index Subgrade
Plastic Limit Subgrade
Moisture Content Subgrade
Silt content in Subgrade
Clay Content in Subgrade
Percent passing No. 200 sieve, Subgrade
Moisture Content Base
Percent Passing No. 200 sieve, Base
Traffic

The results of the evaluation are presented separately for each of the two pavement types. It should be noted, if a pavement is designed "correctly" for the subgrade and climatic conditions at a site, the effect of these factors on roughness of the pavement might not be seen. If a pavement is not designed to take into account the site conditions, the climatic and subgrade parameters may be seen to be affecting the roughness. Therefore, it is important to note because a certain parameter did not show up to be affecting roughness in the analysis, it does not mean that parameter does not have an affect on roughness. A good example is traffic, where no relationship was found between roughness and traffic level. This is most likely because the pavement sections were deigned for the anticipated traffic, and therefore such a relationship was not seen.

AC Pavements on Granular Base: GPS-1

When all GPS-1 sections were evaluated, the factors that had the strongest relationship to the rate of change of roughness were percent material in base passing the No. 200 sieve, freezing index, plasticity index of subgrade, and pavement age. Table 70 presents the factors that were seen to be affecting the roughness progression of GPS-1 sections in each of the environmental zones.

AC Pavements on Stabilized Base: GPS-2

The types of bases that are used in the GPS-2 experiment can be broadly divided into asphalt stabilized or cement stabilized. However, a variety of material types have been used for each of the stabilized base types. For asphalt stabilized bases, the material types that have been used are: hot mix AC, asphalt treated mixtures, sand asphalt, mixed in place cold-laid mixtures, and central plant mix cold-laid mixtures. For cement stabilized bases the material types that have been used are cement aggregate mixtures, soil cement and lean concrete. For each stabilized base type, the properties of the different material types that have been used as base material are very different from each other. Therefore, in order to accurately analyze the data, each of the different

base types in the asphalt and cement stabilized base types should be analyzed separately. However, sufficient sections were not available to do this type of analysis. Generally, only a few causes that contribute to increase in roughness could be found for GPS-2 sections. This may be because of the variety of base types that have been used. A higher rate of increase of IRI was noted for sections with high AC void ratios. For sections on cement treated bases, a high rate of increase of IRI was observed for sections in warmer climates.

Table 70. Factors affecting roughness progression in AC pavements.

Environmental Zone	Parameter	Effect of Higher Value of Parameter on Roughness
Dry Freeze	Annual precipitation	Increases
	Freeze index	Increases
	Plasticity index of subgrade	Increases
	Fines content in base	Increases
Dry No-Freeze	Mean annual temperature	Increases
	Days per year > 32° C	Increases
	Plastic limit subgrade	Increases
Wet Freeze	Total pavement thickness	Decreases
	Asphalt content	Note 1
	Annual precipitation	Note 2
	Wet days per year	Note 3
	Freeze index	Increases
	Fines content in base	Increases
	Silt content in coarse grained subgrade	Note 4
Wet No-Freeze	Fines content in base	Increases
	Fines content in subgrade	Increases
	Moisture content of subgrade	Increases
	Plasticity index of subgrade	Increases
	Days per year > 32° C	Increases

Note 1: Some sections with low AC content had higher roughness
Note 2: Sections with lower annual precipitation had higher roughness
Note 3 : Sections with lower wet days had higher roughness
Note 4: Sections on coarse grained subgrade with silt contents 5-15% had high roughness

Factors Affecting Roughness Progression of PCC Pavements

The three pavement types analyzed were, JPC (GPS-3), JRCP (GPS-4), and CRCP (GPS-5). The effect of parameters presented in table 71on the roughness level of these three pavement types was evaluated.

Table 71. Parameters evaluated for PCC pavements.

Parameter
Surface Thickness
Base Thickness
Total Pavement Thickness
Structural Number
Overburden Pressure
Annual Precipitation
Intense Precipitation Days per year
Annual Wet Days
Mean Temperature
Days with Temperature > 32 °C, per year
Days with Temperature < 0 °C, per year
Annual Freezing Index
Freeze Thaw Cycles per Year
Plasticity Index Subgrade
Plastic Limit Subgrade
Moisture Content Subgrade
Silt content in Subgrade
Clay Content in Subgrade
Percent passing No. 200 sieve, Subgrade
Moisture Content Base
Percent Passing No. 200 sieve, Base
Joint Spacing PCC
PCC Elastic Modulus
PCC Compressive Strength
PCC Tensile Strength
PCC Poisson's Ratio
PCC Unit Weight
PCC - Coarse Aggregate, Weight
PCC - Fine Aggregate, Weight
PCC - Cement, Weight
PCC - Water Cement Ratio
PCC – Air
Traffic

The results of the evaluation are presented separately for each of the three pavement types. It should be noted if a pavement is designed "correctly" for the subgrade and climatic conditions at a site, the effect of these factors on roughness of the pavement might not be seen. If a pavement is not designed to allow for the site conditions the effect of climatic and subgrade parameters may be seen to be affecting the roughness. This is true for PCC properties too. So because a particular parameter was not identified to be affecting roughness in this analysis, it does not mean that parameter is not important for roughness. Pavement designers can make use of the information presented in this section to identify factors that cause higher roughness levels. The pavements can then be designed to adequately address the causes that lead to higher roughness.

Jointed Plain Concrete Pavements: GPS-3

In the dry zone (dry freeze and dry no-freeze), there were only a few doweled sections, and a comparison of performance between doweled and non-doweled pavements cannot be performed. In the wet zone (wet freeze and wet no-freeze) there was a distinct difference in performance between doweled and non-doweled pavement, with non-doweled sections showing a much higher rate of increase of roughness than doweled pavements. In the wet-freeze zone, a rate of change of IRI of less than 0.02 m/km/yr was noted at 72 percent of the sections with dowels, and for 36 percent of the sections without dowels, while a rate of change of IRI of over 0.05 m/km/yr was seen for 16 percent of the sections with dowels and 43 percent of sections without dowels. In the wet no-freeze zone, a rate of change of IRI of less than 0.02 m/km/yr was noted at 58 percent of the sections with dowels and at 38 percent of the sections without dowels, while a rate of change of IRI greater than 0.05 m/km/yr was seen for 11 percent of sections with dowels and 26 percent of sections without dowels. Most of the pavements that do not have dowels and are over 15 years old are showing very high rates of increase of roughness. The factors that were identified to be contributing to higher levels of roughness in non-doweled pavements are listed in table 72.

Table 72. Factors affecting roughness progression in non-doweled PCC pavements.

Parameter	Effect of Higher Value of Parameter on Roughness	Comment
PCC elastic modulus	Increases	Note 1
PCC compressive strength	Increases	Note 2
PCC Poisson's ratio	Increases	-
Ratio between PCC elastic modulus and tensile strength	Increases	Note 3
Subgrade clay content	Increases	Stronger Relationship in Wet Zone
Subgrade plasticity index	Increases	
Subgrade moisture content	Increases	
Annual precipitation	Increases	
Mean Temperature	Decreases	-
Faulting	Increases	-
Note 1: Seen for PCC modulus > 35,000 MPa Note 2: Seen for PCC compressive strength > 60 MPa Note 3: Seen for ratio > 8000		

As indicated in table 72, for non-doweled pavements, higher IRI values were associated with pavements that had high PCC modulus (greater than 35,000 Mpa). There were only four doweled sections that had PCC modulus values greater than 35,000 Mpa, and therefore such a relationship not seen for doweled pavements. For doweled pavements, higher IRI values were associated with high number of wet days. There were several sections with low PCC split tensile strength (less than 3.6 Mpa) that had high rates of increase of IRI. No relationship between total faulting and IRI was observed for doweled pavements. A total faulting greater than 50 mm was observed at 7 percent of the doweled sections compared to 41 percent for non-doweled sections. These results show that having dowels in pavements reduce faulting in pavements, which in turn result in lower IRI values.

Jointed Reinforced Concrete Pavements: (GPS-4)

All JRCP sections are located either in the wet freeze or the wet no-freeze zone. The factors that were identified to be contributing to higher levels of roughness in JRCP pavements are listed in table 73. Several sections that had low cement contents (less than 300 kg/m^3) had

high IRI values. Some sections that had water cement ratios in excess of 0.50 also had high rates of increase of IRI.

Table 73. Factors affecting roughness progression in JRCP pavements.

Parameter	Effect of Higher Value of Parameter on Roughness
PCC compressive strength	Decreases
PCC unit weight	Decreases
PCC elastic modulus	Increases
Ratio between PCC elastic modulus and tensile strength	Increases
PCC Poisson's ratio	Increases
Moisture content subgrade	Increases
Clay content of subgrade	Increases
Plastic limit of subgrade	Increases
Annual precipitation	Increases
Wet days	Increases
Mean temperature	Increases
Joint spacing	Increases

Continuously Reinforced Concrete Pavements (GPS-5)

Ninety percent of CRCP sections are located in the wet zone (wet freeze and wet no-freeze). The CRCP pavements have not shown much change in roughness over the monitored period, with 68 percent of sections showing an IRI change of less than 0.1 m/km over the monitored period. The factors that were identified to be contributing to higher levels of roughness in CRCP pavements are listed in table 74.

Factors Affecting Roughness in AC Overlays

AC Overlay of AC Pavements: GPS-6

No relationship between IRI before the overlay and IRI immediately after overlay was noted. The IRI after overlay for a majority of the sections fell between 0.8 and 1.2 m/km. Thin

Table 74. Factors affecting roughness progression in CRCP pavements.

Environmental Zone	Parameter	Effect of Higher Value of Parameter on Roughness
For Both Wet Freeze and Wet No-Freeze	PCC elastic modulus	Increases
	Ratio between PCC elastic modulus and tensile strength	Increases
	PCC water cement ratio	Decreases
Wet Freeze	Fines content in subgrade	Increases
	Moisture content in subgrade	Increases
	Wet days per year	Increases
Wet No-Freeze	Steel content	Decreases
	Wet days	Decreases
	Days per year > 32 °C	Increases
	Mean annual temperature	Increases

overlays were seen to be capable of reducing the roughness of a pavement substantially. For example, a 76 mm thick AC overlay was capable of achieving an IRI after overlay of 0.7 m/km for a pavement that had a roughness of 3.4 m/km prior to the overlay.

However, the IRI development of overlaid pavements was related to the IRI prior to overlay. The sections that had an IRI greater than 2.0 m/km prior to overlay generally showed a higher rate of increase of IRI compared to sections that had an IRI of less than 2.0 m/km prior to overlay. The majority of pavements that had an IRI prior to overlay of less than 2.0 m/km showed a rate of increase of roughness that were less than 0.04 m/km/year over the initial life of the overlay (4 to 7 years). Placing overlays on pavements that have an IRI of less than 2.0 m/km appear to be an effective rehabilitation strategy in extending the life of the pavement. However, the section should have sufficient structural capacity to carry the anticipated traffic volume.

AC Overlay of PCC Pavements: GPS-7

The PCC pavement types on which the AC overlay has been placed included JPC pavements (with and without dowels), JRCP pavements and CRCP pavements. The factors affecting the increase in roughness for each of these pavement types is expected to influence the

roughness progression of the overlaid pavement. However, sufficient sections were not available to perform separate analysis for each of these PCC pavement types. There was no relationship between IRI before and IRI immediately after overlay for these pavements. The IRI after overlay for a majority of the sections fell between 0.8 and 1.0 m/km. The roughness progression in the overlays did not depend on the IRI prior to overlay. The majority of the overlaid pavements were showing a rate of increase of IRI that was less than 0.04 m/km. High rates of increase of roughness was observed for overlays on PCC sections that had high PCC elastic modulus.

General Observations on Roughness Progression

The cause for the high rate of increase of roughness that were observed on some of the sections prior to the end of their design life can be attributed to several causes. If a pavement is subjected to its design traffic volume in a time period that is less than its intended design life, the roughness of the section is expected to increase rapidly. Also, if the pavement is not adequately designed based on the subgrade and environmental conditions at the site, the roughness of the section can increase at a high rate. It was noted that the pavements that are at higher levels of roughness generally were subjected to a several factors that were identified to be causing high roughness levels. There were many sections that were old, but have maintained their smoothness level over time. Many of these sections appear to have carried low traffic volumes relative to the theoretical traffic volume that can be carried by the pavement section. It was observed that pavements that were of similar age show a parallel trend in roughness progression, indicating pavements that are built smoother provide a smoother pavement over its design life.

SUGGESTIONS FOR FUTURE RESEARCH

1. A comprehensive analysis of the SPS-1, SPS-2, SPS-5 and SPS-6 experiments are recommended when more time-sequence IRI values, material test data and traffic data are available.

2. The evaluation of SPS-2 sections showed that slab curvatures have a large influence on changes in roughness. An analysis of GPS-3 sections to evaluate changes in curvature over time, and its effect on roughness levels and roughness progression is recommended. Such a research can identify PCC material properties, subgrade or environmental conditions that increase the potential for curvature in PCC slabs.

3. Every effort should be made to keep LTPP sections in service beyond the 1.5 m/km roughness level. Without letting these sections deteriorate, future modeling will always be limited.

5. Several areas of data deficiencies have been identified in this report. The LTPP staff is making a concerted effort to close gaps in the database. This level of effort should be increased or at least maintained.

APPENDIX A

IRI PLOTS FOR SPS-1 PROJECTS

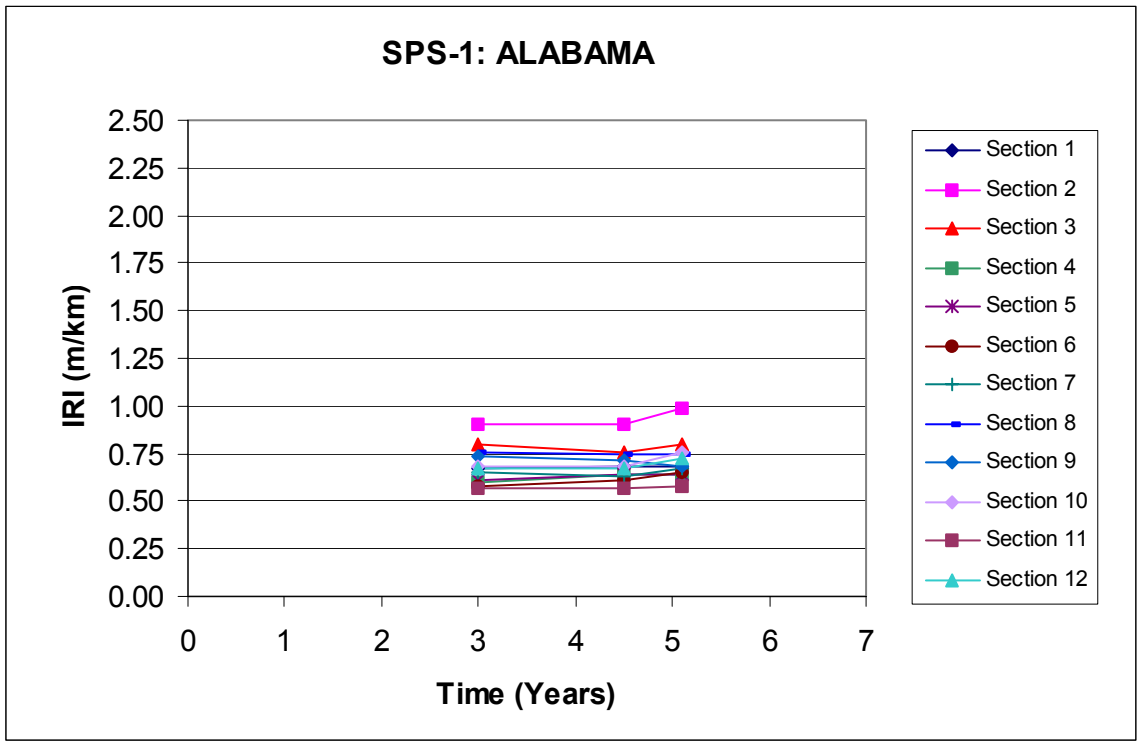
SPS-1: ALABAMA
IRI (m/km)
2.50
2.25
2.00
1.75
1.50
1.25
1.00
0.75
0.50
0.25
0.00
0
1
2
3
4
5
6
7
Time (Years)
Section 1
Section 2
Section 3
Section 4
Section 5
Section 6
Section 7
Section 8
Section 9
Section 10
Section 11
Section 12

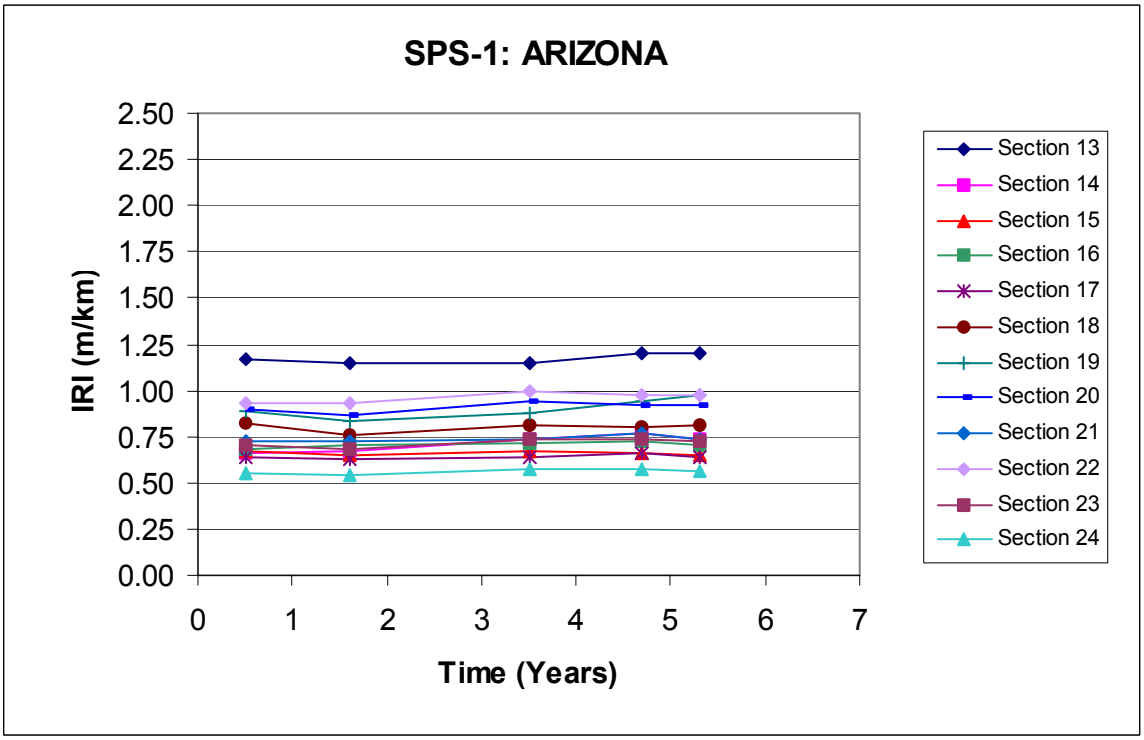
SPS-1: ARIZONA
IRI (m/km)
2.50
2.25
2.00
1.75
1.50
1.25
1.00
0.75
0.50
0.25
0.00
0
1
2
3
4
5
6
7
Time (Years)
Section 13
Section 14
Section 15
Section 16
Section 17
Section 18
Section 19
Section 20
Section 21
Section 22
Section 23
Section 24

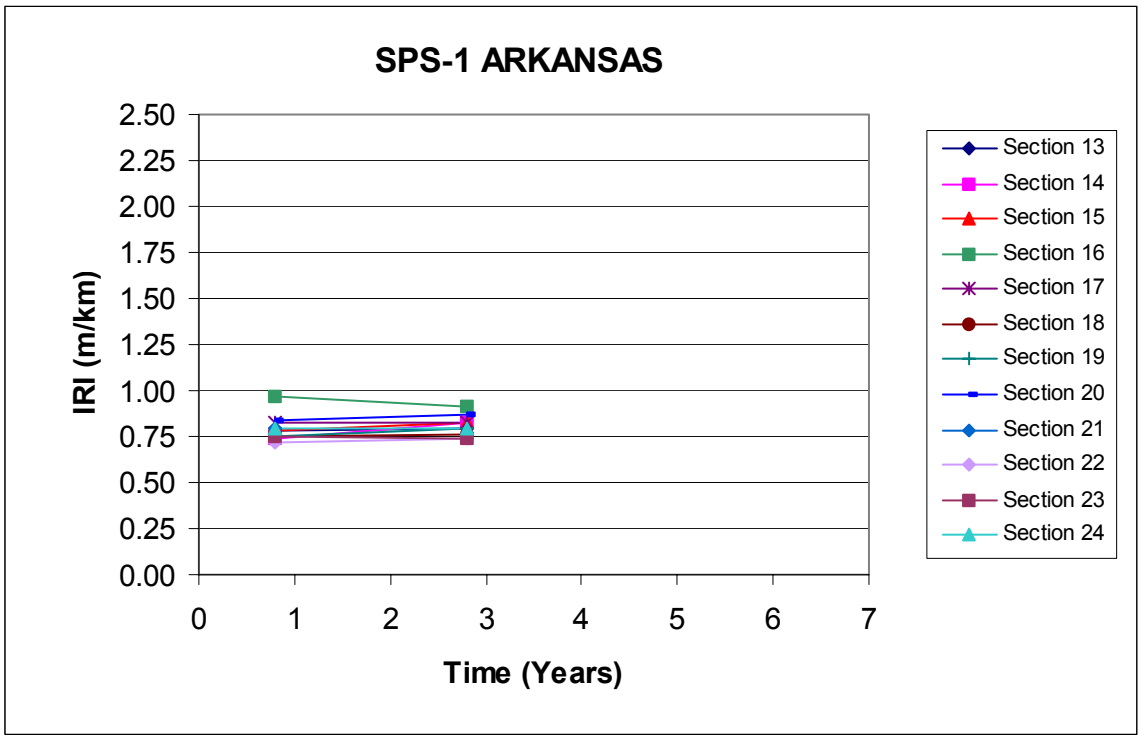
SPS-1 ARKANSAS
IRI (m/km)
2.50
2.25
2.00
1.75
1.50
1.25
1.00
0.75
0.50
0.25
0.00
0
1
2
3
4
5
6
7
Time (Years)
Section 13
Section 14
Section 15
Section 16
Section 17
Section 18
Section 19
Section 20
Section 21
Section 22
Section 23
Section 24

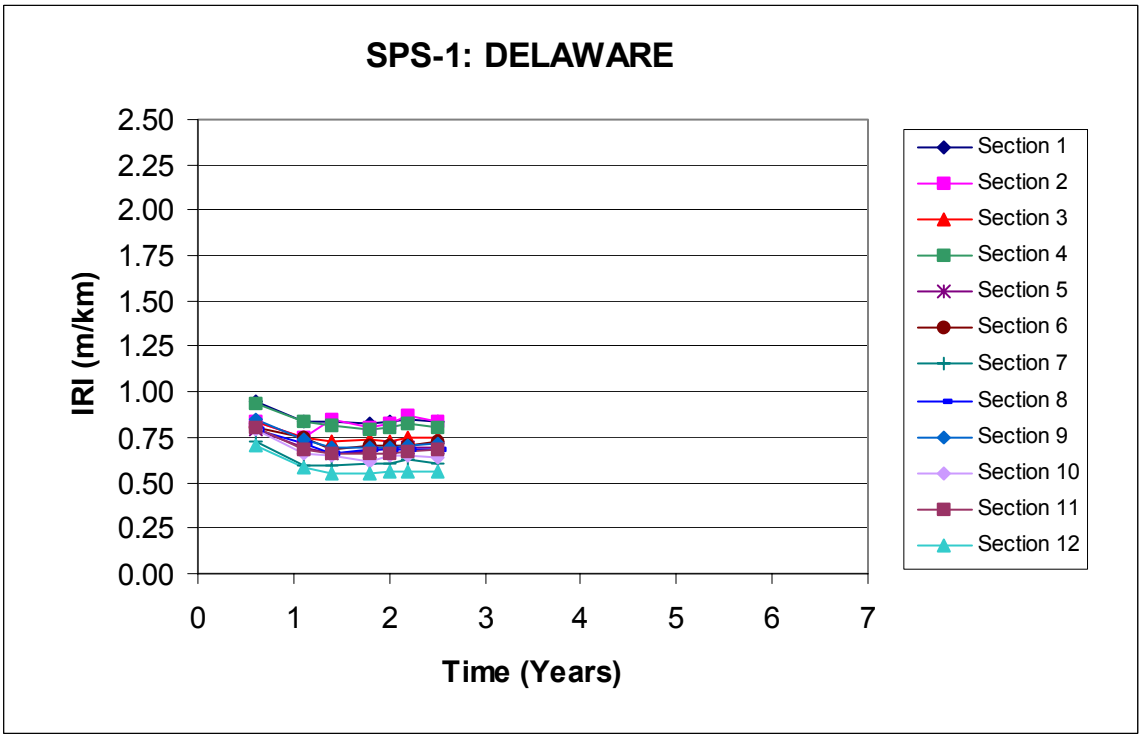
SPS-1: DELAWARE
IRI (m/km)
2.50
2.25
2.00
1.75
1.50
1.25
1.00
0.75
0.50
0.25
0.00
0
1
2
3
4
5
6
7
Time (Years)
Section 1
Section 2
Section 3
Section 4
Section 5
Section 6
Section 7
Section 8
Section 9
Section 10
Section 11
Section 12

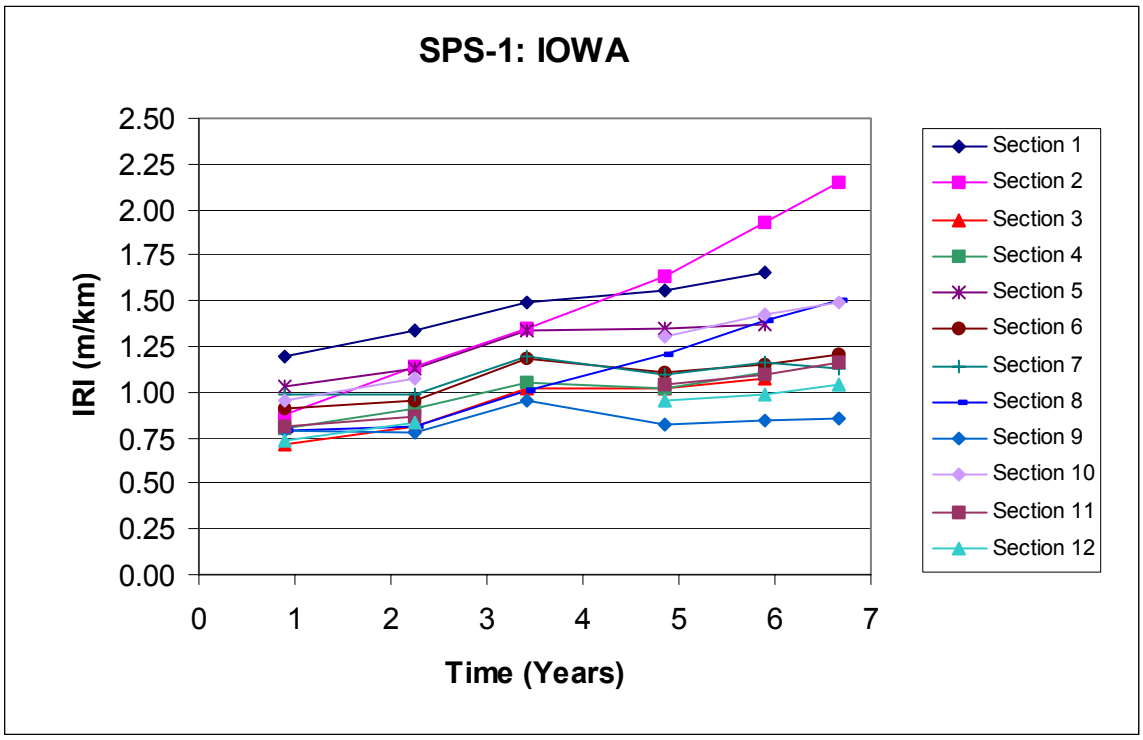
SPS-1: IOWA
IRI (m/km)
2.50
2.25
2.00
1.75
1.50
1.25
1.00
0.75
0.50
0.25
0.00
0
1
2
3
4
5
6
7
Time (Years)
Section 1
Section 2
Section 3
Section 4
Section 5
Section 6
Section 7
Section 8
Section 9
Section 10
Section 11
Section 12

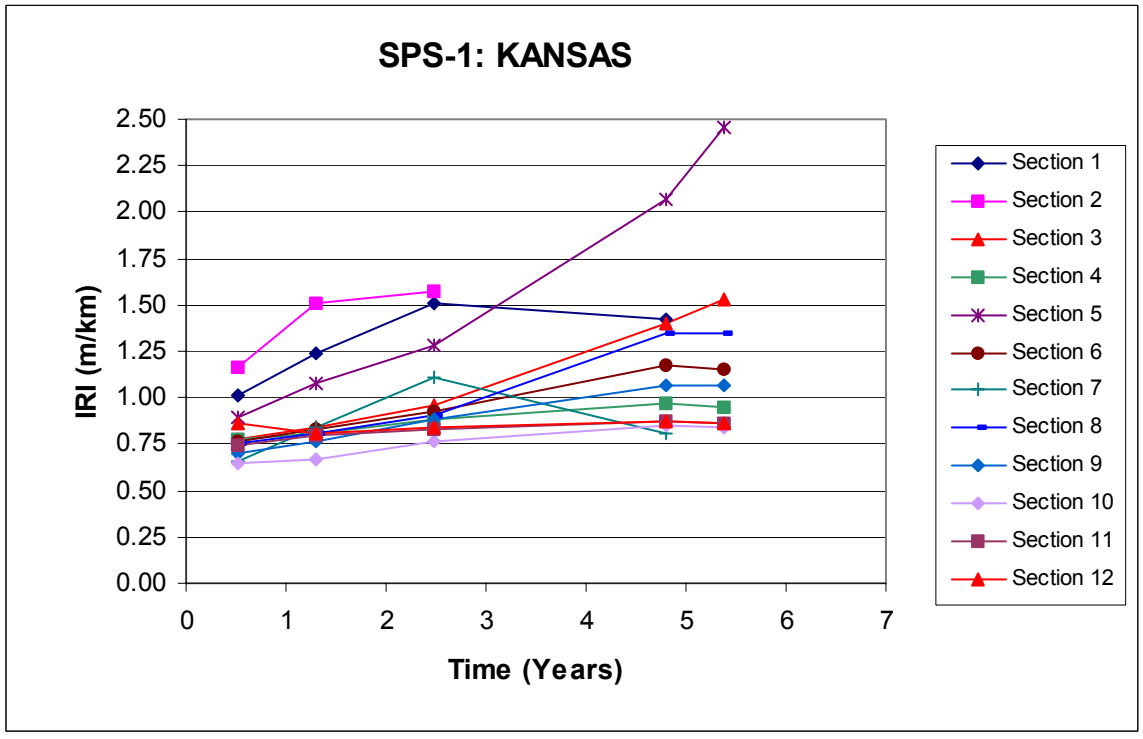
SPS-1: KANSAS
IRI (m/km)
2.50
2.25
2.00
1.75
1.50
1.25
1.00
0.75
0.50
0.25
0.00
0
1
2
3
4
5
6
7
Time (Years)
Section 1
Section 2
Section 3
Section 4
Section 5
Section 6
Section 7
Section 8
Section 9
Section 10
Section 11
Section 12

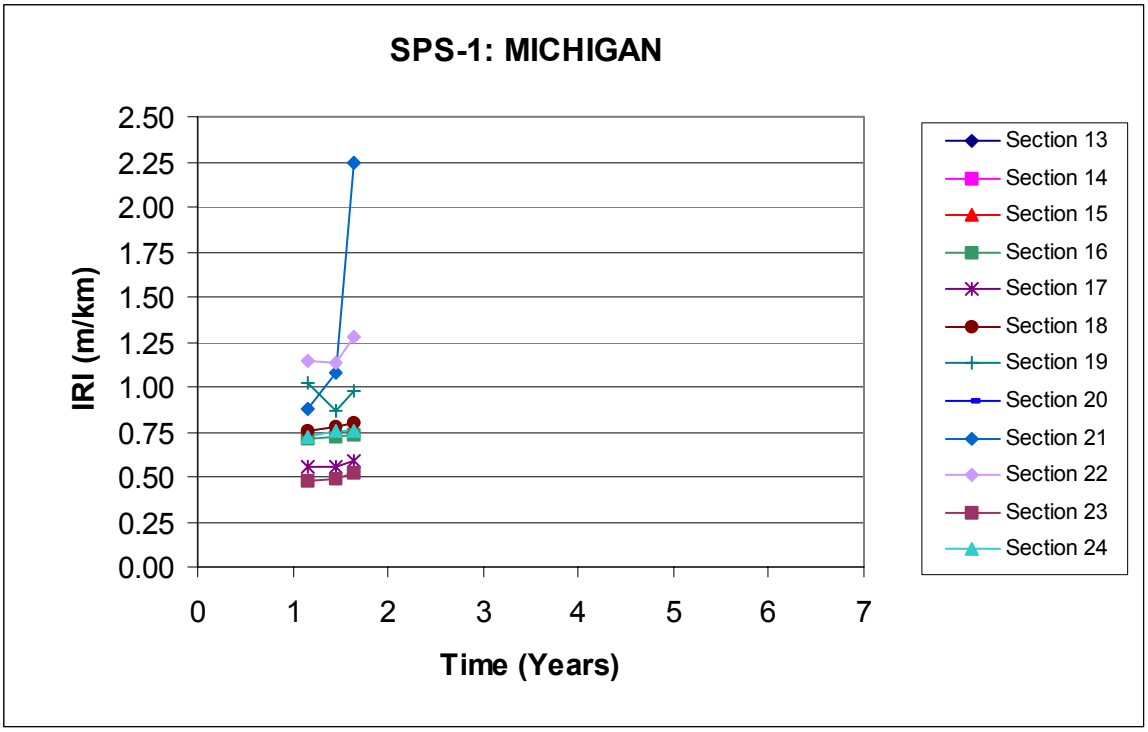
SPS-1: MICHIGAN
IRI (m/km)
2.50
2.25
2.00
1.75
1.50
1.25
1.00
0.75
0.50
0.25
0.00
0
1
2
3
4
5
6
7
Time (Years)
Section 13
Section 14
Section 15
Section 16
Section 17
Section 18
Section 19
Section 20
Section 21
Section 22
Section 23
Section 24

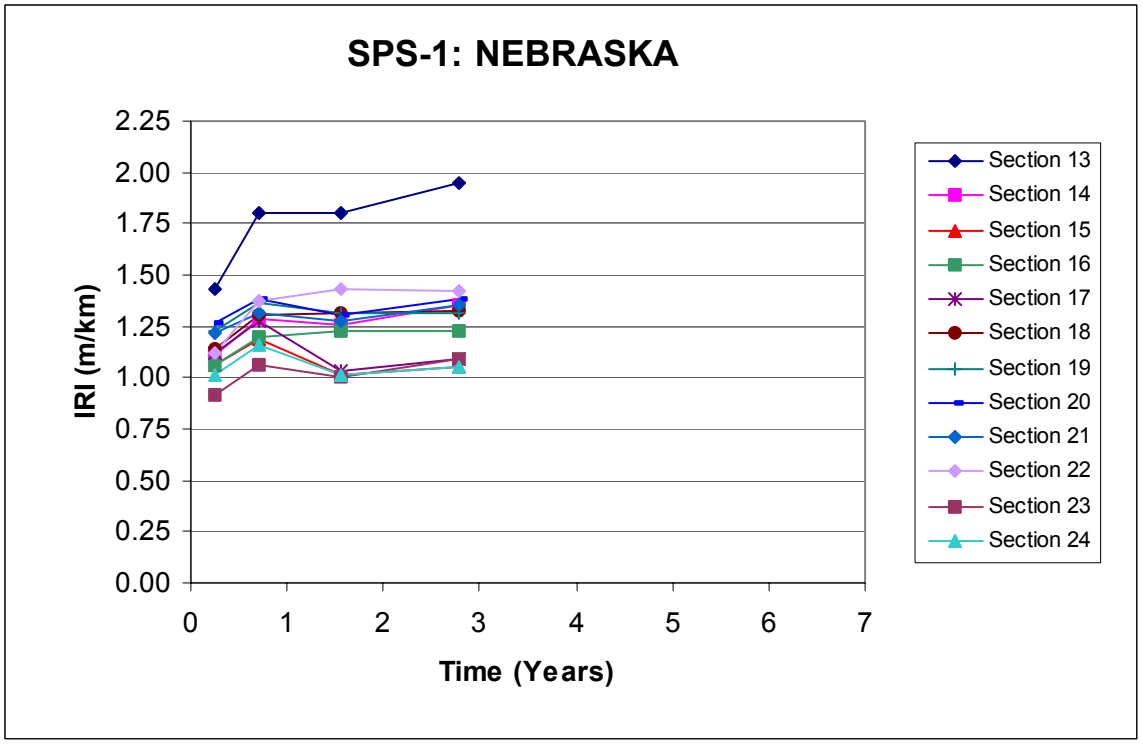
SPS-1: NEBRASKA
IRI (m/km)
2.25
2.00
1.75
1.50
1.25
1.00
0.75
0.50
0.25
0.00
0
1
2
3
4
5
6
7
Time (Years)
Section 13
Section 14
Section 15
Section 16
Section 17
Section 18
Section 19
Section 20
Section 21
Section 22
Section 23
Section 24

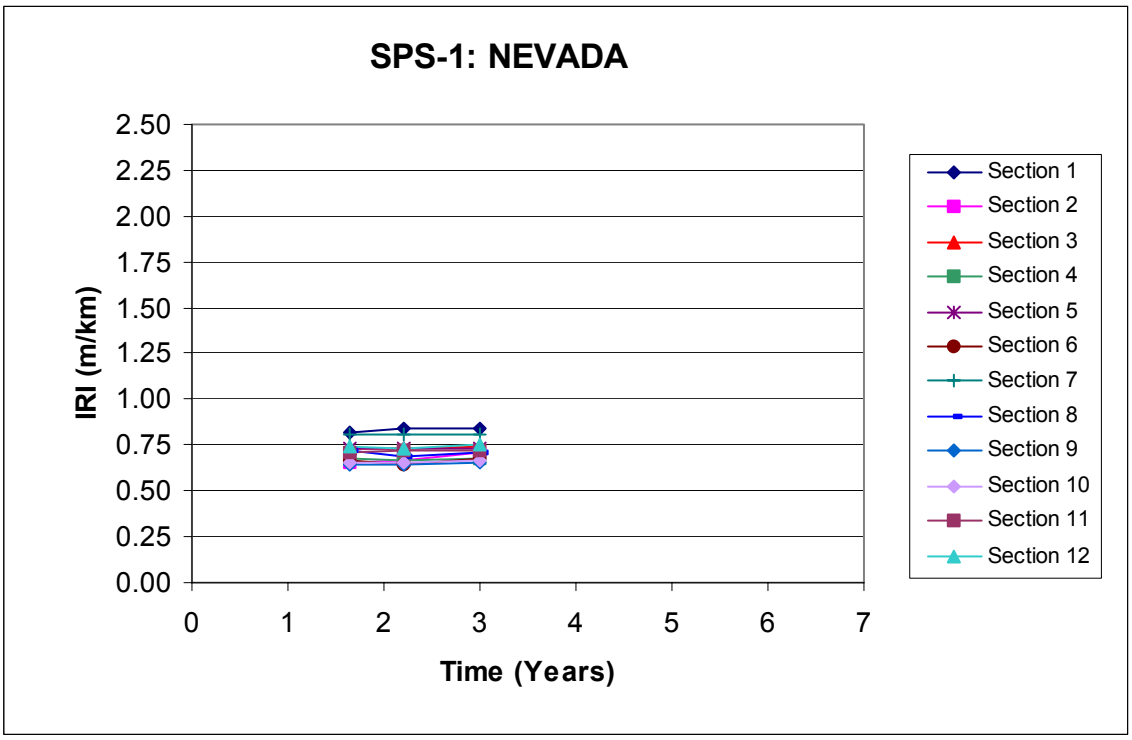
SPS-1: NEVADA
IRI (m/km)
2.50
2.25
2.00
1.75
1.50
1.25
1.00
0.75
0.50
0.25
0.00
0
1
2
3
4
5
6
7
Time (Years)
Section 1
Section 2
Section 3
Section 4
Section 5
Section 6
Section 7
Section 8
Section 9
Section 10
Section 11
Section 12

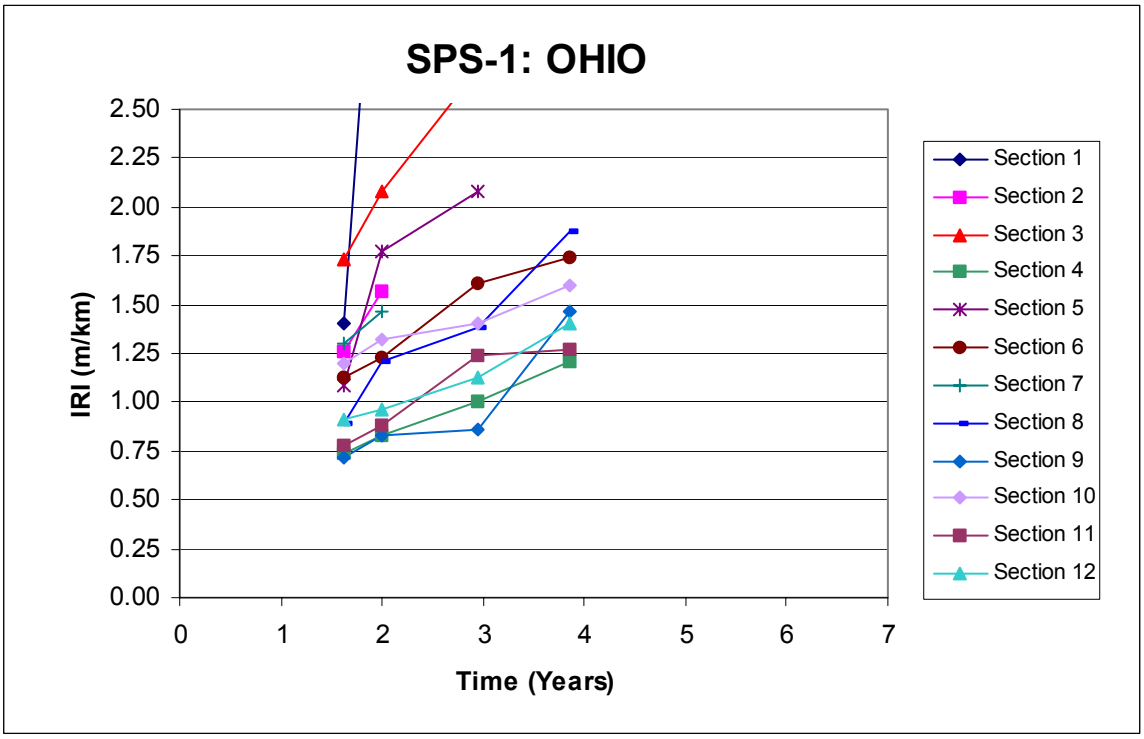
SPS-1: OHIO
IRI (m/km)
2.50
2.25
2.00
1.75
1.50
1.25
1.00
0.75
0.50
0.25
0.00
0
1
2
3
4
5
6
7
Time (Years)
Section 1
Section 2
Section 3
Section 4
Section 5
Section 6
Section 7
Section 8
Section 9
Section 10
Section 11
Section 12

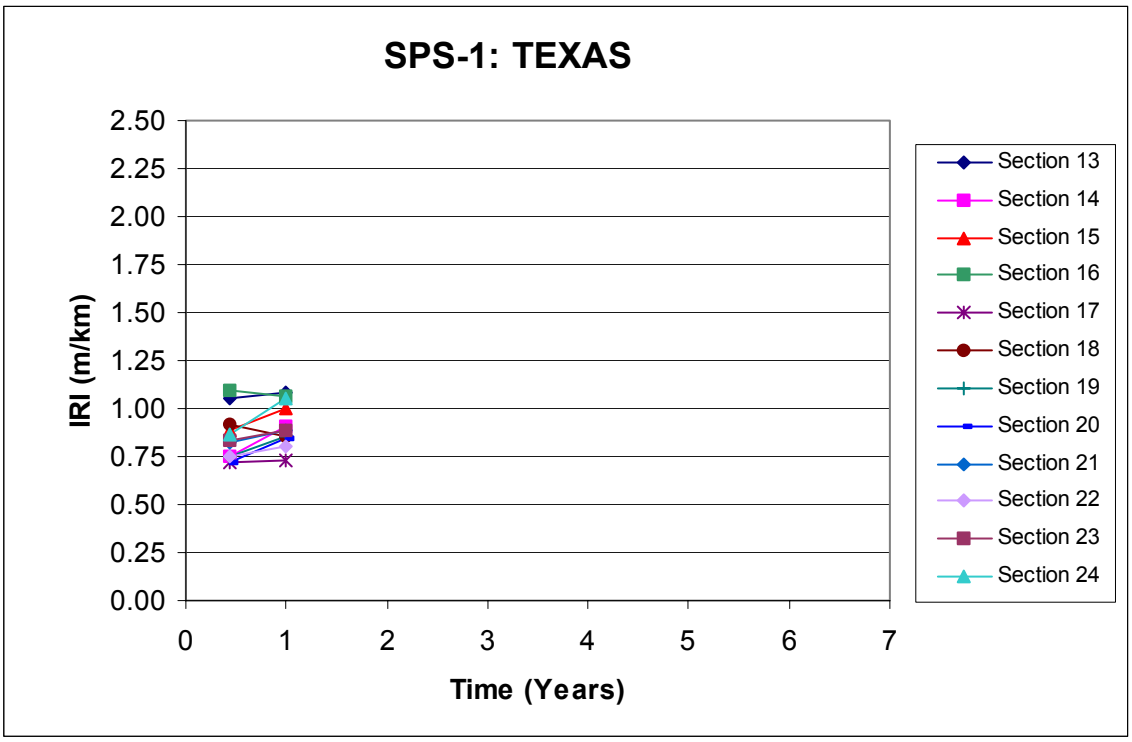
SPS-1: TEXAS
IRI (m/km)
2.50
2.25
2.00
1.75
1.50
1.25
1.00
0.75
0.50
0.25
0.00
0
1
2
3
4
5
6
7
Time (Years)
Section 13
Section 14
Section 15
Section 16
Section 17
Section 18
Section 19
Section 20
Section 21
Section 22
Section 23
Section 24

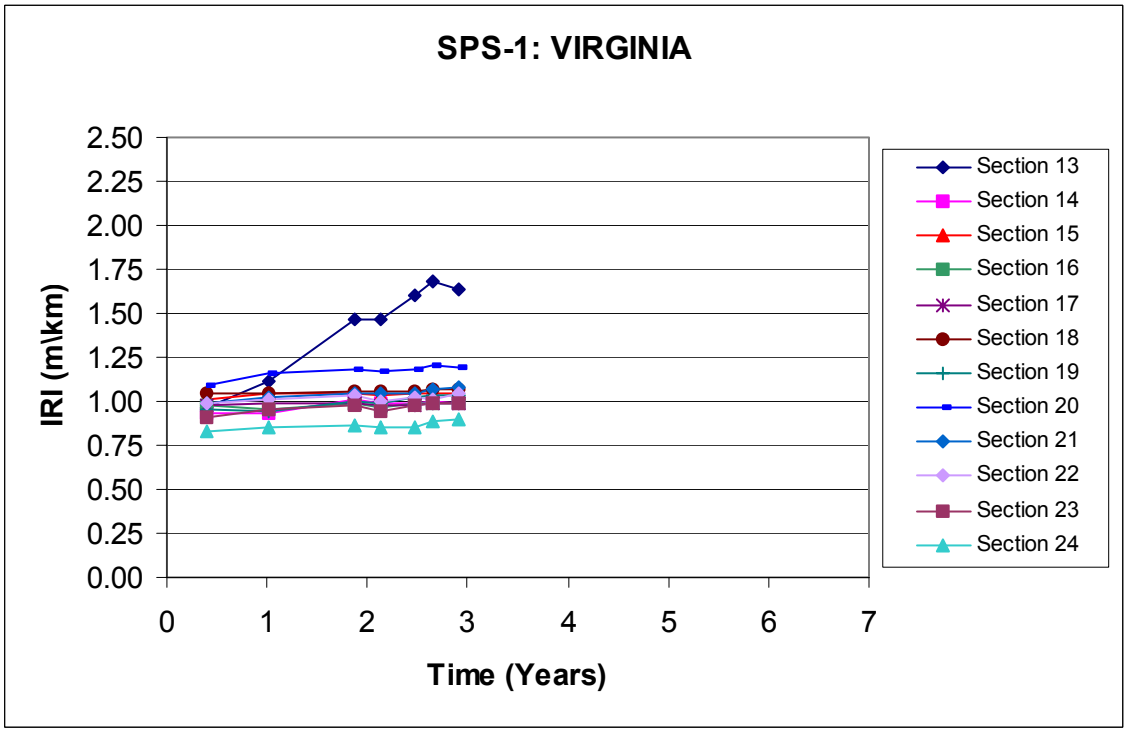
SPS-1: VIRGINIA
IRI (m\km)
2.50
2.25
2.00
1.75
1.50
1.25
1.00
0.75
0.50
0.25
0.00
0
1
2
3
4
5
6
7
Time (Years)
Section 13
Section 14
Section 15
Section 16
Section 17
Section 18
Section 19
Section 20
Section 21
Section 22
Section 23
Section 24

APPENDIX B

IRI PLOTS FOR SPS-2 PROJECTS

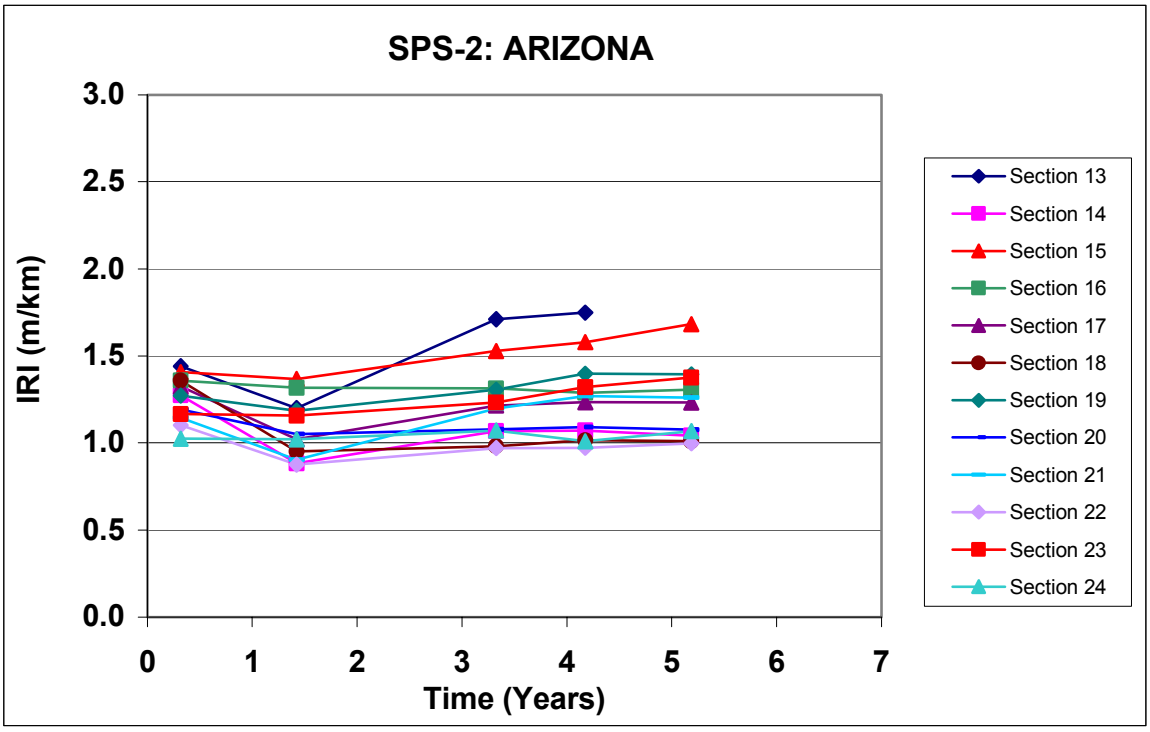
SPS-2: ARIZONA
IRI (m/km)
3.0
2.5
2.0
1.5
1.0
0.5
0.0
0
1
2
3
4
5
6
7
Time (Years)
Section 13
Section 14
Section 15
Section 16
Section 17
Section 18
Section 19
Section 20
Section 21
Section 22
Section 23
Section 24

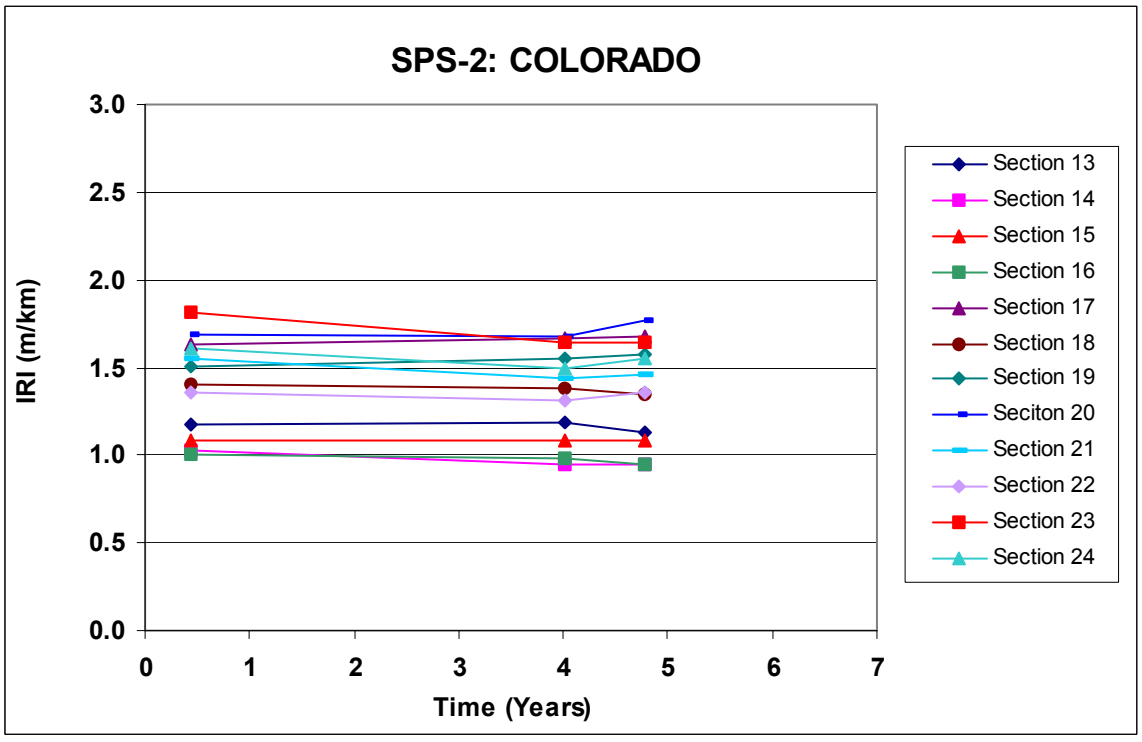
SPS-2: COLORADO
IRI (m/km)
3.0
2.5
2.0
1.5
1.0
0.5
0.0
0
1
2
3
4
5
6
7
Time (Years)
Section 13
Section 14
Section 15
Section 16
Section 17
Section 18
Section 19
Seciton 20
Section 21
Section 22
Section 23
Section 24

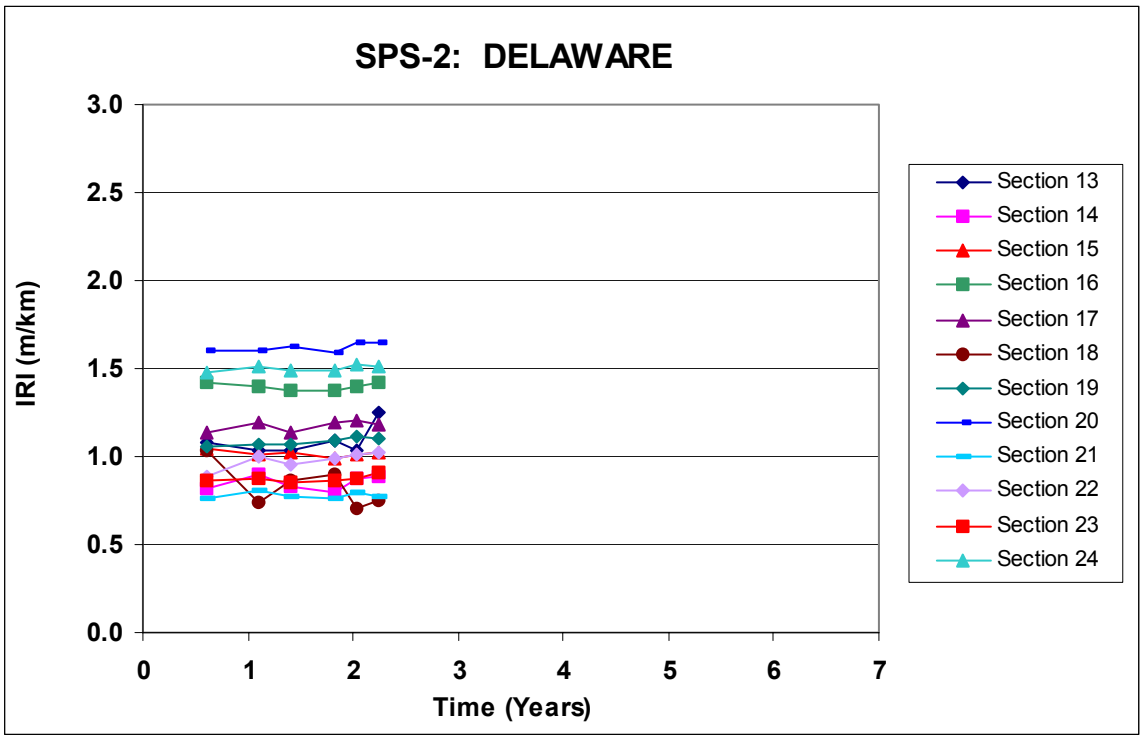
SPS-2: DELAWARE
IRI (m/km)
3.0
2.5
2.0
1.5
1.0
0.5
0.0
0
1
2
3
4
5
6
7
Time (Years)
Section 13
Section 14
Section 15
Section 16
Section 17
Section 18
Section 19
Section 20
Section 21
Section 22
Section 23
Section 24

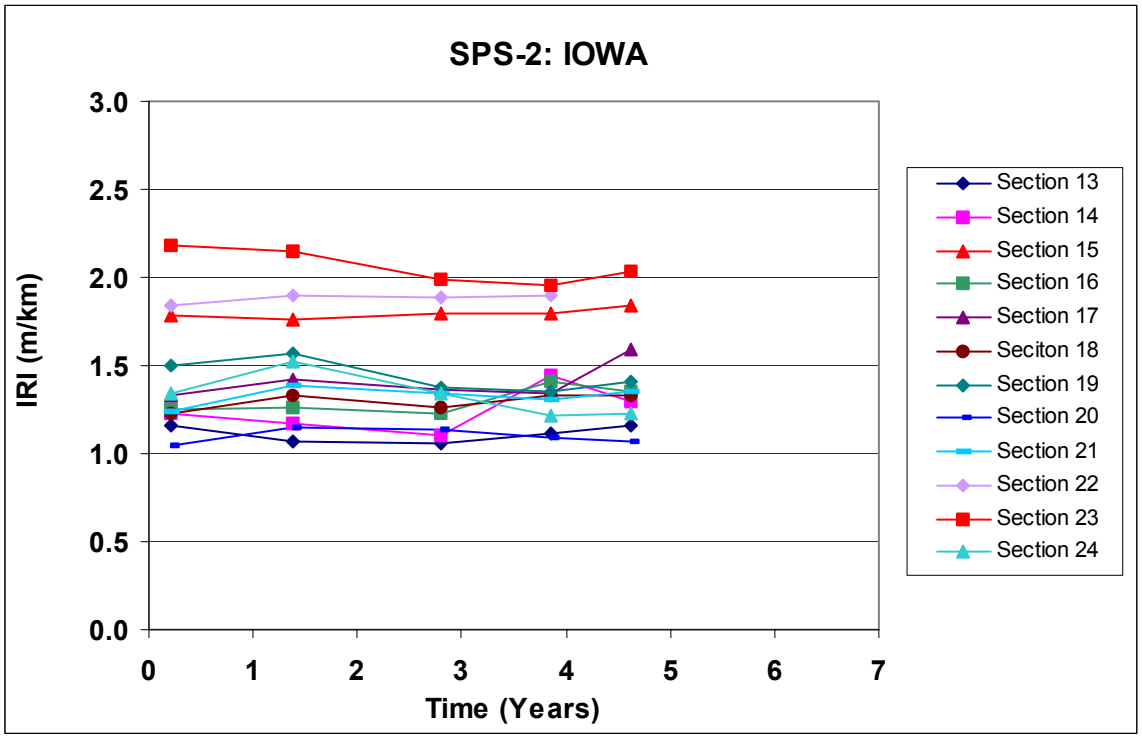
SPS-2: IOWA
IRI (m/km)
3.0
2.5
2.0
1.5
1.0
0.5
0.0
0
1
2
3
4
5
6
7
Time (Years)
Section 13
Section 14
Section 15
Section 16
Section 17
Seciton 18
Section 19
Section 20
Section 21
Section 22
Section 23
Section 24

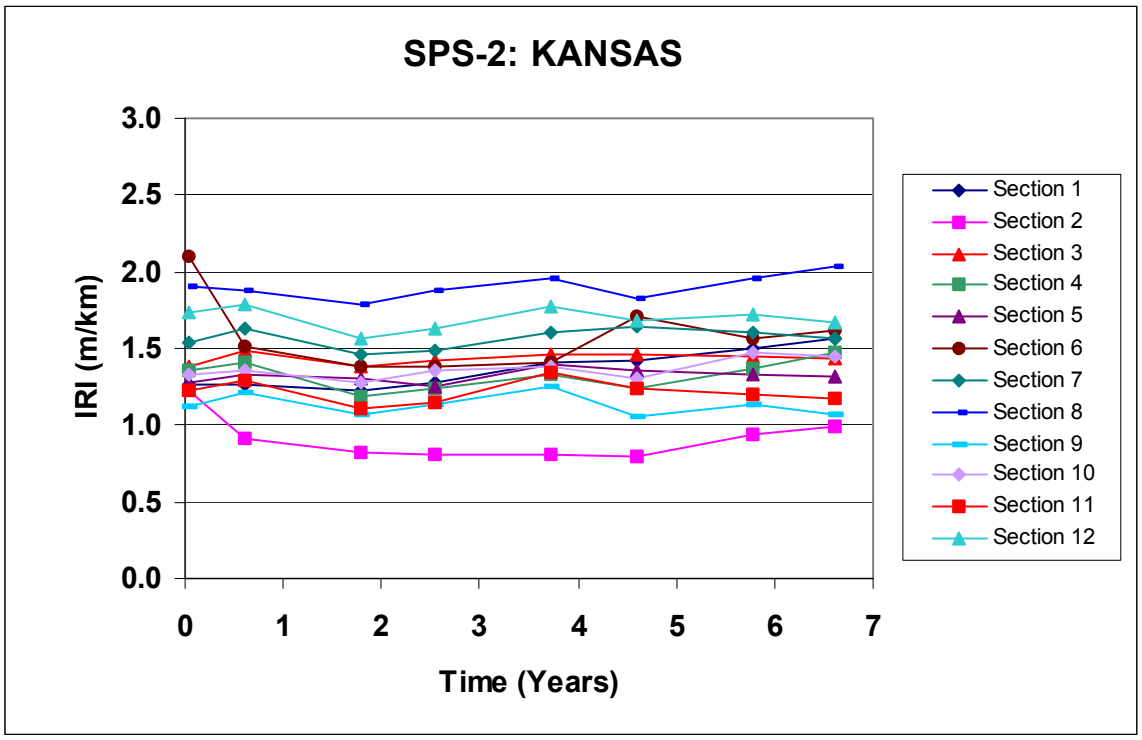
SPS-2: KANSAS
IRI (m/km)
3.0
2.5
2.0
1.5
1.0
0.5
0.0
0
1
2
3
4
5
6
7
Time (Years)
Section 1
Section 2
Section 3
Section 4
Section 5
Section 6
Section 7
Section 8
Section 9
Section 10
Section 11
Section 12

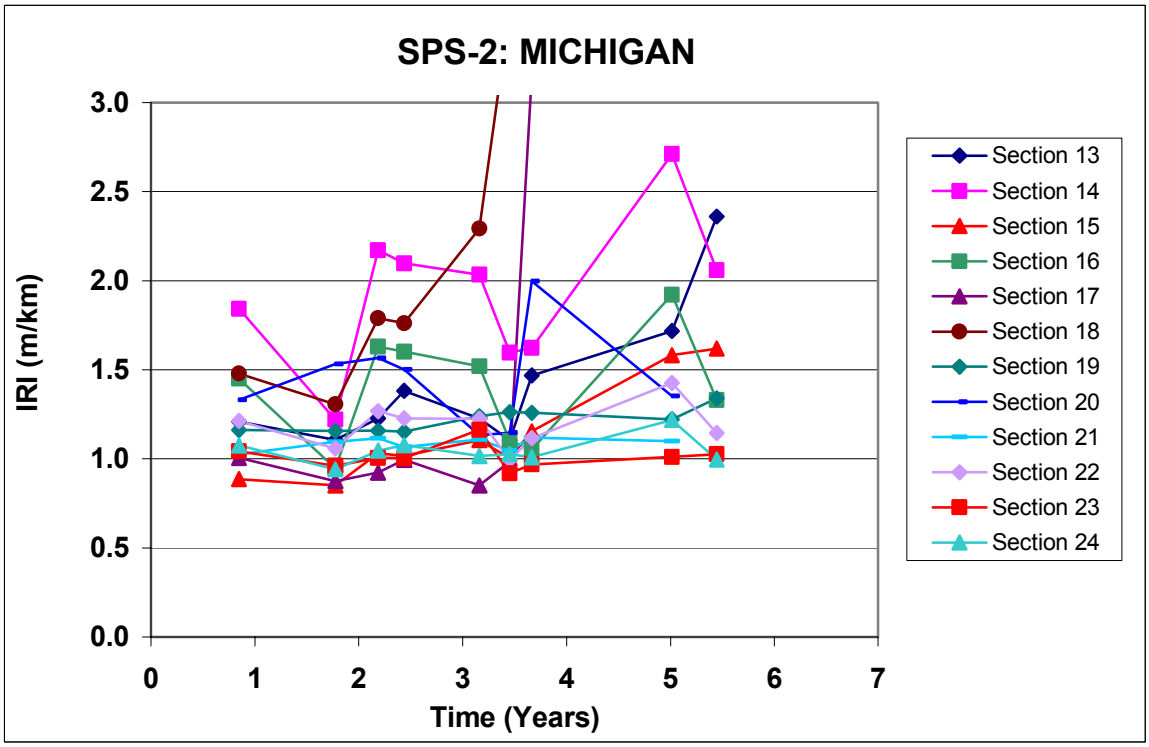
SPS-2: MICHIGAN
IRI (m/km)
3.0
2.5
2.0
1.5
1.0
0.5
0.0
0
1
2
3
4
5
6
7
Time (Years)
Section 13
Section 14
Section 15
Section 16
Section 17
Section 18
Section 19
Section 20
Section 21
Section 22
Section 23
Section 24

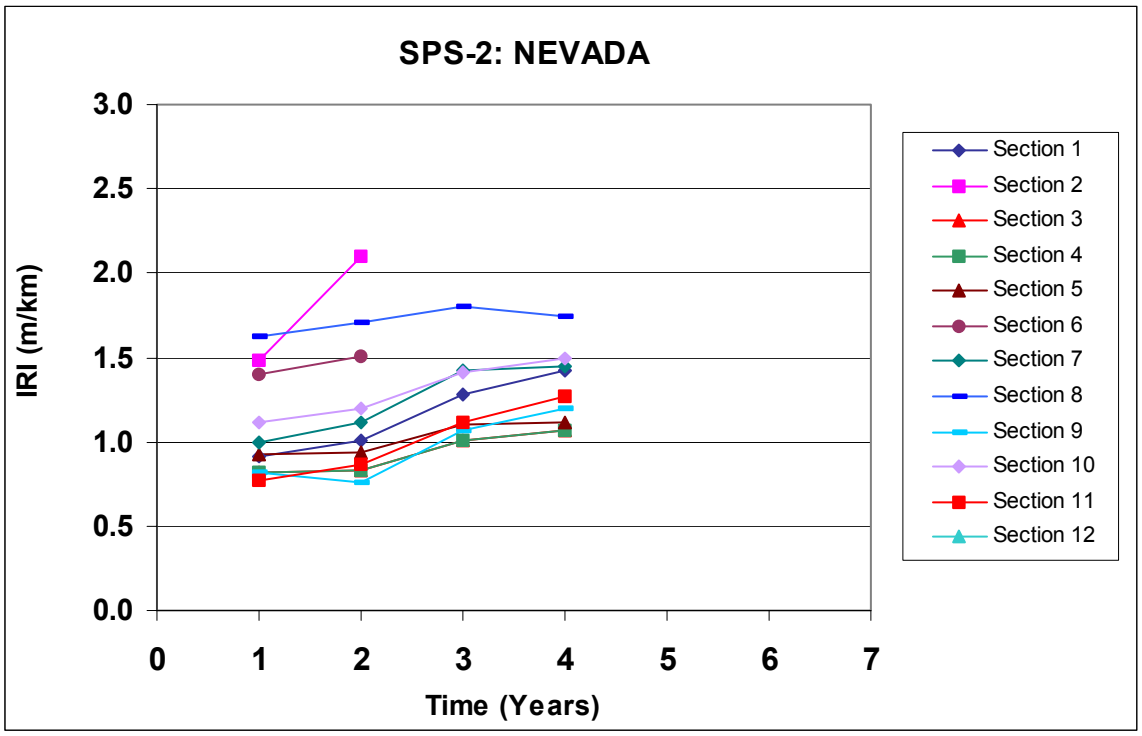
SPS-2: NEVADA
IRI (m/km)
3.0
2.5
2.0
1.5
1.0
0.5
0.0
0
1
2
3
4
5
6
7
Time (Years)
Section 1
Section 2
Section 3
Section 4
Section 5
Section 6
Section 7
Section 8
Section 9
Section 10
Section 11
Section 12

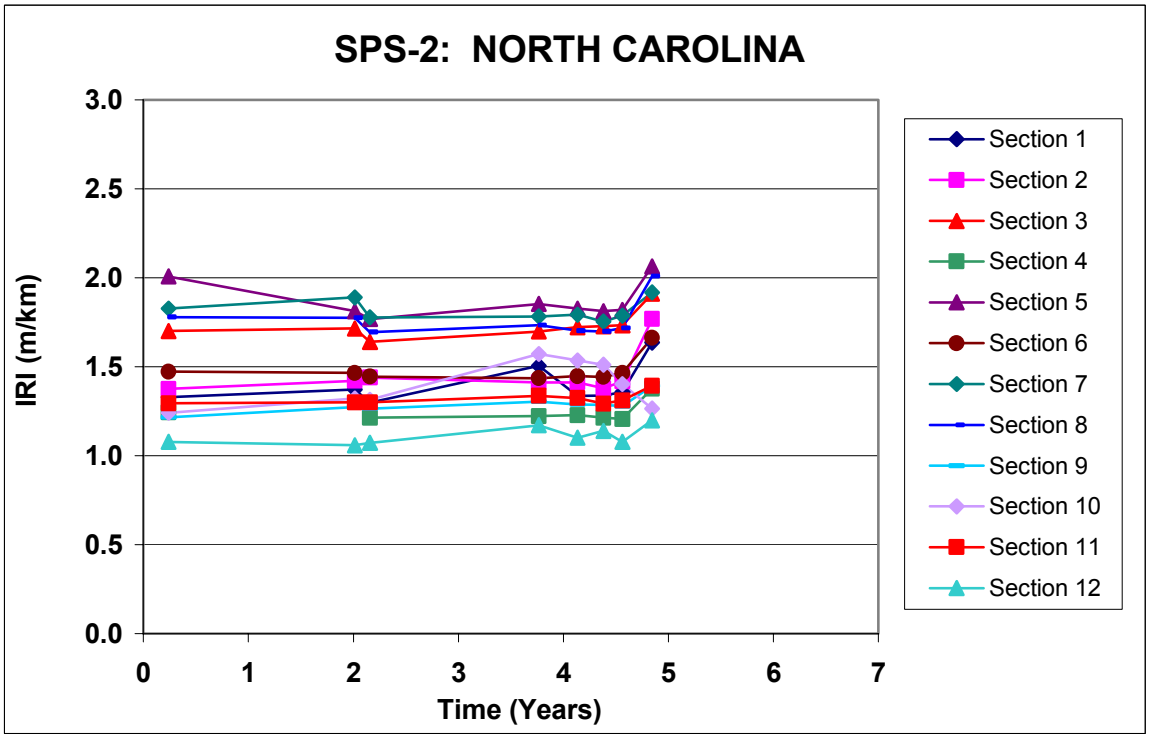
SPS-2: NORTH CAROLINA
IRI (m/km)
3.0
2.5
2.0
1.5
1.0
0.5
0.0
0
1
2
3
4
5
6
7
Time (Years)
Section 1
Section 2
Section 3
Section 4
Section 5
Section 6
Section 7
Section 8
Section 9
Section 10
Section 11
Section 12

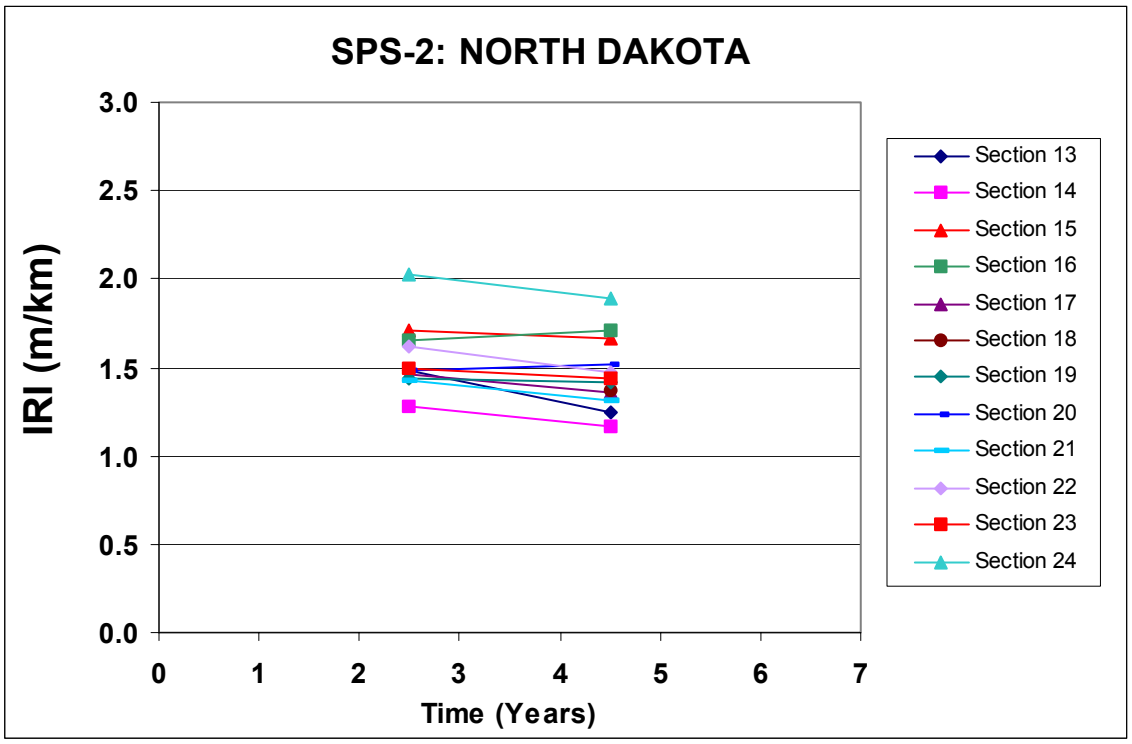
SPS-2: NORTH DAKOTA
IRI (m/km)
3.0
2.5
2.0
1.5
1.0
0.5
0.0
0
1
2
3
4
5
6
7
Time (Years)
Section 13
Section 14
Section 15
Section 16
Section 17
Section 18
Section 19
Section 20
Section 21
Section 22
Section 23
Section 24

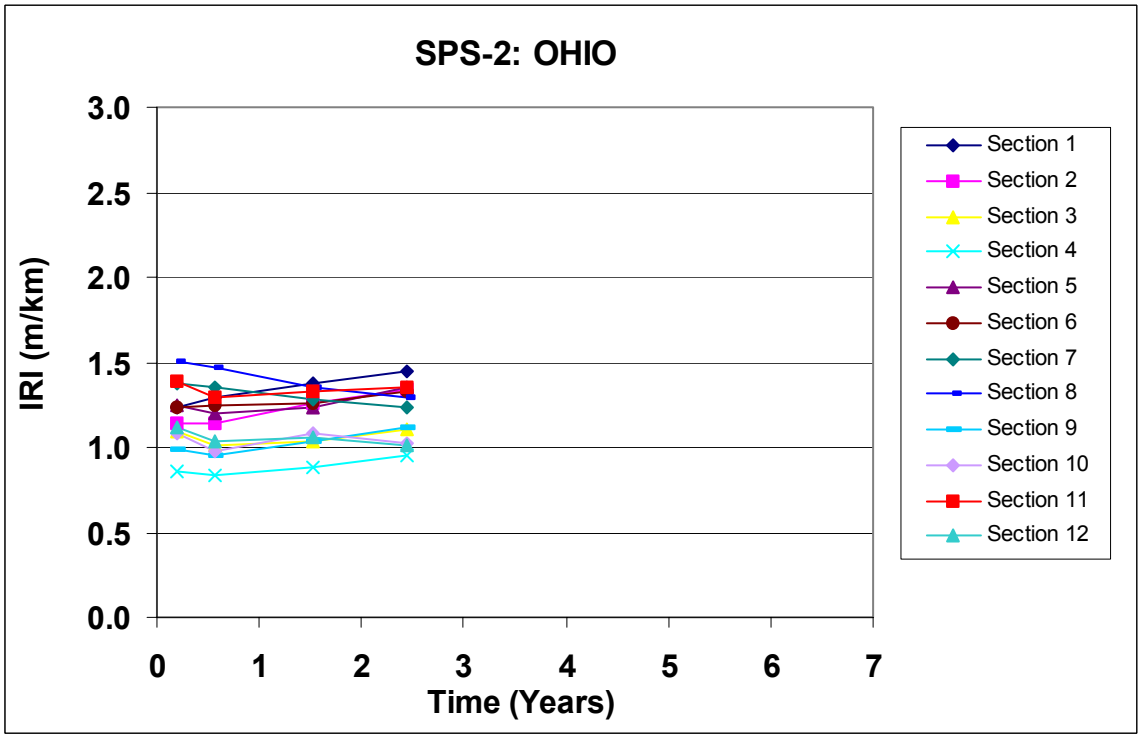
SPS-2: OHIO
IRI (m/km)
3.0
2.5
2.0
1.5
1.0
0.5
0.0
0
1
2
3
4
5
6
7
Time (Years)
Section 1
Section 2
Section 3
Section 4
Section 5
Section 6
Section 7
Section 8
Section 9
Section 10
Section 11
Section 12

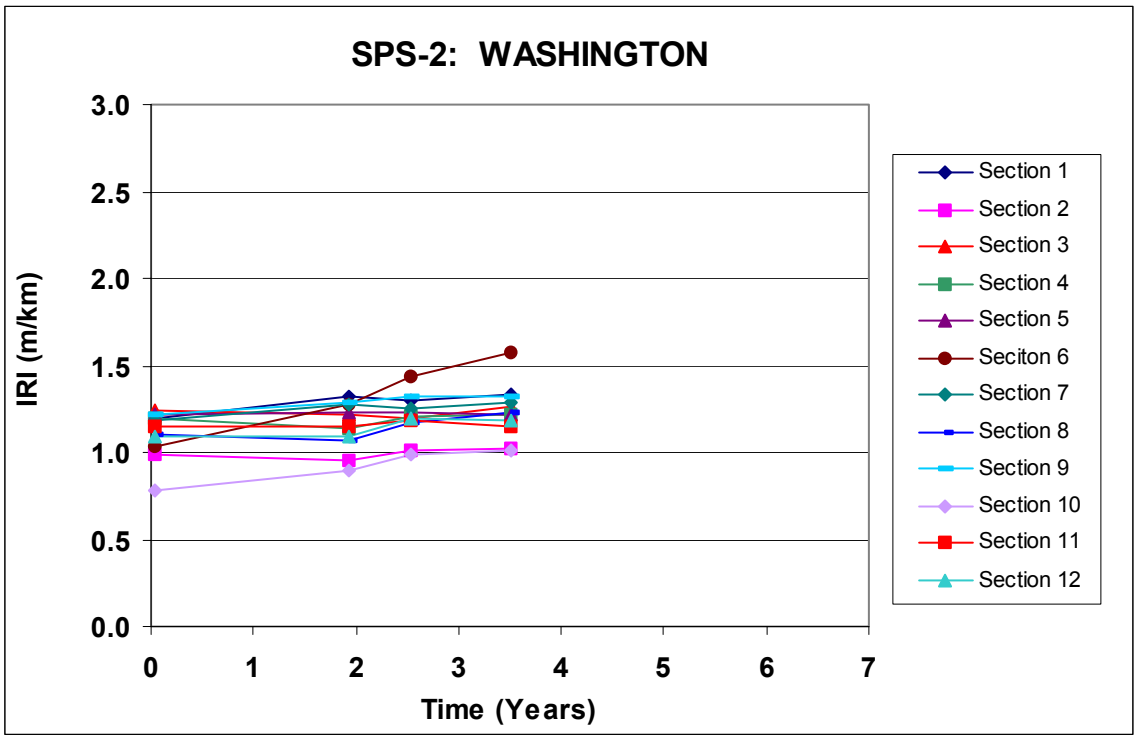
SPS-2: WASHINGTON
IRI (m/km)
3.0
2.5
2.0
1.5
1.0
0.5
0.0
0
1
2
3
4
5
6
7
Time (Years)
Section 1
Section 2
Section 3
Section 4
Section 5
Seciton 6
Section 7
Section 8
Section 9
Section 10
Section 11
Section 12

APPENDIX C

IRI PLOTS FOR SPS-5 PROJECTS

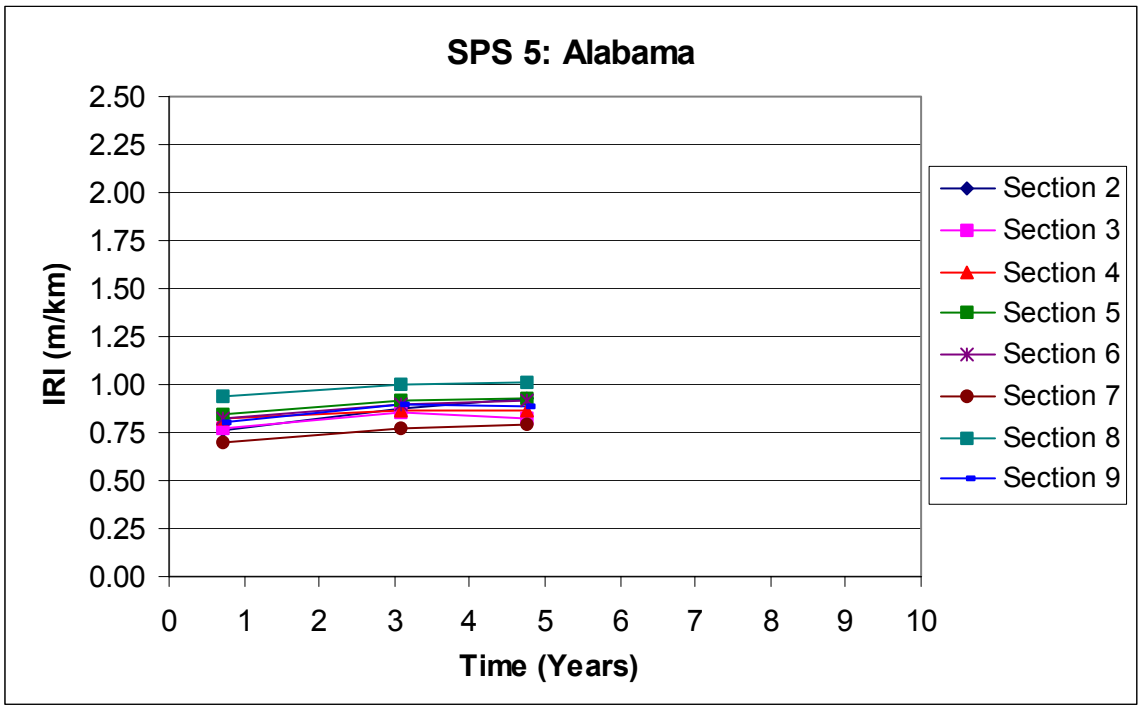
SPS 5: Alabama
IRI (m/km)
2.50
2.25
2.00
1.75
1.50
1.25
1.00
0.75
0.50
0.25
0.00
0
1
2
3
4
5
6
7
8
9
10
Time (Years)
Section 2
Section 3
Section 4
Section 5
Section 6
Section 7
Section 8
Section 9

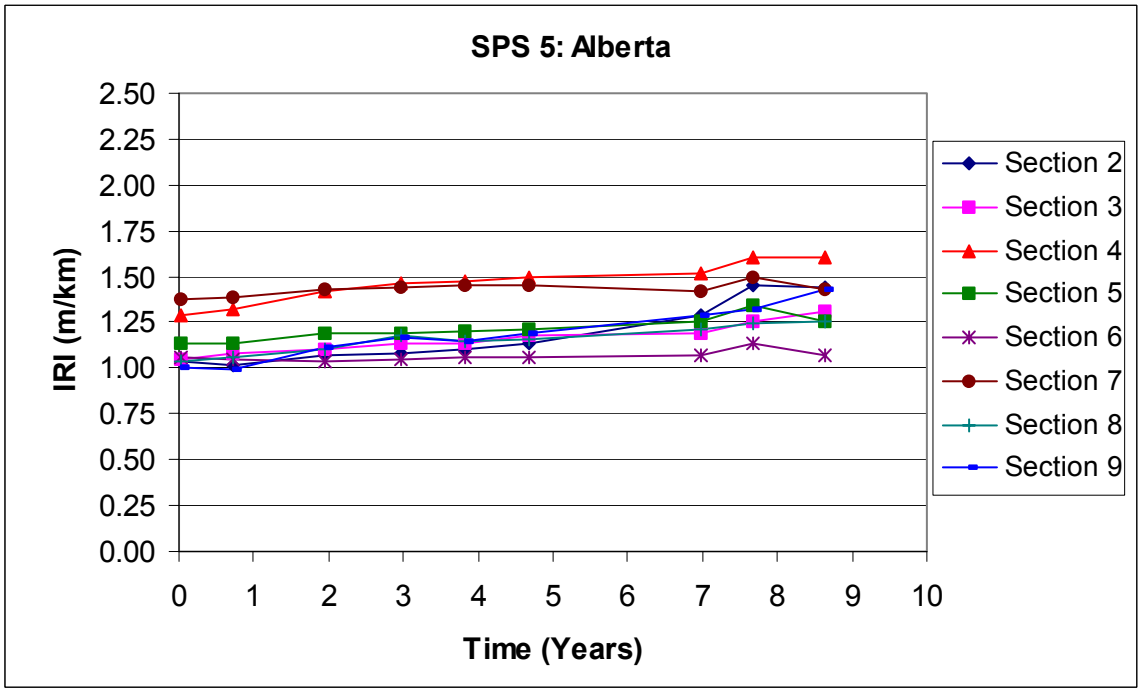
SPS 5: Alberta
IRI (m/km)
2.50
2.25
2.00
1.75
1.50
1.25
1.00
0.75
0.50
0.25
0.00
0
1
2
3
4
5
6
7
8
9
10
Time (Years)
Section 2
Section 3
Section 4
Section 5
Section 6
Section 7
Section 8
Section 9

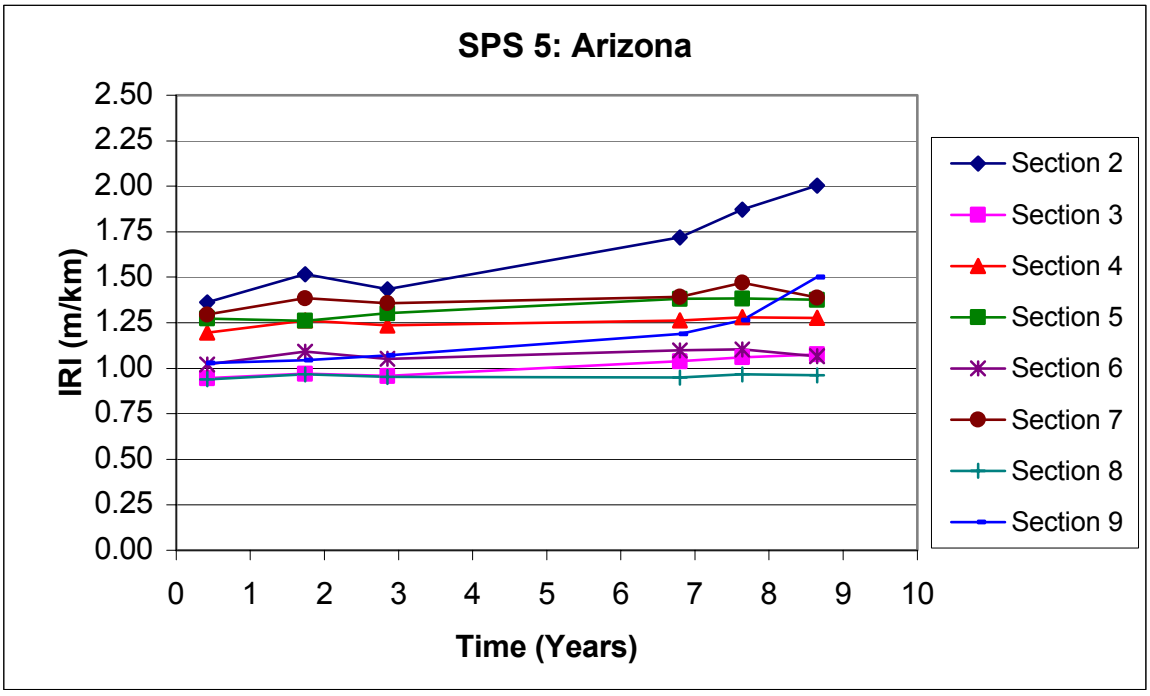
SPS 5: Arizona
IRI (m/km)
2.50
2.25
2.00
1.75
1.50
1.25
1.00
0.75
0.50
0.25
0.00
0
1
2
3
4
5
6
7
8
9
10
Time (Years)
Section 2
Section 3
Section 4
Section 5
Section 6
Section 7
Section 8
Section 9

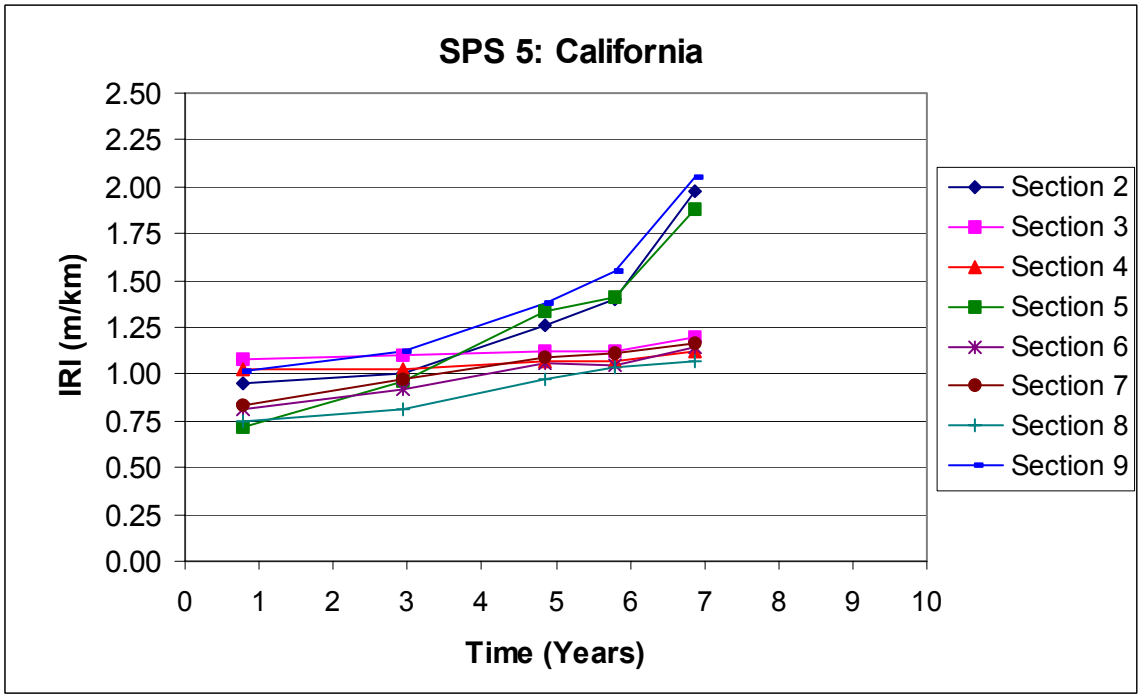
SPS 5: California
IRI (m/km)
2.50
2.25
2.00
1.75
1.50
1.25
1.00
0.75
0.50
0.25
0.00
0
1
2
3
4
5
6
7
8
9
10
Time (Years)
Section 2
Section 3
Section 4
Section 5
Section 6
Section 7
Section 8
Section 9

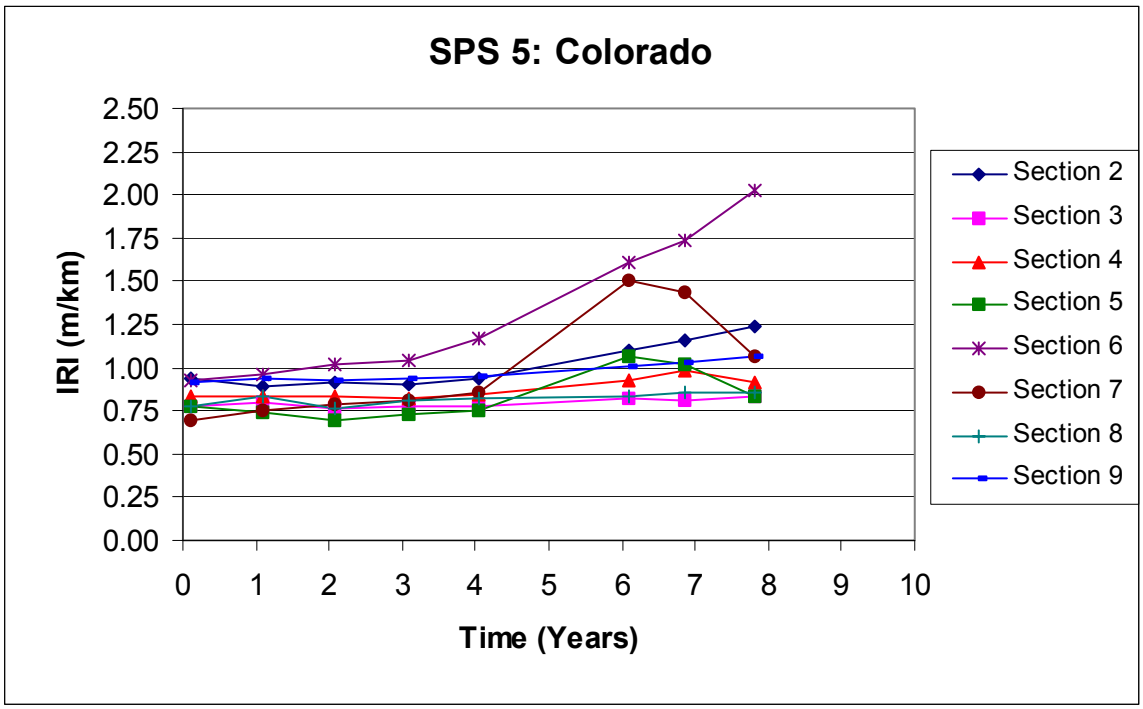
SPS 5: Colorado
IRI (m/km)
2.50
2.25
2.00
1.75
1.50
1.25
1.00
0.75
0.50
0.25
0.00
0
1
2
3
4
5
6
7
8
9
10
Time (Years)
Section 2
Section 3
Section 4
Section 5
Section 6
Section 7
Section 8
Section 9

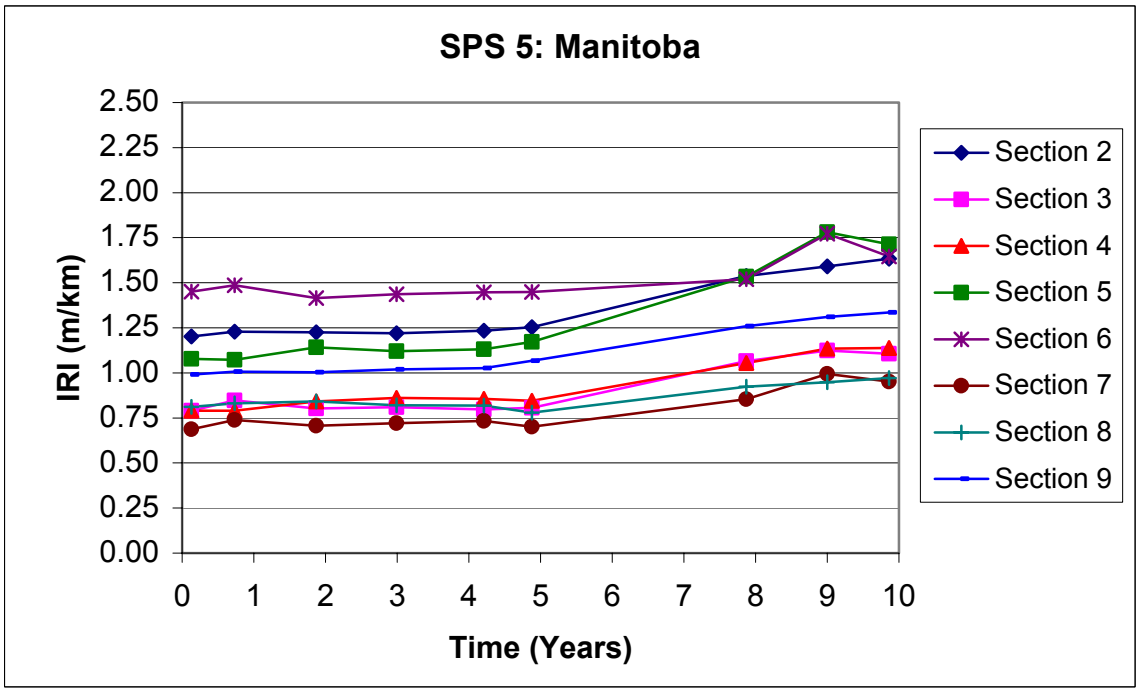
SPS 5: Manitoba
IRI (m/km)
2.50
2.25
2.00
1.75
1.50
1.25
1.00
0.75
0.50
0.25
0.00
0
1
2
3
4
5
6
7
8
9
10
Time (Years)
Section 2
Section 3
Section 4
Section 5
Section 6
Section 7
Section 8
Section 9

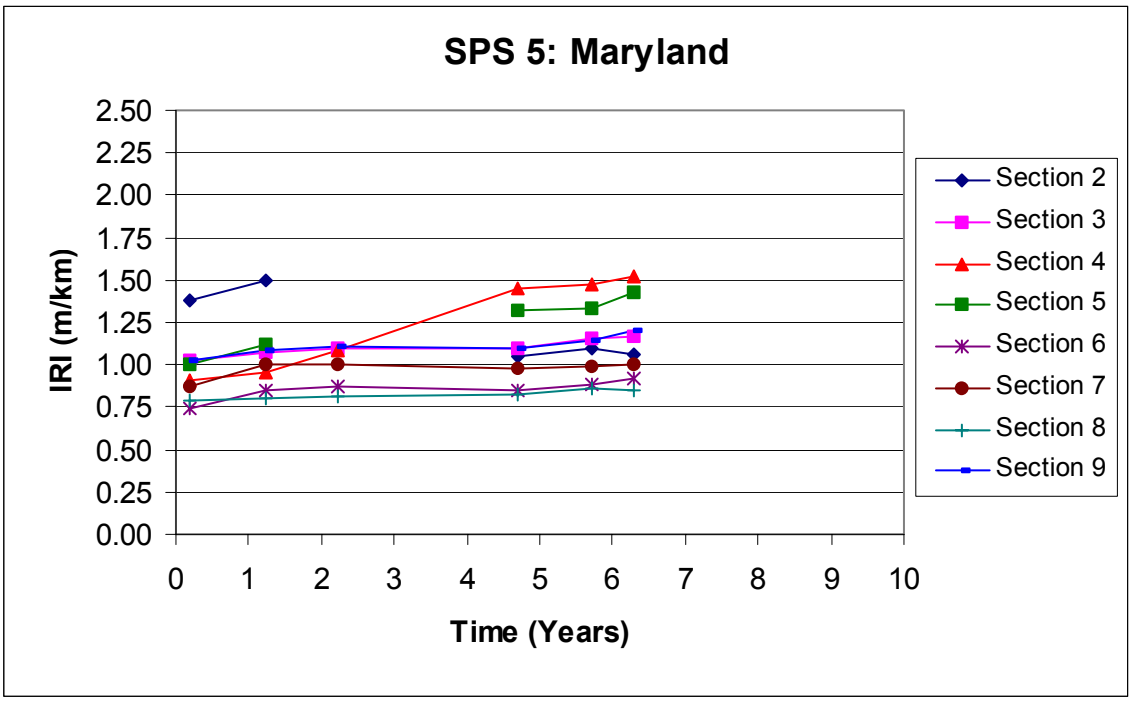
SPS 5: Maryland
IRI (m/km)
2.50
2.25
2.00
1.75
1.50
1.25
1.00
0.75
0.50
0.25
0.00
0
1
2
3
4
5
6
7
8
9
10
Time (Years)
Section 2
Section 3
Section 4
Section 5
Section 6
Section 7
Section 8
Section 9

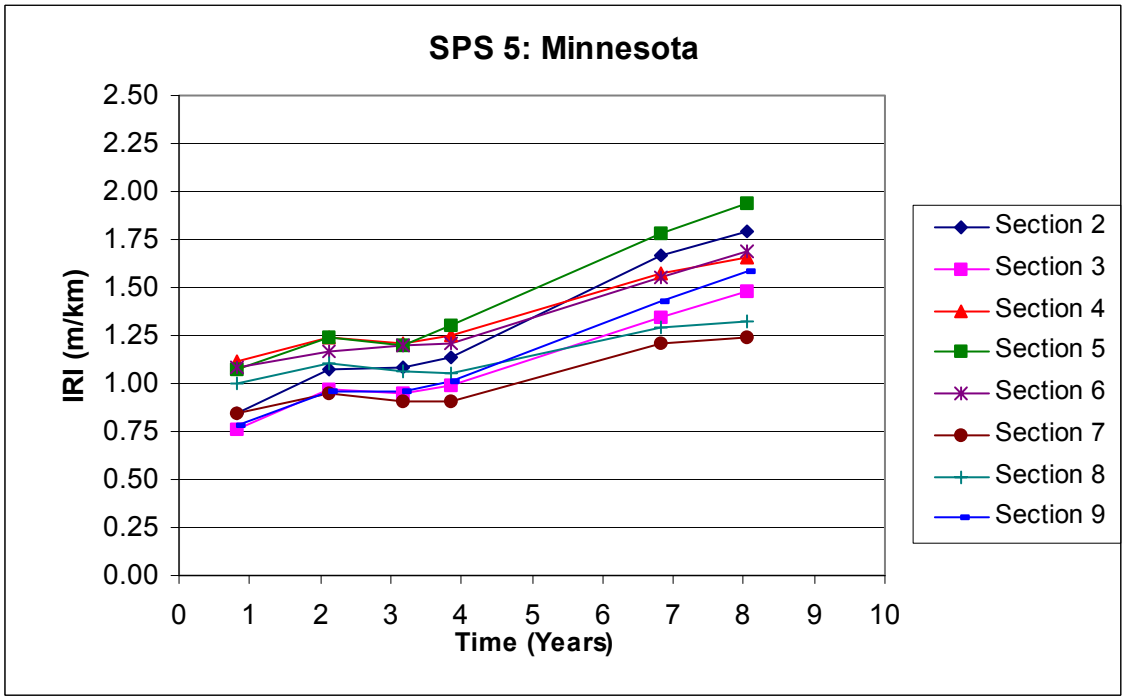
SPS 5: Minnesota
IRI (m/km)
2.50
2.25
2.00
1.75
1.50
1.25
1.00
0.75
0.50
0.25
0.00
0
1
2
3
4
5
6
7
8
9
10
Time (Years)
Section 2
Section 3
Section 4
Section 5
Section 6
Section 7
Section 8
Section 9

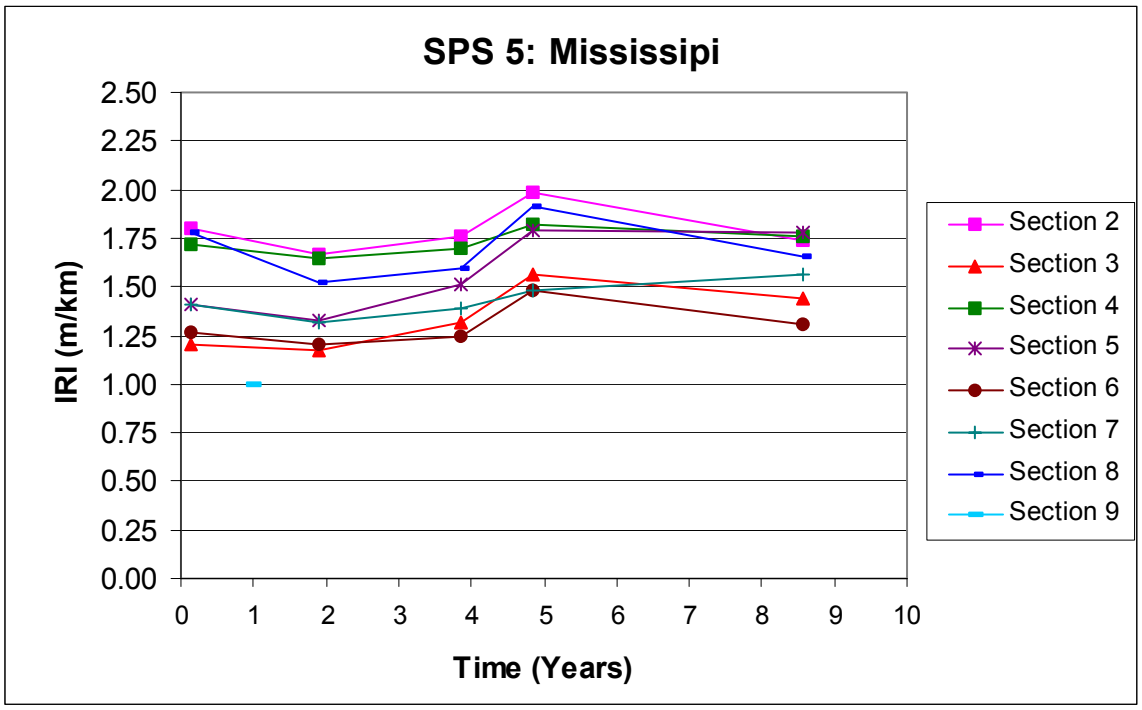
SPS 5: Mississipi
IRI (m/km)
2.50
2.25
2.00
1.75
1.50
1.25
1.00
0.75
0.50
0.25
0.00
0
1
2
3
4
5
6
7
8
9
10
Time (Years)
Section 2
Section 3
Section 4
Section 5
Section 6
Section 7
Section 8
Section 9

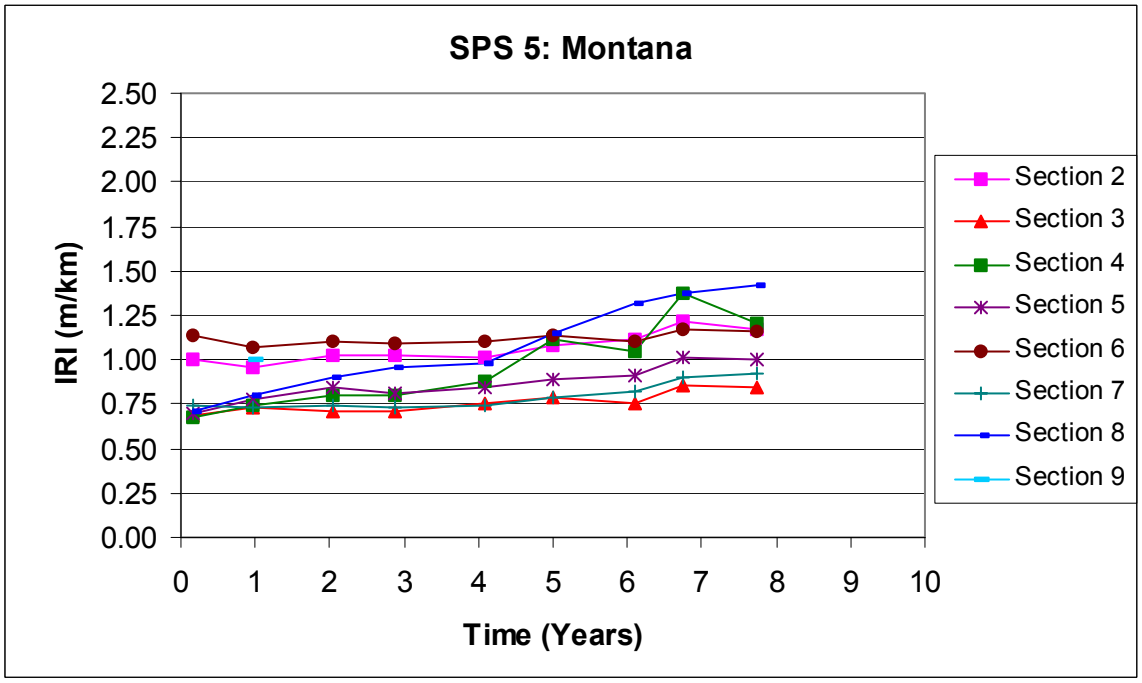
SPS 5: Montana
IRI (m/km)
2.50
2.25
2.00
1.75
1.50
1.25
1.00
0.75
0.50
0.25
0.00
0
1
2
3
4
5
6
7
8
9
10
Time (Years)
Section 2
Section 3
Section 4
Section 5
Section 6
Section 7
Section 8
Section 9

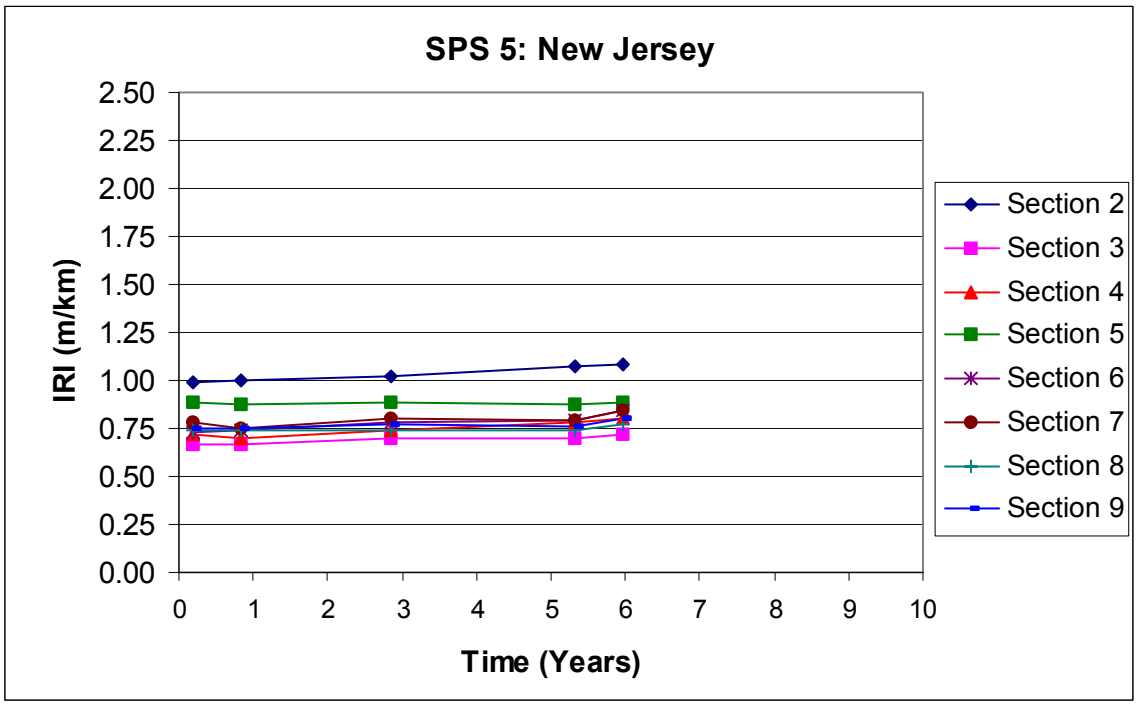
SPS 5: New Jersey
IRI (m/km)
2.50
2.25
2.00
1.75
1.50
1.25
1.00
0.75
0.50
0.25
0.00
0
1
2
3
4
5
6
7
8
9
10
Time (Years)
Section 2
Section 3
Section 4
Section 5
Section 6
Section 7
Section 8
Section 9

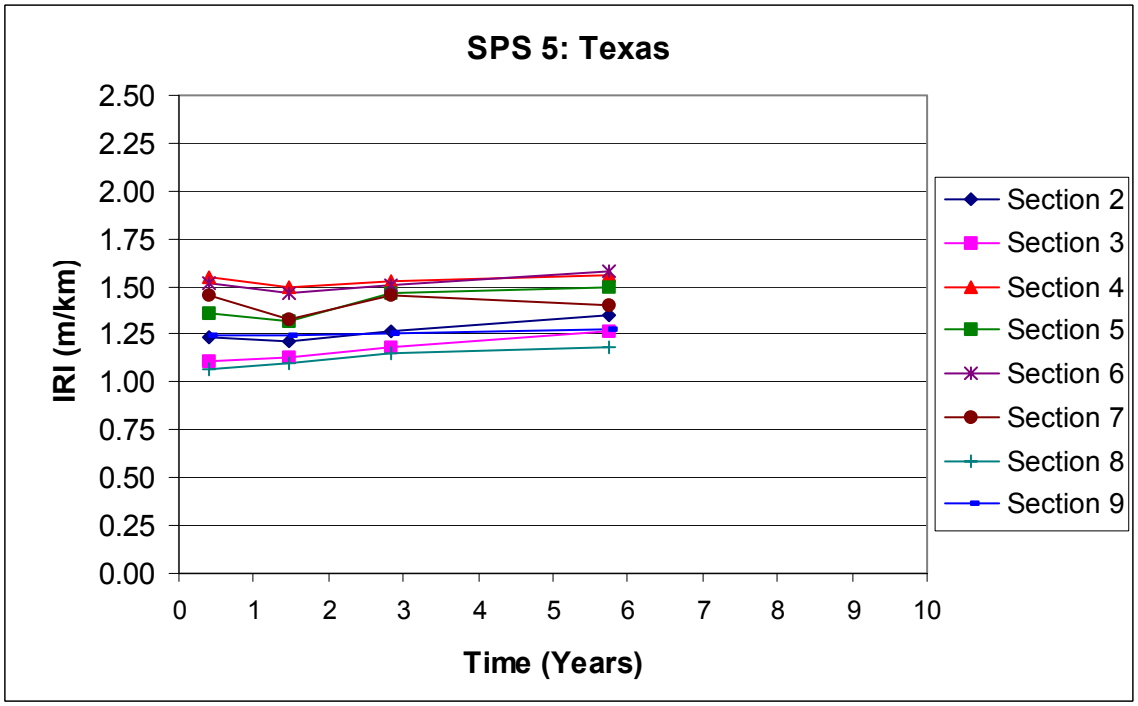
SPS 5: Texas
IRI (m/km)
2.50
2.25
2.00
1.75
1.50
1.25
1.00
0.75
0.50
0.25
0.00
0
1
2
3
4
5
6
7
8
9
10
Time (Years)
Section 2
Section 3
Section 4
Section 5
Section 6
Section 7
Section 8
Section 9

APPENDIX D

IRI PLOTS FOR SPS-6 PROJECTS

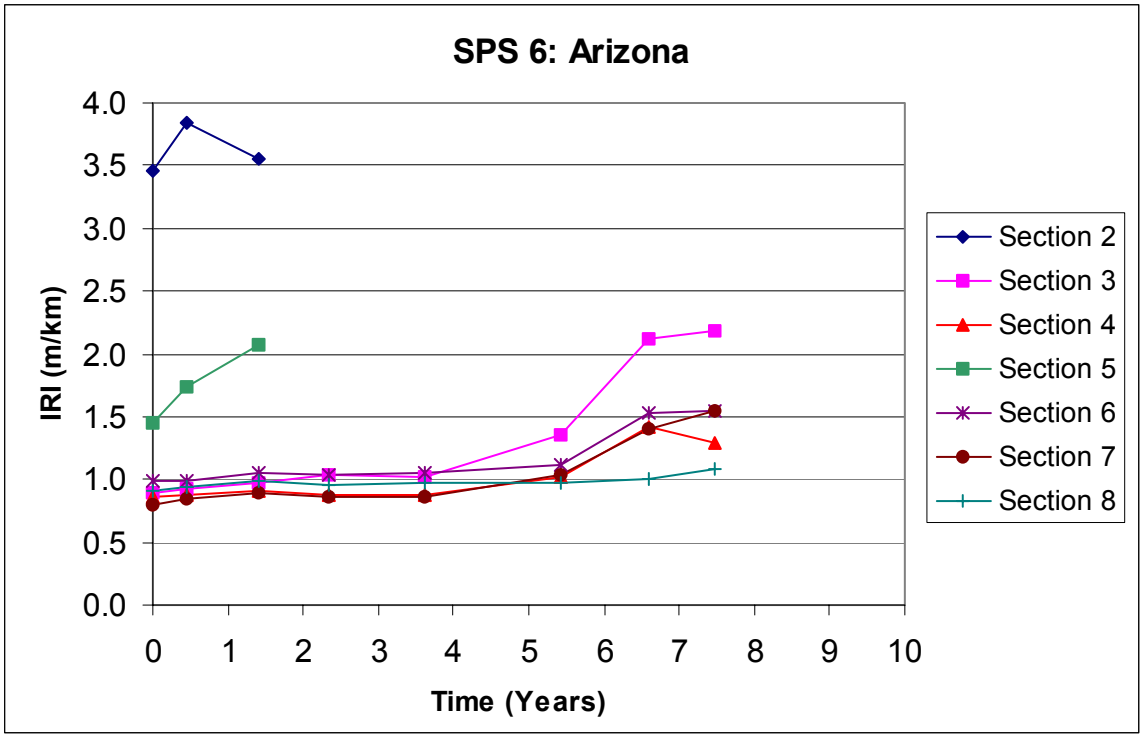
SPS 6: Arizona
IRI (m/km)
4.0
3.5
3.0
2.5
2.0
1.5
1.0
0.5
0.0
0
1
2
3
4
5
6
7
8
9
10
Time (Years)
Section 2
Section 3
Section 4
Section 5
Section 6
Section 7
Section 8

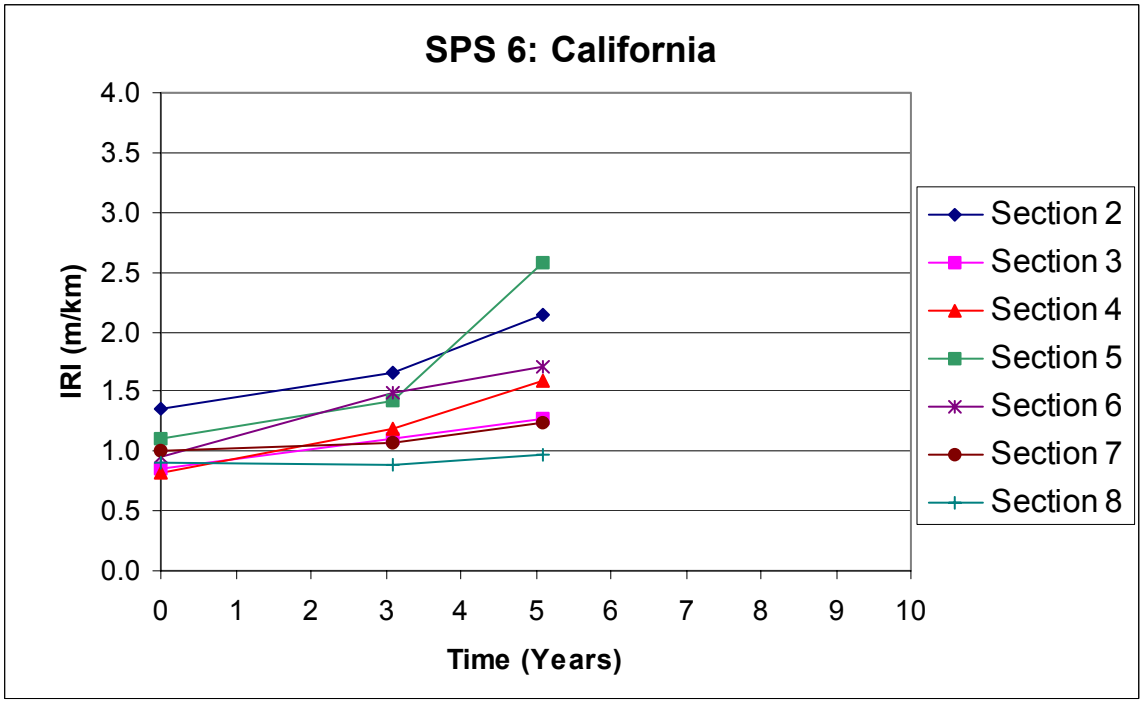
SPS 6: California
IRI (m/km)
4.0
3.5
3.0
2.5
2.0
1.5
1.0
0.5
0.0
0
1
2
3
4
5
6
7
8
9
10
Time (Years)
Section 2
Section 3
Section 4
Section 5
Section 6
Section 7
Section 8

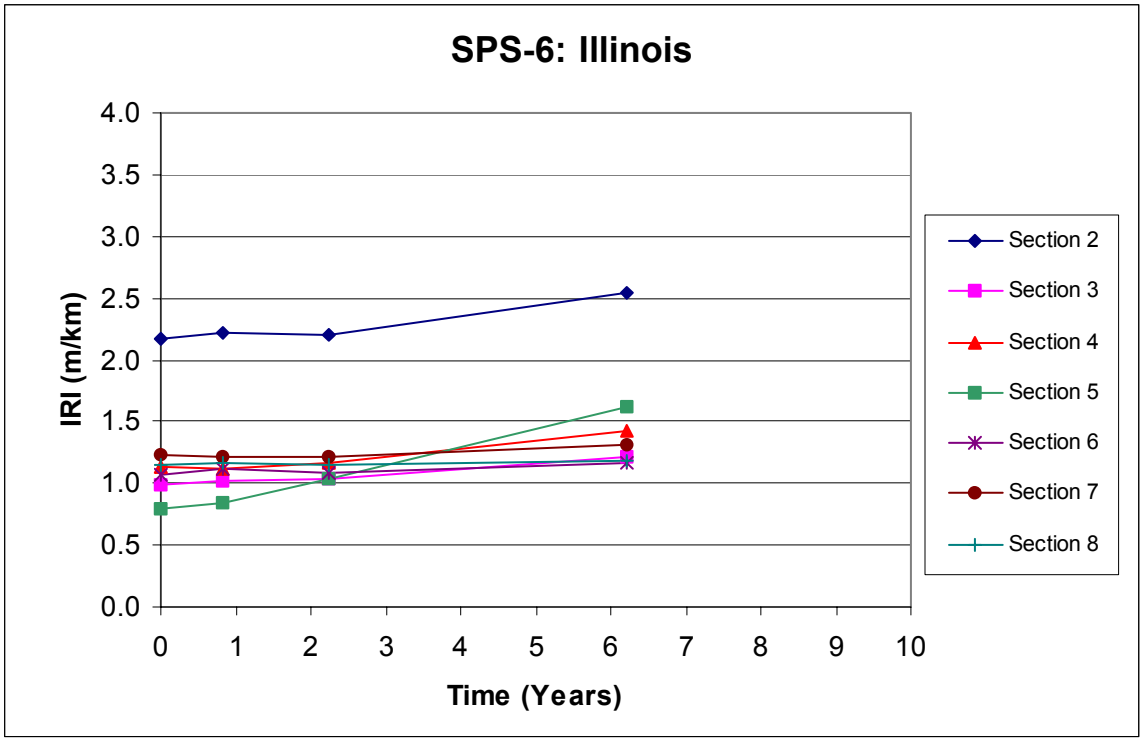
SPS-6: Illinois
IRI (m/km)
4.0
3.5
3.0
2.5
2.0
1.5
1.0
0.5
0.0
0
1
2
3
4
5
6
7
8
9
10
Time (Years)
Section 2
Section 3
Section 4
Section 5
Section 6
Section 7
Section 8

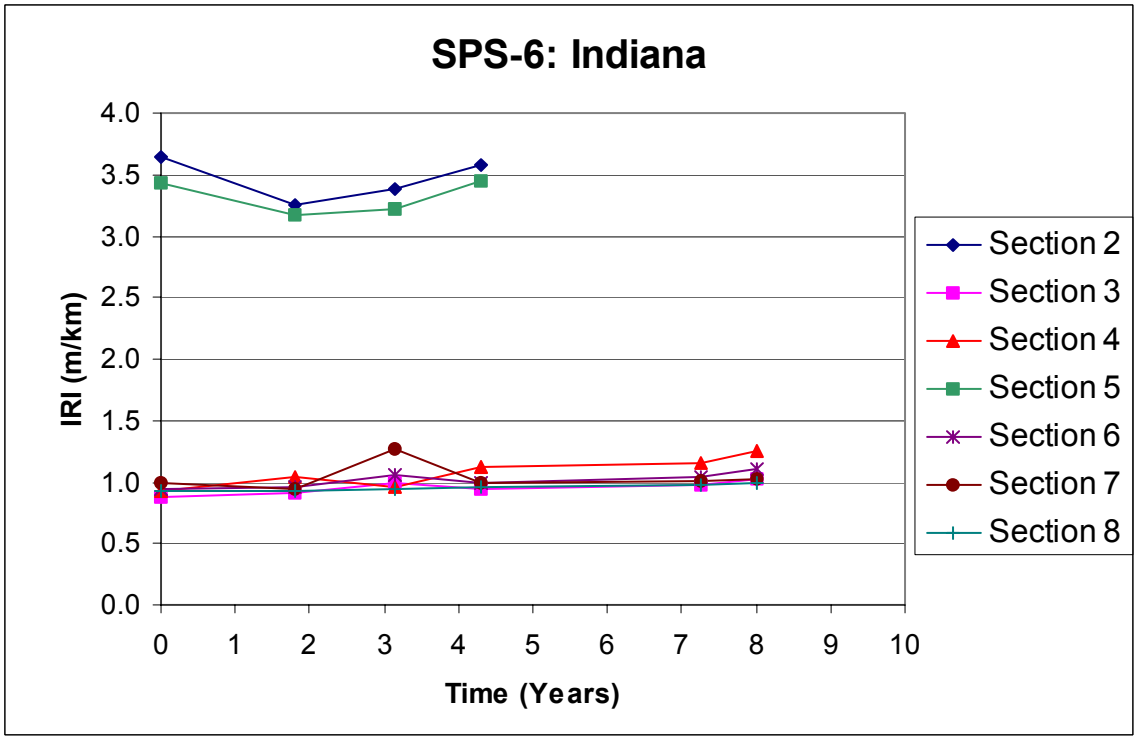
SPS-6: Indiana
IRI (m/km)
4.0
3.5
3.0
2.5
2.0
1.5
1.0
0.5
0.0
0
1
2
3
4
5
6
7
8
9
10
Time (Years)
Section 2
Section 3
Section 4
Section 5
Section 6
Section 7
Section 8

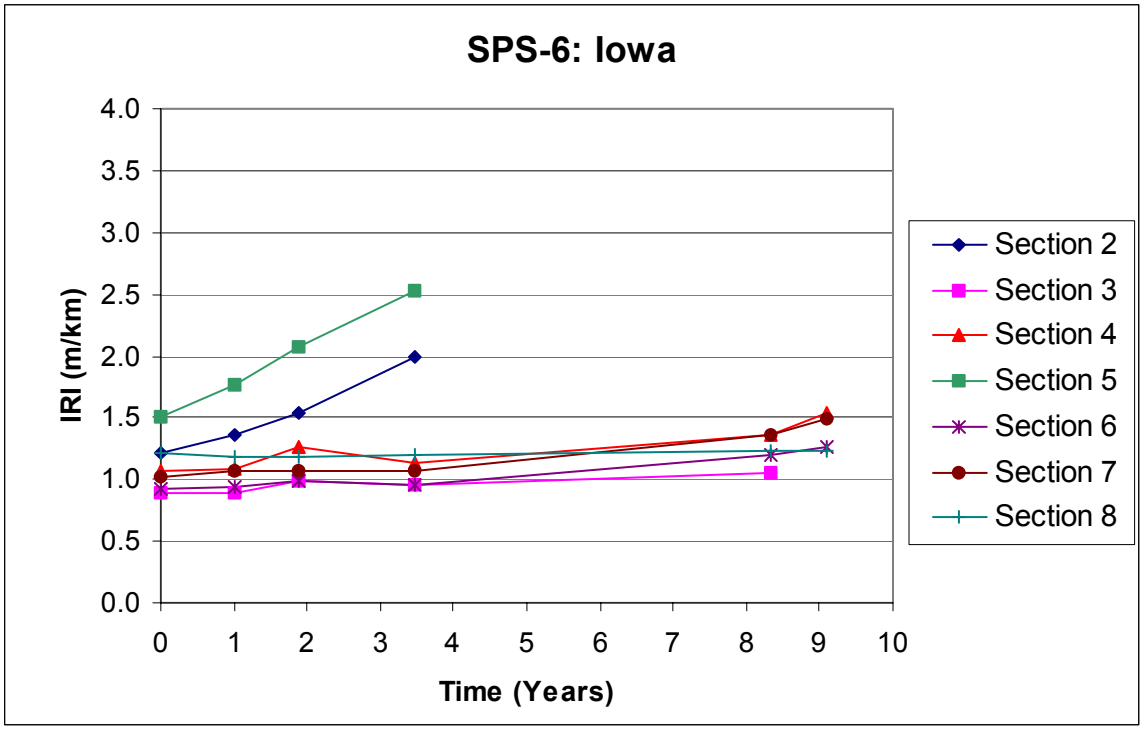
SPS-6: Iowa
IRI (m/km)
4.0
3.5
3.0
2.5
2.0
1.5
1.0
0.5
0.0
0
1
2
3
4
5
6
7
8
9
10
Time (Years)
Section 2
Section 3
Section 4
Section 5
Section 6
Section 7
Section 8

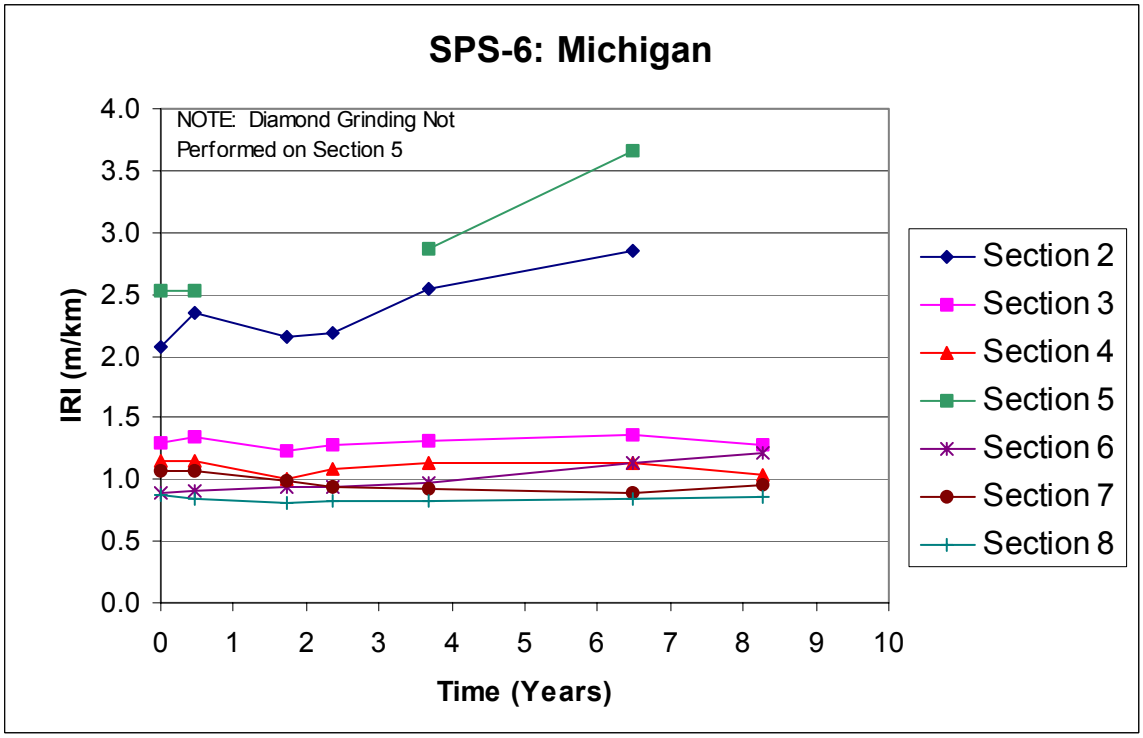
SPS-6: Michigan
NOTE: Diamond Grinding Not Performed on Section 5
IRI (m/km)
4.0
3.5
3.0
2.5
2.0
1.5
1.0
0.5
0.0
0
1
2
3
4
5
6
7
8
9
10
Time (Years)
Section 2
Section 3
Section 4
Section 5
Section 6
Section 7
Section 8

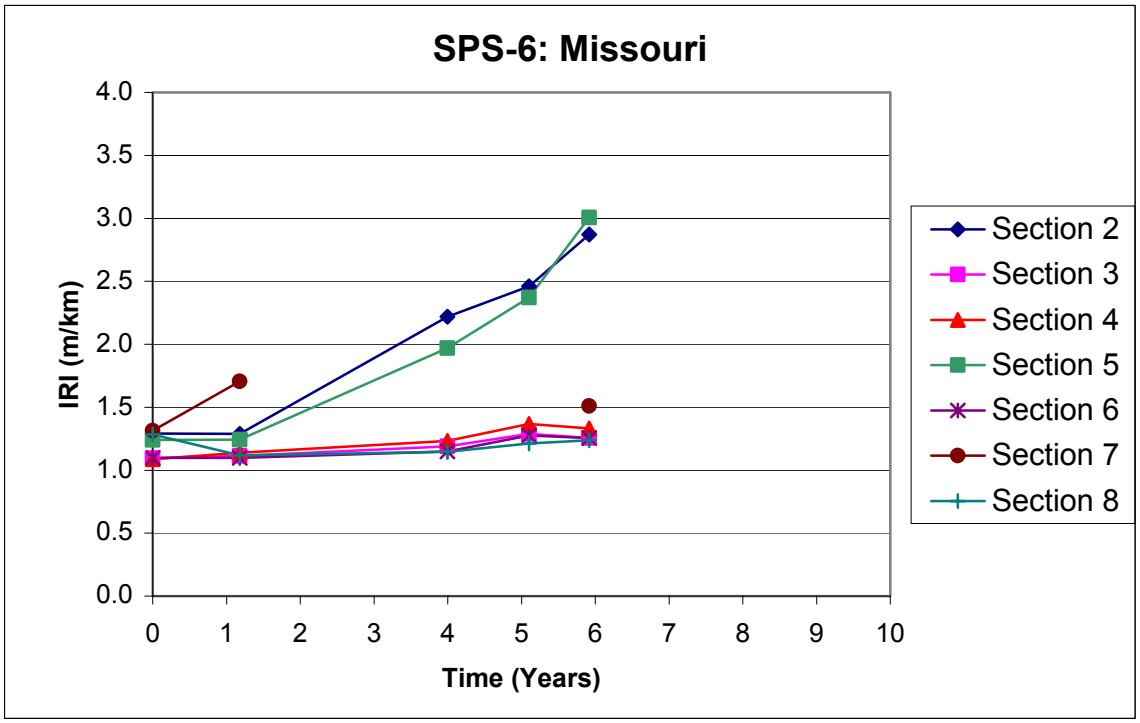
SPS-6: Missouri
IRI (m/km)
4.0
3.5
3.0
2.5
2.0
1.5
1.0
0.5
0.0
0
1
2
3
4
5
6
7
8
9
10
Time (Years)
Section 2
Section 3
Section 4
Section 5
Section 6
Section 7
Section 8

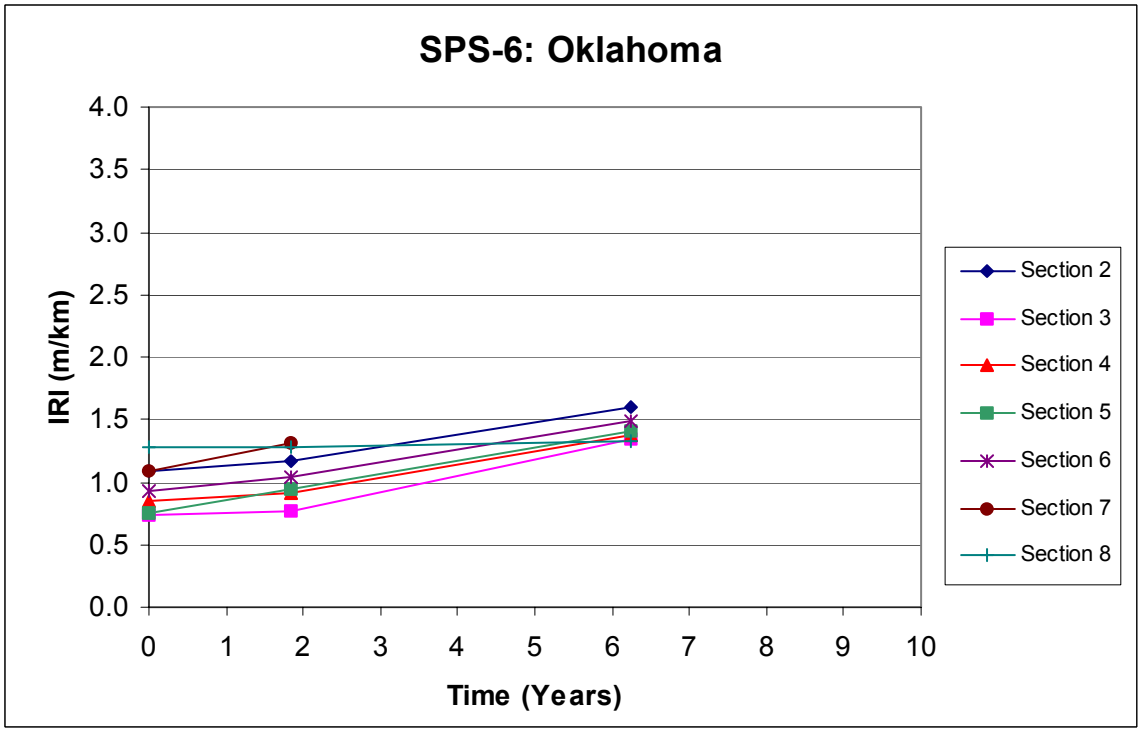
SPS-6: Oklahoma
IRI (m/km)
4.0
3.5
3.0
2.5
2.0
1.5
1.0
0.5
0.0
0
1
2
3
4
5
6
7
8
9
10
Time (Years)
Section 2
Section 3
Section 4
Section 5
Section 6
Section 7
Section 8

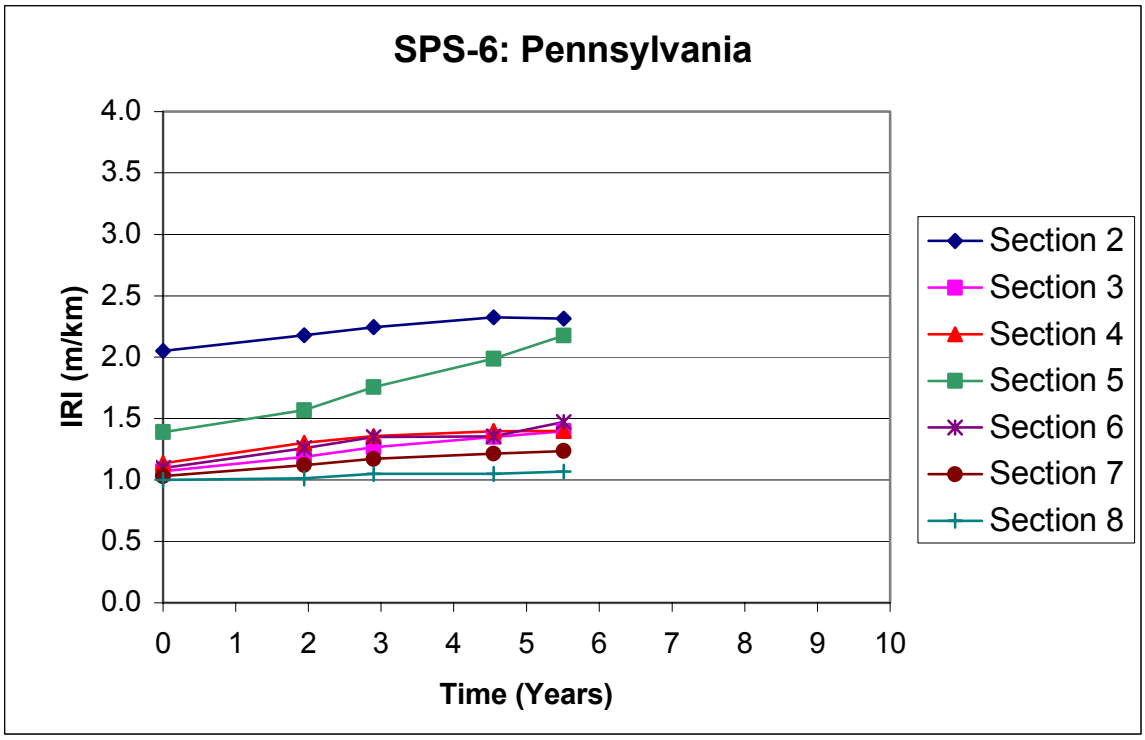
SPS-6: Pennsylvania
IRI (m/km)
4.0
3.5
3.0
2.5
2.0
1.5
1.0
0.5
0.0
0
1
2
3
4
5
6
7
8
9
10
Time (Years)
Section 2
Section 3
Section 4
Section 5
Section 6
Section 7
Section 8

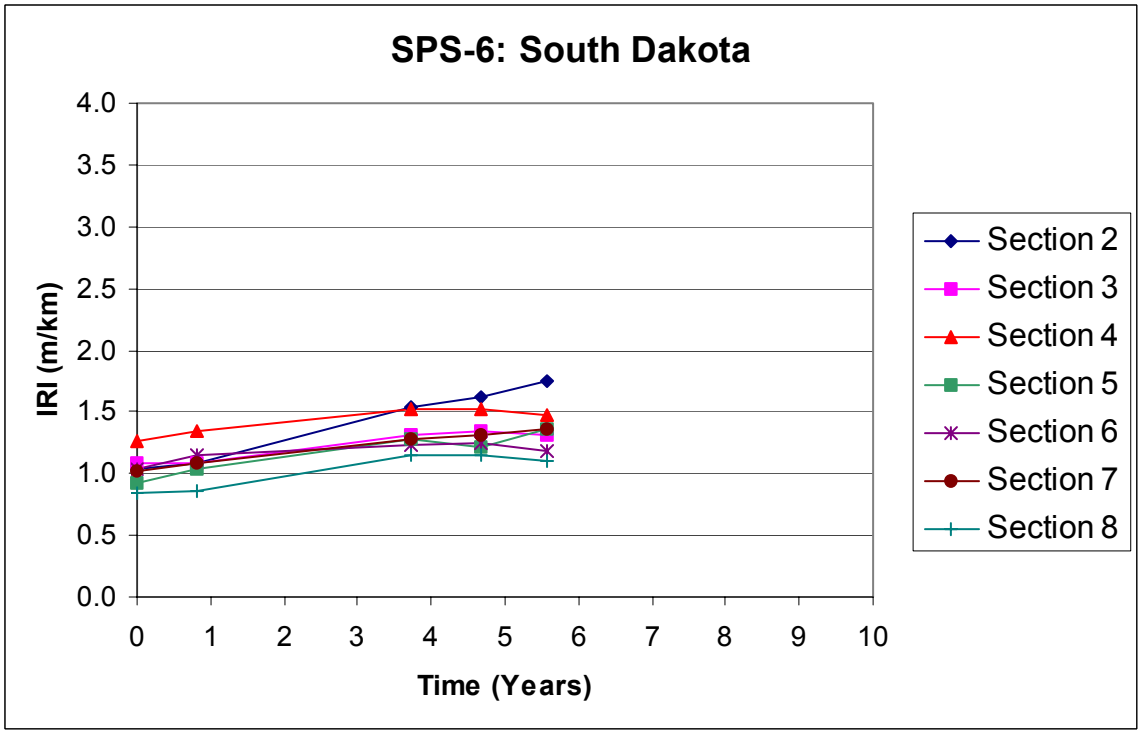
SPS-6: South Dakota
IRI (m/km)
4.0
3.5
3.0
2.5
2.0
1.5
1.0
0.5
0.0
0
1
2
3
4
5
6
7
8
9
10
Time (Years)
Section 2
Section 3
Section 4
Section 5
Section 6
Section 7
Section 8

APPENDIX E

GPS-1 MODELS

In a previous study on roughness at LTPP sites that was performed by Perera et al (1), a non-linear optimization method was used to develop models to predict roughness development. The modeling approach that was adopted in this study was to develop a model that would back predict the initial roughness of the section based on the time sequence IRI data and also predict the actual IRI value at any point in time. In the modeling, a growth rate parameter was modeled such that the key parameters affecting both the initial IRI and growth of the IRI could be determined. The model form that was used for flexible pavements was:

$$IRI(t) = IRI_0 e^{\left[\frac{r_0 t^A}{B}\right]}$$

Where:

IRI0	=	estimated initial IRI (after some initial traffic loading)
	=	f(pavement structure and subgrade properties)
r0	=	growth rate constant
	=	f(climate, traffic, subgrade, layer properties of the pavement)
t	=	time in years
e	=	the exponential function
A and B	=	modeling constants

In this model, IRI0 represents the initial IRI value of the pavement. The initial IRI value is assumed to be the IRI value of the pavement after it has been constructed and it has been opened to traffic and has been subjected to some initial traffic loading. The initial IRI is back predicted as a non linear function of the structural properties of the pavement and subgrade properties. The growth rate is modeled as a non linear function of time, structural properties of the pavement, subgrade properties, climate parameters, and traffic loading. The modeling utilized a non-linear optimization methodology referred to as the Reduced Gradient Algorithm (GRG2). A detailed description of this modeling approach is described by Perera et al [(1)].

In this research project, the models that were previously developed were reviewed with the new time-sequence data and a new set of models were developed. The following models were developed for the GPS-1 sections.

1. Dry freeze regions.
2. Dry no-freeze regions.
3. Wet freeze, for sections on subgrade that has less than 20 percent material passing the no. 200 sieve.
4. Wet freeze, for sections on subgrade that has between 20 and 50 percent material passing the no. 200 sieve.
5. Wet freeze, for sections on subgrade that has greater than 50 percent material passing the no. 200 sieve.
6. Wet no-freeze, for sections on subgrade that has less than 20 percent material passing the no. 200 sieve.
7. Wet no-freeze, for sections on subgrade that has between 20 and 50 percent material passing the no. 200 sieve.
8. Wet no-freeze, for sections on subgrade that has more than 50 percent material passing the no. 200 sieve.

The developed models are presented in figures E-1 through E-8. The variables that are used in these models are described in table E1.

Table E1. Description of variables used in models.

Variable	Description
%AcinSN	Fraction of structural number (SN) by asphalt layers.
%Sand	Percent sand in the subgrade material.
ACBulkSG	Bulk specific gravity for the asphalt concrete.
ACcontent	Asphalt cement content in bituminous mixture, %.
Acthick	Asphalt concrete thickness, in.
AnnPrecip	Annual precipitation, in.
Basewash	Loss by wash for the aggregate base material, %.
Days0.5+	Days per year having more than 0.5 inch of precipitation.
Days90+	Days per year having temperatures over 90 F(.
Dayswet	Days per year having more than 0.1 inch of precipitation.
FrzThwCyc	Number of freeze thaw cycles per year.
FZI	Corps. Of Engineers freeze index, F(-days/yr.
KESAL/yr	Kilo-ESAL per year over the design life.
LI	Liquidity Index for the subgrade material.
LL	liquid limit for the subgrade material.
P200	Percent passing the #200 sieve for the subgrade material.
PI	Plasticity Index for the subgrade material.
Po	Overburden pressure on the subgrade, psf.
SN	AASHTO-based structural number.
Snowcover	Days per year with snow cover.
Snowfall	Annual snowfall amount, in.
w%	Moisture content in subgrade, % by weight.

$$IRI(t) = IRI_0 e^{r_0 \frac{t^U}{V}}$$

$IRI_0 = A(P200)^B + C(P_o)^D + E(\%Sand)^F + G(\%ACinSN)^H + I(ACthick)^J$

$r_0 = [K(KESAL/yr)^L / M(SN)^N] + O(AnnPrecip/1000)^P + Q([(FZI)(P200)(w\%)/P_o]/1E07)^R + S([(\%ACinSN)(P200)(AnnPrecip)]/1000)^T + W(Snowcover/100)^X$

A=	-2802.940378
B=	0.003242708
C=	-216116.2798
D=	-2.348026827
E=	-0.463580
F=	0.80487146
G=	27.60660283
H=	1009.402741
I=	2887.838423
J=	-0.002256239
K=	20
L=	1
M=	498.7543032
N=	4.1270549
O=	-49463428.62
P=	2.716853757
Q=	-105555134.7
R=	268.9428275
S=	2897.459767
T=	0.61101832
U=	0.494697673
V=	5875.36145
W=	1008.873718
X=	1.611560219

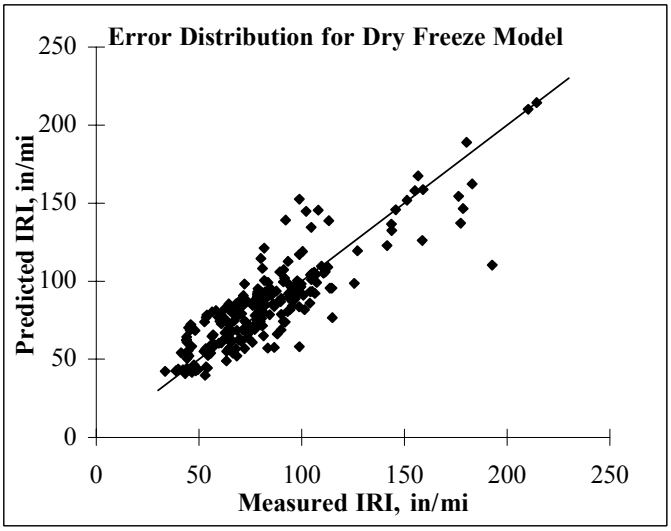

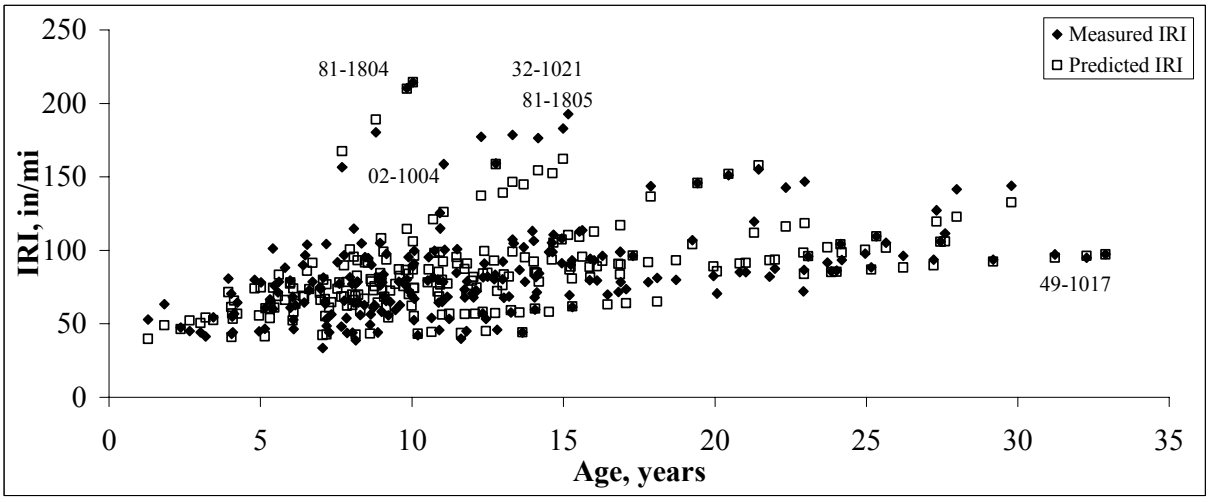

$r^2 = 0.77$, Std. Error = 15.5 in/mi, n=234

1 in/mi = 0.0158 m/km

Figure E-1. GPS-1 dry freeze IRI model.

$$IRI(t) = IRI_0 e^{r_0 \frac{t^S}{T}}$$

$IRI_0 = A(P200/P_o)^B+C(P_o)^D+E(ACThick)^F+G(SN)^H$

$r_0 = [I(KESAL/yr)^J/K(SN)^L+M(AnnPrecip(1+FrzThwCyc)/P_o)^N+ O(FZI+1)^P+Q(P200/P_o)^R+W(ACBulkSG)^X+Y(ACcontent)^Z]/1000$

A=	-0.717582273
B=	-0.998834892
C=	-425437.7902
D=	-1.859139296
E=	134.7405872
F=	-0.226609317
G=	2764.323794
H=	-6.153565853
I=	1173.881628
J=	1.001046117
K=	1
L=	9.88537867
M=	-22.0000
N=	0.01
O=	0.000337316
P=	2.512347581
Q=	6.856926717
R=	-0.83134048
S=	0.81153355
T=	1.056209981
W=	-14.26560139
X=	-1.663635787
Y=	1.3618E-05
Z=	7.362975478

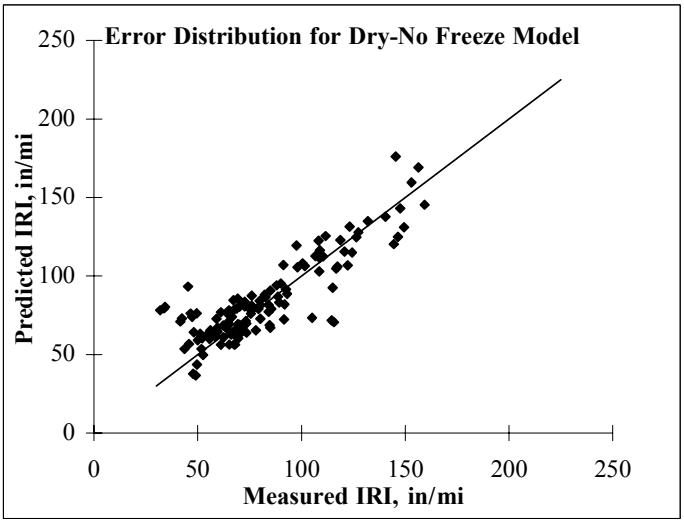

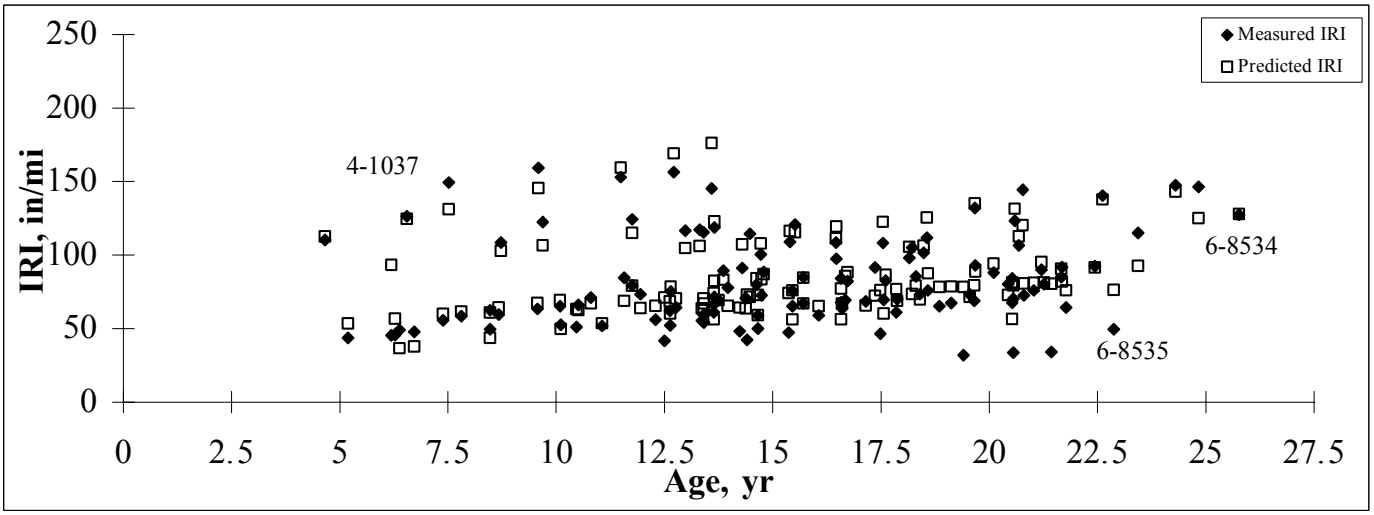

$r^2 = 0.75$, Std. Error = 15.5 in/mi, n=121

1 in/mi = 0.0158 m/km

Figure E-2. GPS-1 dry-no freeze IRI model.

$$IRI(t) = IRI_0 e^{r_0 \frac{t^U}{V}}$$

$IRI_0 = A(P200)^B+C(\%ACinSN)^D+E(ACThick)^F+G(P_o)^H+Y(Basewash)^Z$

$r_0 = [I(KESAL/yr)^J/K(SN)^L+M(FZI)^N+O(FrzThwCyc)^P+ Q(Days0.5+)^R+W(w\%)^X+W(Basewash)^X]/1000$

A=	1.84757E-05
B=	5.178505704
C=	78.86404414
D=	6.034422782
E=	-0.568583607
F=	1.413330208
G=	118.4906028
H=	-0.136439347
I=	117448.8575
J=	1.580745282
K=	65629.45636
L=	0.898753419
M=	4.2049E-06
N=	6.0994
O=	-6868.6833
P=	-0.1380
Q=	424.9595
R=	0.6669
S=	4.2969
T=	-0.2083
U=	0.83476
V=	31.26160316
W=	324.1638723
X=	0.567071508
Y	-5.56754E-07
Z	6.733326557

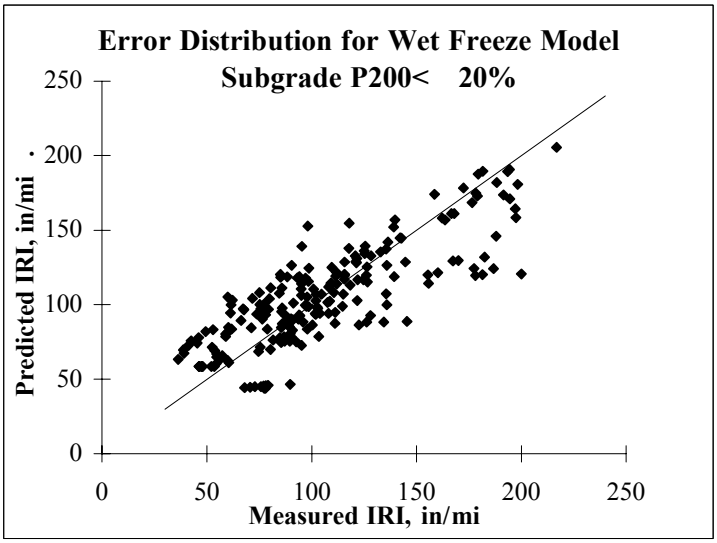

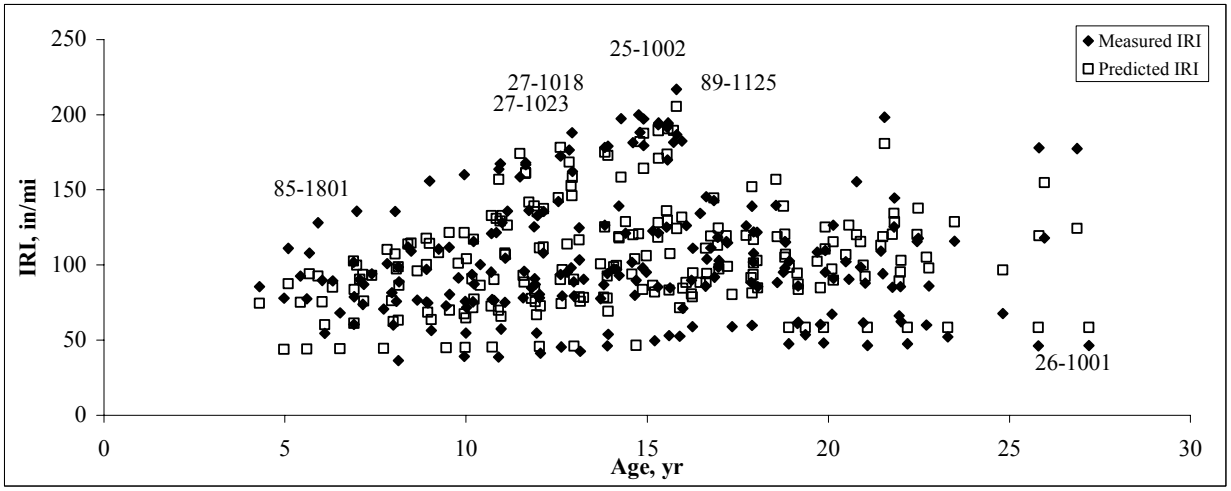

$r^2 = 0.66$, Std. Error = 20.1 in/mi, n=214

1 in/mi = 0.0158 m/km

Figure E-3. GPS-1 wet freeze (P200<20%) IRI model.

$$IRI(t) = IRI_0 e^{r_0 \frac{t^S}{T}}$$

$IRI_0 = A(P200/P_o)^B+C(\%Sand)^D+E(SN)^F+G(\%ACinSN)^H$

$r_0 = [I(KESAL/yr)^J/K(SN)^L+M(FrzThwCyc)^N+O(\%Sand)^P+ Q(P_o)^R]/1000$

A=	47.98758376
B=	3.585951949
C=	334.5737013
D=	-0.478065548
E=	1.729675567
F=	-0.624252196
G=	0.860289289
H=	-4.888487133
I=	0.001
J=	6.462614073
K=	275.5866853
L=	19.95202785
M=	1.58526E-04
N=	2.188617766
O=	-0.597353161
P=	0.353780916
Q=	1224.340057
R=	-1.537572722
S=	1.643895178
T=	0.762023162

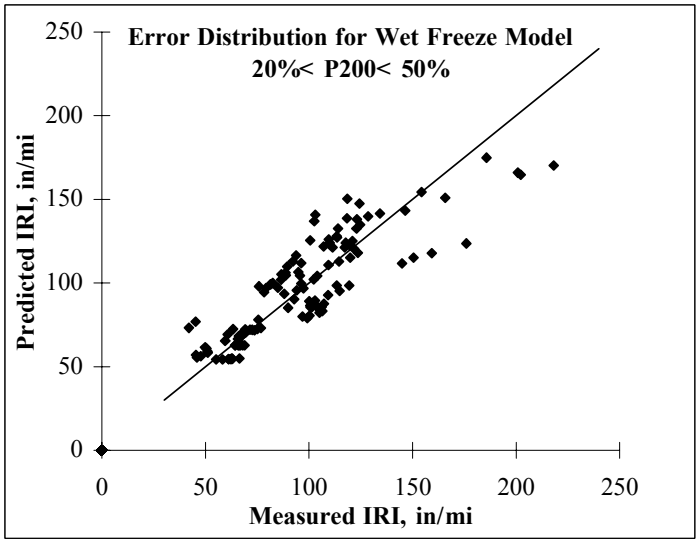

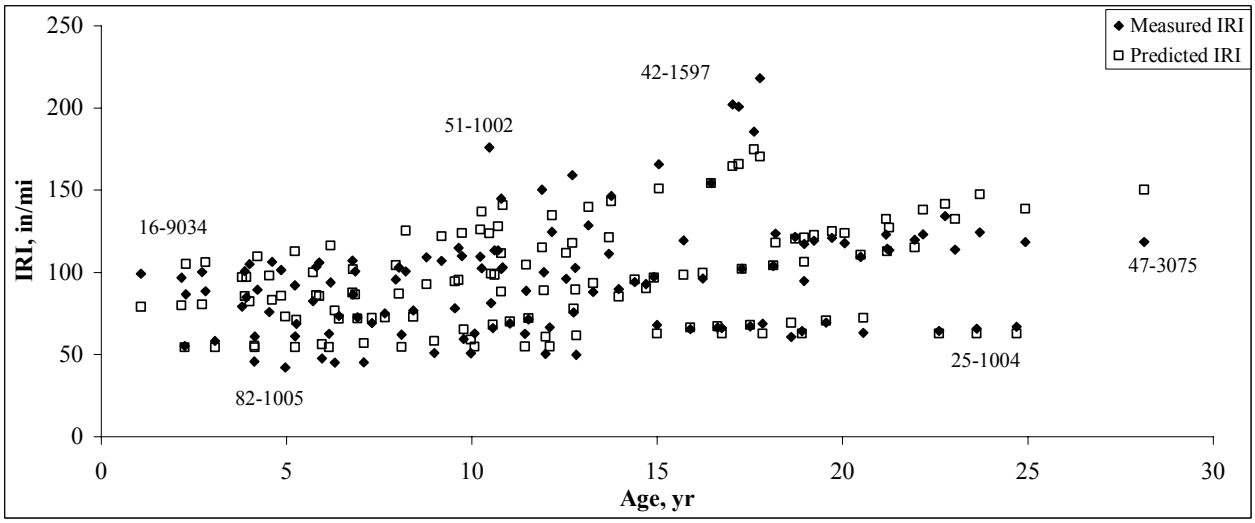

$r^2 = 0.77$, Std. Error = 16.6 in/mi, n=123

1 in/mi = 0.0158 m/km

Figure E-4. GPS-1 wet freeze (20%<P200<50%) IRI model.

$$IRI(t) = IRI_0 e^{r_0 \frac{t^S}{T}}$$

$IRI_0 = A(P200)^B+C(1+PI)^D+E(ACthick)^F+G(w\%)^H$

$r_0 = [I(KESAL/yr)^J/K(SN)^L+M(1+LL)^N+O(w\%(\%Sand)/P_o)^P+ Q(P200)^R+U(Snowfall*25.4)^V]/1000$

A=	130.0353767
B=	-0.1741417
C=	0.426366594
D=	1.337664211
E=	-4.57362E-05
F=	4.52176029
G=	5.53191E+ 03
H=	-24.00727556
I=	15554.28262
J=	1.038662727
K=	1
L=	1.000278427
M=	499.6375074
N=	-4.606587666
O=	4.30558E-06
P=	23.83718933
Q=	3.960422039
R=	-41.99050817
S=	1.01640
T=	47094.70144
U=	1.08989E-06
V=	3.490019358

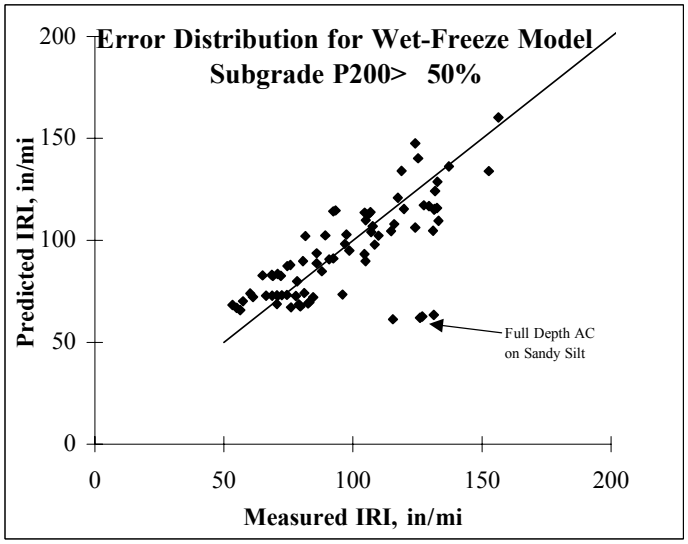

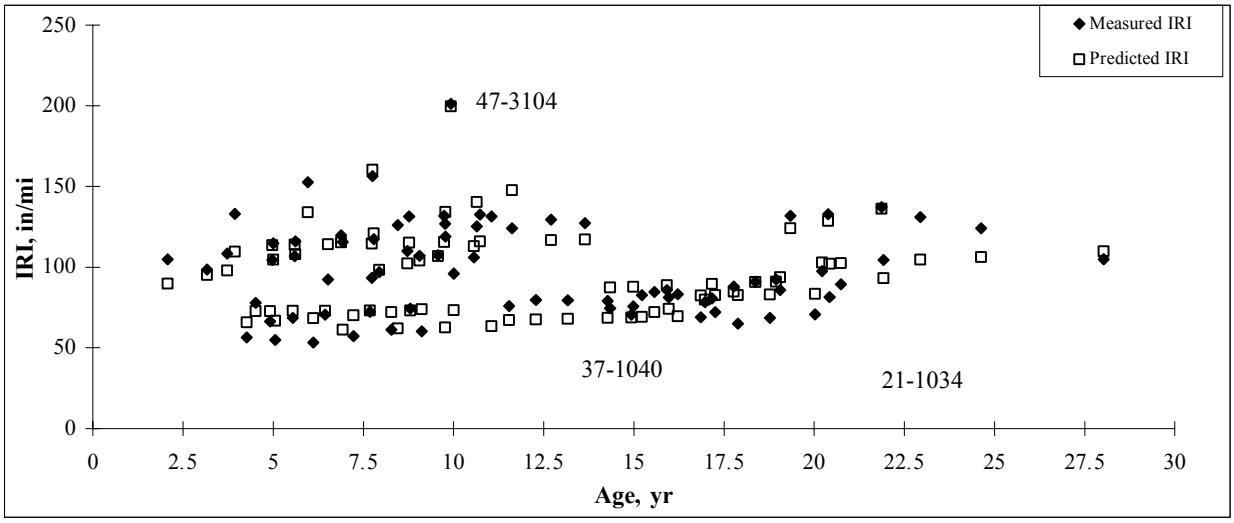

$r^2 = 0.67$, Std. Error = 18.4 in/mi, n=78

1 in/mi = 0.0158 m/km

Figure E-5. GPS-1 wet freeze (P200>50%) IRI model.

$$IRI(t) = IRI_0 e^{r_0 \frac{t^S}{T}}$$

IRI_0 = A(w%)^B+C(SN)^D+E(P200)^F+G(ACthick)^H+U(P$_o$)^V

r_0 = [I(KESAL/yr)^J/K(SN)^L+M(ACthick)^N+O(Days90+)^P+
Q(%ACinSN)^R+W(P200)^X+Y(w%)^Z]/1000

A=	177.1028869
B=	-1.716922883
C=	74.5489505
D=	-0.732326294
E=	-7.39461E-05
F=	0.181451823
G=	18.90878103
H=	0.284274627
I=	324644.6387
J=	0.95
K=	420657.5528
L=	0.95
M=	580.9071107
N=	-227.4827571
O=	7.91895E-05
P=	6.570402829
Q=	-500085.6677
R=	1.000002005
S=	1.03562
T=	72926674.08
U=	-1.04216E-05
V=	2.481747201
W=	-208404.9164
X=	3.199189339
Y=	1006099.735
Z=	3.250664008

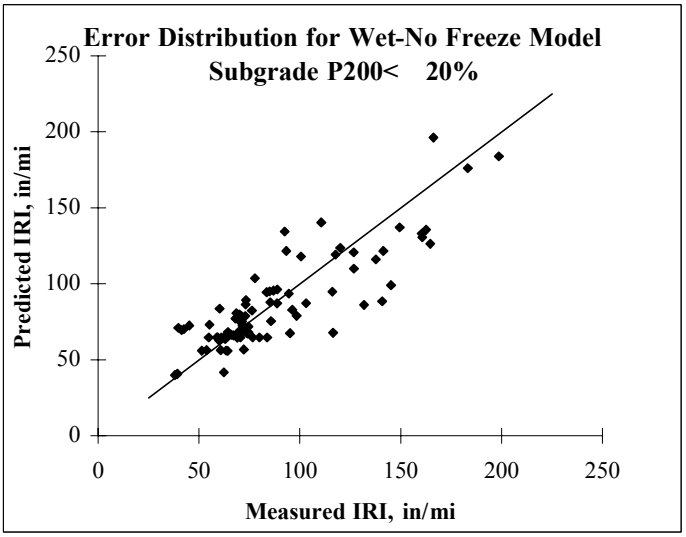

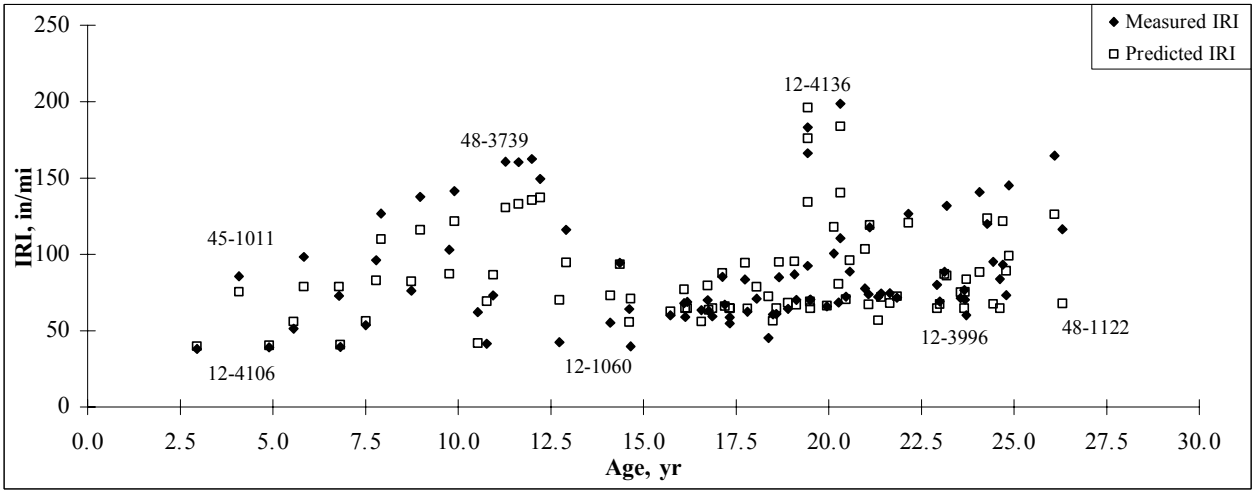

r^2 = 0.73, Std. Error = 18.6 in/mi, n=86

1 in/mi = 0.0158 m/km

Figure E-6. GPS-1 wet no-freeze (P200<20%) IRI model.

$$IRI(t) = IRI_0 e^{r_0 \frac{t^S}{T}}$$

$IRI_0 = A(w\%)^B + C(SN)^D + E(P200)^F + G(P_o)^H$

$r_0 = I(KESAL/yr)^J / K(SN)^L + M(ACthick)^N + O(Days90+)^P + Q(Dayswet)^R$

A=	0.00036776
B=	3.803389945
C=	64.25708572
D=	-7.081849214
E=	73.02626765
F=	-0.074143324
G=	-649.8686819
H=	-0.705966783
I=	0.090
J=	4.337555625
K=	911.0346267
L=	20.67719333
M=	6.691539978
N=	-18.9847011
O=	0.31843241
P=	0.053193018
Q=	-0.00022773
R=	1.439220965
S=	0.963844471
T=	5.942295546

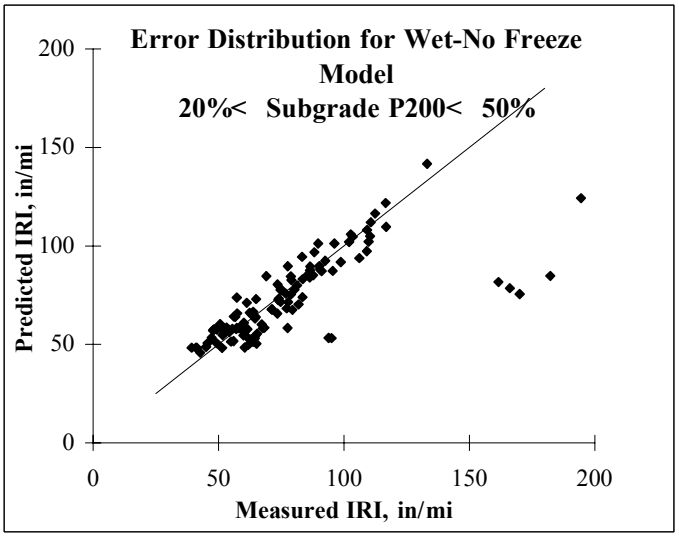

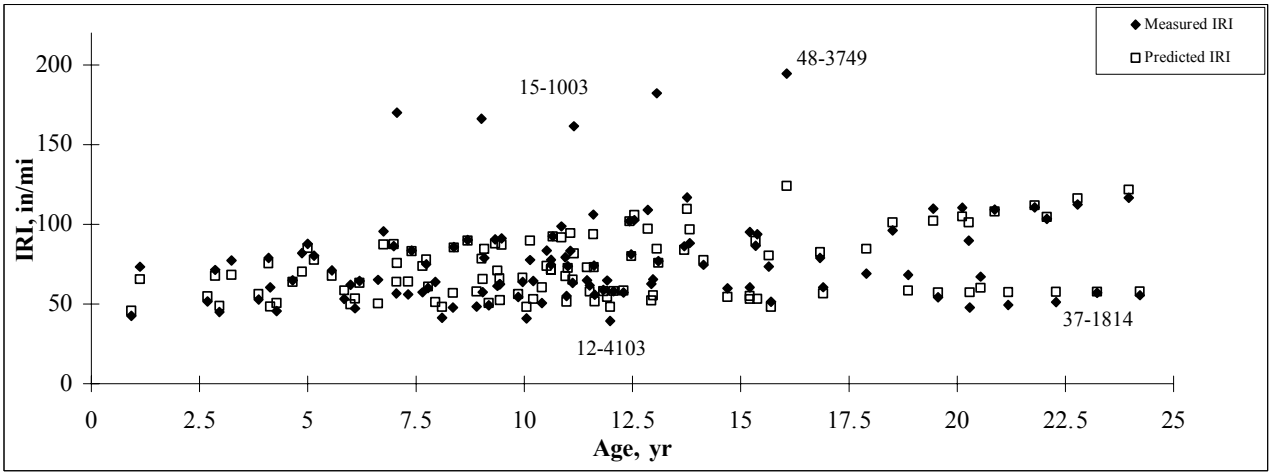

r^2 = 0.50 (0.82), Std. Error = 20.2 (9.1) in/mi, n=86 (w/o outlier)

1 in/mi = 0.0158 m/km

Figure E-7. GPS-1 wet no-freeze (20<P200<50%) IRI model.

$$IRI(t) = IRI_0 e^{r_0 \frac{t^U}{V}}$$

IRI_0 = $A(P_o)^B+C(P200)^D+E(w\%(\%Sand)P_o)^F+G(ACthick/P_o)^H$
$+Y(Basewash)^Z$

r_0 = $[I(KESAL/yr)^J/K(SN)^L+M(0.5+PI)^N+O(1000*(.0001+LI)/P_o)^P$
$Q((0.5+FrzThwCyc)(Days90+)/1000)^R+S(Dayswet)^T+$
$W(Basewash)^X+AA(P200)^{BB}]/1000$

A=	15716.32231
B=	-0.0013943
C=	-15181.6031
D=	-1.103133983
E=	5.487086103
F=	0.255182062
G=	-11016.1579
H=	0.000997796
I=	99734.62533
J=	2.593495872
K=	8799.209017
L=	8.883432783
M=	-0.000136566
N=	4.604158711
O=	-7136.944525
P=	1.951497491
Q=	3.02713E-05
R=	-3.778712582
S=	-11018.02009
T=	-49.01044159
U=	0.924802181
V=	259.1155103
W=	0.002000465
X=	4.305711761
Y=	-4483.899817
Z=	0.002099307
AA=	414.5026142
BB=	0.775821332

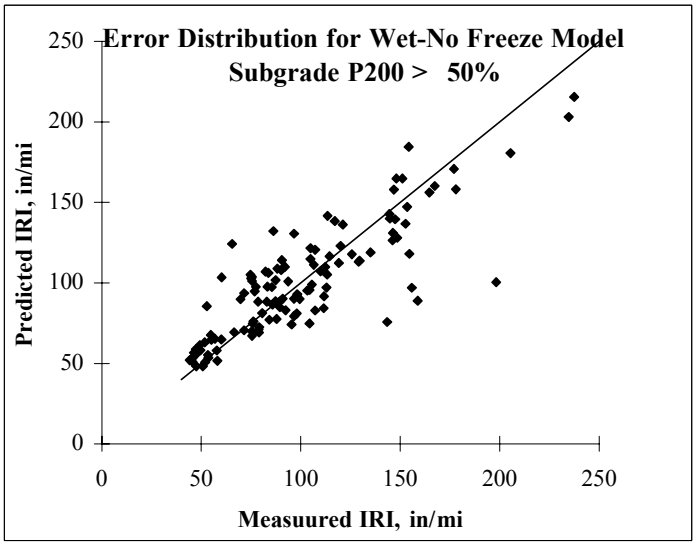

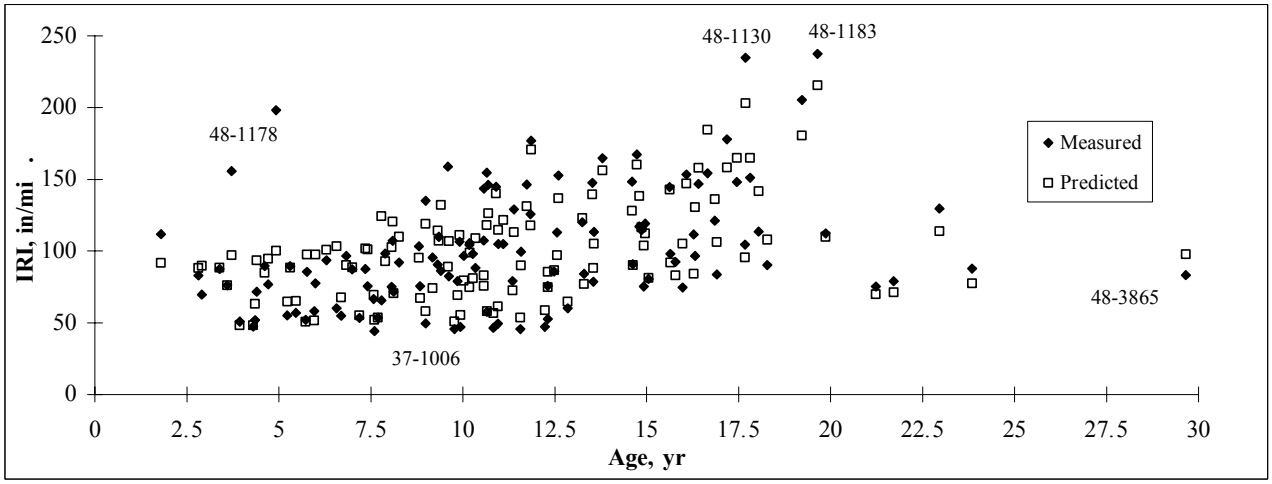

r^2 = 0.71, Std. Error = 21.7 in/mi, n=120

1 in/mi = 0.0158 m/km

Figure E-8. GPS-1 wet no-freeze (P200>50%) IRI model.

REFERENCES

1. Haas, R. and Hudson, W.R., Pavement Management Systems, Robert E. Krieger Publishing Company, Florida, 467p.

2. Sayers, M. On the Calculation of International Roughness Index from Longitudinal Road Profile, TRR 1501, 1995.

3. Strategic Highway Research Program Research Plans, Final Report, Transportation Research Board, 1986, 339 p.

4. Perera, R.W., Byrum. C., and Kohn, S.D., Investigation of Development of Pavement Roughness, FHWA-RD-97-147, May 1998.

5. Khazanovich et al, Common Characteristics of Good and Poorly Performing PCC Pavements, FHWA-RD-97-131, January 1998.

6. Owusu-Antwi, E.B., Titus-Glover, L, and Darter, M.I., Design and Construction of PCC Pavements, Volume I: Summary of Design Features and Construction Practices That Influence Performance of Pavements, Report No. FHWA-RD-98-052, April 1998.

7. Titus-Glover, L, Owusu-Antwi, E.B., Hoener, T., and Darter, M.I., Design and Construction of PCC Pavements, Volume II: Design Features and Practices That Influence Performance of Pavements, Report No. FHWA-RD-98-127, October 1998.

8. Titus-Glover, L., Owusu-Antwi, E.B., and Darter, M.I., Design and Construction of PCC Pavements, Volume II: Design and Construction of PCC Pavements, Volume III: Improved PCC Performance Models, Report No. FHWA-RD-98-113, January 1999.

9. Simpson, A.L., Rauhut, J.B., Jordhal, P.R., Owusu-Antwi, E., Darter, M.I., Ahamad, R., Pendleton, O.J., and Lee, Y., Sensitivity Analyses for Selected Pavement Distresses, SHRP-P-393, National Research Council, 1994.

10. Byrum, C., Analysis by high speed profile of jointed concrete pavement slab curvatures, Transportation Research Record 1730, Transportation Research Board, 2000, pp. 1-9.

11. Daleiden, J.F., Simpson, A., and Rauhut, J.B., Rehabilitation Performance Trends: Early Observations From the Long Term Pavement Performance (LTPP) Specific Pavement Studies (SPS), FHWA-RD-97-099, January 1998.

12. Karamihas, S.M., Gillespie, T.D., Perera, R.W., and Kohn, S.D., Guidelines for Longitudinal Pavement Profile Measurements, NCHRP Report 434, Transportation Research Board, 1999.

13. Paterson, W.D.O., Road Deterioration and Maintenance Effects, Models for Planning and Management. World Bank, 1987.

14. Von Quintus, H.L. and Simpson, A.L., Structural Factors for Flexible Pavements – Initial Evaluation of the SPS-1 Experiment, Final Report, October 2000.

15. Jiang, Y.J. and Darter, M.I., Structural Factors for Jointed Plain Concrete Pavements: SPS-2 - Initial Evaluation and Analysis, Final Report, October 2000.

16. Von Quintus, H.L., Simpson, A.L. and Eltahan, A.A., Rehabilitation of Asphalt Concrete Pavements, Initial Evaluation of the SPS-5 Experiment, Final Report, October 2000.

17. Ambroz, K.A. and Darter, M.I., Rehabilitation of Jointed Portland Cement Concrete Pavements: SPS-6 - Initial Evaluation and Analysis, Final Report, November 2000.

18. Von Quintus, H.L., Eltahan, A., and Yau, A., Smoothness Models for HMA Surfaced Pavements Developed from LTPP Performance Data, Presented at the 80th Annual Meeting, Transportation Research Board, 2001.

19. S-Plus 2000, Modern Statistics and Advanced Graphics, Mathsoft, Seattle, Washington, 1999.

20. Sayers, W. and Karamihas, S.M, The Little Book of Profiling, University of Michigan Transportation Research Center, September 1998.

21. Byrum, C.R., A High Speed Profiler Based Slab Curvature Index for Jointed Concrete Pavement Curling and Warping Analysis, Ph.D. Thesis, University of Michigan, 2001

22. Al-Omari, B. and Darter, M.I., Relationship between International Roughness Index and Present Serviceability Rating, Transportation Research Record 1435, Transportation Research Board, 1994, pp. 130-136